Composite materials: Modeling, Processing, and Characterization

Structural Modeling and Analysis

8-9 June 2021, 14:00-16:00

Speaker: Marco Petrolo, www.mul2.com

Contributors:

Prof. Erasmo Carrera, Dr. Ibrahim Kaleel, Dr. Manish H. Nagaraj

Webinar Organization

- Structural models for composites, Petrolo, 8 June, 14:00-16:00
- Processing methods and simulation, Zobeiry, 8 June, 16:00-18:00
- Multiscale models and failure analysis, Petrolo, 9 June, 14:00-16:00
- Evolution of properties during processing and characterization methods, Zobeiry, 9 June, 16:00-18:00
- Fabrication process of Boeing 777x and 787, Zobeiry, 10 June, 16:00-18:00
- Safety factor, building block and substantiation of composite aircraft, Zobeiry, 11 June, 16:00-18:00

The MUL2 Group

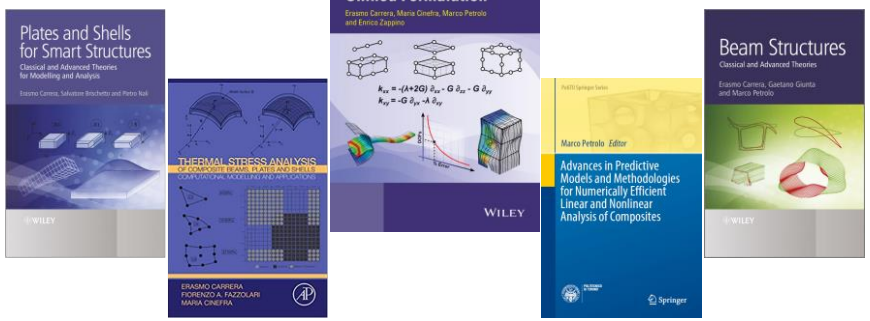

Network and Partners:

MUL2 Staff

Head of the Group

Professor Erasmo Carrera

Associate Professors
Alfonso Pagani
Marco Petrolo

Assistant Professors
Matteo Filippi
Enrico Zappino

Post-Doc
Riccardo Augello

PhD Students
Rodolfo Azzara
Ehsan Daneshkhah
Marco Enea
Jamal Najd
Alberto Racionero Sánchez-Majano
Li Xinzhu
Song Yunqiu
Fangzhou Zhu

Current Projects

- PRIN - DEVISU
- H2020 - ERC - PRE ECO
- Clean Sky 2 - CASTLE
- Clean Sky 2 - Airgreen 2
- Embraer - Global/Local Analysis of composite wing Structures (GLAS) and Validation projects

Research topics

- Aeroelasticity and Fluid-structure Interaction
- Aircraft and Spacecraft Design
- Best Theory Diagrams and Asymptotic/Axiomatic Analysis
- Biomechanics
- Composites
- Damage and Failure
- Inflatable Structures
- Meshless methods
- Multifield Analysis
- Rotor-Dynamics
- Structure Mechanics and FEM
- Global/Local Methods and plug-in for Abaqus/Nastran

Upcoming Events

- Sept 2021 - 26th Congress of the Italian Association of Aeronautics and Astronautics - www.aidaa2021.it
- May 2022 - 10th Design, Modelling and Experiments of Advanced Structures and Systems Conference, DEMEASS20201 Scopello, Italy
- TBD 2022 - 3rd International Conference on Mechanics of Advanced Materials and Structures, ICMAMS2021, College Station, TX, USA
- Sept 2024 - 34th International Council of the Aeronautical Sciences, ICAS2024, Florence, Italy

Node-dependent kinematics

E. Zappino, G. Li, A. Pagani, E. Carrera, A.G. de Miguel
Use of higher-order Legendre polynomials for multilayered plate elements with node-dependent kinematics
Composite Structures, 2018

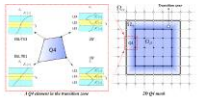

Best Theory Diagrams

E. Carrera, M. Petrolo
Axiomatic/Asymptotic Method and Best Theory Diagram for Composite Plates and Shells
Encyclopedia of Continuum Mechanics. Springer, 2018

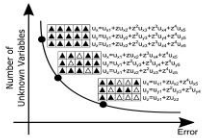

Progressive failure

I. Kaleel, M.Petrolo, A.M. Waas, E. Carrera
Micromechanical Progressive failure Analysis of Fiber-Reinforced Composite Using Refined Beam Models
Journal of Applied Mechanics, 2018

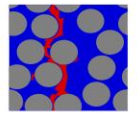

Non-linearity

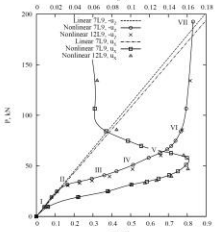

A. Pagani, E. Carrera
Unified formulation of geometrically nonlinear refined beam theories
Mechanics of Advanced Materials and Structures, 2016

Micromechanics

A.G de Miguel, A. Pagani, W. Yu, E. Carrera
Micromechanics of periodically heterogeneous materials using higher-order beam theories and the mechanics of structure genome
Composite Structures, 2017

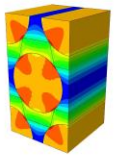

Biomechanics

E. Carrera, D. Guarnera, A. Pagani
Static and free-vibration analysis of dental prosthesis and atherosclerotic human artery by refined finite element models
Biomechanical Modeling and Mechanobiology, 2018.

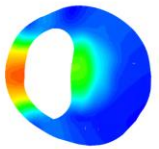

Rotordynamics

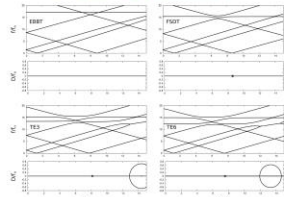

E. Carrera, M. Filippi
Variable kinematic one-dimensional finite elements for the analysis of rotors made of composite materials
Journal of Engineering for Gas Turbines and Power, 2014

Composites and multifield

M. Cinefra, M. Petrolo, G. Li, E. Carrera
Variable kinematic shell elements for composite laminates accounting for hygrothermal effects
Journal of Thermal Stresses, 2017

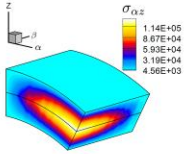

Global/local analysis and plug-in for Abaqus/Nastran

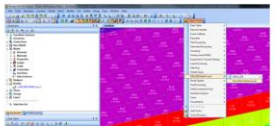

MUL2 – Theories of Structures and FEM

MUL2 is an in-house FE code entirely based on the Carrera Unified Formulation (CUF)

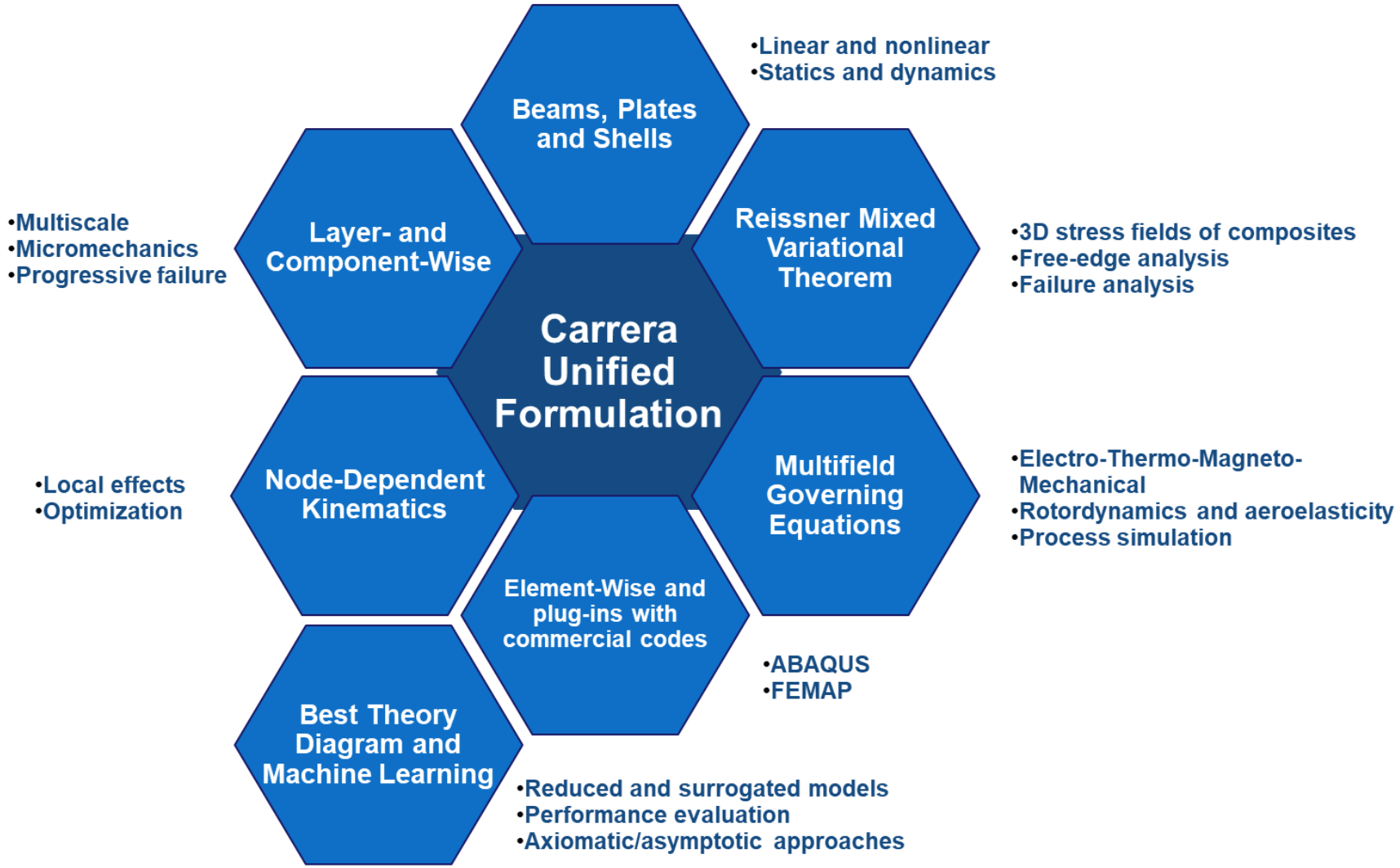

MUL2 – Current Capabilities for Composites

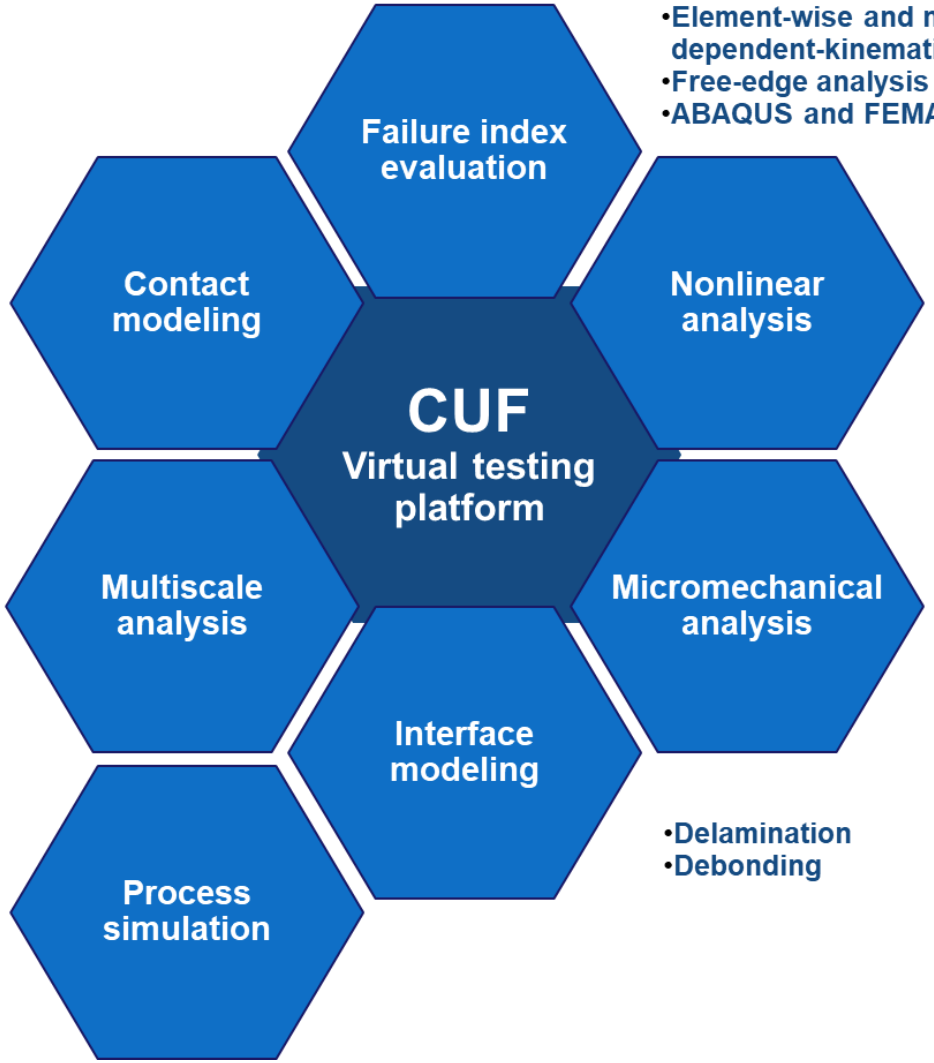

- Element-wise and node-dependent-kinematics
- Free-edge analysis
- ABAQUS and FEMAP plug-in

- Low-velocity impact
- Scalable explicit solver

- Material and geometrical nonlinearities
- CODAM2 damage models

- Concurrent framework
- Highly-scalable – parallel implementation

- 3D RVEs
- Nonlinear analysis
- Defect analysis

- Delamination
- Debonding

- Thermomechanical
- Residual stress analysis
- Spring-in angles

NOTE: this presentation focuses on composites only. Other capabilities are available.

Outline

- Introduction
  - PART I – Structural Theories
- Brief Overview of Theories for Metallic Structures
- Theories for Composite Structures
- Numerical Examples
  - PART II – Failure and Multiscale Analyses
- Failure Onset and Progression
- Micromechanics
- Multiscale

INTRODUCTION

Aims 1/2

- Available **options** for the structural analysis of **metallic and composite structures** concerning the choice of **1D, 2D, and 3D theories**
- Proper **modeling of** various types of **mechanical behaviors** and the associated **solution's efficiency**
- Multiple **problems** are considered, including **linear and nonlinear** analyses and **static and dynamic** settings
- **Guidelines on the proper selection of a model** are outlined, and quantitative **estimations on the accuracy** are provided
- Not many theoretical details, but **warnings, hints and references** for further study

Aims 2/2

Problem	HOST DOF	3D DOF	HOST/3D	Error	Variable and Convergence Pattern
Non-homogeneous atherosclerotic plaque - Beam	23529	761244	3%	3%	Tranverse axial strain, HOST -> 3D
Composite C-section spar - Beam	89175	2276739	4%	25%	Free-edge peeling stress, 3D -> HOST
Composite Omega stringer - Beam	142476	4560150	3%	30%	Free-edge failure index, 3D -> HOST
Composite notched specimen - Plate	10000	10000000	0.1%	3%	Tensile peak stress, HOST -> 3D
Multilayered beam - Beam	23595	63210	37%	0.4%	Plastic strain, HOST -> 3D
Double-swept blade - Beam	13200	203808	6%	1%	Natural frequencies, HOST -> 3D
Viscoelastic beam - Beam	5475	56400	10%	5%	Modal loss factor, HOST -> 3D
Randomly distributed RVE - Beam	13642	31524	43%	2%	Local shear strain, HOST -> 3D
Lattice structure - Beam	13584	617580	2%	1%	Displacement, HOST -> 3D
Three-point bending of a sandwich beam - Beam	14229	201504	1%	0%	Transverse stress, HOST -> 3D
Low-velocity impact on a bi-metallic plate - Plate	10659	856251	1%	16%	Plastic strain, 3D -> HOST
Large deflections in asymmetric cross-ply beams - Beam	5124	573675	1%	7%	Shear stress, HOST -> 3D
Disbonding in sandwich beams - Beam	41160	171888	24%	1%	Peak load, HOST -> 3D
Curing of a composite part - Beam	16569	599571	3%	0%	Spring-in angle, 3D -> HOST

Carrera E. et al, (2021), COMPOSITE STRUCTURES, Vol. 264, DOI:10.1016/j.compstruct.2021.113671

Basic Nomenclature

- 1D, 2D and 3D theories: **beams**, **plates** and **shells**, **solids**
- **Classical theories**: Euler-Bernoulli, Timoshenko, Kirchhoff, Reissner-Mindlin, Classical Lamination Theory (CLT), First-Order Shear Deformation Theory (FSDT)
- **Refined or higher-order theories**: any theory beyond classical ones, e.g., Third-Order Shear Deformation Theory (TSDT)
- **Degrees of Freedom (DOF)**: number of unknown variables, e.g, **Timoshenko** has **five DOF per node**; in **commercial codes**, each node can have up to **six DOF**

A Definition for *Structural Theory*

- A **structural theory** is a set of mathematical relations and assumptions to **reduce/approximate the 3D problem to 2D or 1D ones**
- **2D theory**: the approximation may be seen as a **through-the-thickness integration;** assumptions are made concerning the **through-the-thickness behavior** of the structure, e.g., unstretchable normal; **unknowns** over the **in-plane coordinates**

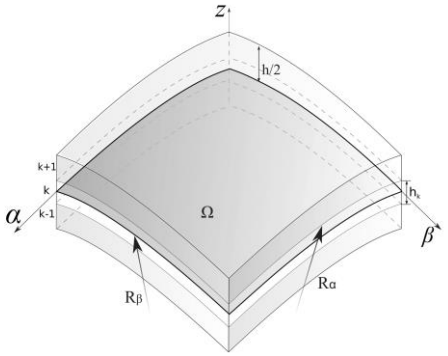

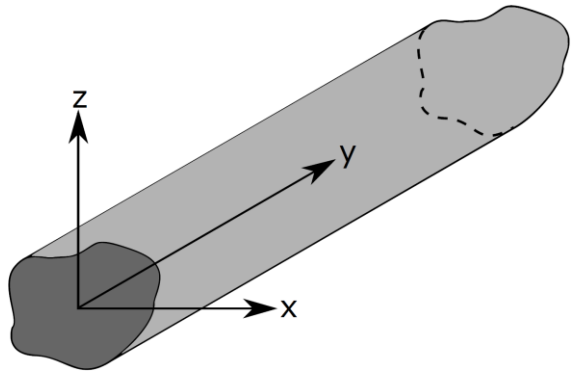

- **1D theory**: the approximation is an **integral over the cross-section**; assumptions are made concerning the **cross-sectional behavior** of the structure, e.g., no shear deformability; **unknowns** over the **axial coordinate**

PART I – Structural Theories

BRIEF OVERVIEW OF THEORIES FOR METALLIC STRUCTURES

Classical Theories 1/2

- Notes:
  1. For the sake of brevity, the **focus is on 2D models**, namely, plates and shells; in most cases, the **assumptions** used to develop such 2D models can be **applied to 1D models as well**
  2. For **shell** theories, the standard notation is based on **curvilinear coordinates** and displacements are u_α, u_β, and u_z; for **plates** and **beams**, the components are u_x, u_y, and u_z
- The **simplest 2D theory** is the **Kirchhoff-Love** (or **Euler-Bernoulli** for 1D):

$$u_x = u_{x1} - z u_{z1,x}$$
$$u_y = u_{y1} - z u_{z1,y}$$
$$u_z = u_{z1}$$

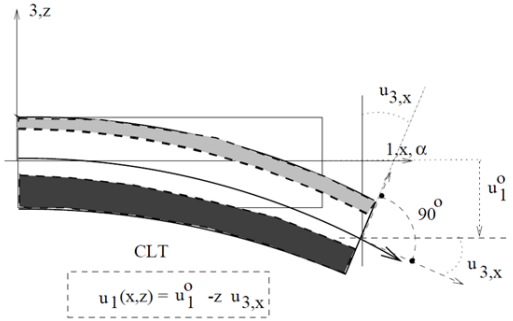

- **3 DOF**
- Assumptions: **no transverse shear stress, no normal stretching**
- The **derivatives** of the transverse displacement have the physical meaning of **rotations of the normals**

Classical Theories 2/2

- The First Order Shear Deformation Theory (**FSDT**) assumes a **constant shear distribution along the thickness**

$$u_x = u_{x1} + z u_{x2}$$
$$u_y = u_{y1} + z u_{y2}$$
$$u_z = u_{z1}$$

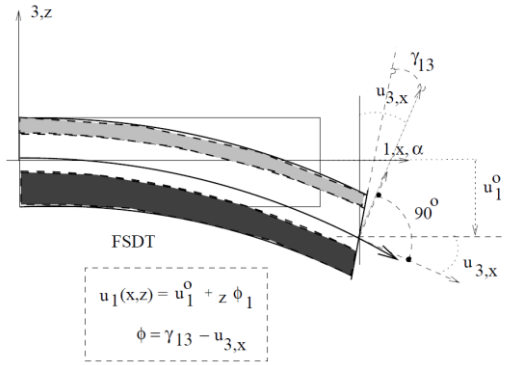

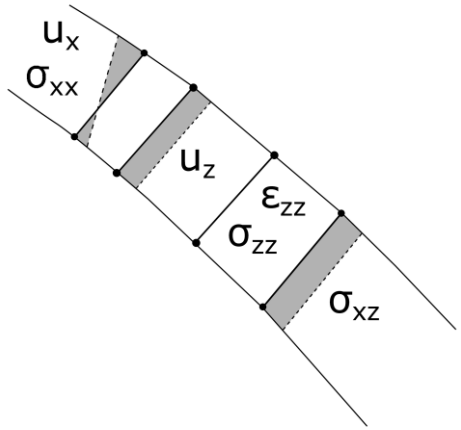

- **5 DOF**
- The **additional two terms** are rotations of the normals corrected by **shear**
- Stress **in-plane components** can be **linear**, the **transverse shear** stress is **constant**, and the **normal stretching and stress null**
- The accuracy for global responses **improved via shear correction factors**. Such factors are **problem-dependent** as they depend on the distribution of shear stresses

A Simple Case with Normal Stretching

- Let us consider a **3D temperature distribution** over an **isotropic plate** with a constant distribution: $T(x, y, z) = T_0$
- Being α the coefficient of thermal expansion, the **normal strains induced** by the heat distribution are $\varepsilon_{xx} = \varepsilon_{yy} = \varepsilon_{zz} = \alpha T_0$
- Assuming linear geometrical relations: $\varepsilon_{zz} = u_{z,z}$
- Integrating: $u_z = u_{z1} + \alpha T_0 z$
- A plate theory with **at least a linear transverse displacement field** is necessary to capture the **normal transverse strain** caused by the **constant distribution of temperature** across the thickness
- With a similar procedure, the **linear distribution of temperature** leads to a **quadratic distribution of transverse displacement**
- In the most general case, T stems from a **heat-conduction problem** and, in the case of **thick multilayered structures**, may assume a **layer-wise nonlinear distribution** and require **higher-order layer-wise displacement fields**

E. Carrera: Journal of Thermal Stresses, 23(9):797-831, 2000; AIAA Journal, 40(9):1885-1896, 2002; AIAA Journal, 43(10):2232-2242, 2005

Higher-Order Structural Theories (HOST)

- The **enrichment of the displacement field** is a common approach to **remove assumptions** from structural theories
- A **2D or 1D** model based on an **infinite expansion** would guarantee the **exact 3D solution**

$u_x = u_{x1} + zu_{x2} + z^2u_{x3} + z^3u_{x4}$ $u_y = u_{y1} + zu_{y2} + z^2u_{y3} + z^3u_{y4}$ $u_z = u_{z1}$	$u_x = u_{x1} + zu_{x2} + z^2u_{x3} + z^3u_{x4}$ $u_y = u_{y1} + zu_{y2} + z^2u_{y3} + z^3u_{y4}$ $u_z = u_{z1} + zu_{z2} + z^2u_{z3} + z^3u_{z4}$
$u_x = u_{x1} + zu_{x2}$ $u_y = u_{y1} + zu_{y2}$ $u_z = u_{z1} + zu_{z2} + z^2u_{z3}$	$u_x = u_{x1} + zu_{x2} + \sin\left(z\pi/h\right)u_{x3} + e^{z/h}u_{x4}$ $u_y = u_{y1} + zu_{y2} + \sin\left(z\pi/h\right)u_{y3} + e^{z/h}u_{y4}$ $u_x = u_{z1} + zu_{z2} + \sin\left(z\pi/h\right)u_{z3} + e^{z/h}u_{z4}$

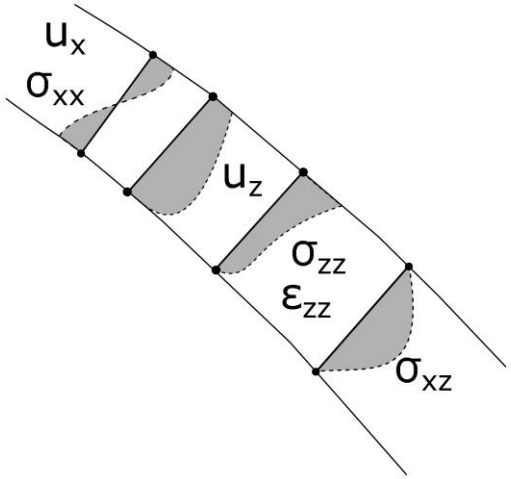

J.N. Reddy, International Journal of Engineering Science, 23(3):319 -330, 1985

K. Washizu, Variational Methods in Elasticity and Plasticity. Pergamon, Oxford, 1968

HOST's Accuracy is Problem Dependent

- S-S 0/90/0 Shell, Free Vibrations, 10 Modes, **a/h = 10**
- The **solid line is the Best Theory Diagram**, i.e., the set of shell theories **minimizing DOF** per node and **maximizing the accuracy**.
- The error distribution is problem-dependent
- **Carrera Unified Formulation**: framework to obtain any theory

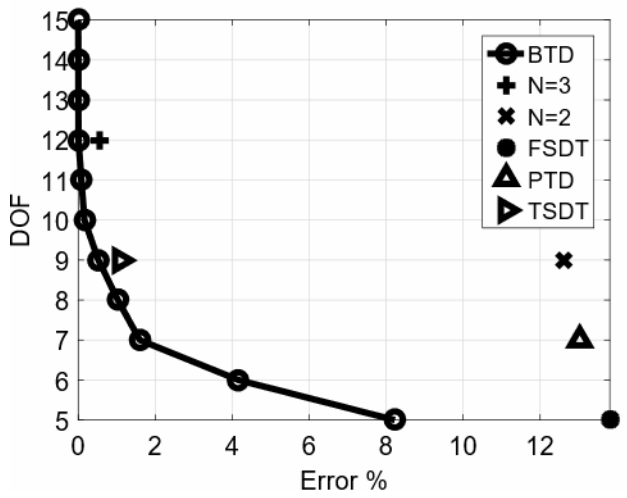

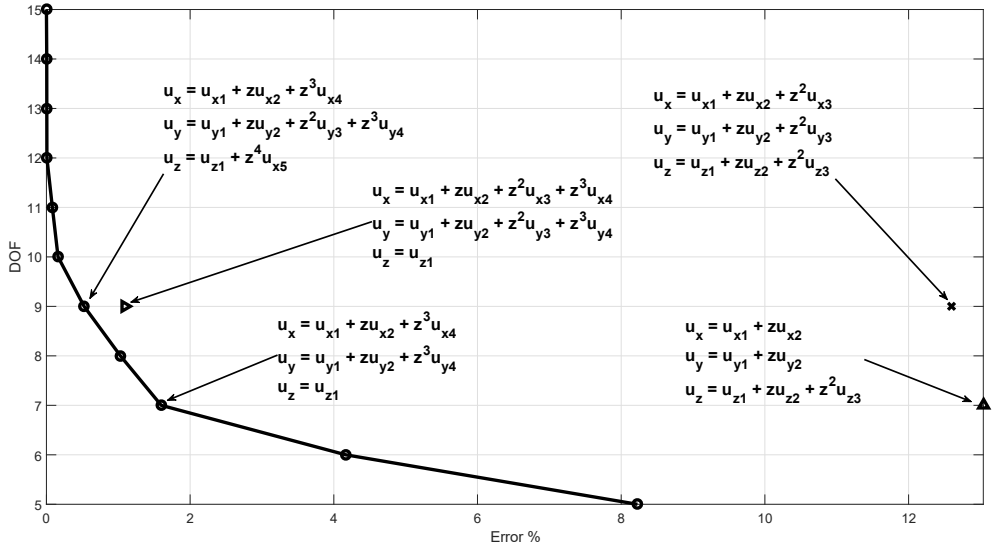

Petrolo M., Carrera E., (2020), ACTA MECHANICA, Vol. 231, pp. 395-434, DOI: 10.1007/s00707-019-02601-w

Carrera Unified Formulation (CUF)

$u_x =$	$u_{x1} +$	$zu_{x2} +$	$z^2u_{x3} +$	$z^3u_{x4} +$	$\cdots$
$u_y =$	$u_{y1} +$	$zu_{y2} +$	$z^2u_{y3} +$	$z^3u_{y4} +$	$\cdots$
$u_z =$	$u_{z1} +$	$zu_{z2} +$	$z^2u_{z3} +$	$z^3u_{z4} +$	$\cdots$
	$N = 0$	$N = 1$	$N = 2$	$N = 3$	$N = \cdots$
	$\tau = 1$	$\tau = 2$	$\tau = 3$	$\tau = 4$	$\tau = \cdots$
	3 DOF	3 DOF	3 DOF	3 DOF	$\cdots$

CUF Displacement Field: $u(x, y, z) = F_\tau(z)u_\tau(x, y)$

FEM: $u = F_\tau N_i u_{\tau i}$

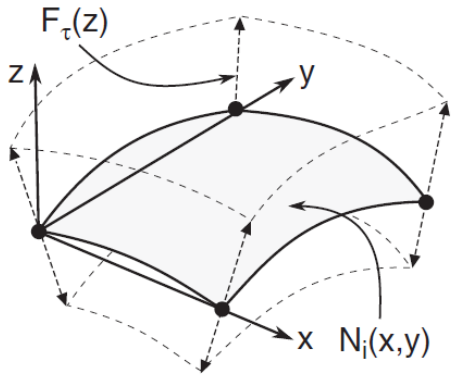

Carrera E., Archives of Computational Methods in Engineering (2003), Vol. 10, 3, pp. 215-296

CUF – Fundamental Nucleus of Stiffness Matrix

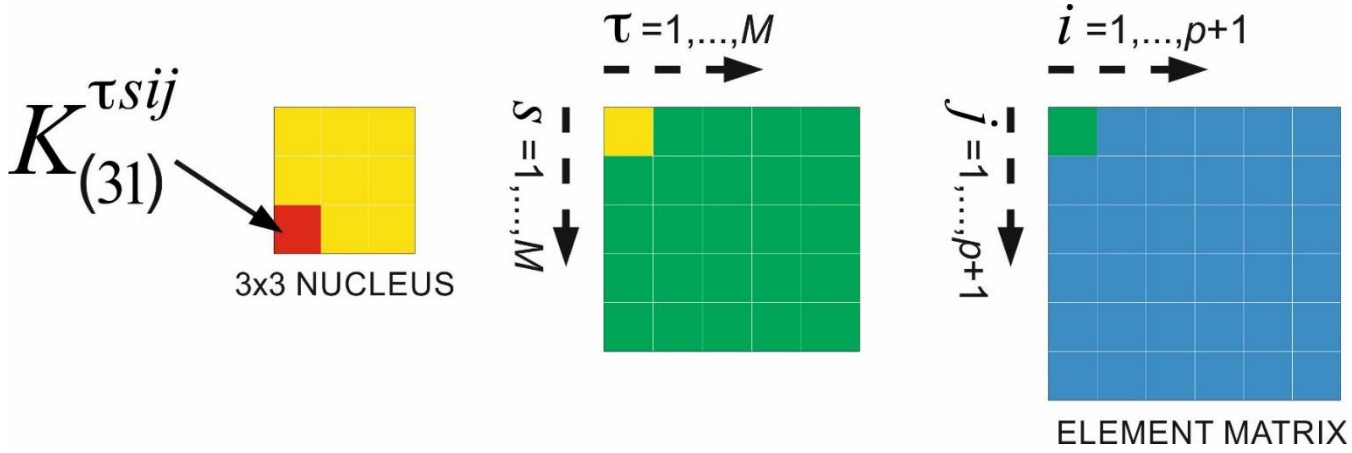

$$K_{xx}^{\tau isj} = \int_\Omega N_i N_j \, d\Omega \int_A C_{55} \, F^i_{\tau,z} F^j_{s,z} \, dz + \int_\Omega N_{i,y} N_{j,y} \, d\Omega \int_A C_{66} \, F^i_\tau F^j_s \, dz + \int_\Omega N_{i,x} N_{j,y} \, d\Omega \int_A C_{16} \, F^i_\tau F^j_s \, dz + \\ + \int_\Omega N_{i,y} N_{j,x} \, d\Omega \int_A C_{16} \, F^i_\tau F^j_s \, dz + \int_\Omega N_{i,x} N_{j,x} \, d\Omega \int_A C_{11} \, F^i_\tau F^j_s \, dz$$

$$K_{xy}^{\tau isj} = \int_\Omega N_i N_j \, d\Omega \int_A C_{45} \, F^i_{\tau,z} F^j_{s,z} \, dz + \int_\Omega N_{i,y} N_{j,y} \, d\Omega \int_A C_{26} \, F^i_\tau F^j_s \, dz + \int_\Omega N_{i,x} N_{j,y} \, d\Omega \int_A C_{12} \, F^i_\tau F^j_s \, dz + \\ + \int_\Omega N_{i,y} N_{j,x} \, d\Omega \int_A C_{66} \, F^i_\tau F^j_s \, dz + \int_\Omega N_{i,x} N_{j,x} \, d\Omega \int_A C_{16} \, F^i_\tau F^j_s \, dz$$

CUF – 1D, 2D, 3D

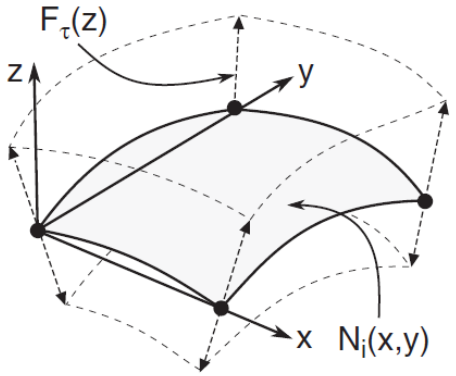

$$u_x = u_{x1} + zu_{x2} + z^2u_{x3} + z^3u_{x4} + \cdots$$
$$u_y = u_{y1} + zu_{y2} + z^2u_{y3} + z^3u_{y4} + \cdots$$
$$u_z = u_{z1} + zu_{z2} + z^2u_{z3} + z^3u_{z4} + \cdots$$

$$u_x = u_{x1} + xu_{x2} + zu_{x3} + x^2u_{x4} + xzu_{x5} + \cdots$$
$$u_y = u_{y1} + xu_{y2} + zu_{y3} + x^2u_{y4} + xzu_{y5} + \cdots$$
$$u_z = u_{z1} + xu_{z2} + zu_{z3} + x^2u_{z4} + xzu_{z5} + \cdots$$

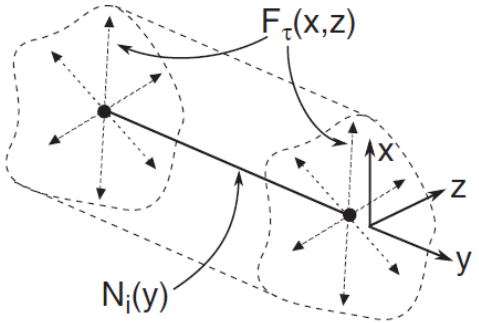

Equilibrium equations in Strong Form $\longrightarrow \delta L_i = \int_V \delta u k u dV + \int_S \ldots dS$

$$\underbrace{\begin{bmatrix} k_{xx} & k_{xy} & k_{xz} \\ k_{yx} & k_{yy} & k_{yz} \\ k_{zx} & k_{zy} & k_{zz} \end{bmatrix}}_{k} \underbrace{\begin{Bmatrix} u_x \\ u_y \\ u_z \end{Bmatrix}}_{u} = \underbrace{\begin{Bmatrix} p_x \\ p_y \\ p_z \end{Bmatrix}}_{p}$$

$k_{xx} = -(\lambda + 2G)\,\partial_{xx} - G\,\partial_{zz} - G\,\partial_{yy}$;
$k_{xy} = -\lambda\,\partial_{xy} - G\,\partial_{yx}$;
$k_{xz} = \ldots$
$\lambda = (E\nu)/[(1+\nu)(1-2\nu)]$; $G = E/[2(1+\nu)]$

$u = u(x, y, z)$
$\delta u = \delta u(x, y, z)$

The diagonal (e.g. k_{xx}) and the non-diagonal (e.g. k_{xy}) terms can be obtained through proper index permutations.

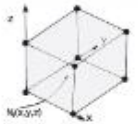

3D FEM Formulation $\longrightarrow \delta L_i = \delta u_j k^{ij} u_i$

$$k^{ij}_{xx} = (\lambda + 2G)\int_V N_{j,x}N_{i,x}dV + G\int_V N_{j,z}N_{i,z}dV + G\int_V N_{j,y}N_{i,y}dV;$$
$$k^{ij}_{xy} = \lambda\int_V N_{j,y}N_{i,x}dV + G\int_V N_{j,x}N_{i,y}dV$$

$u = N_i(x, y, z)u_i$
$\delta u = N_j(x, y, z)\delta u_j$

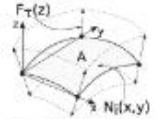

2D FEM Formulation $\longrightarrow \delta L_i = \delta u_{sj} k^{\tau s ij} u_{\tau i}$

$$k^{\tau s ij}_{xx} = (\lambda + 2G)\int_\Omega N_{i,x}N_{j,x}d\Omega \int_h F_\tau F_s dz +$$
$$+G\int_\Omega N_i N_j d\Omega \int_h F_{\tau,z}F_{s,z}dz + G\int_V N_{i,y}N_{j,y}d\Omega \int_h F_\tau F_s dz;$$
$$k^{\tau s ij}_{xy} = \lambda\int_\Omega N_{i,y}N_{j,y}d\Omega \int_h F_\tau F_s dz + G\int_\Omega N_{i,x}N_{j,y}d\Omega \int_h F_\tau F_s dz$$

$u = N_i(x, y)F_\tau(z)u_{\tau i}$
$\delta u = N_j(x, y)F_s(z)\delta u_{sj}$

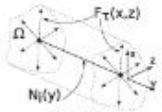

1D FEM Formulation $\longrightarrow \delta L_i = \delta u_{sj} k^{\tau s ij} u_{\tau i}$

$$k^{\tau s ij}_{xx} = (\lambda + 2G)\int_l N_i N_j dy \int_A F_{\tau,x}F_{s,x}dA$$
$$+G\int_l N_i N_j dy \int_A F_{\tau,z}F_{s,z}dA + G\int_l N_{i,y}N_{j,y}dy \int_A F_\tau F_s dA;$$
$$k^{\tau s ij}_{xy} = \lambda\int_l N_{i,y}N_j dy \int_A F_\tau F_{s,x}dA + G\int_l N_i N_{j,y}dy \int_A F_{\tau,x}F_s dA$$

$u = N_i(y)F_\tau(x, z)u_{\tau i}$
$\delta u = N_j(y)F_s(x, z)\delta u_{sj}$

CUF leads to the automatic implementation of any theory of structures through 4 loops (i.e. 4 indexes):

- τ and s deal with the functions that approximate the displacement field and its virtual variation along the plate/shell thickness ($F_\tau(z)$, $F_s(z)$) or over the beam cross-section ($F_\tau(x, z)$, $F_s(x, z)$);
- i and j deal with the shape functions of the FE model, (3D:$N_i(x, y, z)$, $N_j(x, y, z)$; 2D:$N_i(x, y)$, $N_j(x, y)$; 1D:$N_i(y)$, $N_j(y)$).

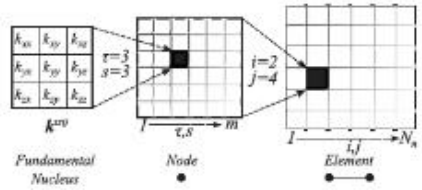

Carrera E., Cinefra M., Petrolo M., Zappino E. (2014) Finite Element Analysis of Structures through Unified Formulation. John Wiley & Sons Ltd.

Error of lower- and higher-order models for various applications involving isotropic structures[1]

Problem	Variable	Lower-order	Higher-order
Thermo-mechanical, linear temperature profile, plate with a/h = 10 [2]	Transverse displacement	FSDT, 37 %	N = 2, 0.3 %
Elastoplastic, bending of a bimetallic cantilever beam [3]	Plastic strain	N = 2, 30 %	LE9, 6 %
Dynamic response of a thin-walled cylinder [4]	Transverse displacement	TBT, 80 %	N = 7, 5 %
Wave propagation in a thin plate [5]	Transverse displacement	N = 1, 30 %	N = 4, 0.1 %

[1] E. Carrera et al. Composite Structures, 264, 2021

[2] E. Carrera. AIAA Journal, 40(9):1885-1896, 2002

[3] I. Kaleel et al. In: Advances in Predictive Models and Methodologies for Numerically Efficient Linear and Nonlinear Analysis of Composites, Springer, 2019

[4] E. Carrera and A. Varello. Journal of Sound and Vibration, 331(24):5268-5282, 2012

[5] A.G. de Miguel et al. Journal of Sound and Vibration, 457:139-155, 2019

PART I – Structural Theories

THEORIES FOR COMPOSITE STRUCTURES

Challenging Features of Composites 1/4

- In-plane anisotropy: **properties** of each layer can change significantly **depending on directions**
- The anisotropy may coexist with **high transverse shear and normal flexibility** and **couplings** between axial and shear strains. Further couplings can arise between in-plane and out-of-plane strains, e.g., in the case of non-symmetric stacking sequences
- Transverse anisotropy: **layer-wise discontinuous physical properties** along the thickness leading to compatibility and equilibrium conditions challenging to model
- The compatibility requires the **discontinuity of the slopes of displacement components** at the layer interfaces, i.e., the **zig–zag shape of the displacement field**. Such a zig–zag shape must coexist with the equilibrium conditions dictating the **continuity of the transverse stresses** at the interfaces, i.e., transverse shear and axial stresses must be interlaminar continuous. The literature refers to the sum of the two conditions as to the $\mathbf{C_0^z}$ **requirements**
- Further challenges may stem from many scenarios: the analysis of **residual stress from the curing process**, the analysis of **damaged structures**, the presence of singularities such as **free edges**, the use of tens of layers, and the use of **sandwich structures with soft cores**

Challenging Features of Composites 2/4

- High transverse deformability:
  - Common values for isotropic cases: $\frac{E_L}{E_T} = 1, \frac{E}{G} = 2.6, \text{with } \nu = 0.3$
  - Common values for an orthotropic layer:

$$5 < \frac{E_L}{E_T} < 40, 2 < \frac{E_T}{G_{LT}} < 5, 10 < \frac{E_L}{G_{LT}} < 200$$

- Transverse displacement and stress:
- Koiter's recommendation:

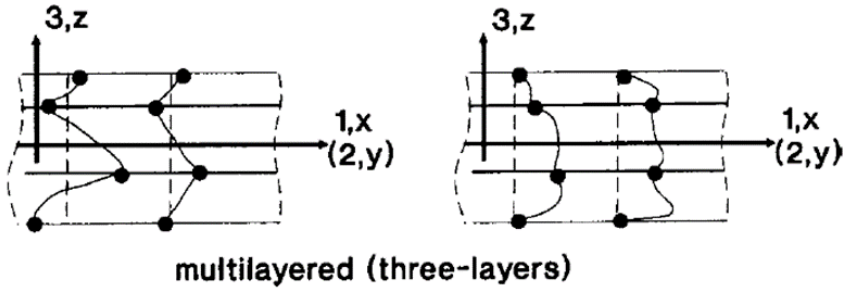

"A refinement of the Love's first approximation theory is indeed meaningless, in general, unless the **effects of transverse shear and normal stresses** are taken into account at same time"

Koiter WT, Proc. Of Symp. On the Theory of Thin Elastic Shells, Amsterdam, 1959

Cicala P, ''Sulla teoria elastica della parete sottile'', Giornale del Genio Civile, 6e(9), 1959

Goldenveizer AL, ''Theory of Thin Elastic Shells'', Pergamon Press, 1961

Challenging Features of Composites 3/4

- **Koiter's** recommendation is **not enough** as **zigzag effects**, and **interlaminar continuity** are **additional requirements**
- The **coupling** between **in-plane and out-of-plane** normal **stresses** makes the fulfillment of the σ_{zz} **interlaminar continuity** particularly **difficult**
- A theory's **accuracy depends on multiple factors**, e.g., the **thickness** and **orthotropic ratios**, the **number of layers, laminations**, and the **outputs**, e.g., **global** ones such as **natural frequencies**, or **local** ones, such as **through-the-thickness stress** distributions

E. Carrera, Journal of Applied Mechanics, 66(4):1004-1012, 12 1999; E. Carrera, Journal of Sound and Vibration, 225(5):803- 829, 1999.

E. Carrera, Composite Structures, 50(2):183-198, 2000; A.G. de Miguel et al, Composites Part B: Engineering, 168:375-386, 2019.

Challenging Features of Composites 4/4

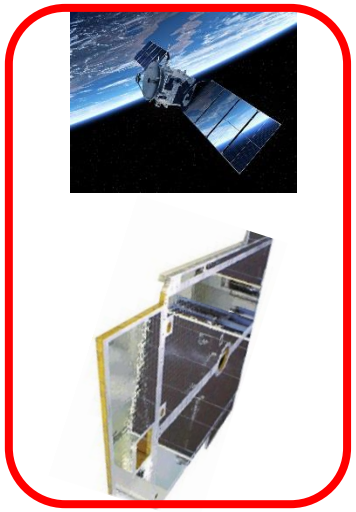

Macro-scale 10^{1} m

Structural response

Classical FEM Models

Macro-scale 10^{0} m

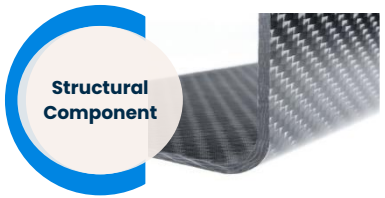

Interlaminar stresses

Free-edge effects

Failure Indexes
- Max Stresses/Strains
- Tsai-Wu, Tsai-Hill
- ...

Delamination Analysis
- Cohesive elements
- ...

Peridynamics
Homogenization
Failure Indexes
- Puck
- Hashin
- LaRC03
- LaRC04
- LaRC05

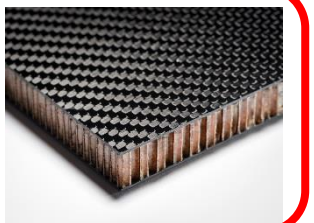

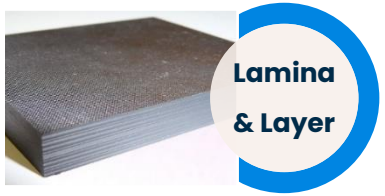

Meso-scale 10^{-2} m

Delamination/ debonding

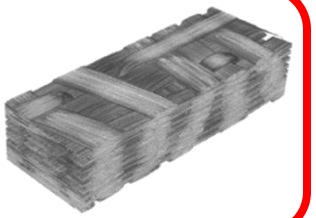

Micro-scale 10^{-6} m

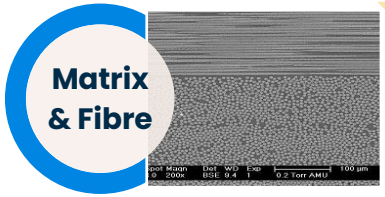

Matrix/Fiber Failure
Crack propagation
Micro-buckling
Etc

Refined 3D models
Crack propagation
...

Overview of Modeling Approaches

CUF provides models for all scales, including 1D, 2D, and 3D models

CUF allows to create **refined equivalent single layer models** able to improve the accuracy of the solution even if an equivalent layer is considered instead the original lamination, **Zig-Zag functions** can be used to improve the solution.

Layer-wise models consider **each layer as an independent entity** that is, the stress fields can be accurately evaluated even when complex laminations or sandwich materials are considered. **MIXED formulation** can be used to ensure the continuity. The **mesoscale** can be investigated using these models.

The **Node-Dependent Kinematic** models can be exploited to perform **global-to-local analyses** where the details of the meso-scale can be included locally using **LW models only where is required** reducing the computational costs.

Component-wise approach allows each component of the structure to be modeled using an independent formulation, that is it can be used **to model independently matrix and fibers**. The **microscale** can be studied using this approach.

Classical Theories – FSDT 1/2

- As in the metallic case, **in-plane** displacement and stress are usually **well-captured**
- The **transverse shear stress fails** to fulfill the top/bottom and interlaminar boundary conditions

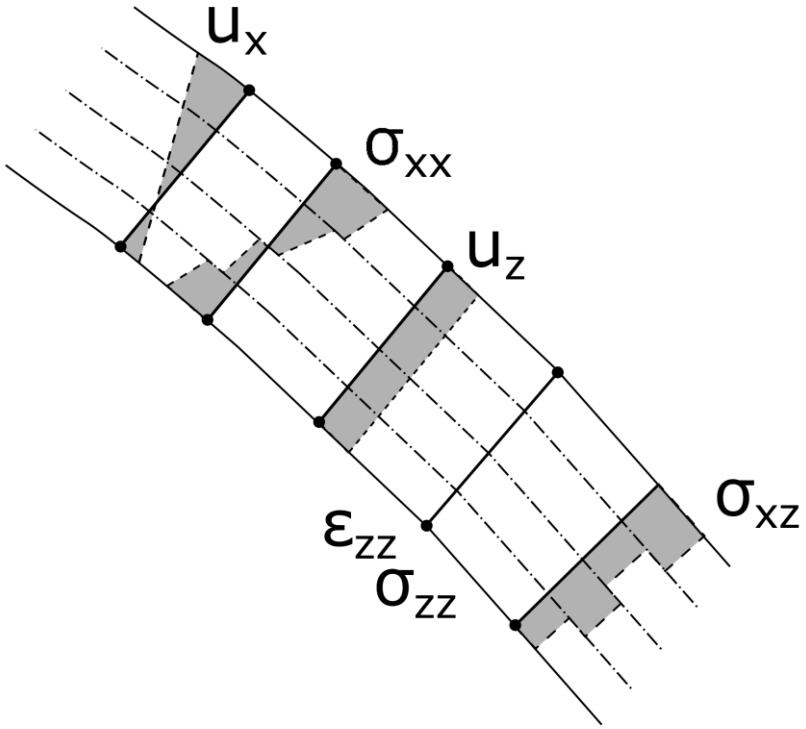

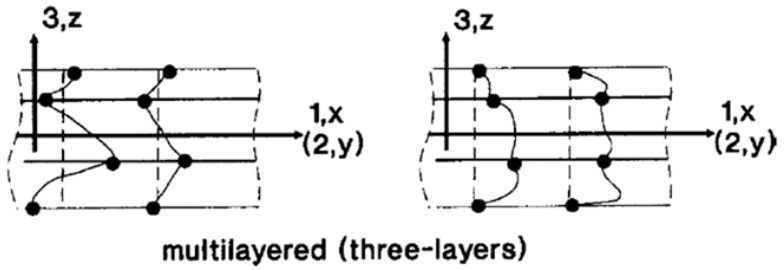

Classical Theories – FSDT 2/2

- **Transverse normal** stresses/strains are **neglected**
- **Transverse shear** strains are considered. There are retained **constant** within the thickness direction
- **Transverse stresses** are **discontinuous** at the interface.
- **Koiter's** recommendation is **not considered**

Consequently:

- FSDT works **well for global response** of **thin and moderately thin** laminated structures
- **No thick** laminated structures
- **No local phenomena**
- Shear **correction factors** can help but highly **problem-dependent**

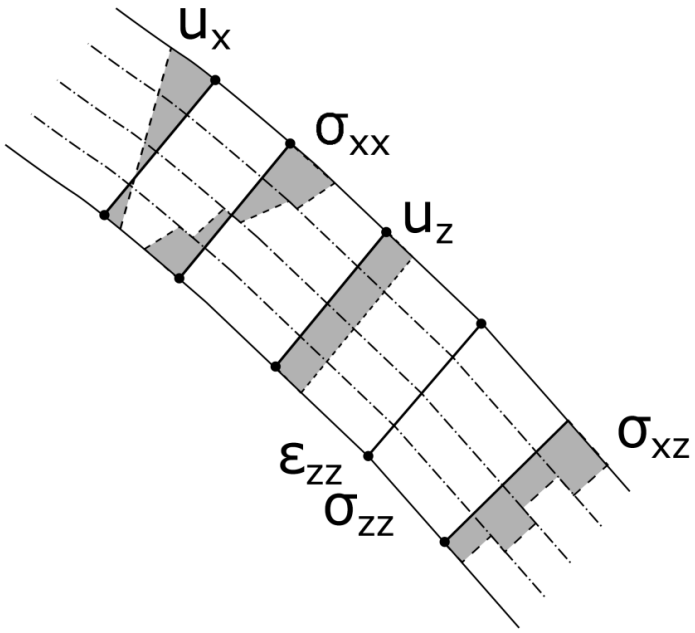

HOST and Equivalent Single Layer (ESL)

- **ESL** is a modeling approach commonly used for CLT, FSDT and HOST
- **ESL** assumes a distribution of variables for the **whole laminate**
- **ESL homogenizes** the **mesoscale properties** (each layer) into **a single macroscale layer**

The **same HOST seen before** may be applied to composites:

- The **inclusion of transverse deformability** is decisive in many cases
- **Further refinements are necessary** as, for instance, the **interlaminar continuity** of transverse stresses is **not achieved**

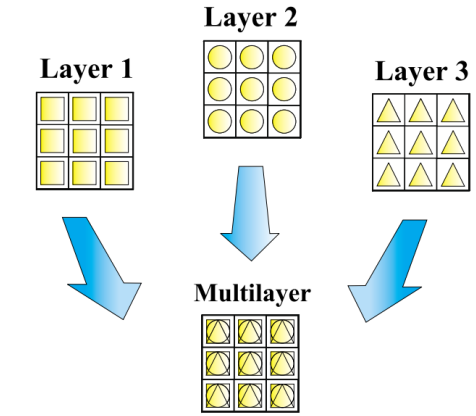

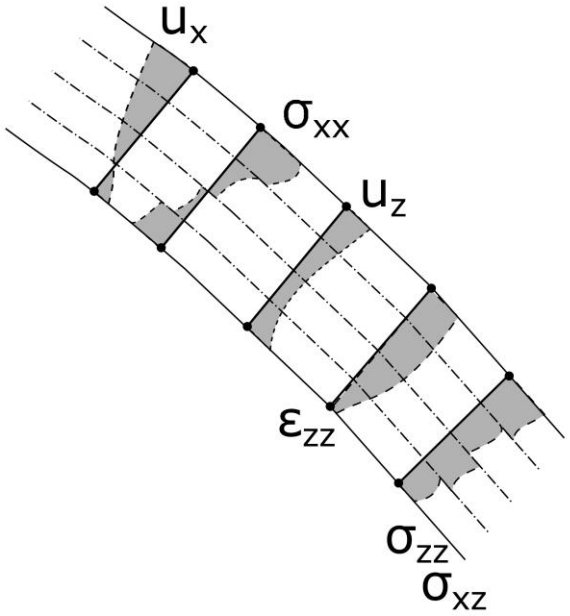

Zig-Zag Models

- **Aim:** improve the C_0^z **requirements**, i.e., **discontinuity** of the slopes of displacement components at the layer interfaces, and the continuity of the transverse stresses at the interfaces while **maintaining total DOF independent of the number of layers**
- There exist three ZZ classes [1]: **Lekhnitskii**–Ren, **Ambartsumian**–Whitney–Rath-Das; Reissner–**Murakami**-Carrera

Examples on the right: **FSDT and TSDT** with **Murakami ZZ**

- u_{xZ}, u_{yZ}, u_{zZ}, are **additional variables** independent of layers
- The **exponent k** changes the sign of the zig-zag term in each layer to **obtain the discontinuity of the first derivative of the displacement variables** in the z-directions and due to transverse anisotropy

[1] Carrera E., Applied Mechanics Reviews (2003), 56, pp. 287-308

$$u_x = u_{x1} + zu_{x2} + (-1)^k \frac{2z_k}{h_k} u_{xZ}$$

$$u_y = u_{y1} + zu_{y2} + (-1)^k \frac{2z_k}{h_k} u_{yZ}$$

$$u_z = u_{z1}$$

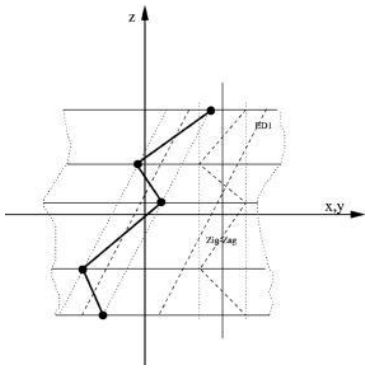

$$u_x = u_{x1} + zu_{x2} + z^2u_{x3} + z^3u_{x4} + (-1)^k \frac{2z_k}{h_k} u_{xZ}$$

$$u_y = u_{y1} + zu_{y2} + z^2u_{y3} + z^3u_{y4} + (-1)^k \frac{2z_k}{h_k} u_{yZ}$$

$$u_z = u_{z1} + zu_{z2} + z^2u_{z3} + z^3u_{z4} + (-1)^k \frac{2z_k}{h_k} u_{zZ}$$

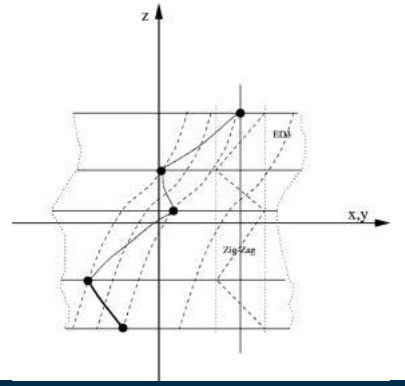

Layer-Wise Approach (LW)

$$u_x^k = F_1 u_{x1}^k + F_2 u_{x2}^k + \sum_{\tau=3}^{N} F_\tau u_{x\tau}^k$$

$$u_y^k = F_1 u_{y1}^k + F_2 u_{y2}^k + \sum_{\tau=3}^{N} F_\tau u_{y\tau}^k$$

$$u_z^k = F_1 u_{z1}^k + F_2 u_{z2}^k + \sum_{\tau=3}^{N} F_\tau u_{z\tau}^k$$

- **LW** leads to **zig-zag** distributions with the **additional** benefit of having **independent layers**
- **DOF** depend on the number of **layers**
- LW leads to **higher computational costs**, but its adoption is **necessary** in many cases, e.g., the precise detection of stress in each layer, **high-stress gradients** along the thickness, **free-edge**, and **local effects**
- Each **k-th layer** has its set of DOF
- Typical choices for F_τ are **Lagrange or Legendre** polynomials
- For compatibility conditions at the interfaces, **'1' and '2'** variables are **displacements at the top and bottom** of the interface
- Usually, **third- or fourth-order** terms guarantee **quasi-3D accuracy**
- **Transverse stresses** are very **well detected** with **minor interlaminar discontinuities**

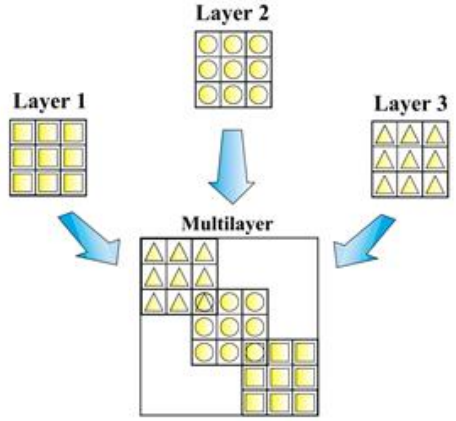

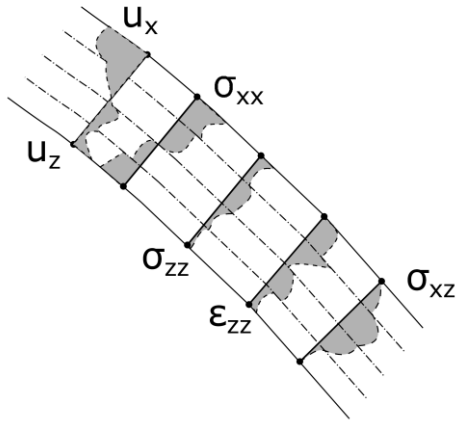

Carrera E., Journal of Applied Mechanics (1998), 65, pp. 820-828

J.N. Reddy. Mechanics of laminated composite plates and shells. Theory and Analysis. CRC Press, 2004

Models based on the Reissner Mixed Variational Theorem (RMVT)

- In mixed formulations, displacements and **stresses are primary variables**
- RMVT is one of the **most powerful tools** for composites, primary variables: the **displacements and the transverse stresses** [1]
- The use of RMVT is **independent of the type of expansion** adopted, Taylor expansions, zig-zag, layer-wise approaches, and **combination thereof can be used**. The example on the right is LW
- RMVT is **convenient** for multilayered structures as the **interlaminar continuity of transverse stresses** and **zig-zag displacements** are easily implementable
- The **post-processing** for transverse stresses is **not necessary**
- An **RMVT third-order zig-zag, ESL model,** can provide **3D-like accuracy in most cases** except for **severe local effects** in which the **layer-wise** version is preferable [2]

$$u_x^k = F_1 u_{x1}^k + F_2 u_{x2}^k + \sum_{\tau=3}^{N} F_\tau u_{x\tau}^k$$

$$u_y^k = F_1 u_{y1}^k + F_2 u_{y2}^k + \sum_{\tau=3}^{N} F_\tau u_{y\tau}^k$$

$$u_z^k = F_1 u_{z1}^k + F_2 u_{z2}^k + \sum_{\tau=3}^{N} F_\tau u_{z\tau}^k$$

$$\sigma_{xz}^k = F_1 \sigma_{xz1}^k + F_2 \sigma_{xz2}^k + \sum_{\tau=3}^{N} F_\tau \sigma_{xz\tau}^k$$

$$\sigma_{yz}^k = F_1 \sigma_{yz1}^k + F_2 \sigma_{yz2}^k + \sum_{\tau=3}^{N} F_\tau \sigma_{yz\tau}^k$$

$$\sigma_{zz}^k = F_1 \sigma_{zz1}^k + F_2 \sigma_{zz2}^k + \sum_{\tau=3}^{N} F_\tau \sigma_{zz\tau}^k$$

[1] E. Reissner, International Journal for Numerical Methods in Engineering, 23(2):193-198, 1986

[2] E. Carrera, Archives of Computational Methods in Engineering, 10(3):216-296, 2003

1D and 2D

- So far, most of the equations focused on 2D – plate, shell- models. All theories can be used for **1D – beam - models**

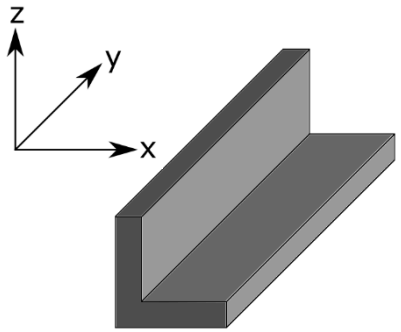

3D Geometry

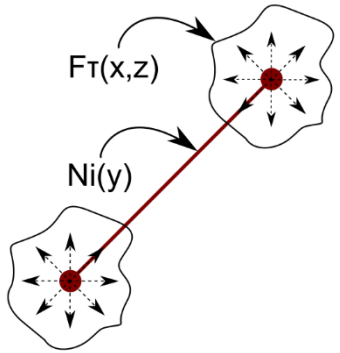

Taylor Expansion

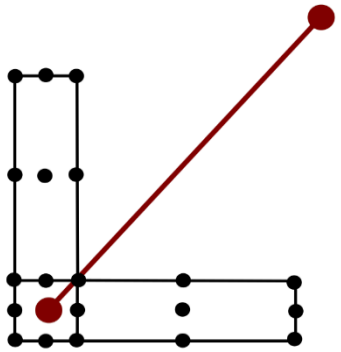

Lagrange Expansion

Classical 1D Finite Element

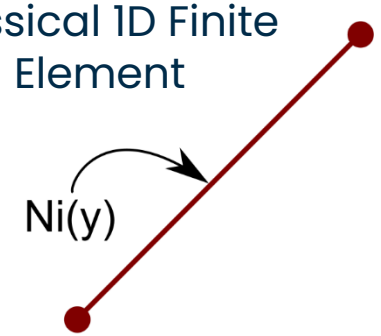

Refined 1D – CUF models

$$u_x = u_{x1} + xu_{x2} + zu_{x3} + x^2u_{x4} + xzu_{x5} + \cdots$$
$$u_y = u_{y1} + xu_{y2} + zu_{y3} + x^2u_{y4} + xzu_{y5} + \cdots$$
$$u_z = u_{z1} + xu_{z2} + zu_{z3} + x^2u_{z4} + xzu_{z5} + \cdots$$

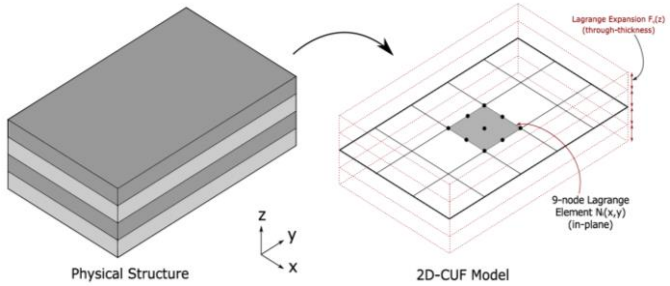

2D layer-wise modelling in CUF

Component-Wise Approach (CW)

- All engineering structures have **multiple components** with various **scales, geometries and materials**
- The **concurrent, proper modeling** of components with different properties may be **difficult**
- Examples of critical **modeling issues**: **coupling of beam, plate, shell, and solid elements**; accurate **3D geometrical modeling**; **homogenization of material properties**; etc.
- **CW** models use **1D CUF models for all components**, independently of their scale, geometry or material
- Advantages: **only pure displacements** as unknowns; **no** need of **reference surfaces** and **retaining of the 3D geometry**; **no** need of **homogenization techniques**

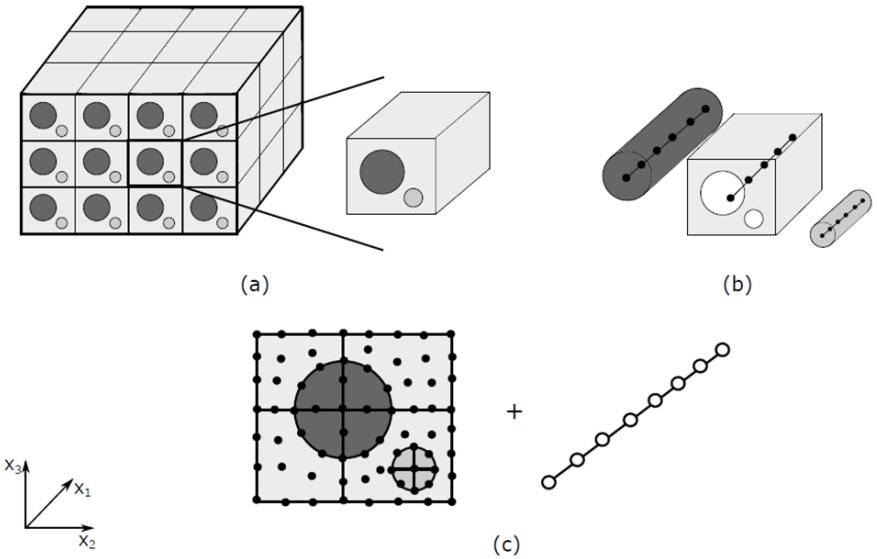

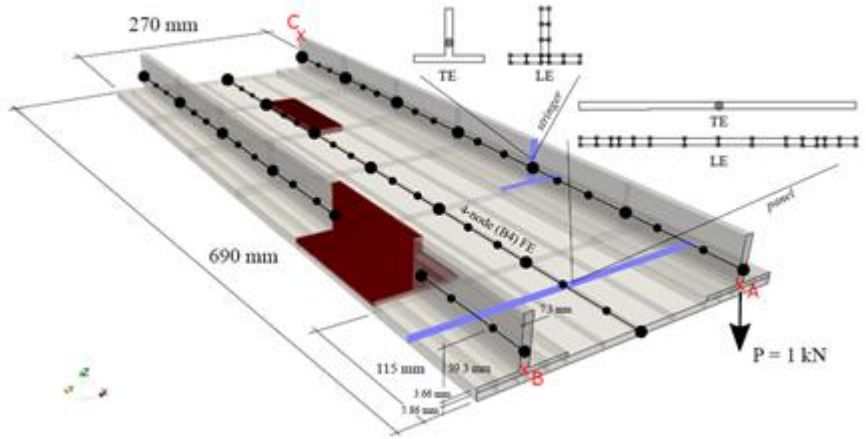

Carrera E. et al, AIAA Journal (2013), Vol. 51, 5, pp. 1255-1268

PART I – Structural Theories

NUMERICAL EXAMPLES

Local Effects in Sandwich Panels

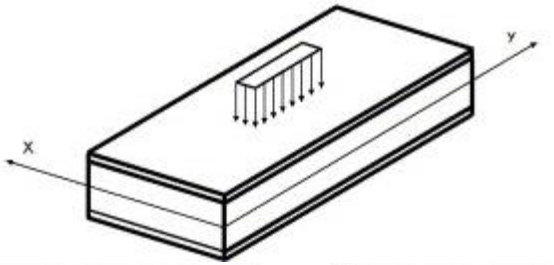

- Sandwich panels with a/h=10 and **soft cores**: the **core deformability** can be, at least, one order of magnitude **higher than that of the faces**, and the **normal transverse deformation** is **necessary** to model the sandwich core
- Plots show the **transverse displacement in the loading region**, with:
  - **LM4**: LW, fourth-order model based on RMVT
  - **EMZC3**: ESL, third-order model based on RMVT with zig-zag and interlaminar continuity
  - **EMZC3d**: EMZC3 without transverse normal strain
  - **ED1**: ESL, first-order model

Error wrt LM4	Top Face	Bottom Face
LM4	-	-
EMZC3	20%	18%
EMZC3d	25%	18%
ED1	99%	99%

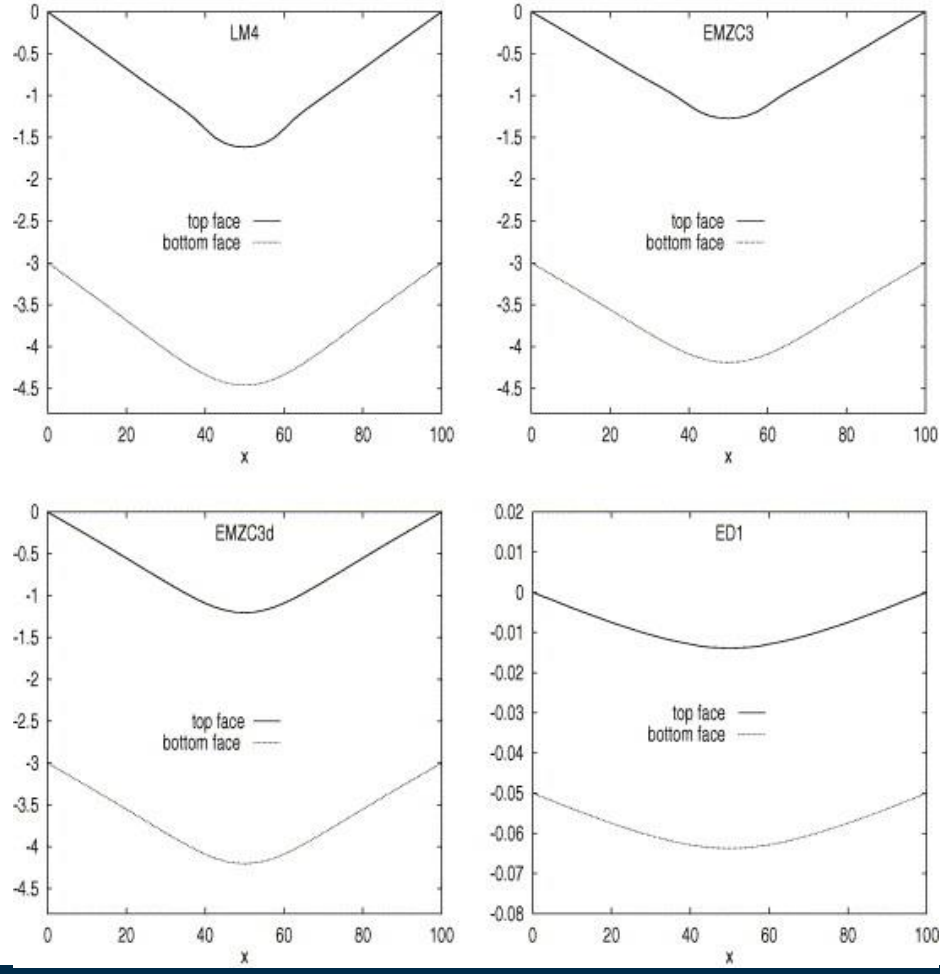

E. Carrera and A. Ciuffreda, Composite Structures, Volume 68, Issue 2, 2005, Pages 185-202

Examples of σ_{zz} effect

- Three-layer plate 0/90/0, simply-supported, a/h=4, distributed **load on the top surface**
- Plots show the **transverse shear stress** with:
  - **RMZC**: ESL, first-order model based on RMVT with zig-zag and interlaminar continuity
  - **3D**: exact solution
  - **RH and RF**: HOST without σ_{zz}
- The **3D (exact) solution** is **not symmetric**
- The **inclusion of σ_{zz}** is **necessary** to capture this effect

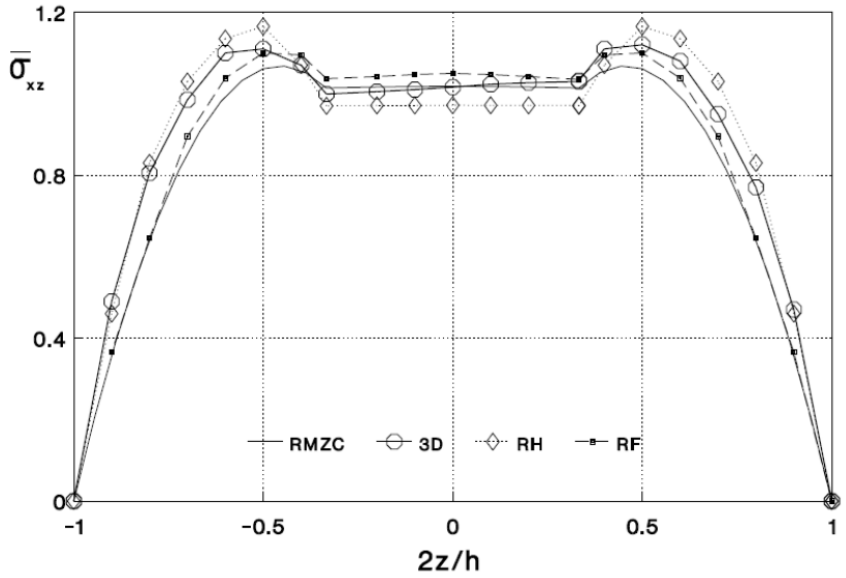

Carrera E., International Journal for Numerical Methods in Engineering (1996), 39, pp. 1797-1820

Notes on Post-Processing of Transverse Stress

Transverse stress can be computed via **three approaches**

1) Stress components are evaluated using **the constitutive laws**
2) The second method exploits the **indefinite equilibrium equations of 3D elasticity**. In the 2D case, the **in-plane stress components are integrated over the thickness** to obtain the transverse ones.
3) Mixed formulations lead to **mixed cases** as assumed transverse stress is directly available - a priori - as primary variables or can be evaluated - a posteriori, as in the previous cases - via constitutive laws or by integration

- The use of **constitutive laws** has the advantage of **simplicity**, but **its accuracy is satisfactory in LW models** with, at least, **third-order expansions**.
- The integration of the indefinite **equilibrium equations provides good accuracy**, but it may **sometimes fail to fulfill boundary conditions**. Furthermore, such a procedure **may be inaccurate as the number of layers increases**.
- **LW mixed formulations** provide the **best results**

Carrera E., Composite Structures (2000), 48, pp. 245-260

Stress Analysis of Adhesively Bonded Joints 1/2

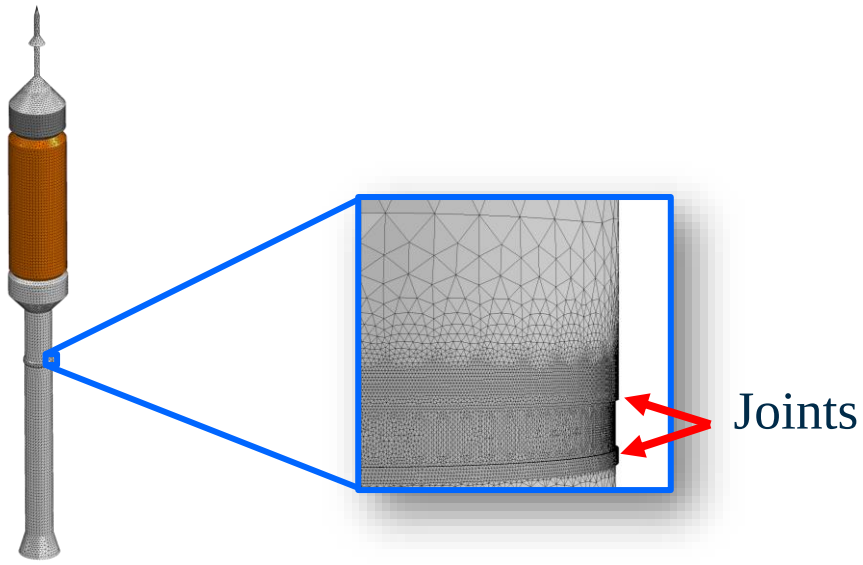

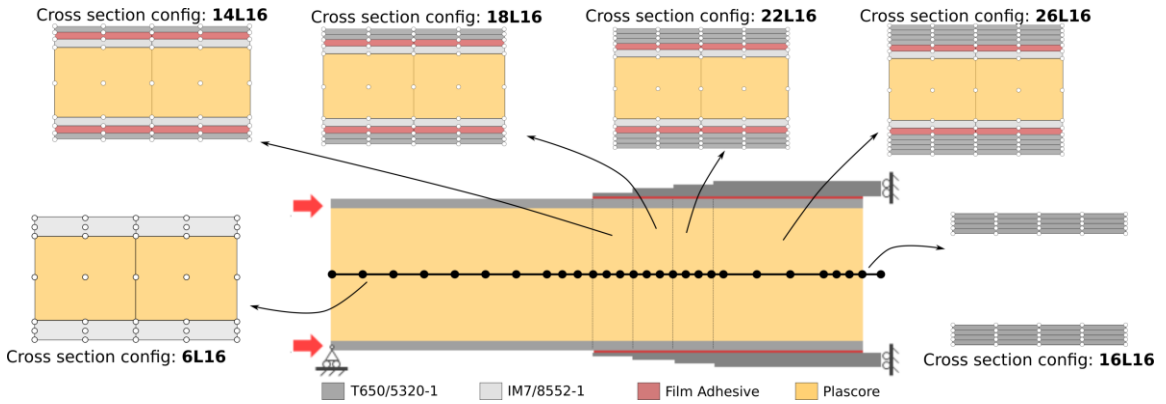

- CUF 1D CW: Mesh with **four-node beam elements** and Lagrange cross-section kinematics
- Converged 3D FEM as benchmark: **10 linear brick elements per layer and 20 for core**

Stapleton S.E. et al. (2021), MECHANICS OF ADVANCED MATERIALS AND STRUCTURES, Vol. 28, pp. 791-811

Stress Analysis of Adhesively Bonded Joints 2/2

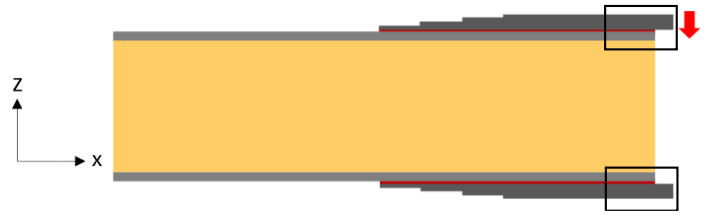

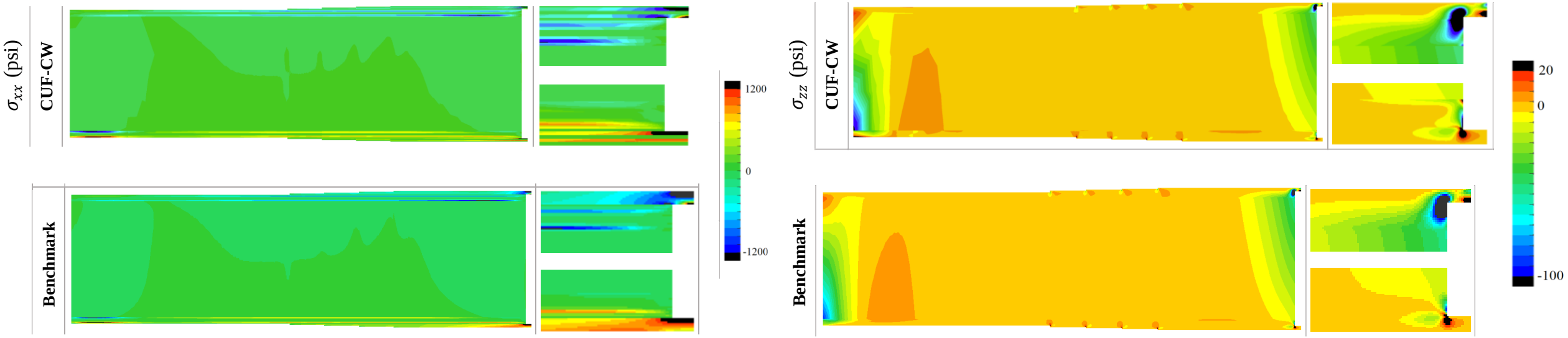

- **Accurate** capturing the **stress reversals** observed close to the **free surface**
- **Traction-free** conditions are **captured** along the free surface

Stapleton S.E. et al. (2021), MECHANICS OF ADVANCED MATERIALS AND STRUCTURES, Vol. 28, pp. 791-811

Free-Edge Effects 1/3

- Defined as **stress states** at the **interfaces** between **dissimilar layers** in the vicinity of **geometrical or mechanical discontinuities** in the structure
- **Classical theories cannot** model free-edge effects; specific models continue to be developed for understanding the mechanics of this complex problem [1-3]
- The Poisson effect and the **various elastic moduli** of the material **over different plies** let them **behave differently in the in-plane direction**.
- To satisfy the **compatibility of the displacements** at the interfaces, **transverse stresses appear near the free edge**.
- A **correct evaluation** of these stresses is **necessary**, for instance, to prevent damage mechanisms such as **delamination**.
- Free-edge **3D stress fields** have **strong gradients** - as the **region is roughly equal** to the **total thickness of the laminate** - and may lead to remarkably **high peak values**.

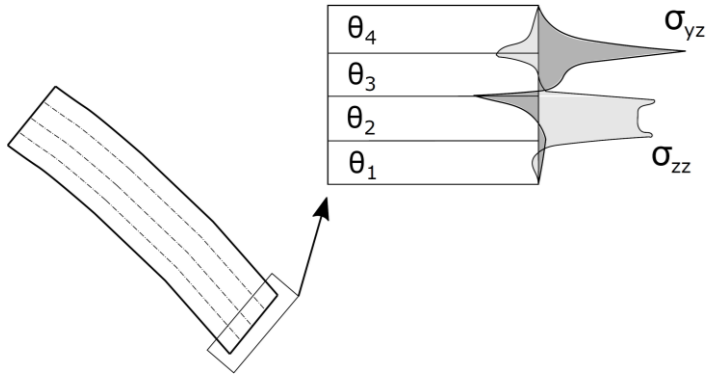

[1] T. Hayashi, vol 66, Transaction of Japan Society for Aeronautical Engineering and Space Science (1967), pp. 43-48

[2] A.H. Puppo, H.A. Evensen, J Compos Mater, 4 (2) (1970), pp. 204-220

[3] R.B. Pipes, N.J. Pagano, J Compos Mater, 4 (4) (1970), pp. 538-548

Free-Edge Effects 2/3

- The peeling stress (σ_{zz}) at the free-edge via **1D is more accurate than 3D** with five elements per node; **no stress recovery**; no aspect ratio constraints

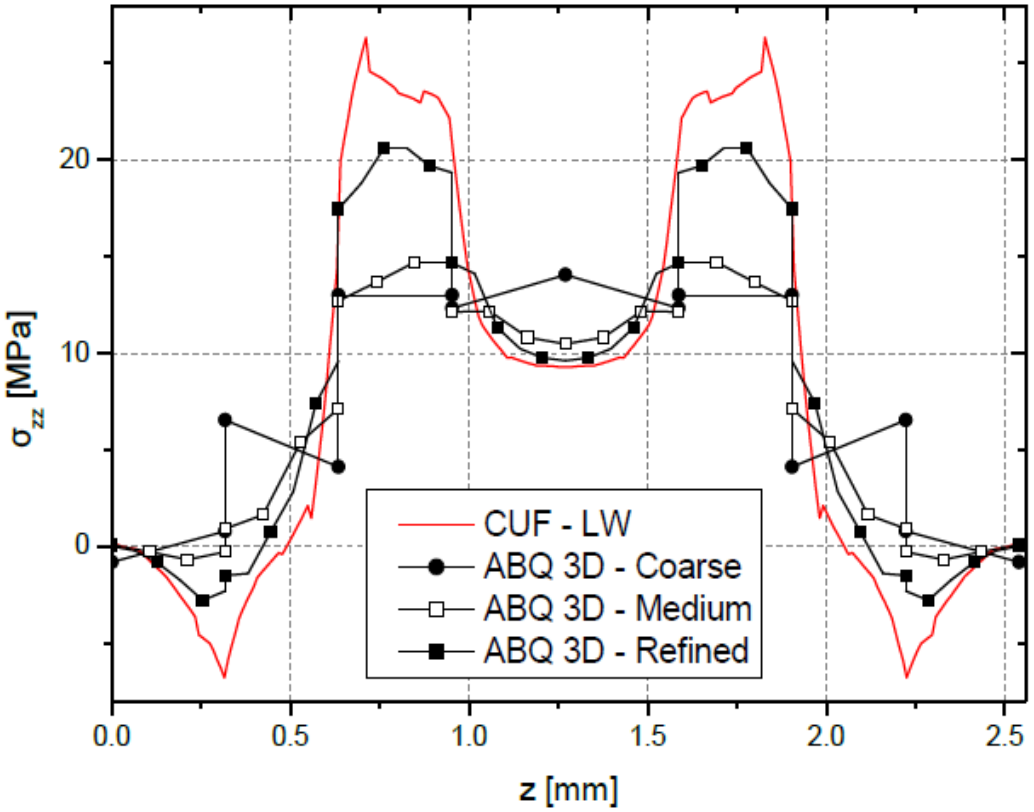

de Miguel A.G. et al. (2019), COMPOSITES. PART B, ENGINEERING, Vol. 168

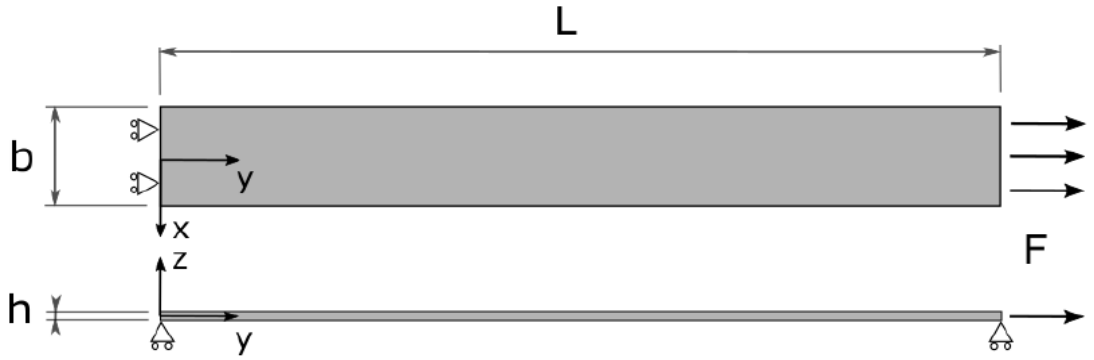

$$[45\ -45\ 90\ 0]_s$$

Model	DOF	Time (s)
CUF – LW (4 elements/ply)	**77,805**	**82**
3D FEM – Coarse (1 element/ply)	**168,237**	**27**
3D FEM – Medium (3 elements/ply)	**467,325**	**261**
3D FEM – Refined (5 elements/ply)	**3,501,933**	**3526**

Free-Edge Effects 3/3

Global-Local plug-in for NASTRAN and ABAQUS

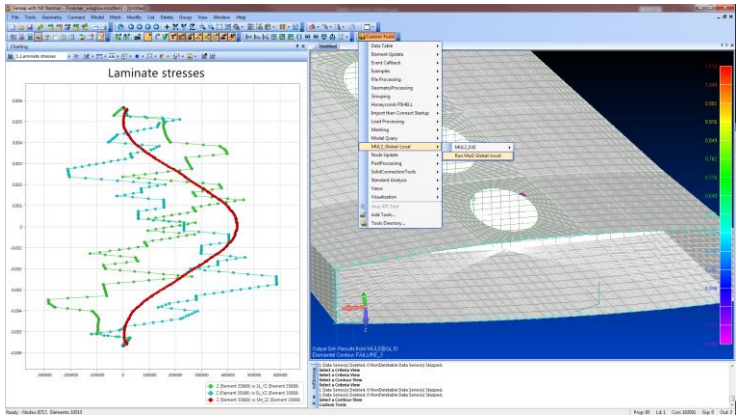

Criteria	Shell Nastran Centroid	Mul2@GL Centroid	Mul2@GL Free Edge
Hoffman	0.307	0.307	0.510
LaRC5 Fiber Tension		0.208	0.206
LaRC5 Fiber Kinking		0.079	0.542
LaRC5 Matrix Failure		0.029	0.657

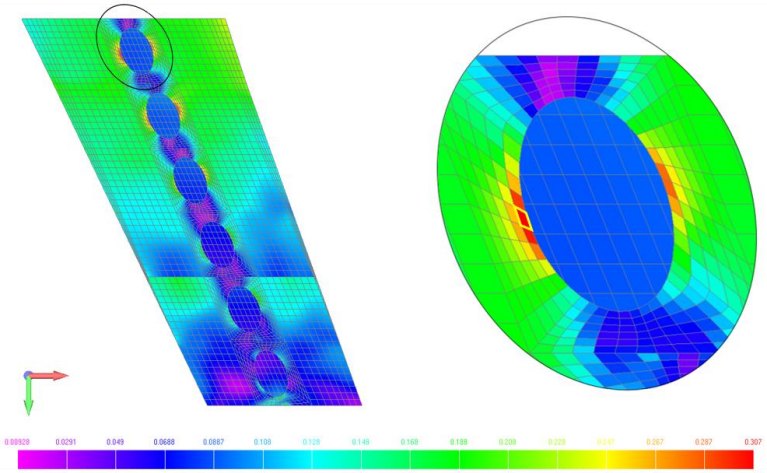

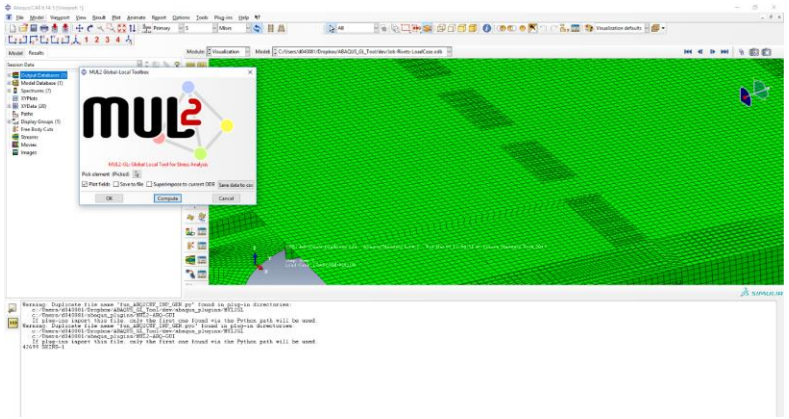

- **Global**: commercial **QUAD4**
- **Local: CUF LW**
- Centroid: center of the element on the edge
- **Dramatic increase of stress and failure indexes** at the free-edge

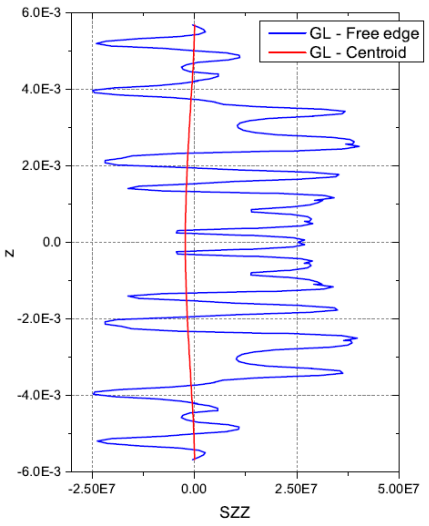

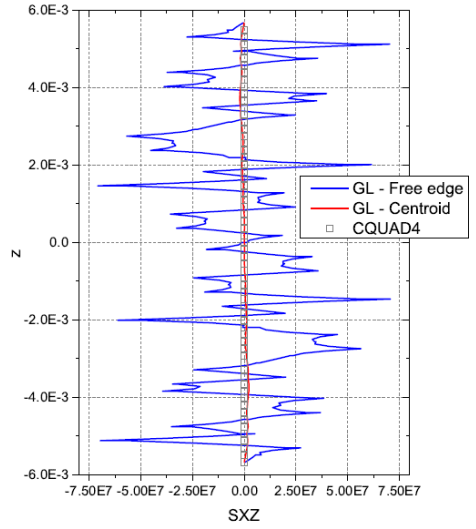

Carrera, E. et al. (2021), MECHANICS OF ADVANCED MATERIALS AND STRUCTURES, Vol. 28, pp. 1121-1127

Carrera, E. et al. (In Press), MECHANICS OF ADVANCED MATERIALS AND STRUCTURES, doi: doi.org/10.1080/15376494.2019.1676938

PART I Wrap-Up 1/2

- Feature: zig-zag displacements along the thickness

  Guideline: The computationally **cheapest** option is the **ESL model with zig-zag functions**. Mixed models, both ESL and LW, provide such capabilities as well as 3D

- Feature: interlaminar continuity of transverse shear and normal stress

  Guideline: **Mixed** ESL and LW **models** are the only models providing this capability. Otherwise, increasing the expansion order can improve the interface stresses, although the continuity is not guaranteed. Similarly, the use of **refined 3D meshes (5+ elements per layer)** can reach similar results

- Feature: Accurate description of transverse normal stress

  Guideline: **LW models** or 3D are essential to obtain **accurate distributions of** σ_{zz}. As stated above, only mixed models can guarantee the interface continuity of this stress component

- Feature: Accurate transverse stress without integration of equilibrium equations

  Guideline: The use of **LW is fundamental** to obtain this capability. Mixed models provide the best accuracy but increasing the order of LW models without mixed features can improve the results significantly

PART I Wrap-Up 2/2

- Minimization of the number of degrees of freedom

  Guideline: **3D** is the most expensive option due to the **aspect ratio constraints** in which the **thickness of each ply** plays a decisive role. **2D or 1D LW models are less costly** but are still dependent on the number of layers. **ESL is the cheapest solution** as the number of variables is independent of the number of layers. As a **general guideline** based on a trade-off between accuracy and efficiency, **a third-order ESL mixed model with zig-zag functions** can be a **robust option** unless **severe local effects** are present as they **require LW capabilities**

PART II – Failure and Multiscale Analyses

FAILURE ONSET AND PROGRESSION

Failure Onset

- Failure mechanisms in composite structures are **complex phenomena** and **dependent** not only **on** the constituent **material properties**, but also **geometric features**, such as the **ply stacking sequence** and **fiber orientation**
- The **first step** in the analysis is the **determination of the failure onset**; that is, the **point-wise location** and the **load value**
- The typical strategy employs a **linear analysis** and **failure criteria** indicating the probability of **failure point-wise** and based on **strain and stress states**
- Failure criteria provide **failure indices**; values **greater than or equal to unity** indicate the **failure onset**
- One of the factors influencing the **accuracy of failure indexes** is the **quality of the strain or stress field** used in the analysis
- A **3D stress field** may be required to **accurately predict** the behavior of composite laminates

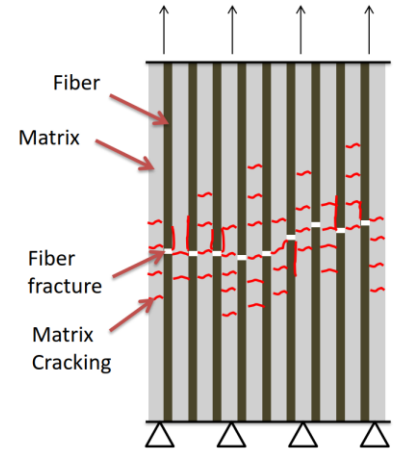

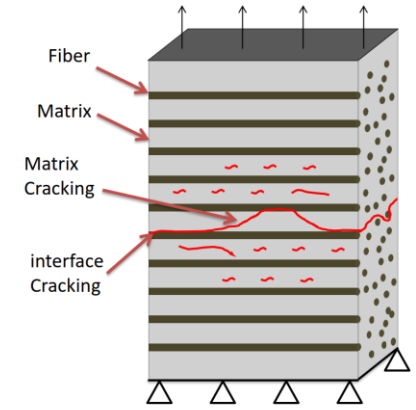

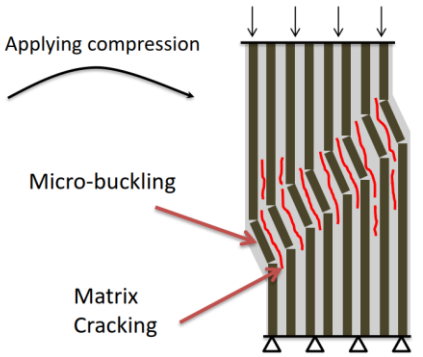

de Miguel A.G. et al. (2018) Composite Science and Technology, 167, pp 174-189; S.W. Tsai and H.T. Hahn, Winter annual Meeting of ASME, 1975, pp. 73–96; J.N. Reddy and A.K. Pandey, Comput. Struct. 25 (3) (1987) 371–393.; Y.S.N. Reddy and J.N. Reddy, Compos. Sci. Technol. 44 (3) (1992) 227–255; Z. Hashin, J. Appl. Mech. 47 (2) (1980) 329–334

Failure Indexes

- Over the year, **many indexes have been proposed**, e.g., Puck , Hashin, LaRC03-05, etc.
- The **aim** of this webinar is not to discuss pro and cons of indexes, but **analyze the influence of structural modeling on the failure onset**
- The next examples has the **Hashin 3D** failure criteria [1] for the prediction of **ply failure** and the **mixed mode quadratic criteria** to determine the onset of **delamination** [2]

Fiber	**Matrix**	**Delamination**
T: $\left(\frac{\sigma_{11}}{X_T}\right)^2 + \frac{\sigma_{12}^2+\sigma_{13}^2}{S_{12}^2} \geq 1$	T: $\frac{(\sigma_{22}+\sigma_{33})^2}{Y_T^2} + \frac{\sigma_{23}^2-\sigma_{22}\sigma_{33}}{S_{23}^2} + \frac{\sigma_{12}^2+\sigma_{13}^2}{S_{12}^2} \geq 1$	$\left(\frac{\langle\sigma_{33}\rangle}{Z_T}\right)^2 + \left(\frac{\sigma_{23}}{S_{23}}\right)^2 + \left(\frac{\sigma_{13}}{S_{13}}\right)^2 \geq 1$
C: $\left(\frac{\sigma_{11}}{X_C}\right)^2 \geq 1$	C: $\left[\left(\frac{Y_C}{2S_{23}}\right)^2 - 1\right]\left(\frac{\sigma_{22}+\sigma_{33}}{Y_C}\right) + \frac{(\sigma_{22}+\sigma_{33})^2}{4S_{23}^2} + \frac{\sigma_{23}^2-\sigma_{22}\sigma_{33}}{S_{23}^2} + + \frac{\sigma_{12}^2+\sigma_{13}^2}{S_{12}^2} \geq 1$	
T: Tension; C: Compression; X, Y: Material Strengths along the fiber and transverse directions; S: Shear material strengths; Z: Interlaminar normal strength		

[1] Z. Hashin, J. Appl. Mech. 47 (2) (1980) 329–334; [2] J.C. Brewer, P.A. Lagace, J. Compos. Mater. 22 (12) (1988) 1141–1155

Virtual Tensile Test 1/4

- Lamination: $[45\ -45\ 90\ 0]_s$
- **Failure indexes** from various models are compared
- **In-plane stress** components **coincide**
- **Differences** due to **transverse stress**

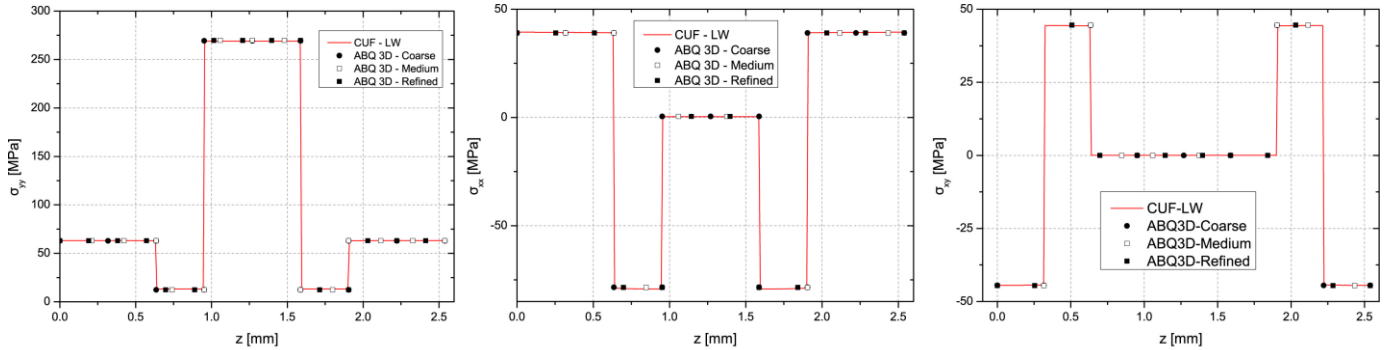

(a) σ_{yy} (b) σ_{xx} (c) σ_{xy}

Model	Delamination	Matrix-T	Fiber-T	Fiber-T*
Load [N]	14288	11938	27178	34417
CUF-LW	1.00	1.00	1.00	1.00
ABAQUS – Coarse	0.28	0.40	0.70	0.94
ABAQUS – Medium	0.31	0.45	0.71	1.05
ABAQUS - Refined	0.60	0.73	0.82	1.07

*Modified Hashin 3D criteria with only in-plane components

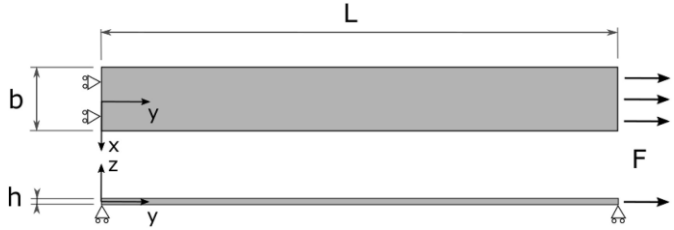

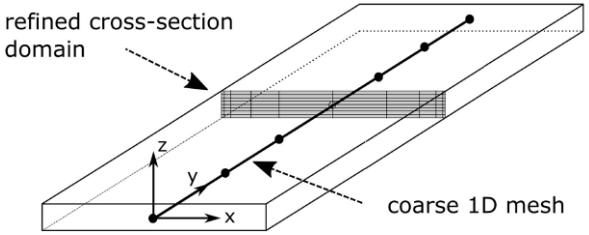

Model	DOF	Time (s)
CUF – LW (4 elements/ply)	**77,805**	**82**
3D FEM – Coarse (1 element/ply)	**168,237**	**27**
3D FEM – Medium (3 elements/ply)	**467,325**	**261**
3D FEM – Refined (5 elements/ply)	**3,501,933**	**3526**

de Miguel A.G. et al. (2018) Composite Science and Technology, 167, pp 174-189

Virtual Tensile Test 2/4

Failure **onset** along **free-edges**

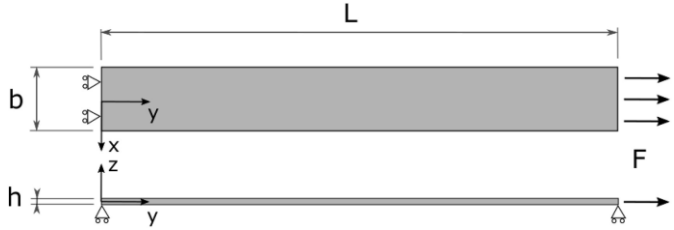

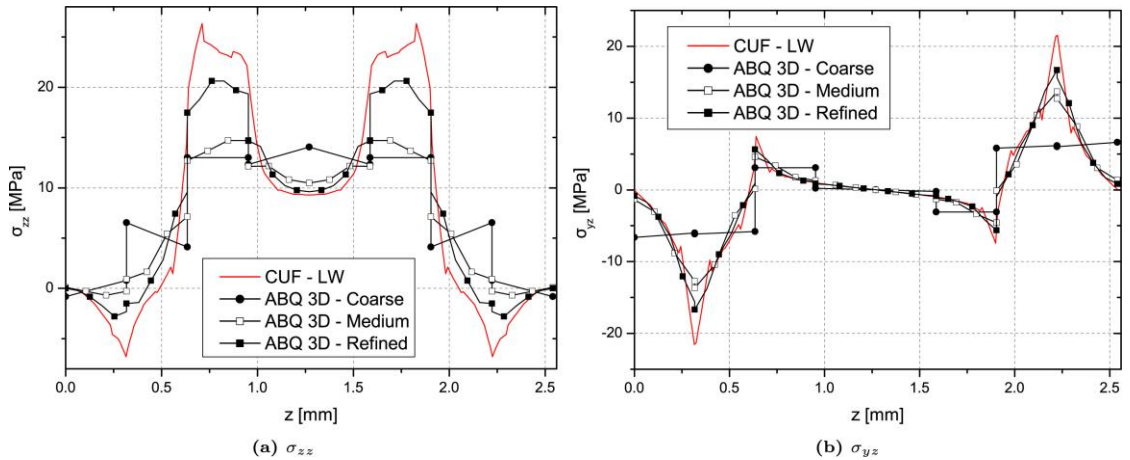

(a) σ_{zz} (b) σ_{yz}

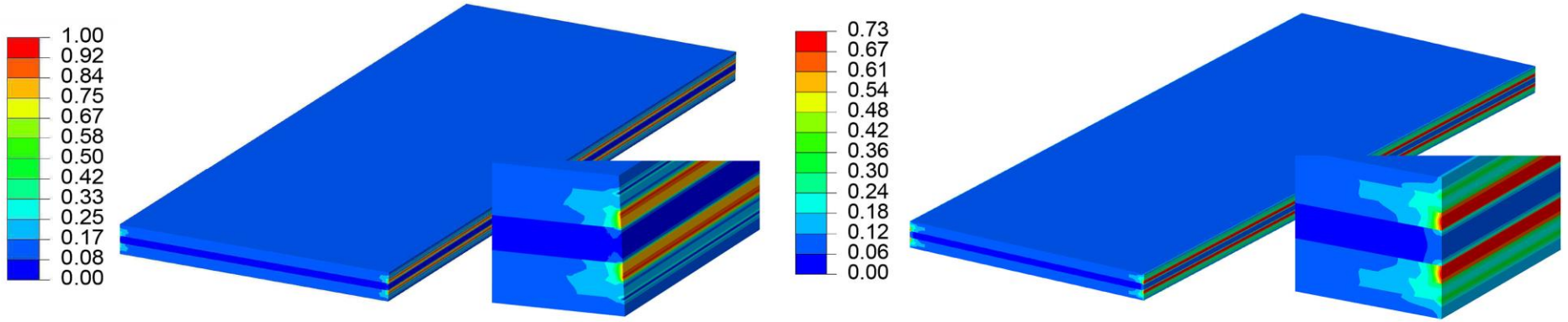

(a) CUF-LW **(b)** ABQ3D - refined

de Miguel A.G. et al. (2018) Composite Science and Technology, 167, pp 174-189

Virtual Tensile Test 3/4

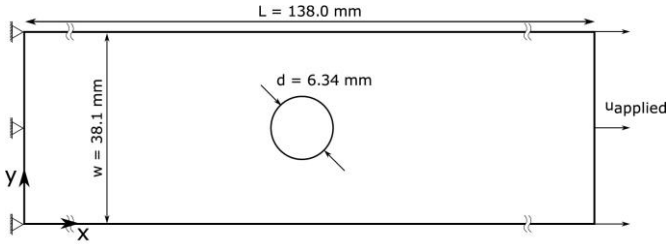

- Lamination: $[45\ -45\ 90\ 0]_s$
- CUF: 53346 DOF, ABAQUS (4 linear solid per layer): 1306977
- Matrix Tension FI:

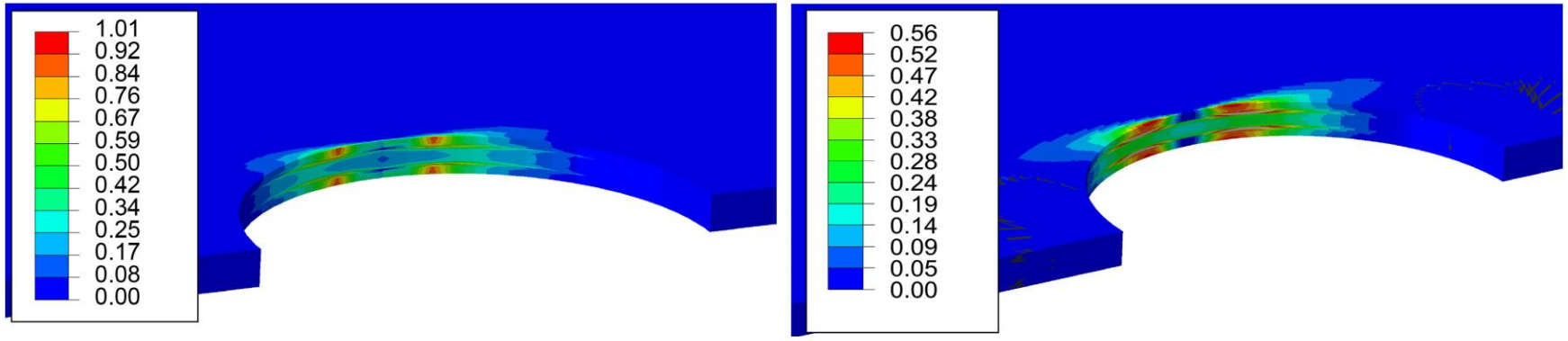

(a) CUF-LW2 (53,346 DOF)

(b) ABQ3D-4L (1,306,977 DOF)

de Miguel A.G. et al. (2018) Composite Science and Technology, 167, pp 174-189

Virtual Tensile Test 4/4

- Laminations: skin: $[45\backslash 90\backslash -45\backslash 0]_s$; stringer: $[-45\backslash 0\backslash 45\backslash 0\backslash 45\backslash 0\backslash -45]$
- Refined models: **CUF: 277326 DOF**, **ABAQUS** (2 linear solid per layer): **4560150**

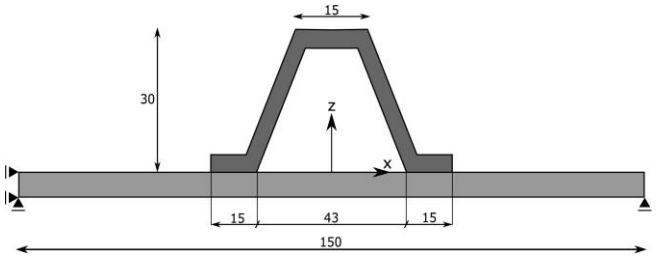

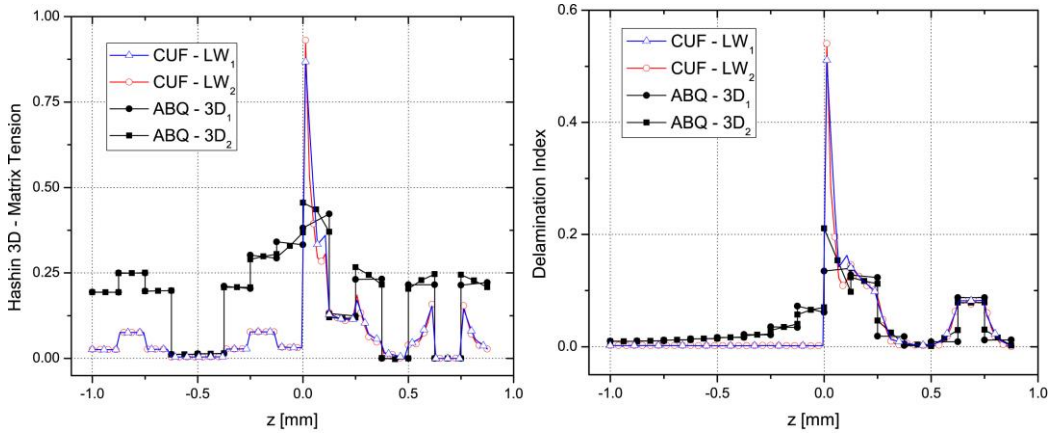

(a) Hashin 3D - Matrix Tension (b) Delamination Inde

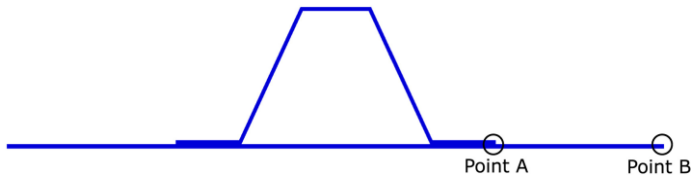

Model	Delamination	Matrix-T	Fiber-T
	Free-Edge Stringer		
CUF-LW	0.54	0.93	0.19
ABAQUS	0.21	0.44	0.18
	Free-Edge Skin		
CUF-LW	0.24	1.01	0.76
ABAQUS	0.19	0.68	0.21

de Miguel A.G. et al. (2018) Composite Science and Technology, 167, pp 174-189

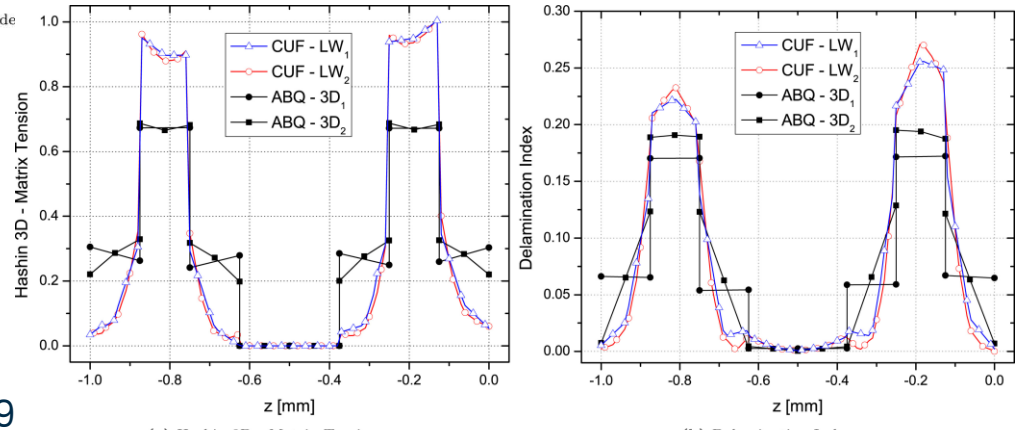

(a) Hashin 3D - Matrix Tension (b) Delamination Index

Damage Progression

- After the onset of failure, **material properties are degraded** and there is the **progressive extension** of the **damaged area**
- Basic example: **intralaminar damage under tension**
  1. Matrix damage initiation in the 90° layer
  2. Fiber damage initiation in the 0° layer
  3. The fibers of the $\pm 45^{\circ}$ layers start to degrade
  4. The fiber damage in the 0° layer saturates
  5. Damage is completely saturated, no more load-carrying capacity
- As the loading, e.g., **compression**, or the **stacking sequence changes**, the progression of damage can change. Also, this example does not include **delamination**
- The area under the $\sigma - \epsilon$ curve is the **fracture energy release rate density**, g_f

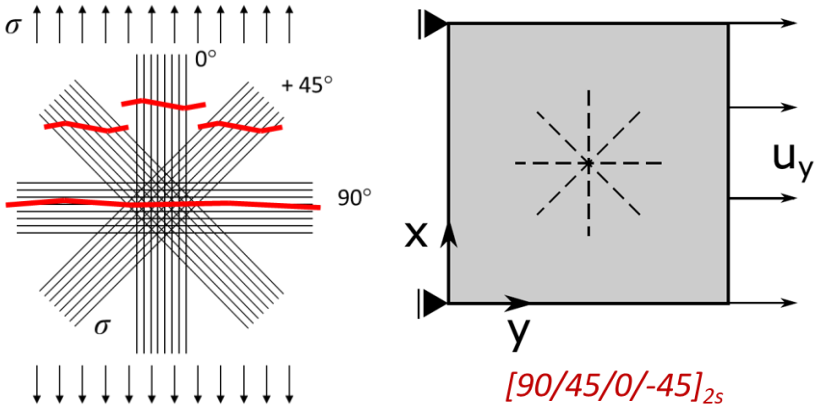

$[90/45/0/-45]_{2s}$

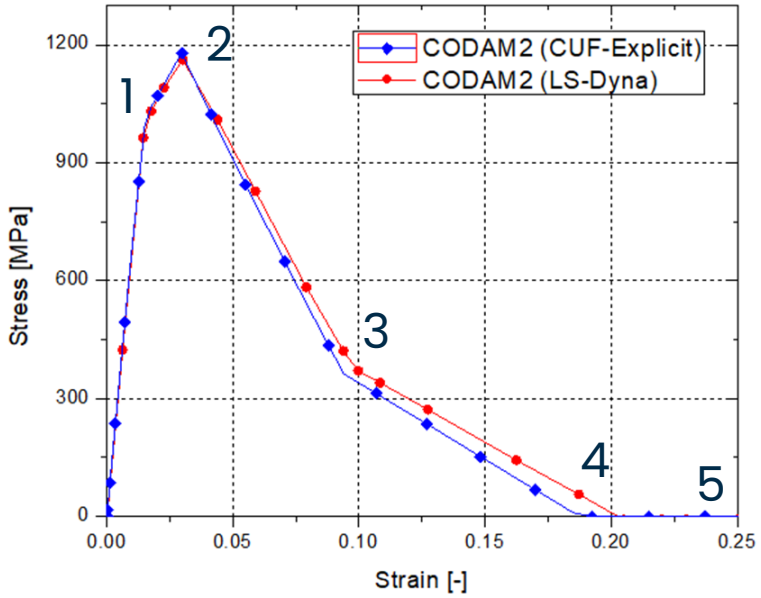

Forghani, A. et al. (2013), Journal of Composite Materials, 47(20-21), 2553-2573

Nagaraj, M.H. et al. (2020), COMPOSITES. PART B, ENGINEERING, Vol. 190

Damage Progression: Modeling Strategies

Approaches:

- **Discrete** damage modelling (xFEM, phase field, floating node etc.)
- **Continuum** damage modelling – smeared approach
- **Combined** approach – Continuum damage (intralaminar) + discrete damage (interlaminar)

Challenges:

- **Computational cost** – analysis time and memory required
- Trade-off between cost and **fidelity**
- **Scalability** – aspect ratio constraints of finite elements

Bouvet, C. et al. (2009), International Journal of Solids and Structures, 46(14-15), 2809-2821.

Kim, E. H. et al. (2013), Composite Structures, 95, 123-134.

Lopes, C. S. et al. (2009), Composites Science and Technology, 69(7-8), 937-947.

Intralaminar Continuum Damage

- COmposite DAMage model (**CODAM2**) developed at the University of British Columbia [1]
- Stress-based failure initiation criteria (**Hashin**)
- **Crack-band** approach [2]: **smearing** the gradual effect of **micro-cracking** over a band of material with known dimension. The **scaling of fracture energy** is necessary to **avoid mesh-dependency and** ensure **total energy release** upon complete failure equal to **fracture toughness**
- **Damage variables** used to **reduce the stiffness matrix**
  1. The damage variable is a function of the strain state, $\mathrm{d} = \mathrm{f}(\epsilon)$
  2. The material properties are degraded according to the damage variable, $\mathrm{C} = \mathrm{f}(\mathrm{d})$
  3. A nonlinear analysis is required
- Solved using an **explicit time integration scheme**
- Available in **LS-DYNA** and in **MUL2**

$$\mathbf{C}^{dam} = \frac{1}{\Delta}\begin{bmatrix} (1-R_2\nu_{23}\nu_{32})R_1E_1 & (\nu_{21}+\nu_{23}\nu_{31})R_1R_2E_1 & (\nu_{31}+R_2\nu_{21}\nu_{32})R_1E_1 & 0 & 0 & 0 \\ & (1-R_1\nu_{31}\nu_{13})R_2E_2 & (\nu_{32}+R_1\nu_{31}\nu_{12})R_2E_2 & 0 & 0 & 0 \\ & & (1-R_1R_2\nu_{21}\nu_{12})E_3 & 0 & 0 & 0 \\ & & & \Delta R_1R_2G_{12} & 0 & 0 \\ & sym. & & & \Delta G_{23} & 0 \\ & & & & & \Delta G_{13} \end{bmatrix}$$

[1] Forghani, A. et al. (2013), Journal of Composite Materials, 47(20-21), 2553-2573; [2] Bazant, Z. and Oh, B. H. (1983), Materials and Structures, 16:155–177;

Implicit vs Explicit

Explicit *nonlinear analysis in CUF*

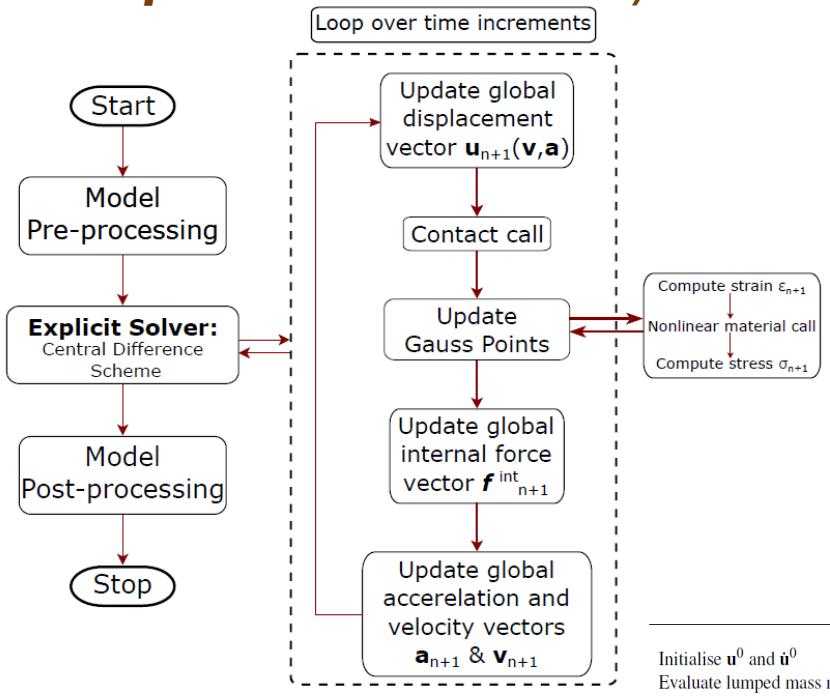

Central difference scheme algorithm

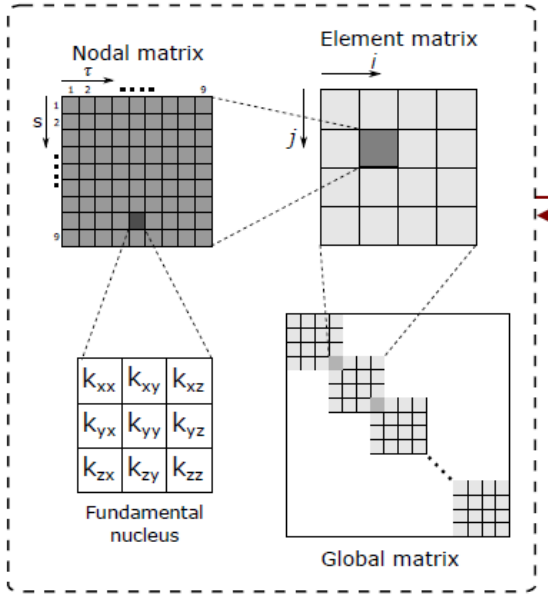

Stiffness matrix assembly in CUF

Initialise $\mathbf{u}^0$ and $\dot{\mathbf{u}}^0$
Evaluate lumped mass matrix $\mathbf{M}$
Compute initial mid-interval velocity: $\dot{\mathbf{u}}^{\frac{1}{2}\Delta t} = \dot{\mathbf{u}}^0 + \frac{1}{2}\Delta t\ \ddot{\mathbf{u}}^0$

For each time increment:

1. Evaluate new displacements: $\mathbf{u}^{t+\Delta t} = \mathbf{u}^t + \Delta t\ \dot{\mathbf{u}}^{t+\frac{1}{2}\Delta t}$
2. Compute displacement increment: $\Delta\mathbf{u} = \mathbf{u}^{t+\Delta t} - \mathbf{u}^t$
3. At each integration point:
→ Compute updated strains: $\boldsymbol{\varepsilon}^{t+1} = \boldsymbol{\varepsilon}^t + \mathbf{B}\Delta\mathbf{u}$
→ Compute updated stress: $\boldsymbol{\sigma}^{t+1} = \mathbf{C}^{sec}\boldsymbol{\varepsilon}^{t+1}$
4. Compute internal force vector: $\mathbf{F}^{t+\Delta t}_{int} = \int_V \mathbf{B}^T\boldsymbol{\sigma}^{t+\Delta t}\ dV$
5. Compute new accelerations: $\ddot{\mathbf{u}}^{t+\Delta t} = \mathbf{M}^{-1}\{\mathbf{F}^{t+\Delta t}_{ext} - \mathbf{F}^{t+\Delta t}_{int}\}$
6. Compute new mid-interval velocities: $\dot{\mathbf{u}}^{t+\frac{3}{2}\Delta t} = \dot{\mathbf{u}}^{t+\frac{1}{2}\Delta t} + \Delta t\ \ddot{\mathbf{u}}^{t+\Delta t}$

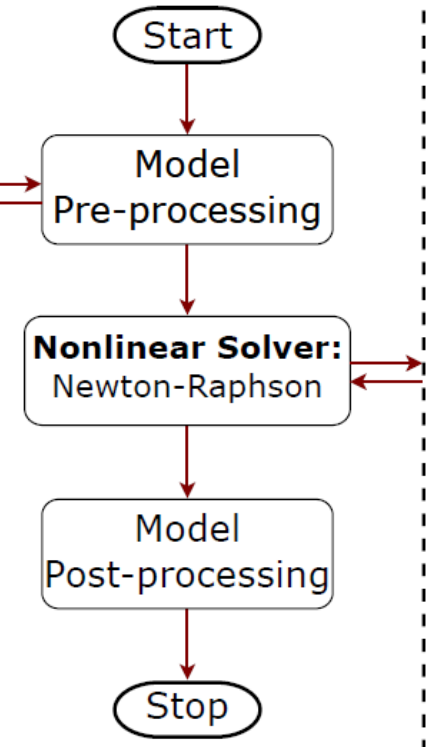

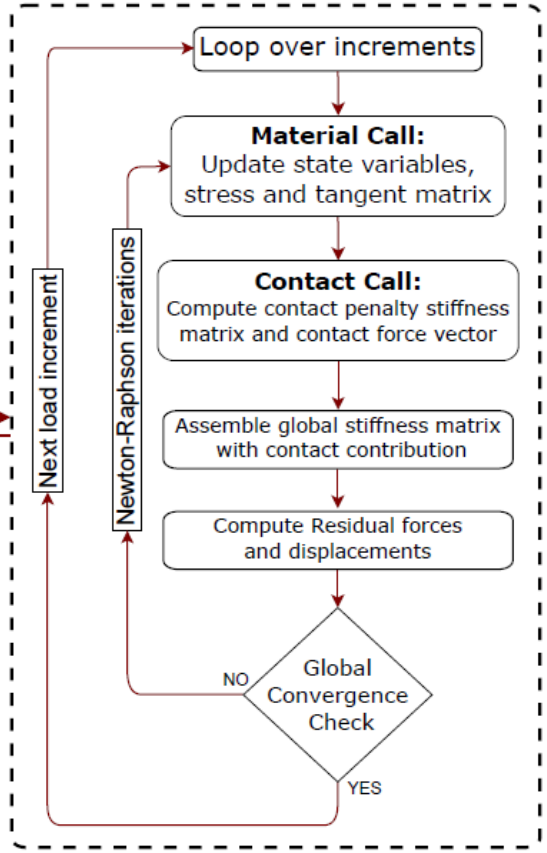

Implicit *nonlinear analysis in CUF*

Kaleel I., PhD Thesis, http://hdl.handle.net/11583/2729362; Nagaraj M.H., PhD Thesis, http://hdl.handle.net/11583/2872328

Interlaminar Damage: Delamination

- Delamination is one of the **most predominant failure** in laminated composite structure
- Typical causes: run-way debris **impact**, tool-drop during maintenance, **high interlaminar stresses** and geometric discontinuities, e.g., **free-edge**
- Modeling strategies: **cohesive** zone models[1, 2], **virtual crack closure** technique [3]
- Precursor to **precise delamination** analysis: **accurate transverse fields**
- Challenges:

1. Accurate stress resolution dictates the need of **computationally intensive FE models**
2. Appropriate **constitutive modeling** of the cohesive surface
3. Extremely **refined mesh** near the cohesive zone
4. Convergence issues in **tracing the equilibrium path**
5. Scalability to **large-scale structures** is still computationally **infeasible**

[1] Dugdale, D. (1960), Journal of the Mechanics and Physics of Solids, 8(2):100 – 104

[2] Barenblatt, G. I. (1962). Volume 7 of Advances in Applied Mechanics, pages 55 – 129

[3] Rybicki, E. and Kanninen, M. (1977), Engineering Fracture Mechanics, 9(4):931 – 938.

Cohesive Elements

- Basic idea: existence of a **narrow band of vanishing thickness** ahead of a **crack tip**
- The narrow band has **two virtual surfaces across the crack tip** with presence of **resistive cohesive forces**
- Cohesive **constitutive law** relates the **cohesive traction** to the **displacement jump across the interface surface**
- The area under the **traction-separation curve** corresponds to **fracture toughness**
- Failure **onset**: $\left(\frac{\langle\sigma_{33}\rangle}{Z_T}\right)^2 + \left(\frac{\sigma_{23}}{S_{23}}\right)^2 + + \left(\frac{\sigma_{13}}{S_{13}}\right)^2 \geq 1$

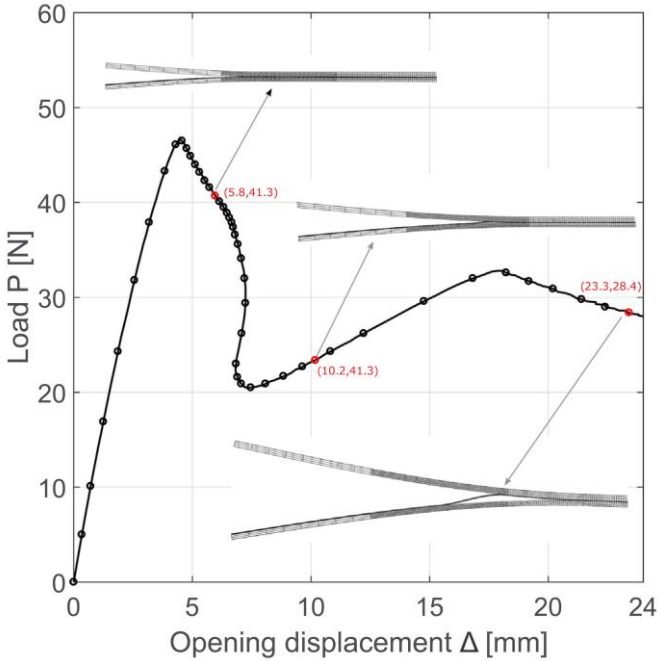

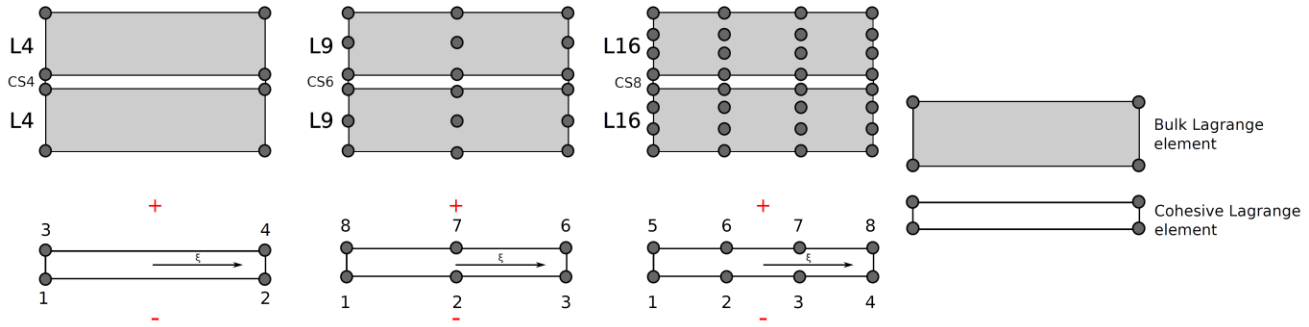

Kaleel I. et al. (2020), Composite Structures, Vol. 235

Example: Low-Velocity Impact 1/2

- In a low-velocity impact event, **all damage mechanisms** can be activated
- Besides the modeling challenges seen above, to model impact the implementation of **contact** algorithms are necessary

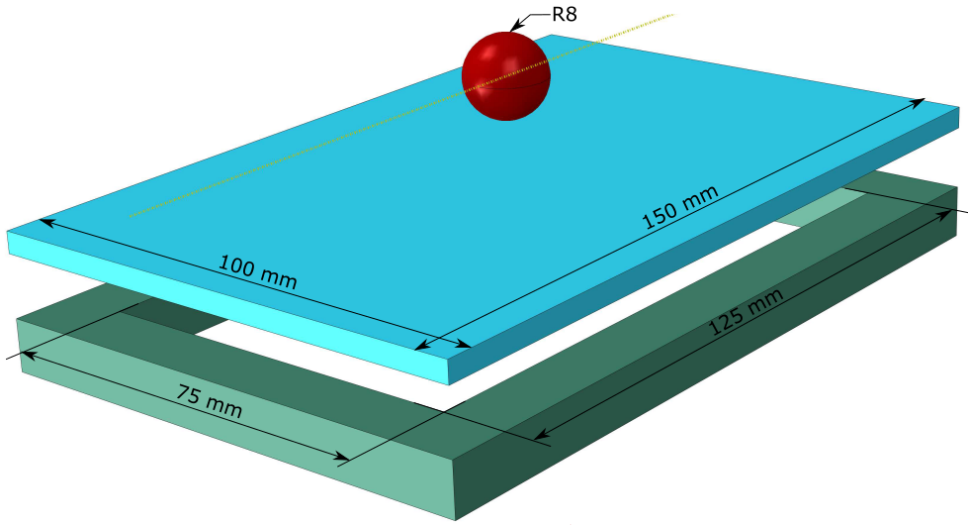

$[0_2/45_2/90_2/-45_2]_2$ T laminate = 4.16 mm
T700/M21 CFRP T ply = 0.26 mm
Quasi-isotropic laminate

Vertical deflection u_z of composite plate

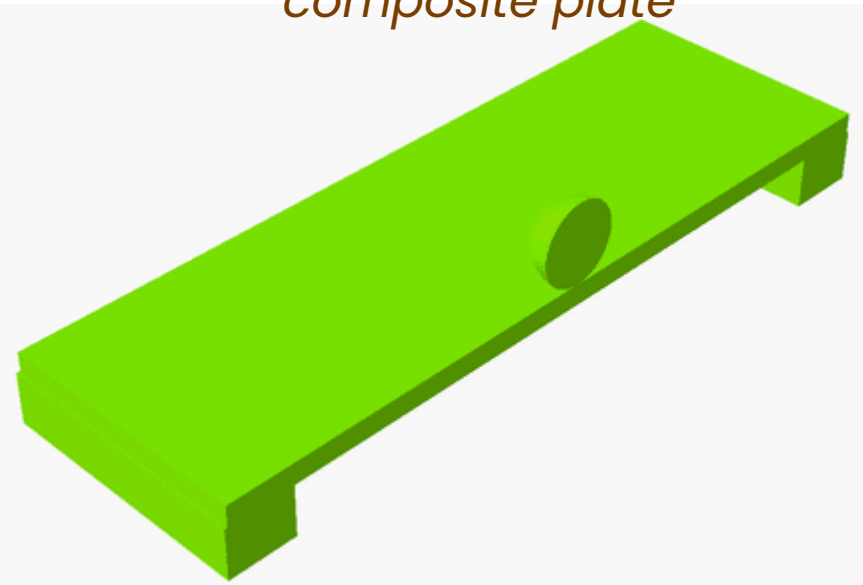

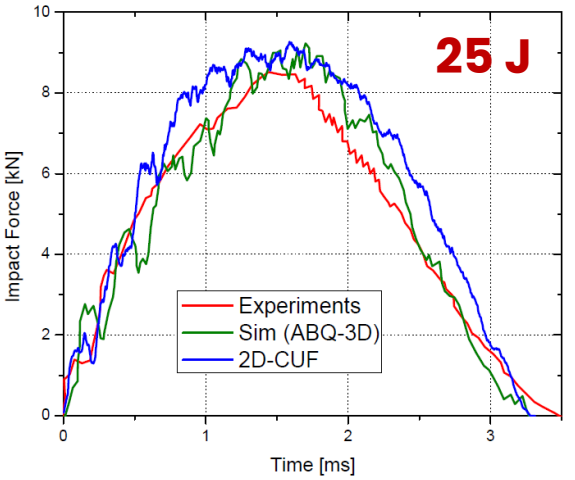

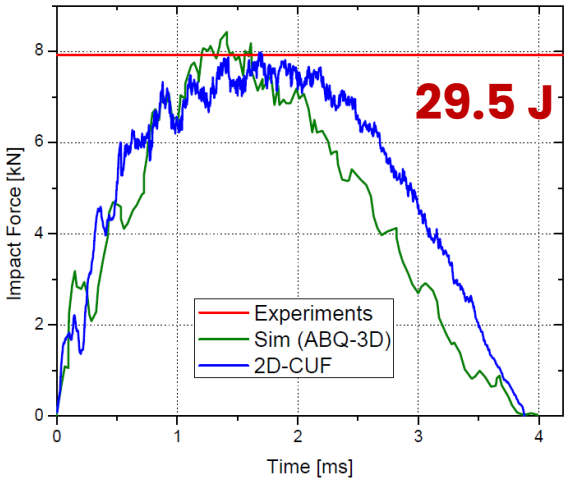

Impact force – time response

Nagaraj, M. H. et al. (2020), INTERNATIONAL JOURNAL OF NON-LINEAR MECHANICS, Vol. 127

Example: Low-Velocity Impact 2/2

Impact-face **Back-face**

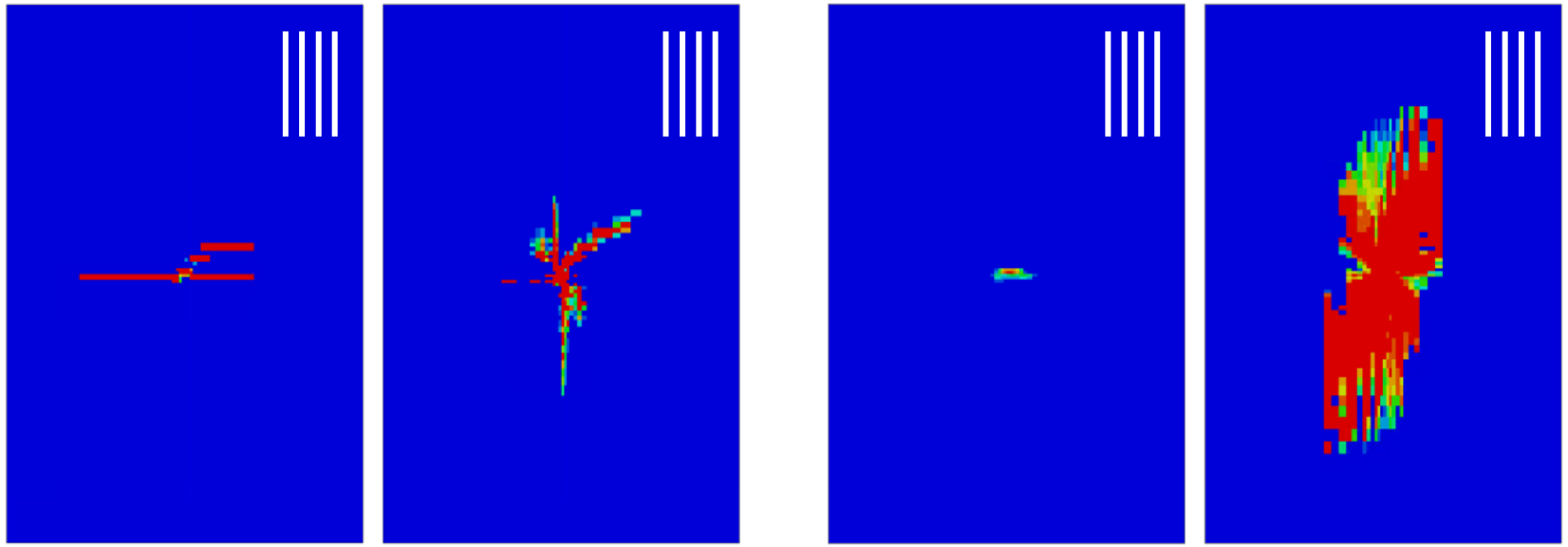

Fibre damage compression | Matrix damage compression | Fibre damage tension | Matrix damage tension

Damage profile of $[0_2/45_2/90_2/-45_2]_2$ quasi-isotropic laminate under 29.5J impact

COMPUTATIONAL COST

Ref ABQ-3D:
~10 hours @ 32 CPUs

2D-CUF (LW):
~4 hours @ 4 CPUs

Nagaraj, M. H. et al. (2020), INTERNATIONAL JOURNAL OF NON-LINEAR MECHANICS, Vol. 127

PART II – Failure and Multiscale Analyses

MICROMECHANICS

Motivations

- The **homogeneous continuum** is assumed to **retain** its bulk material **properties irrespective of the scale**.
- In case of real materials, the **assumption starts to fade at lower scales** as they turn **heterogeneous in nature**
- Hierarchical material systems, such as composites, necessitate micromechanics to **capture lower scales phenomena** for reliable simulations
- Micromechanics captures the **effective behavior of heterogeneous systems** through **homogenization** (up-scaling) and **localization** (down-scaling) for a given representative volume element (**RVE**)
- Micromechanics often **enriches physically nonlinear simulations** such as progressive failure in composites, as they are greatly stimulated by **underlying lower scale features**
- Effectiveness is greatly influenced by **proper constitutive modeling** at lower scales and the ability of these models to generate **accurate local fields** at the constituent level
- The former requires rigorous validation through **in-situ experiments**
- The latter greatly depends on the **mathematical approaches employed**

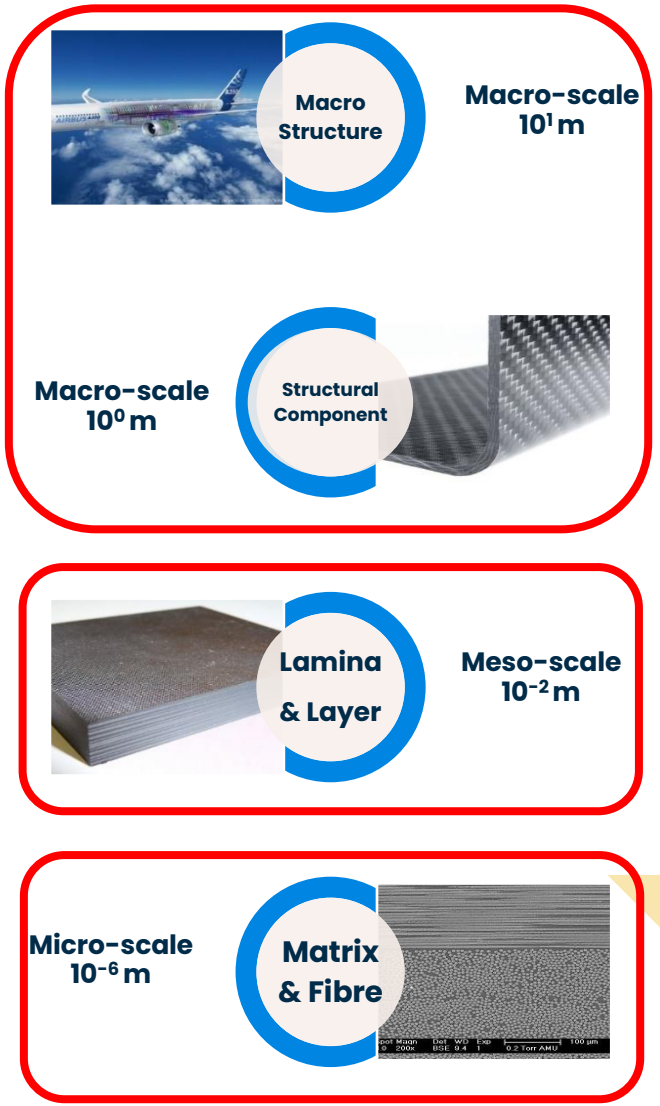

Bednarcyk, B. A. et al. (2010), AIAA Journal, 48(7):1367–1378

Liu, X. et al. (2018), Vision 2040: A roadmap for integrated, multiscale modeling and simulation of materials and systems. NASA Glenn Research Center

Aims and Approaches

- ISSUE: the **direct numerical simulation** of a composite structure accounting for **all scales** concurrently **is not feasible**

AIMS

- RVE: a **volume of the structure** including a representative description of the microscale **architecture of the constituents**, e.g., **fibers, matrix, honeycomb packing, voids, defects**
- Homogenization (up-scaling): provide homogenized material **properties for the upper scales** starting **from the constituent properties**
- Localization or de-homogenization (down-scaling): provide **stress and strain fields at the microscale** for a given **macroscale load**
- The micromechanical formulations intends to **capture the explicit heterogeneous nature of the microstructure** and provide an **effective continuum to the higher-scale** by defining **representative volume elements** (RVE)

STRATEGIES AND CHALLENGES

- **Analytical, semi-analytical** and full numerical methods are available. In MUL2, **fully numerical methods** via FE
- The main **challenge** is to develop a model having **accurate homogenization and de-homogenization** while **keeping the computational cost low** to favor **multiscale and nonlinear analyses**
- The main **novelty in MUL2** is the use of **1D models instead of 3D** leading to **superior de-homogenization and computational cost performances**

Aboudi J., Arnold S., Bednarcyk B. (2021), Practical Micromechanics of Composite Materials, Butterworth-Heinemann

W. Yu, J Mech Mater Struct, 11 (4) (2016), pp. 379-411

RVE's Basic Concepts

- Define the **RVE architecture**; typical choices: one fiber + matrix; multiple fibers + matrix; honeycomb; textiles
- Build an **RVE model**; typical choices: **3D FEM** or, with CUF, **1D Component-Wise** models
- Although in composites the actual **fiber distribution is quite random** across the cross-section, the micromechanical formulation is postulated based on the **assumption of periodicity**. An RVE is the basic unit of the periodic structure. To maintain compatibility of displacements along different faces of RVE, **periodic boundary conditions** are applied
- In a composite, fibers and matrix have **vastly different properties.** All the **RVE are identical** and must have **identical stress and strain fields;** that is, the stress and strain fields are **periodic**
- The periodicity boundary conditions are imposed to displacements of **external faces**

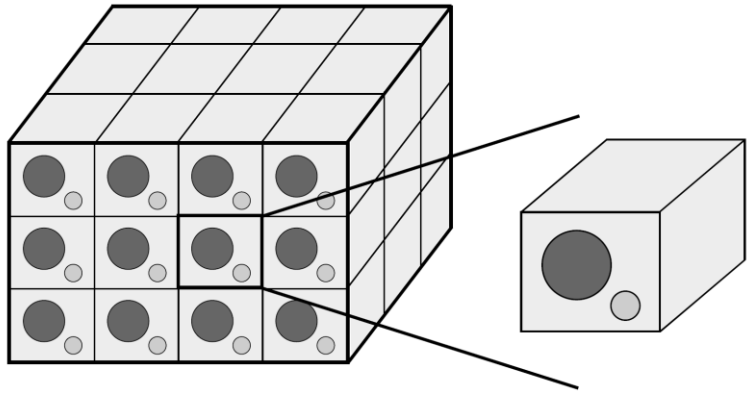

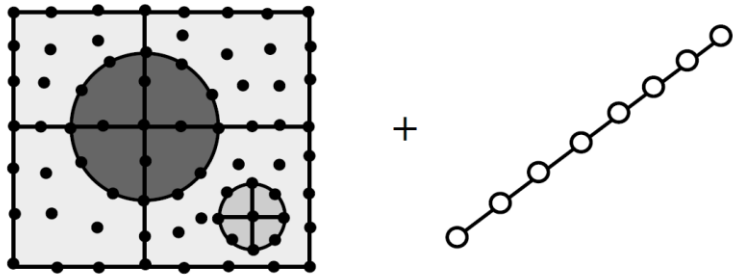

Sun, C. T. and Vaidya, R. S. (1996), Composites Science and Technology, 56(2):171–179

Xia, Z. et al. (2003), International Journal of Solids and Structures, 40(8):1907–1921

Homogenization and Localization

- Homogenization provides **effective properties** based on the **individual constituents** of the RVE; homogenization is achieved through **volume averaging** the **stress and strain** fields: $\bar{\epsilon}_{ij} = \frac{1}{V}\int \epsilon_{ij} dV$, $\bar{\sigma}_{ij} = \frac{1}{V}\int \sigma_{ij} dV$, V is the volume of the RVE, σ_{ij} and ϵ_{ij} are the **local stress** and **local strain** within the individual constituents of the RVE, respectively
- Six individual **unit strains are applied** and the **effective material matrix**, $\bar{\mathbf{C}}$, of the homogenized RVE is populated through $\bar{\boldsymbol{\sigma}} = \bar{\mathbf{C}}\bar{\boldsymbol{\epsilon}}$
- Localization requires the application of $\bar{\boldsymbol{\epsilon}}$ to obtain σ_{ij} and ϵ_{ij}
- Nonlinear **constitutive laws** can be applied. For instance, **plasticity of the matrix** for progressive failure analyses
- Defects, e.g., **voids**, can be included
- The **computational size of the RVE** determines the cost of the analysis
- In a multiscale scenario, **each Gauss point** of the macroscale model **has its own RVE**

Sun, C. T. and Vaidya, R. S. (1996), Composites Science and Technology, 56(2):171–179

Xia, Z. et al. (2003), International Journal of Solids and Structures, 40(8):1907–1921

Examples: Linear Elastic Homogenization

Aim: avoid 3D elements and favor multiscale analyses

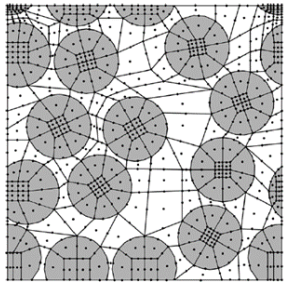

Normal transverse stress

CUF-CW
DOF: 19,080
Runtime: 18s

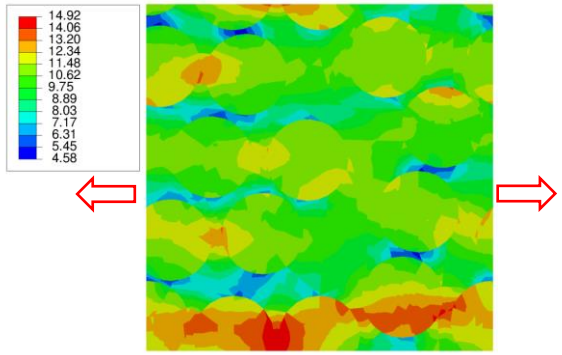

3D FEM
DOF: 91,305
Runtime: 324s

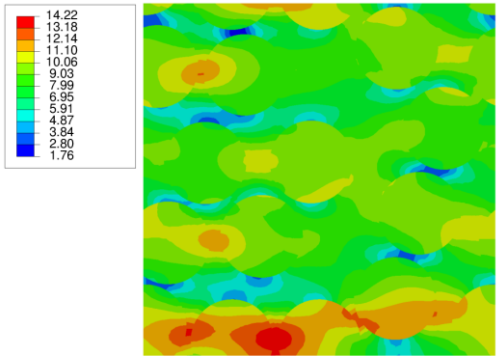

Effective moduli of periodical cellular structure

Architecture of hexagonal honeycomb

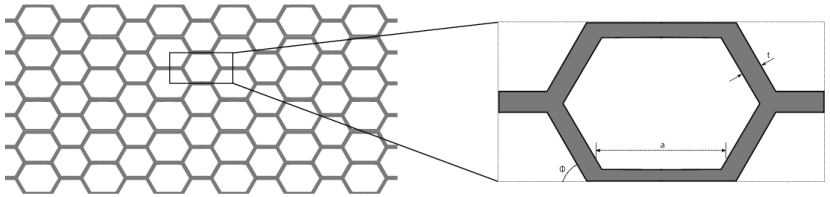

CW discretization of RVE – 18L9

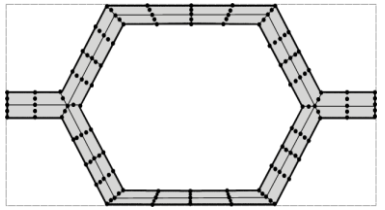

Predicted transverse Young's modulus

CUF-CW	FEM 3D	G-A MMM (Gibson et al.)
0.0504	0.0498	0.0485

3D von-Mises stress contour σ_{vm}

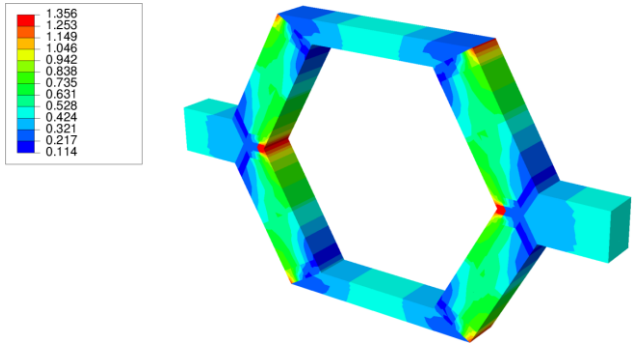

CUF-CW | DOF: 6,993

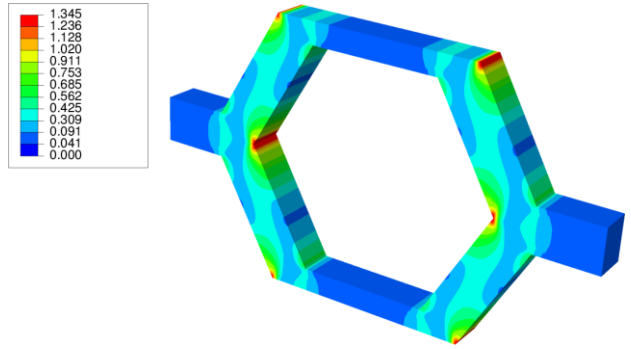

3D FEM | DOF: 79,104

Kaleel I. et. al. "Integration of CUF micromechanics framework into NASMAT for multiscale analysis of fiber-reinforced composites", In: Proceedings of ICMAMS 2019, Nanjing, China, 19-22 October 2019

Examples: Progressive Damage

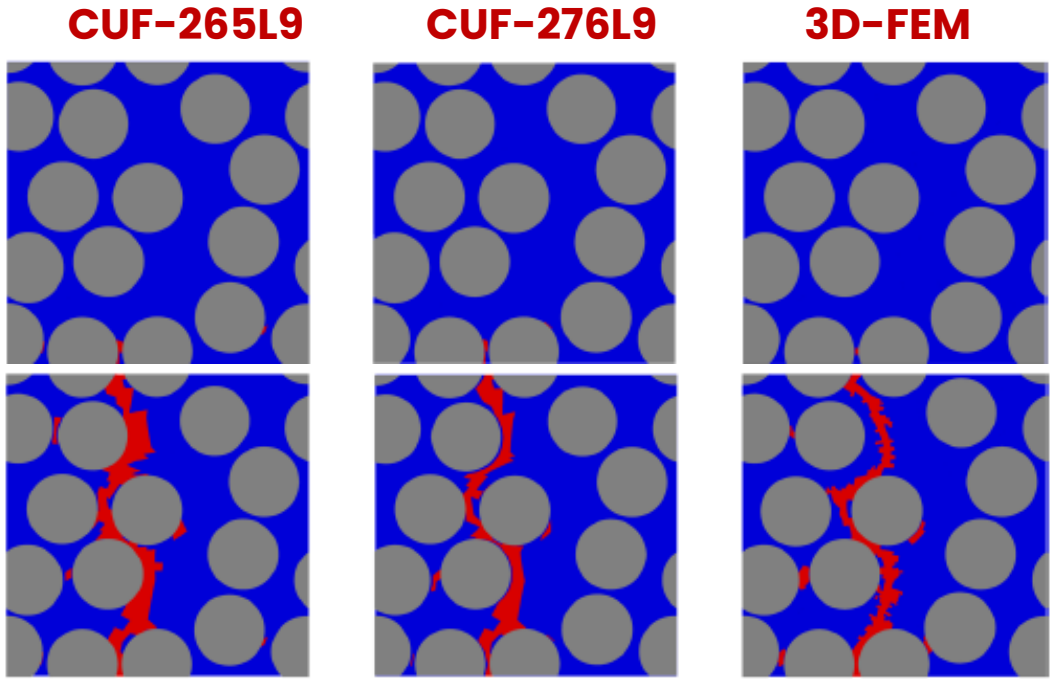

Matrix damage progression under applied transverse strain [1]

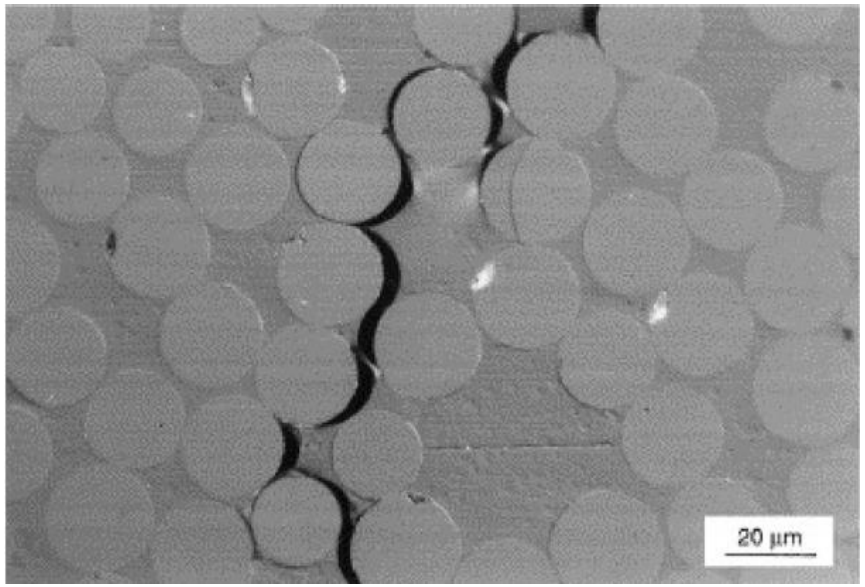

Formation of micro-cracks in static tension tests of cross-ply laminates [2]

Model	DOF	Time (min)
1D	**23711**	**48**
3D	**91305**	**108**

~4x DOF
~2.2x Time

[1] Kaleel I. et al. Journal of Applied Mechanics (2018), 85

[2] Gamstedt, E. K., & Sjögren, B. A. (1999). Composites Science and Technology, 59(2), 167-178

Examples: Voids 1/3

- Randomly distributed voids in matrix
- Void volume fraction given as an input
- Use of distribution functions to randomly select matrix GP
- Material properties of selected GPs modified to exhibit void-like behaviour

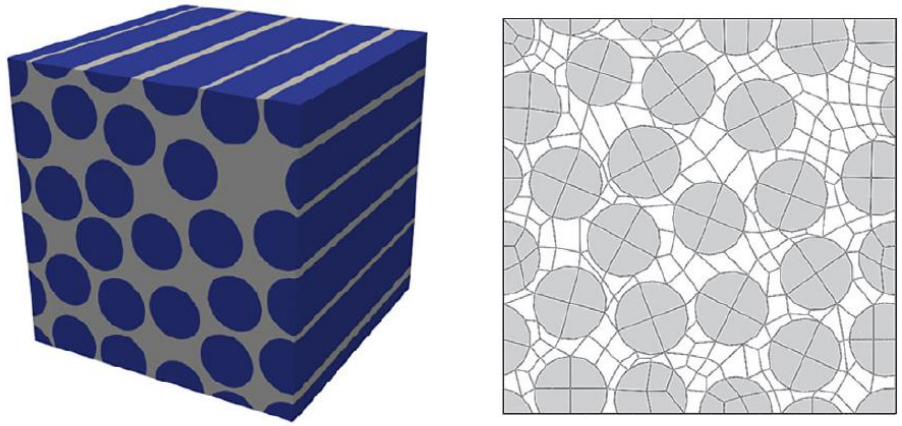

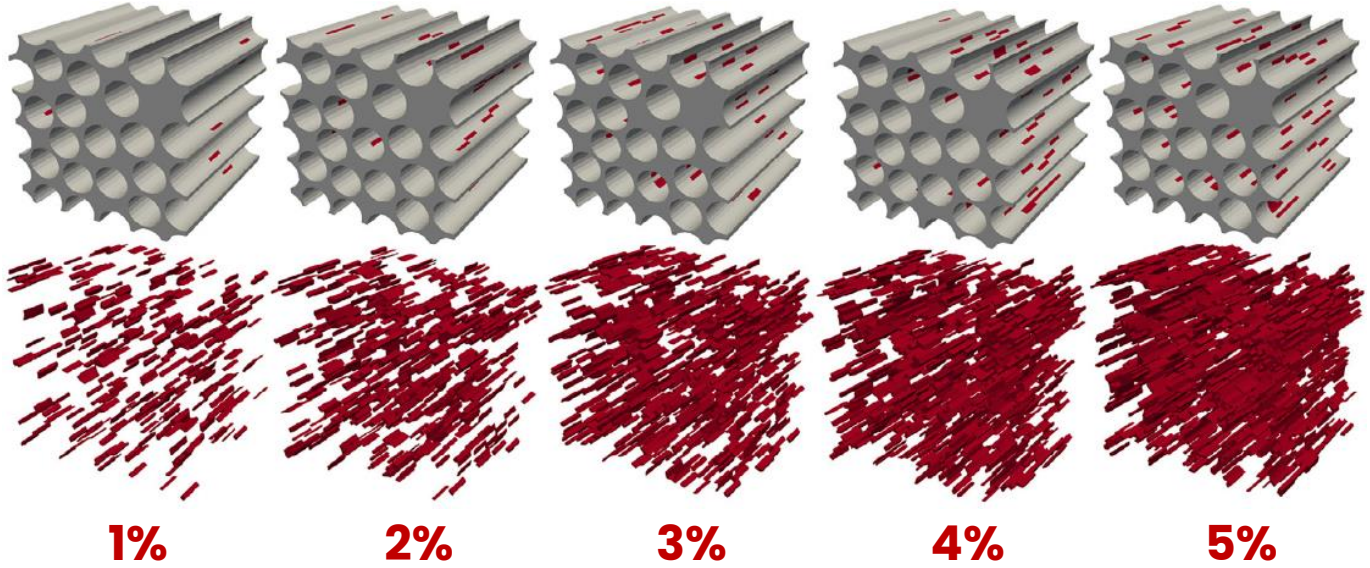

RVE models with increasing void content [1]

Carrera, E. et al. (2020). Composite Structures, 254, 112833

Examples: Voids 2/3

Homogenised Properties

		Void content (%)				
		1	2	3	4	5
$\bar{x}$ (GPa)	E_{11}	135.846	135.809	135.772	135.734	135.697
	E_{22}	9.887	9.818	9.749	9.679	9.609
Mean	E_{33}	9.836	9.766	9.696	9.625	9.555
	G_{12}	5.156	5.127	5.098	5.069	5.040
	G_{13}	4.993	4.964	4.935	4.906	4.878
	G_{23}	3.125	3.103	3.080	3.057	3.034
s (MPa)	E_{11}	0.508	0.680	0.784	0.850	0.963
	E_{22}	1.470	2.174	2.231	2.910	3.108
Std. dev.	E_{33}	1.307	2.036	2.761	2.405	3.127
	G_{12}	1.064	1.673	1.835	1.979	2.064
	G_{13}	0.969	1.304	1.894	1.790	2.165
	G_{23}	0.456	0.580	0.647	0.790	0.868

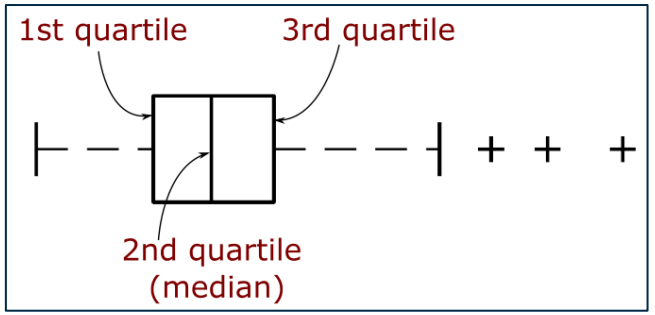

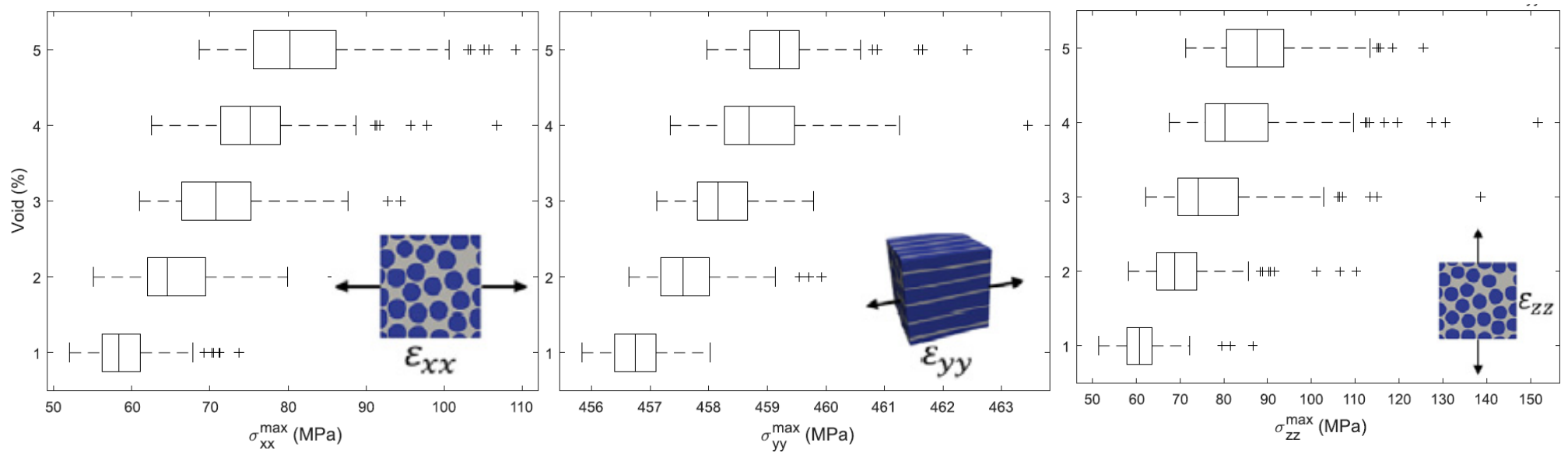

Carrera, E. et al. (2020). Composite Structures, 254, 112833

Maximum local stress components as a function of void content

Examples: Voids 3/3

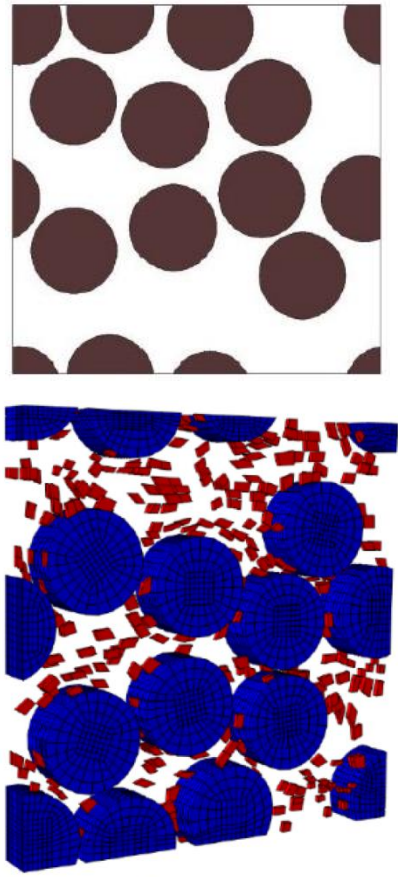

1-D RVE model with 2% randomly distributed voids

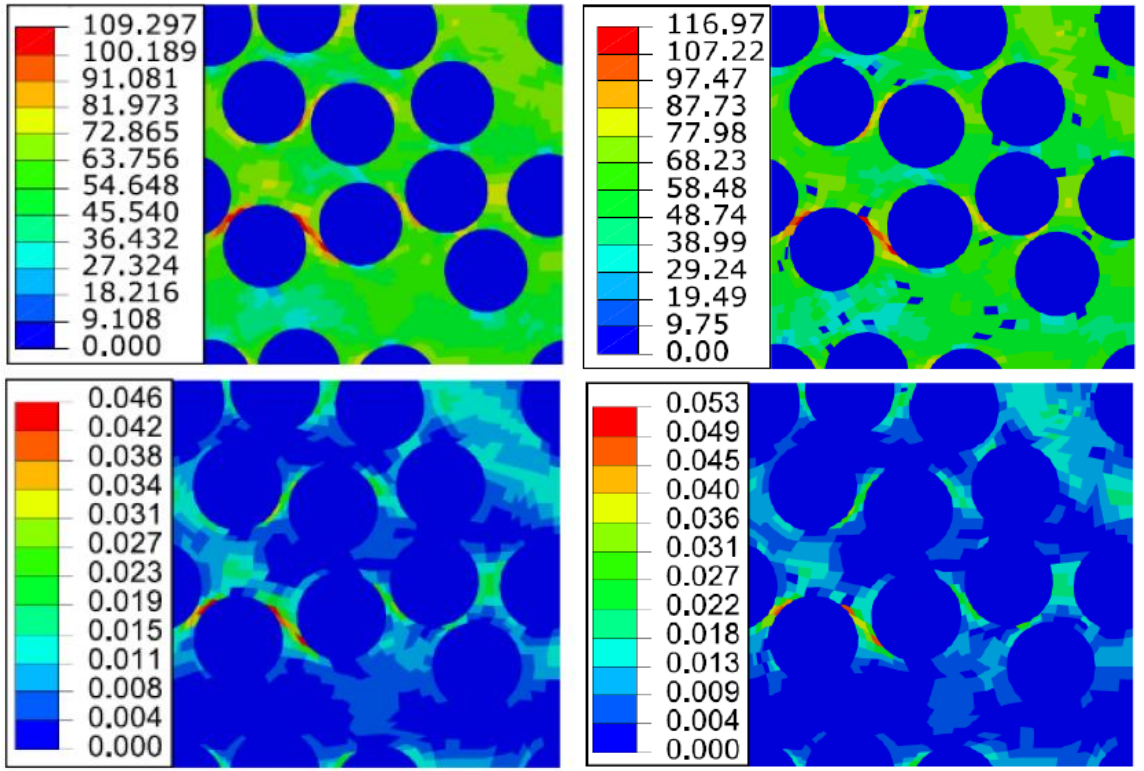

Local von Mises stress (top) and eq. plastic strain (bottom, for applied -22 global strain

PART II – Failure and Multiscale Analyses

MULTISCALE

Motivations

- Understanding the source of physical behavior at **lower scales** and **bridging** the effect accurately to **upper scales** can significantly **boost the fidelity** of such simulations
- Continuum-based constitutive modeling has proven to be well-suited for predicting the overall response of structures, modeling **localized phenomena** such as damage and failure propagation using such approaches remains questionable as such mechanisms are **heavily influenced by the underlying lower-scale features**
- Macroscale constitutive modeling assumes the **material point as a homogeneous** and **heterogeneity** such as inclusions, voids etc. are accounted through **implicit mathematical formulations**.
- Within a multiscale framework, the constitutive response at **a material point is interfaced** with a lower scale with **explicit heterogeneous definitions** through homogenization

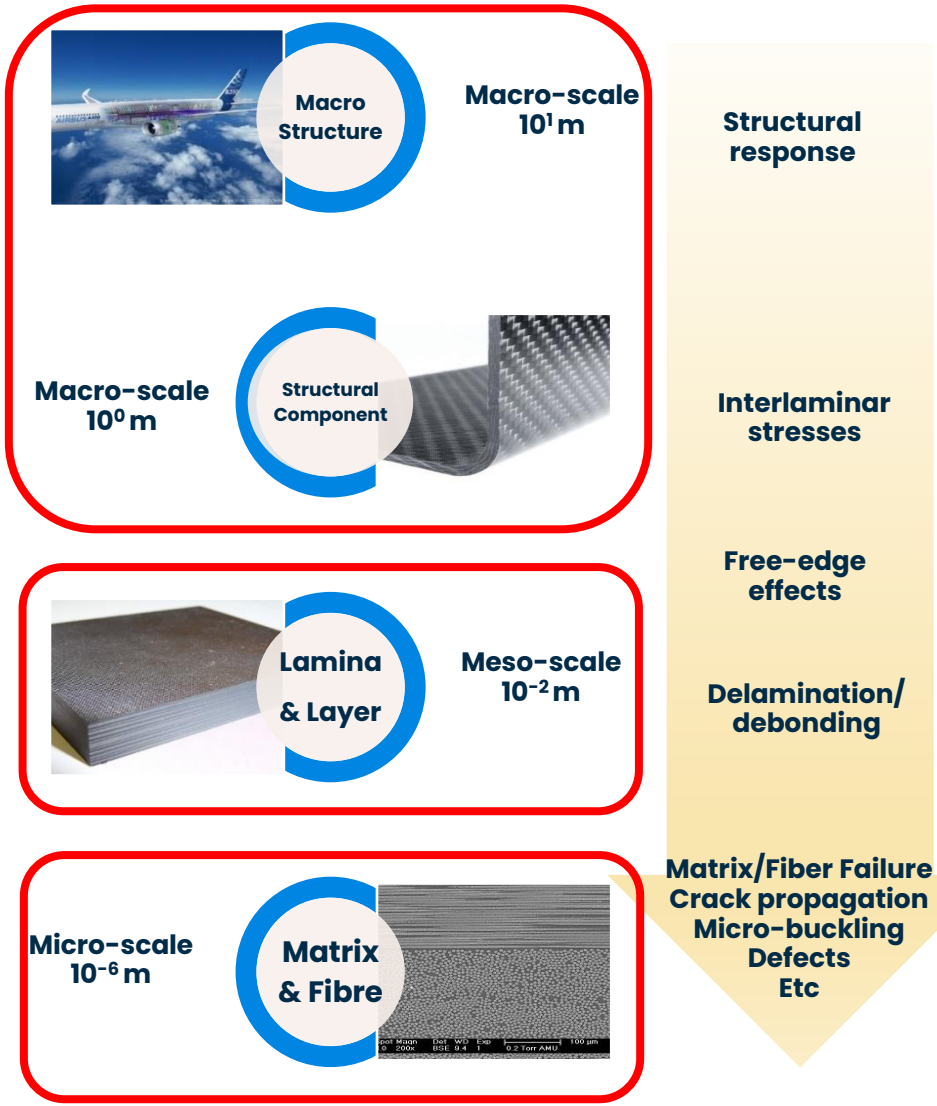

Sullivan, R. W. and Arnold, S. M. (2010). An annotative review of multiscale modeling and its application to scales inherent in the field of ICME. In Models, Databases, and Simulation Tools Needed for the Realization of Integrated Computational Materials Engineering. ASM International.

Approaches

- Hierarchical: based on **one-way coupling** with information passed **either bottom-up** (homogenization) **or top-down** (localization)
- Concurrent: **fully-coupled information interfacing** with bottom-up and top-down occur concurrently with **all scales handled simultaneously** in space and time
- Synergistic: fully coupled, **hierarchical in space, concurrent in time**
- As in micromechanics, there are **analytical, semi-analytical**, and **fully numerical** approaches
- **Most common fully-numerical** approaches are based on finite element models applied at both scales, often referred to as **FE² method**

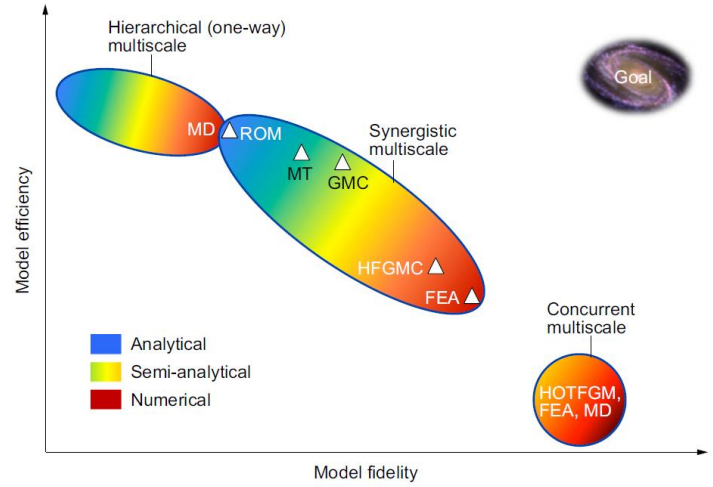

Aboudi, J. et al. (2013), Micromechanics of Composite Materials: A Generalized Multiscale Analysis Approach. Elsevier

Ladevèze, P., et al. (2001), International Journal for Numerical Methods in Engineering, 52(1-2):121–138

Multiscale in MUL2

- **Synergistic** multiscale framework, potentially concurrent
- RVE at **microscale via 1D CUF**
- **1D or 2D CUF** models for **macroscale**
- Highly scalable due to **parallel implementation** (Hybrid OpenMP + MPI)

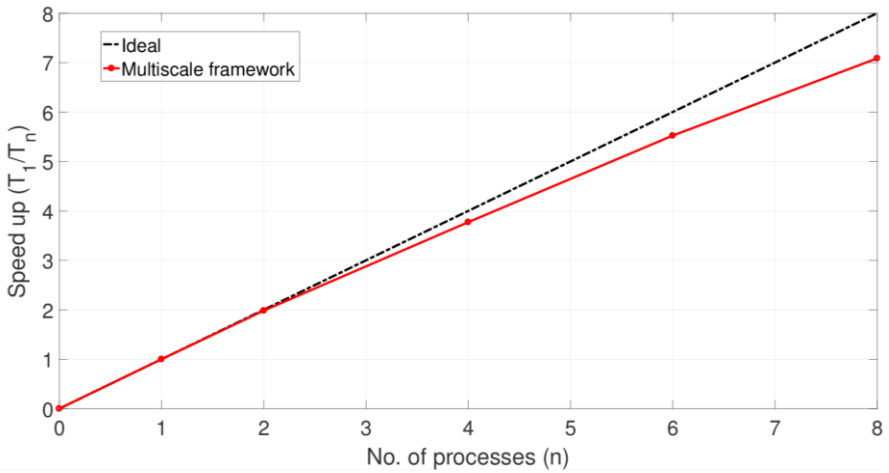

Speed-up Vs. No. of processors

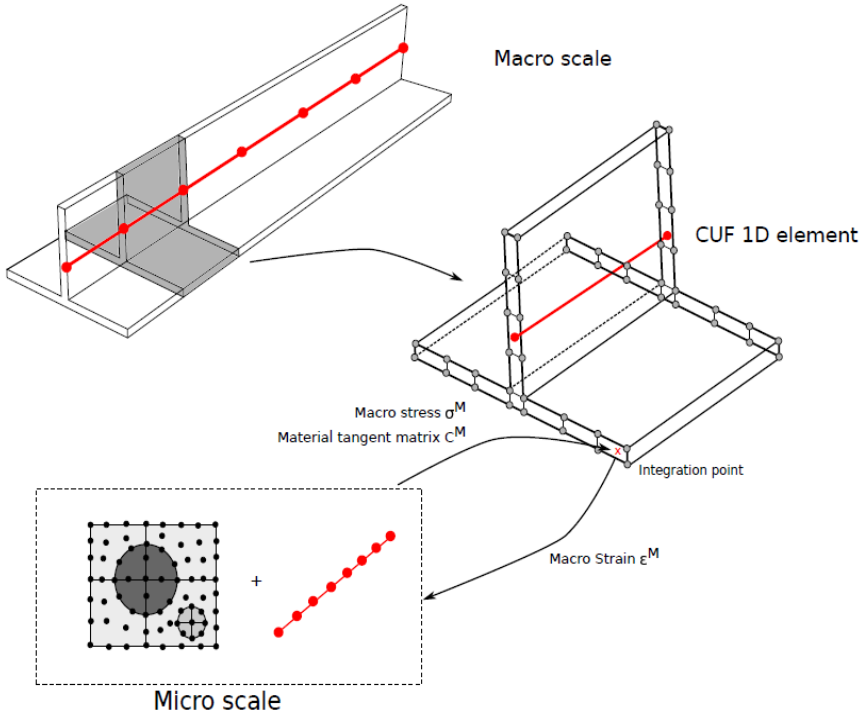

Schematic representation of the multiscale analysis procedure

Kaleel I. et al. (2019), AIAA Journal, 57(9), pp. 4029-4041

Kaleel I. et al. (2019), AIAA Journal, 57(9), pp. 4019-4028

Multiscale in MUL2/Implicit

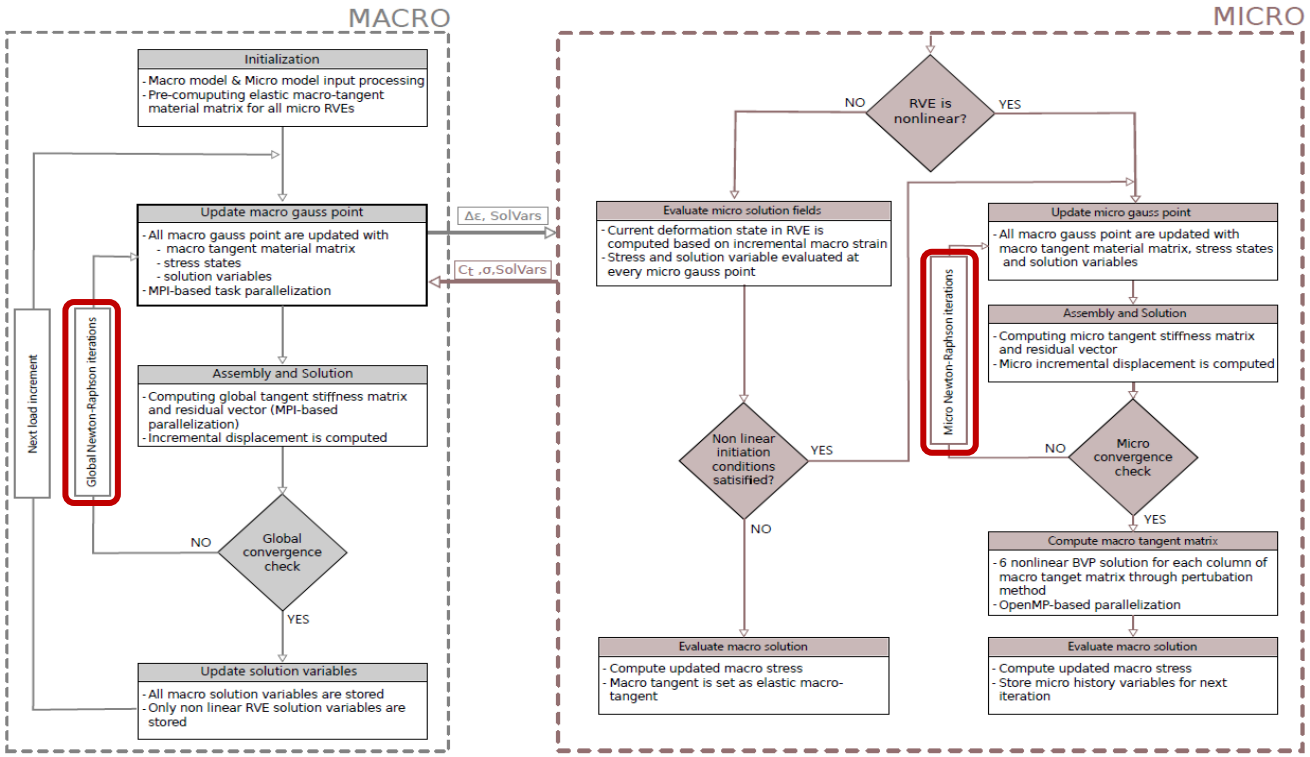

- **Fully implicit** multiscale framework
- Nonlinear solver based on Newton-Raphson at **both scales**
- Typical performances shown in the Table below
- Composite **open-hole specimen**, material nonlinearity

Model	Memory Requirement (Gb)	Time
1D /1D	**2.02**	**2 hrs**
3D coarse/1D	**7.28**	**5.5 hrs**
3D refined/1D	**8.75**	**8.5 hrs**

Kaleel I. et al. (2019), AIAA Journal, 57(9), pp. 4029-4041

Kaleel I. et al. (2019), AIAA Journal, 57(9), pp. 4019-4028

Multiscale in MUL2/Explicit

1D CUF-Micromechanics toolkit based on Newton-Raphson for micromechanical analysis

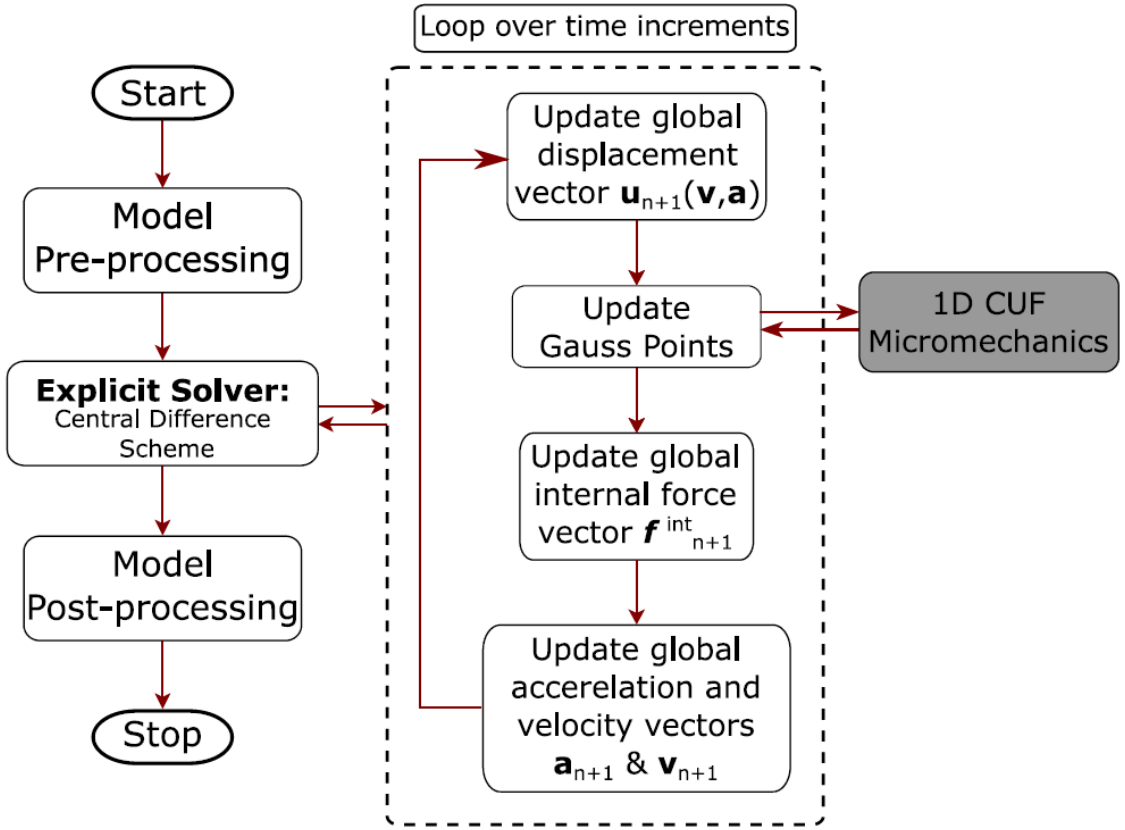

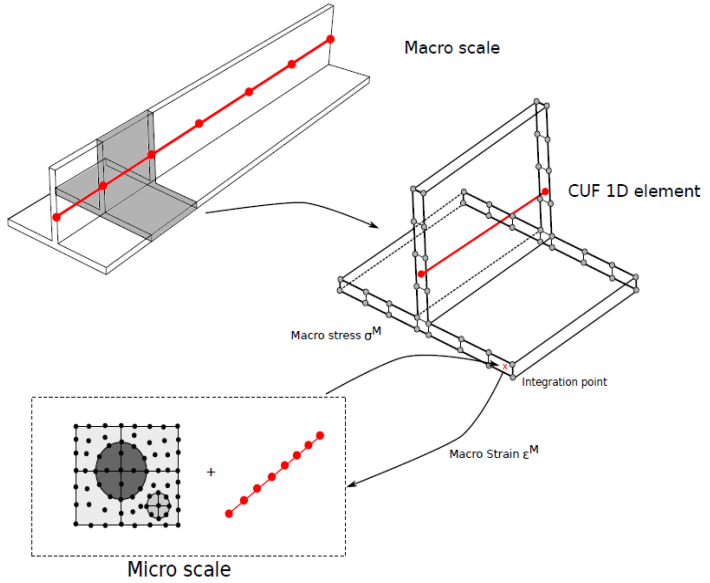

Use of explicit solver improves numerical convergence – feasibility of damage analysis

Model	Time
2D /1D	**3.5 hrs**
3D coarse/1D	**6.0 hrs**
3D refined/1D	**8.5 hrs**

Kaleel I. et al. (2019), AIAA Journal, 57(9), pp. 4029-4041

Kaleel I. et al. (2019), AIAA Journal, 57(9), pp. 4019-4028

Example: stiffness prediction of laminates

- Fiber volume fraction: 65%
- **Open-hole** specimen
- Macro specimen interfaced with a **square packed RVE**
- **Tensile stiffness prediction** for three layups

	Experimental	MAC/GMC	CUF 1D/1D
$[0\backslash 45\backslash 90\backslash -45]_{2s}$	48.3	49.1 (1.66%)	49.4 (2.28%)
$[60\backslash 0\backslash 60]_{3s}$	48.8	48.9 (0.20%)	50.44 (3.36%)
$[30\backslash 60\backslash 90\backslash 30-60]_{3s}$	32.4	33.7 (4.01%)	33.25 (2.62%)

All units in GPa. Quantities in parenthesis represent error with respect to experimental result

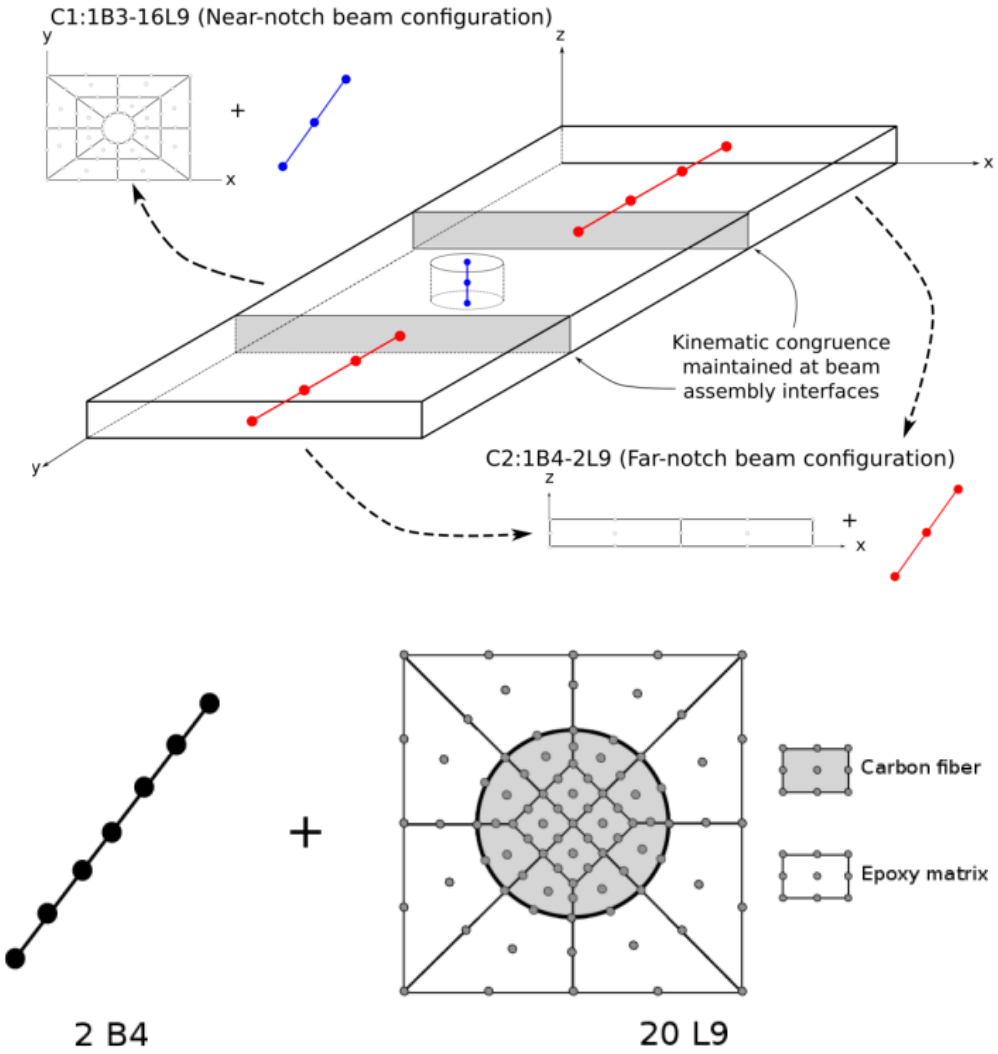

Kaleel I. et al. (2019), AIAA Journal, 57(9), pp. 4029-4041

Kaleel I. et al. (2019), AIAA Journal, 57(9), pp. 4019-4028

Example: linear multiscale analysis with randomly distributed RVE

- Two multiscale models
  - 1. **1D/1D** (Macro and micro model: CUF);
  - 2. **1D/3D** (Macro: CUF beam and micro: 3D)
- 1D (**left**) and 3D (**right**)

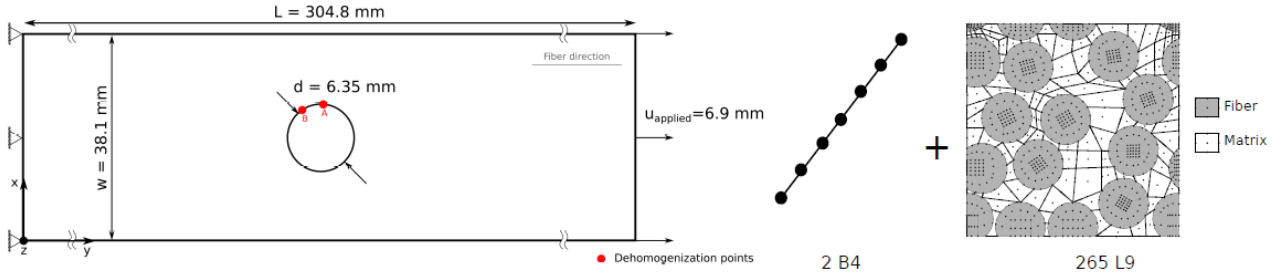

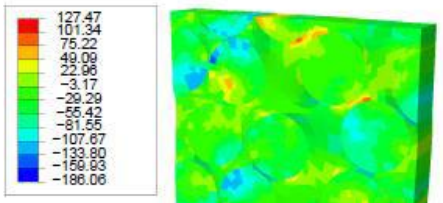

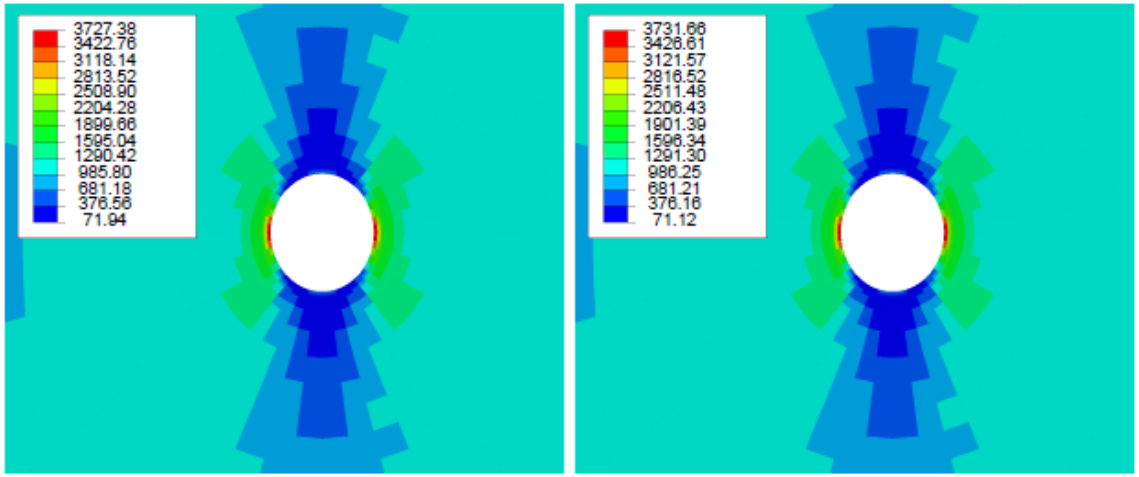

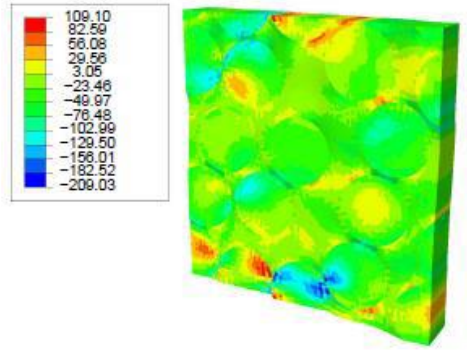

Model	Time (s)
1D /1D	**10**
1D/3D	**42**

Kaleel I. et al. (2019), AIAA Journal, 57(9), pp. 4029-4041

Kaleel I. et al. (2019), AIAA Journal, 57(9), pp. 4019-4028

Example: linear multiscale analysis of a honeycomb sandwich plate 1/2

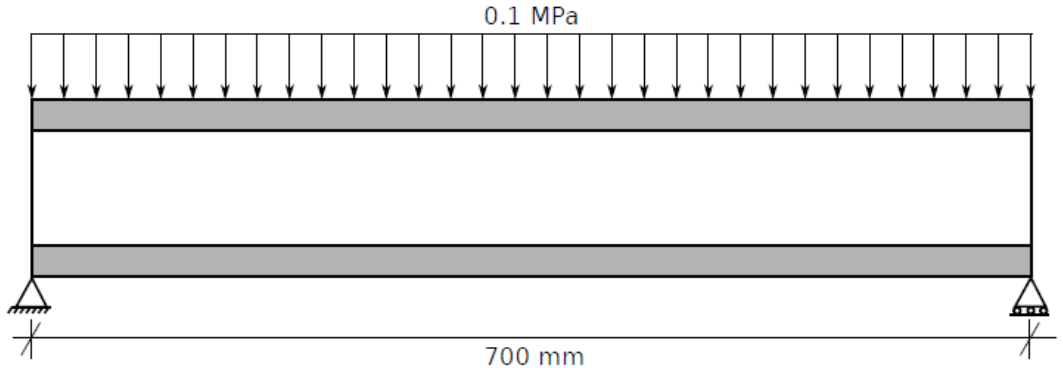

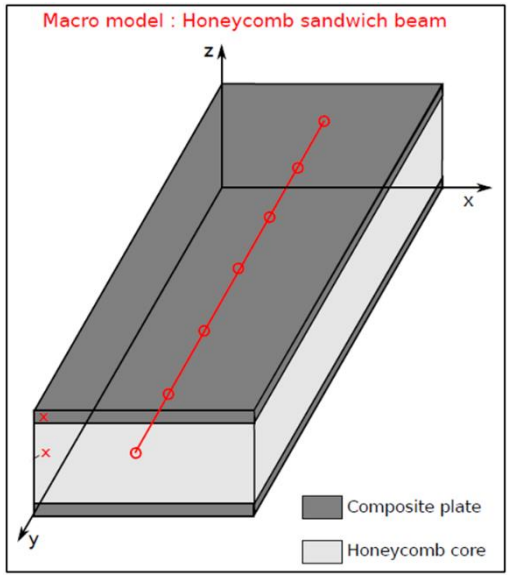

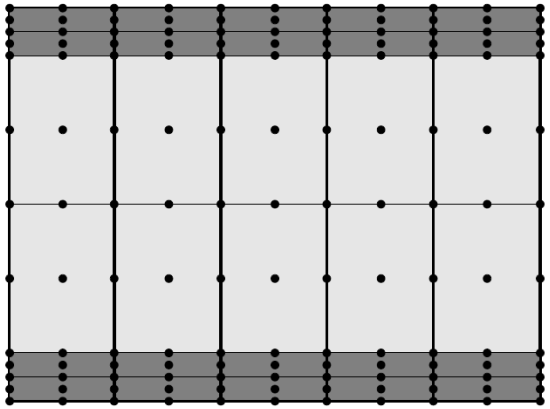

Macroscale cross-section mesh

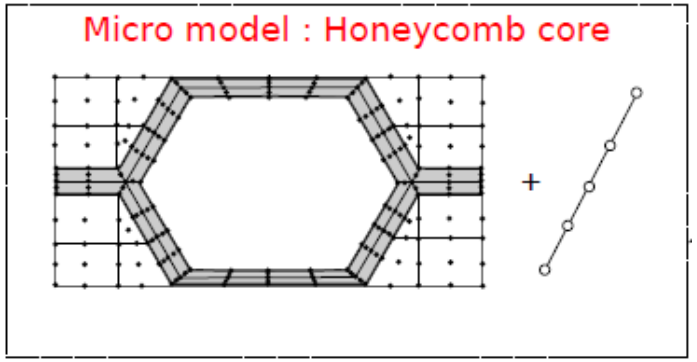

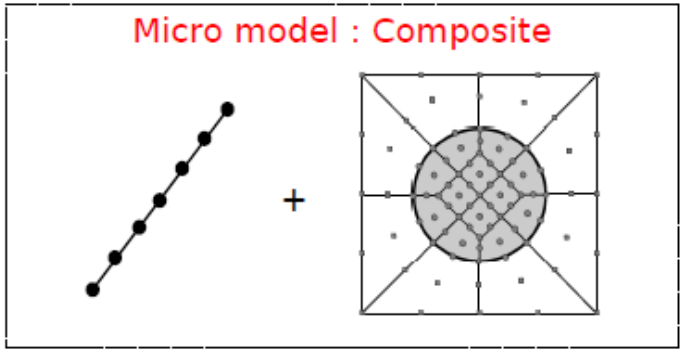

RVE discretization at the microscale

Kaleel I. et al. (2019), AIAA Journal, 57(9), pp. 4029-4041

Kaleel I. et al. (2019), AIAA Journal, 57(9), pp. 4019-4028

Example: linear multiscale analysis of a honeycomb sandwich plate 2/2

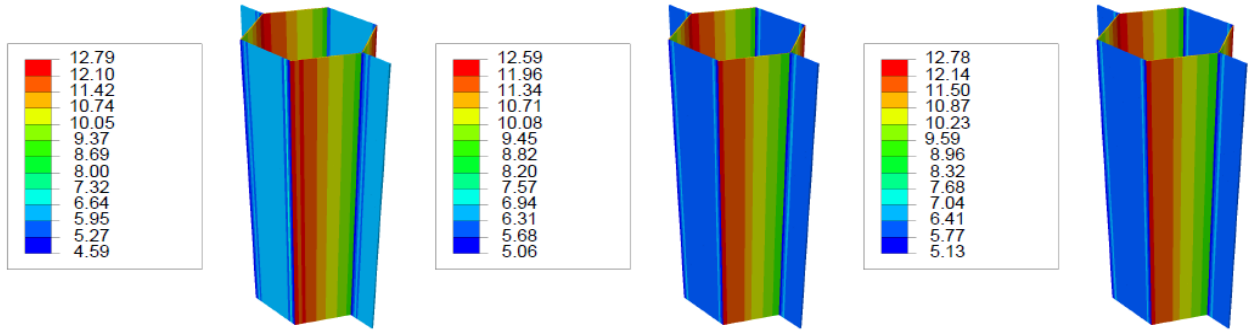

(a) 1D-1D (b) 3D-1D(Coarse) (c) 3D-1D(Refined)

Local von Mises stress field

Analysis	Mesh	DOF	Gauss Pts.	No. of CPUs	Analysis Time (s)		Memory required for macro – GP (GB)
					Without Local Fields	With Local Fields	
1D – 1D	36 L9 – 15 B4	19,734	16,200	1	14.9	64.0	2.95
3D – 1D (coarse)	12,500 linear brick	43,758 **(~2.2x)**	100,000	4	27.9 **(~1.9x)**	181.2 **(~2.8x)**	19.8 **(~6.7x)**
3D – 1D (refined)	20,000 linear brick	69,498 **(~3.5x)**	160,000	4	44.0 **(~2.9x)**	287.0 **(~4.5x)**	31.6 **(~10.7x)**

Kaleel I. et al. (2019), AIAA Journal, 57(9), pp. 4029-4041

Kaleel I. et al. (2019), AIAA Journal, 57(9), pp. 4019-4028

Example: elastoplastic response of open-hole tensile coupon

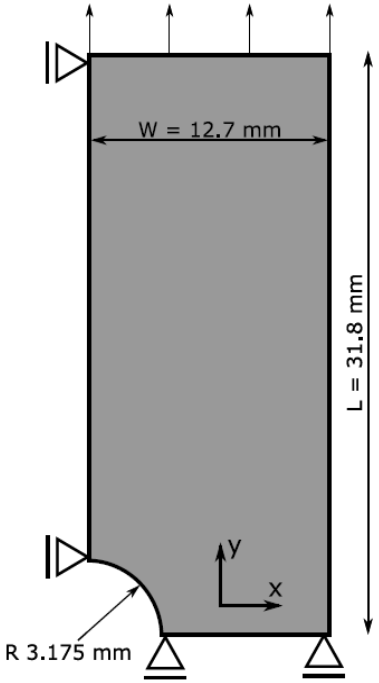

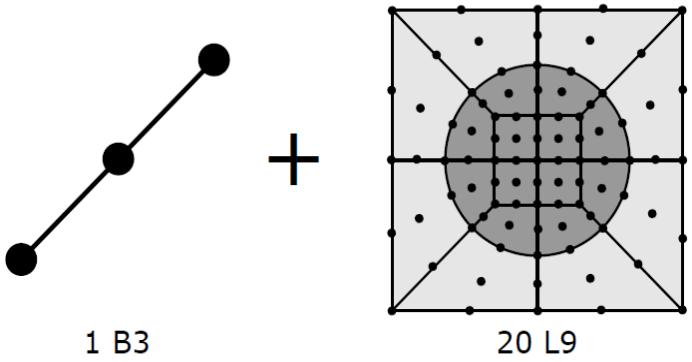

MICROSCALE: Square-packed RVE with 1B3/20L9 discretisation

MACROSCALE: Open-hole [0/90/0] tension coupon (1/4 model)

Model	Time
2D /1D	**3.5 hrs**
3D coarse/1D	**6.0 hrs**
3D refined/1D	**8.5 hrs**

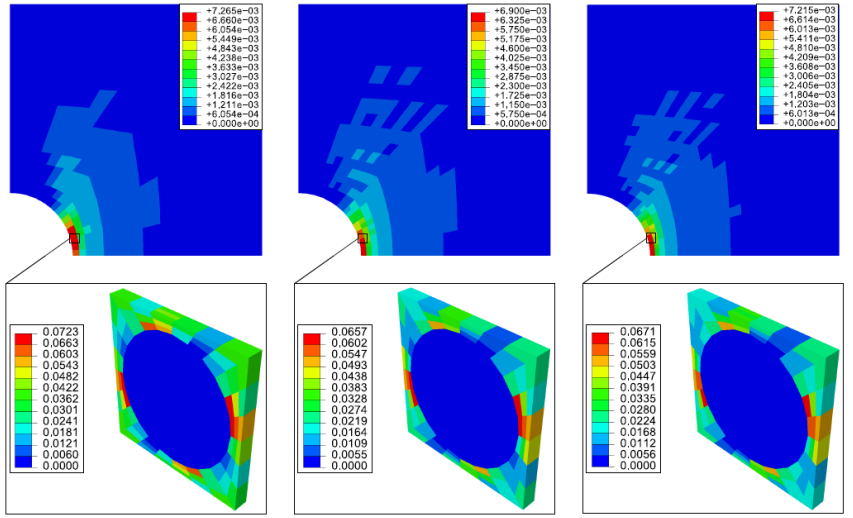

Inelastic strain fields at macro- and micro-scales

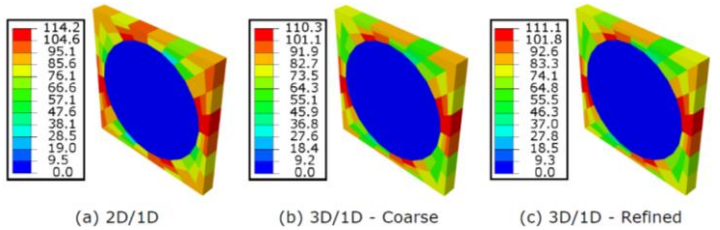

Von Mises stresses at the microscale

Kaleel I. et al. (2019), AIAA Journal, 57(9), pp. 4029-4041

Kaleel I. et al. (2019), AIAA Journal, 57(9), pp. 4019-4028

NASA Multiscale Analysis Tool (NASMAT)

- **New** state-of-the-art **multiscale framework** developed at the **NASA Glenn Research Center** for use on **high performance computing systems**
- Already **includes several** semi-analytical micromechanics **theories**, constitutive and **damage models**
- Uses recursive data structures and subroutines to facilitate analyses utilizing an **arbitrary number of length scales**
- Several application program interfaces developed to support **interoperability with third party software**
- The **MUL2 micromechanics** is now one of the tools **available in NASMAT**

Main features:

- An **Abaqus** GUI generates CUF/**MUL2** meshes
- NASMAT can **combine CUF/MUL2 models** with **any material model** available in its libraries
- A library of **predefined CUF architectures** implemented in NASMAT (Square-packed, square-packed with coating, hex-packed, hex-packed with coating)

Aboudi J., Arnold S., Bednarcyk B. (2021), Practical Micromechanics of Composite Materials, Butterworth-Heinemann

Further Topics and Reading

- Geometrical Nonlinearity

  Pagani, A. et al. (2019), AIAA JOURNAL, Vol. 57, pp. 3524-3533

- Multifield problems

  Nali P. et al., International Journal for Numerical Methods in Engineering (2011), 85, pp. 869-919;

  Carrera E., AIAA Journal (2005), Vol. 43, N° 10, pp. 2232-2242;

  Carrera E. and Nali P., International Journal for Numerical Methods in Engineering (2009), 80, pp. 403-424

- Node-Dependent-Kinematics and Global/Local

  Zappino, E., Carrera, E., (2018) AIAA Journal, 56:4, pp 1647-1661

- Rotordynamics

  Filippi, M. et al. (2019), JOURNAL OF THE AMERICAN HELICOPTER SOCIETY, Vol. 64, pp. 1-10

- Virtual Manufacturing

  Zappino, E. et al. (2020), COMPOSITE STRUCTURES, Vol. 241

- Axiomatic/Asymptotic Method, Best Theory Diagrams, Neural Networks

  Carrera E., Petrolo M., AIAA Journal (2010), Vol. 48, N° 12, pp.2852-2866

  Petrolo M., Carrera E., (2019), Advanced Modeling and Simulation in Engineering Science, 6(4), pp. 1-23

  Petrolo, M., Carrera, E., (2021), COMPUTERS & STRUCTURES, Vol. 244

Full list: http://www.mul2.polito.it/index.php/publications/journal-articles

Composite materials: Modeling, Processing, and Characterization

Structural Modeling and Analysis

8-9 June 2021, 14:00-16:00

Speaker: Marco Petrolo, www.mul2.com

Contributors:

Prof. Erasmo Carrera, Dr. Ibrahim Kaleel, Dr. Manish H. Nagaraj

Processing methods and simulation of composites

2021-06-07

Navid Zobeiry, PhD (navidz@uw.edu)
Assistant Professor
Materials Science & Engineering
University of Washington

BE BOUNDLESS

What are Advanced Composites?

- Composite Materials or 'Composites' are:
  - *Made from two or more constituent materials with different properties (mechanical, chemical …)*
  - *Remain separate and distinct within the finished structure*
- In typical industrial applications, one material is much stronger than the other one. The weaker material acts is a binding agent.

Example of Advanced Composites (or composites)

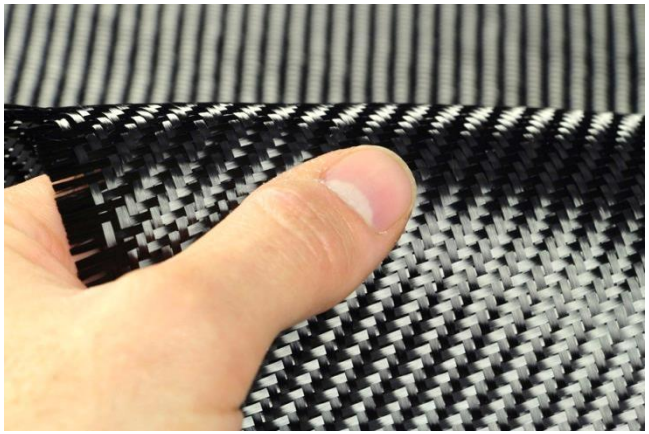

Advanced Fibers
(example Carbon fiber)

+

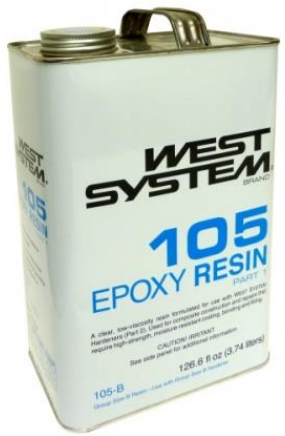

Matrix
(example Epoxy)

→

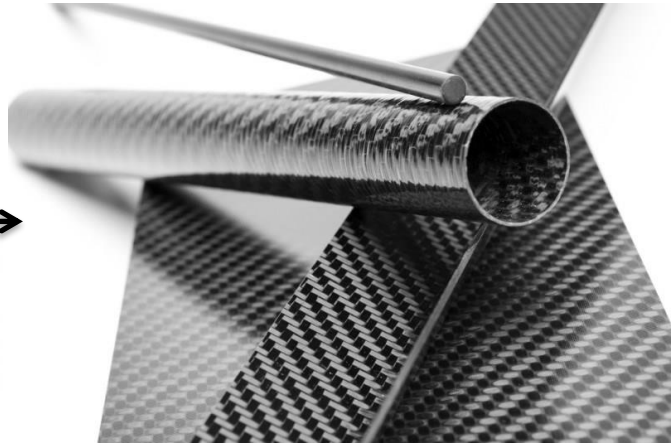

Advanced Composite parts

Introduction: A Cooking Analogy

- Composites processing and cooking have a lot in common
- We'll use a cooking analogy to go through a typical manufacturing process

Cooking food

=

Processing composites

Introduction: A Cooking Analogy

Choose the ingredients

Choose the constituent materials

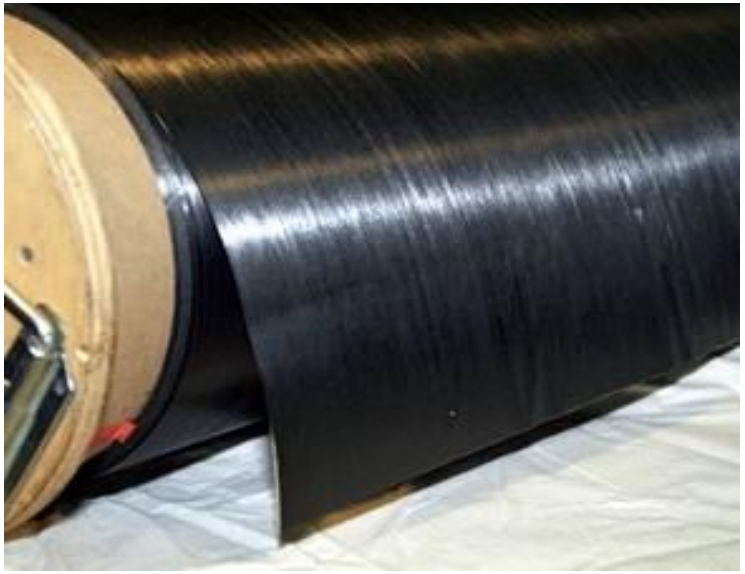

Introduction: A Cooking Analogy

Choose the cooking method

Choose the process

Introduction: A Cooking Analogy

Choose the cookware

Choose the tool

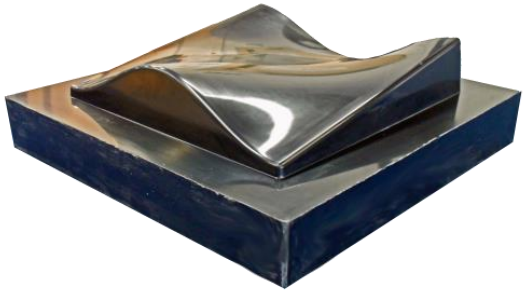

Introduction: A Cooking Analogy

Prepare the ingredients

Prepare the materials

Introduction: A Cooking Analogy

Grease the pan

Apply release agent

Introduction: A Cooking Analogy

Mix ingredients and place in pan

Deposit material on tool

Introduction: A Cooking Analogy

Cover with foil

Apply vacuum bag

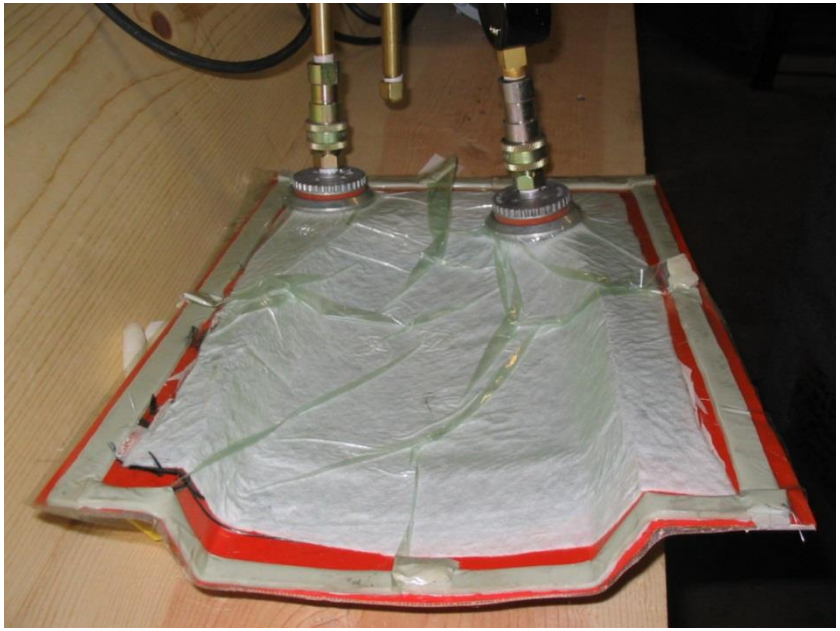

Introduction: A Cooking Analogy

Bake in oven

Apply cure cycle

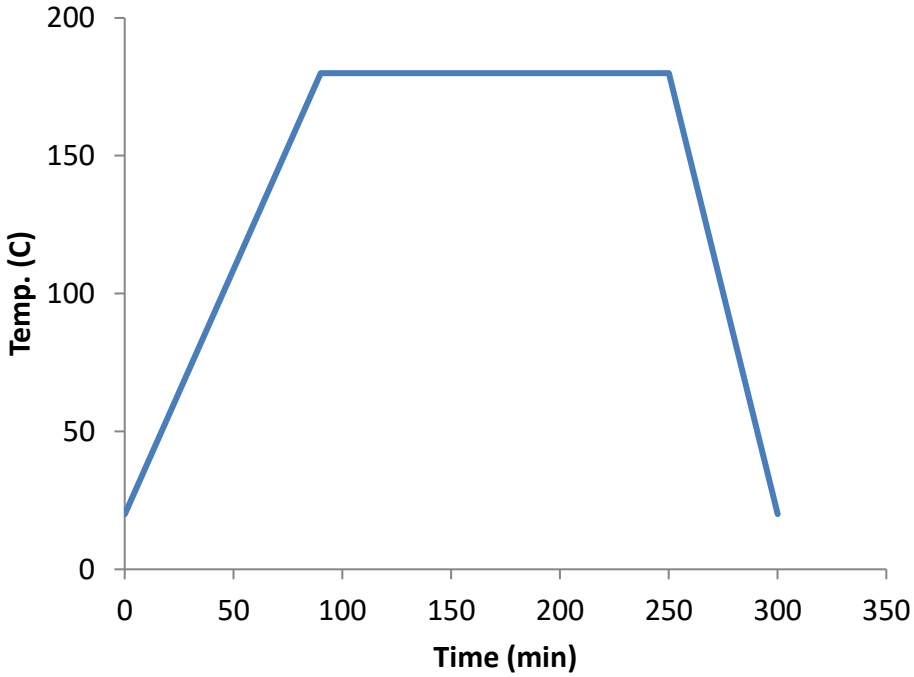

Introduction: A Cooking Analogy

Cut and serve

Demould and trim
(post processing)

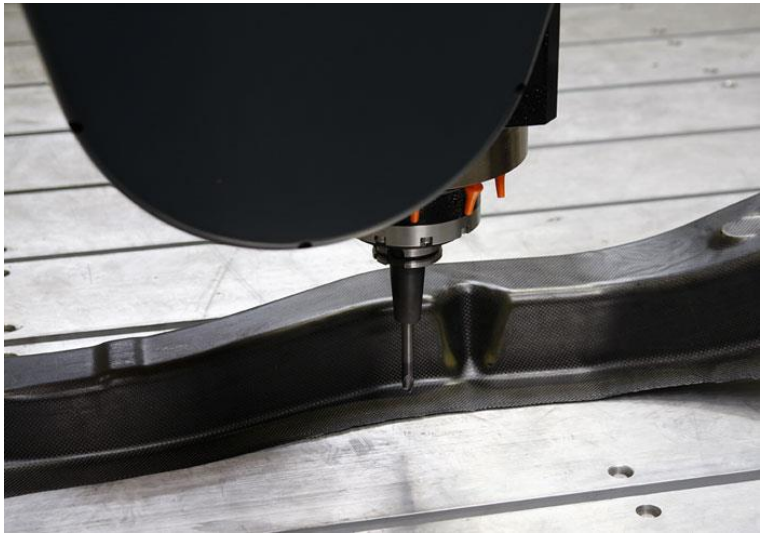

Composites Manufacturing

- Raw material
  - Fiber
  - Resin
  - Prepreg
  - …
- Material deposition
  - Hand lay-up
  - Automated fiber placement (AFP)
  - Liquid composite molding (LCM)
  - …
- Curing process
  - Autoclave
  - Out-of-autoclave
  - …

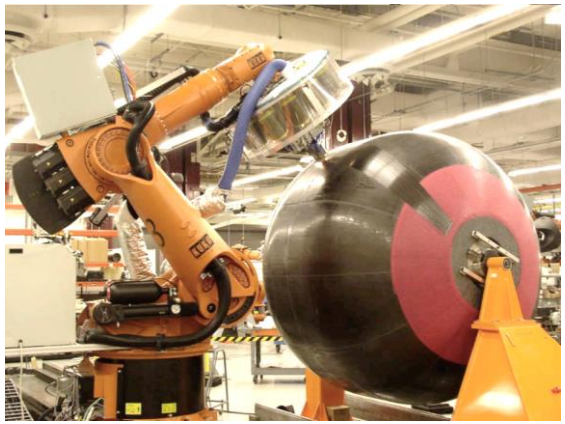

Advanced Fibers

- Advanced composite materials are characterized by high performance fibres:
  - Small diameter to reduce the probability of imperfections
  - High aspect ratio to effectively transfer the load
  - High flexibility for ease of processing

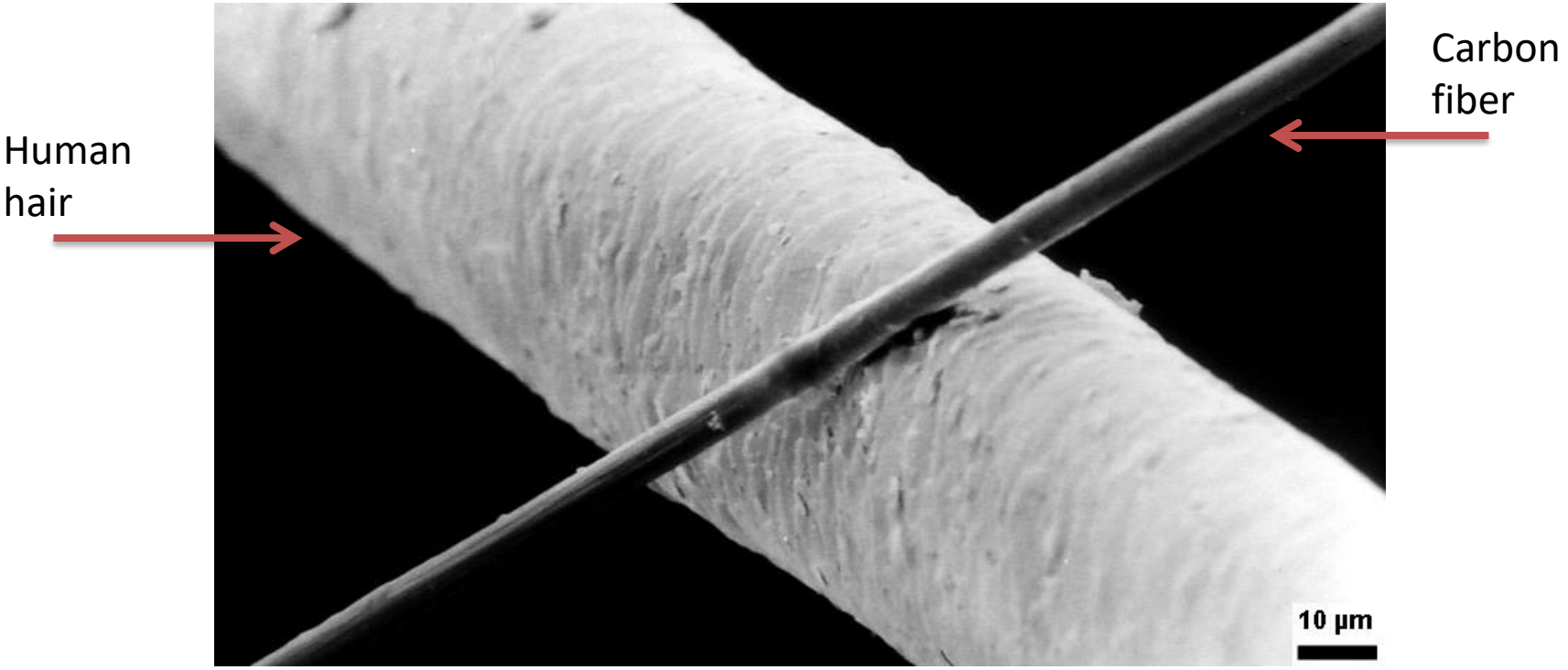

Commonly used Advanced Composites

Carbon Fiber

CFRP

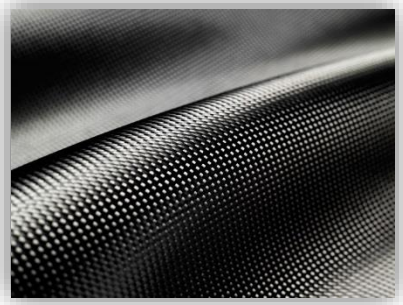

Glass Fiber

GFRP

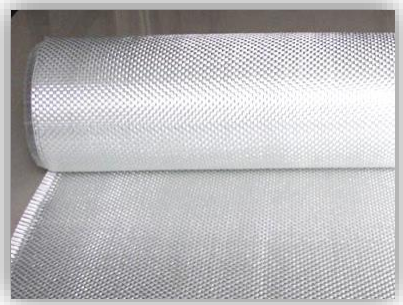

+

Thermoset Resins

- Epoxy
- Vinyl ester
- Polyester
- …

Thermoplastic Resins

- Polypropylene
- PEI
- PEEK
- …

Fiber Architecture: Unidirectional

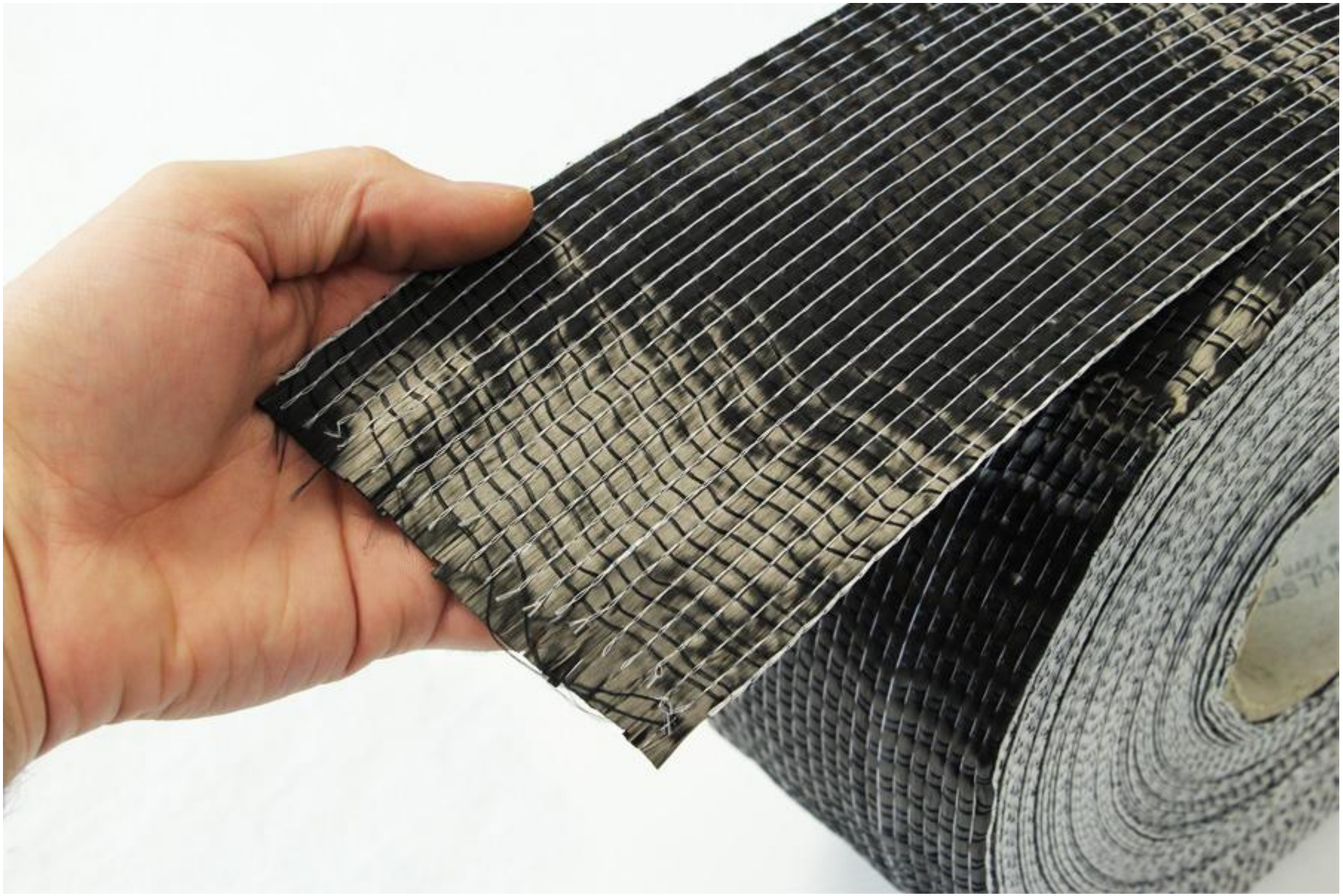

Fiber Architecture: Plain Weave Fabric

- Consists of tows that are interlaced in an alternating fashion (over one, under one, over one, under one…)

Raw Material: Prepreg

- Prepreg material refers to fiber that is already combined with resin

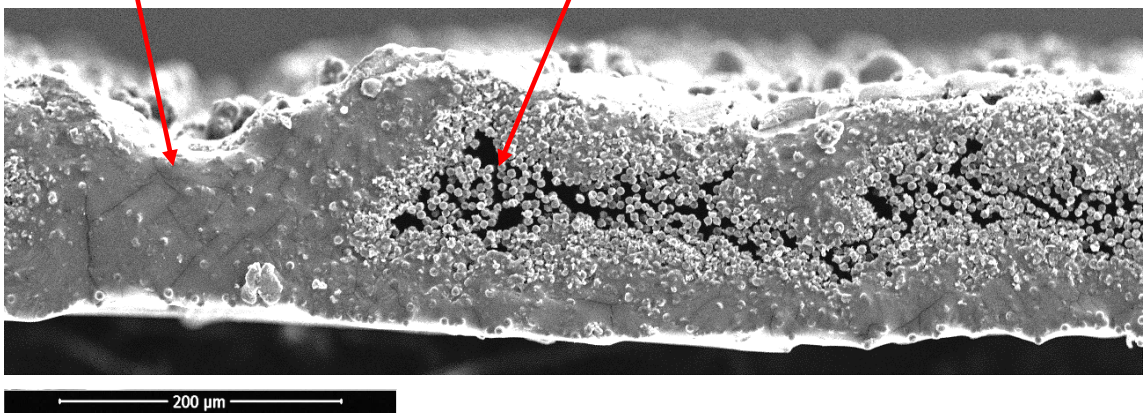

e.g. Prepreg roll of carbon fiber (60%) and epoxy (40%)

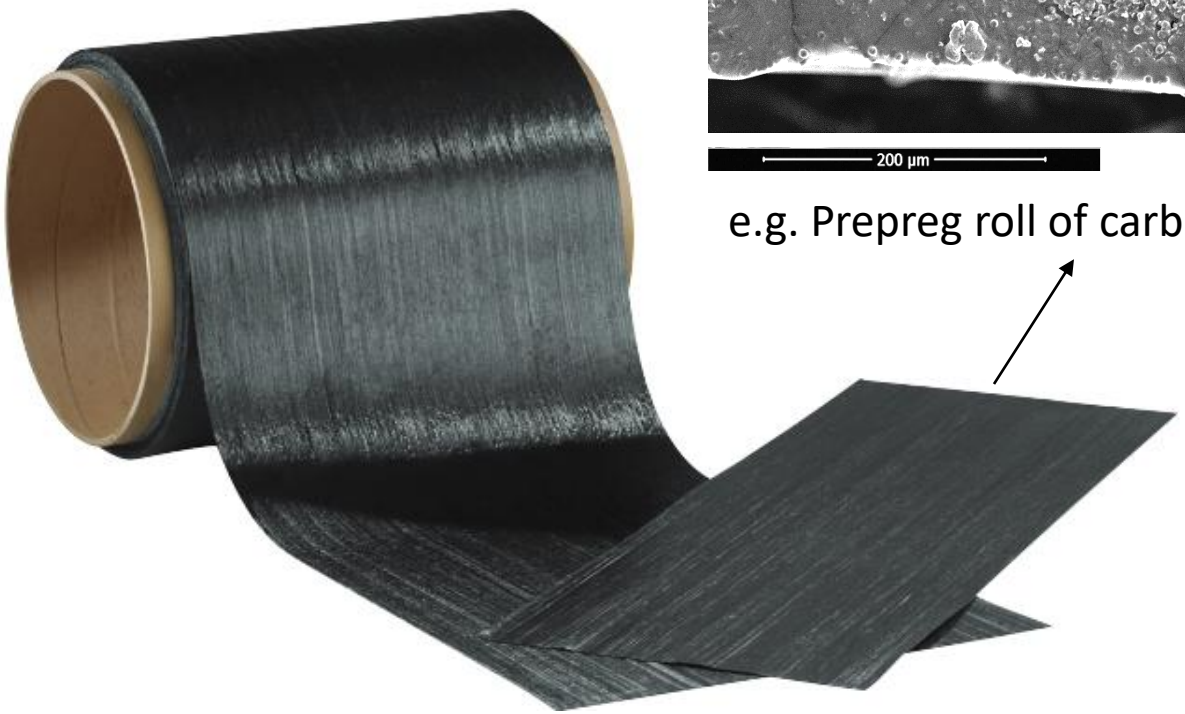

Material Deposition Methods

- There are three main methods to combine resin and fiber to deposit onto a tool:
  - **Wet Processes:** Mixing liquid resin and dry fiber directly in the mold
  - **Liquid Composite Molding (LCM) processes:** Infusing dry fabric with resin using a pressure gradient
  - **Prepreg Processes:** Laying-up using prepreg where resin and fiber are already combined

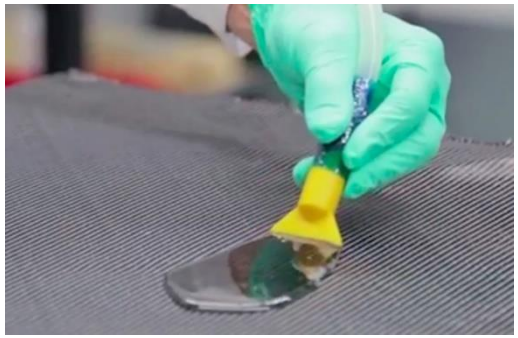

Wet Process

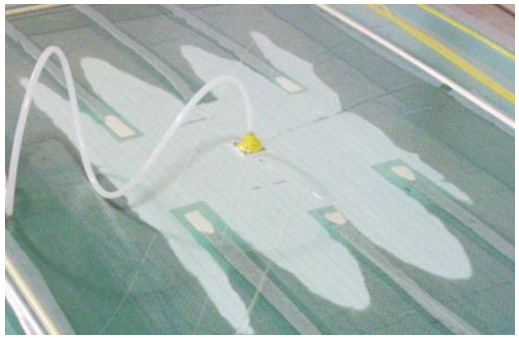

LCM

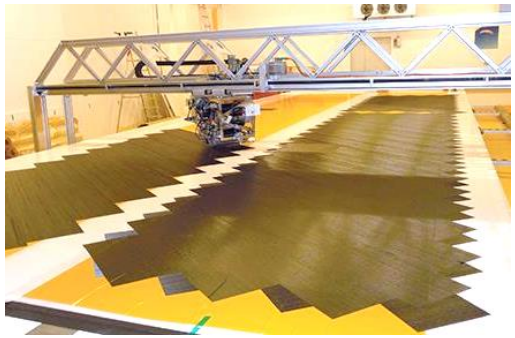

Prepreg Process

Main Processing Methods

Autoclave Processing

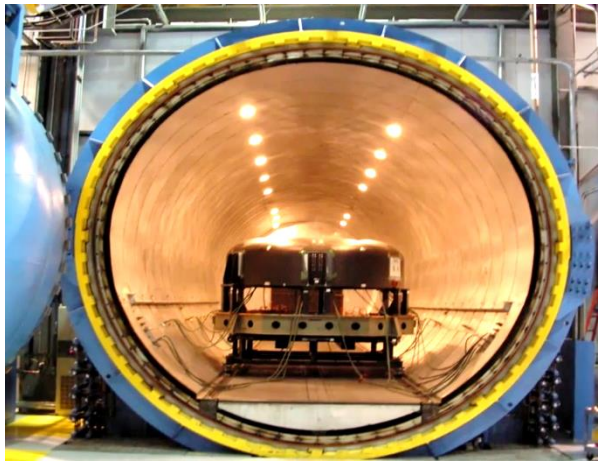

Out-of-Autoclave (OOA) Processing

Oven

Microwave

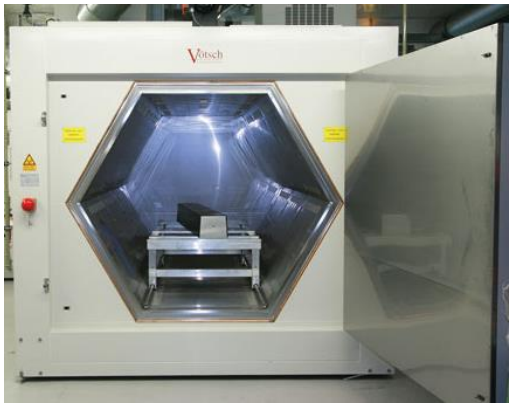

Hot press

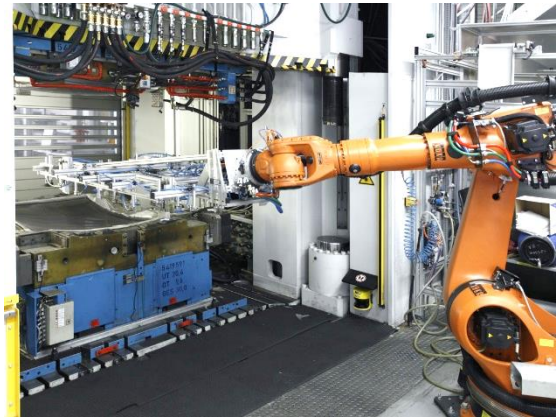

Heated tools

Autoclave

- Essentially, an autoclave is a heated pressure vessel
- Typical max pressures: ~7-10 bars
- Typical operating temperatures: ~200-400 ℃
- Autoclaves are utilized where the highest of material performance standards are required such as void contents of less than 2%.
- It takes a lot of time and energy to produce parts using the Autoclave which make the end products very expensive.

Autoclave: Major Cost in Aerospace

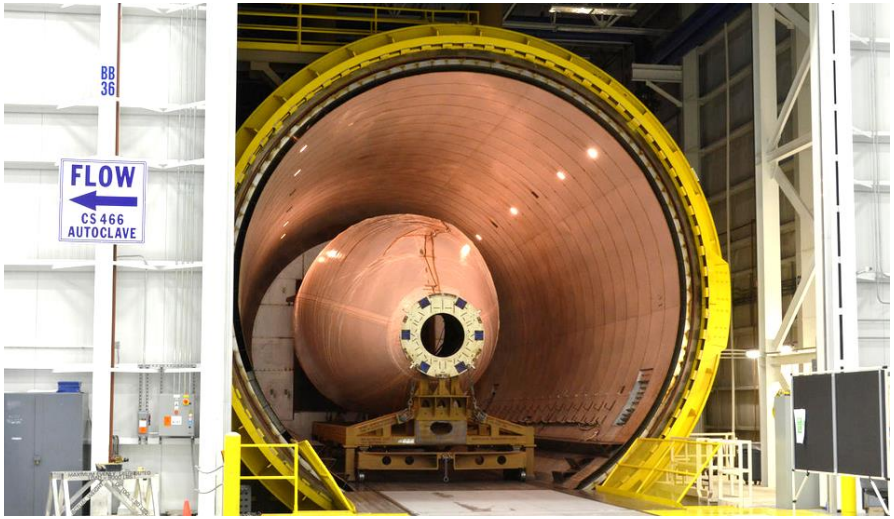

Boeing Autoclave for 787 fuselage

Boeing Autoclave for 777x Wing

Mitsubishi Autoclave for 787 wing

OOA: Microwave Curing

- GKN Aerospace has developed microwave curing processing.
- An 80 percent reduction in energy use compared to autoclave cure, and a 40 percent shorter cycle-time was achieved.
- The end-part quality is lower than the autoclave part.

microwave oven-cured section of C-channel.

OOA: Oven Curing

- In oven curing, parts are vacuumed bagged and cured in an oven with 1 atmospheric pressure compared to 7-10 bars in an autoclave. The process is extremely sensitive to process parameters.
- The Lockheed Martin X-55 Advanced Composite Cargo Aircraft (ACCA) is a transport aircraft which was built using a specific prepreg built for oven curing.

OOA: Oven Curing

The Advanced Composite Cargo Aircraft‘s fuselage comprises eight pieces molded from OOA-cured MTM-45 prepreg

OOA Processing Challenges

Bombardier Learjet 85: Advanced Full Composite Structure

- Program launched in 2007
- Originally scheduled for entry into service in 2013
- Program delayed to 2014 due to several new technical challenges (Fuselage and empennage manufactured using an out-of-autoclave process (average elevation 2,000m, vacuum pressure -20%)
- Program suspended and 1,000 associated jobs lost January 2015

Hand Lay-up Application

- NASA Composite Space Capsule
- Primary structure: Carbon epoxy composite (IM7/977-2) and aluminium honeycomb for sandwich structure
- Manufacturing method: hand lay-up, vacuum bagging and autoclave curing

Hand Lay-up Application

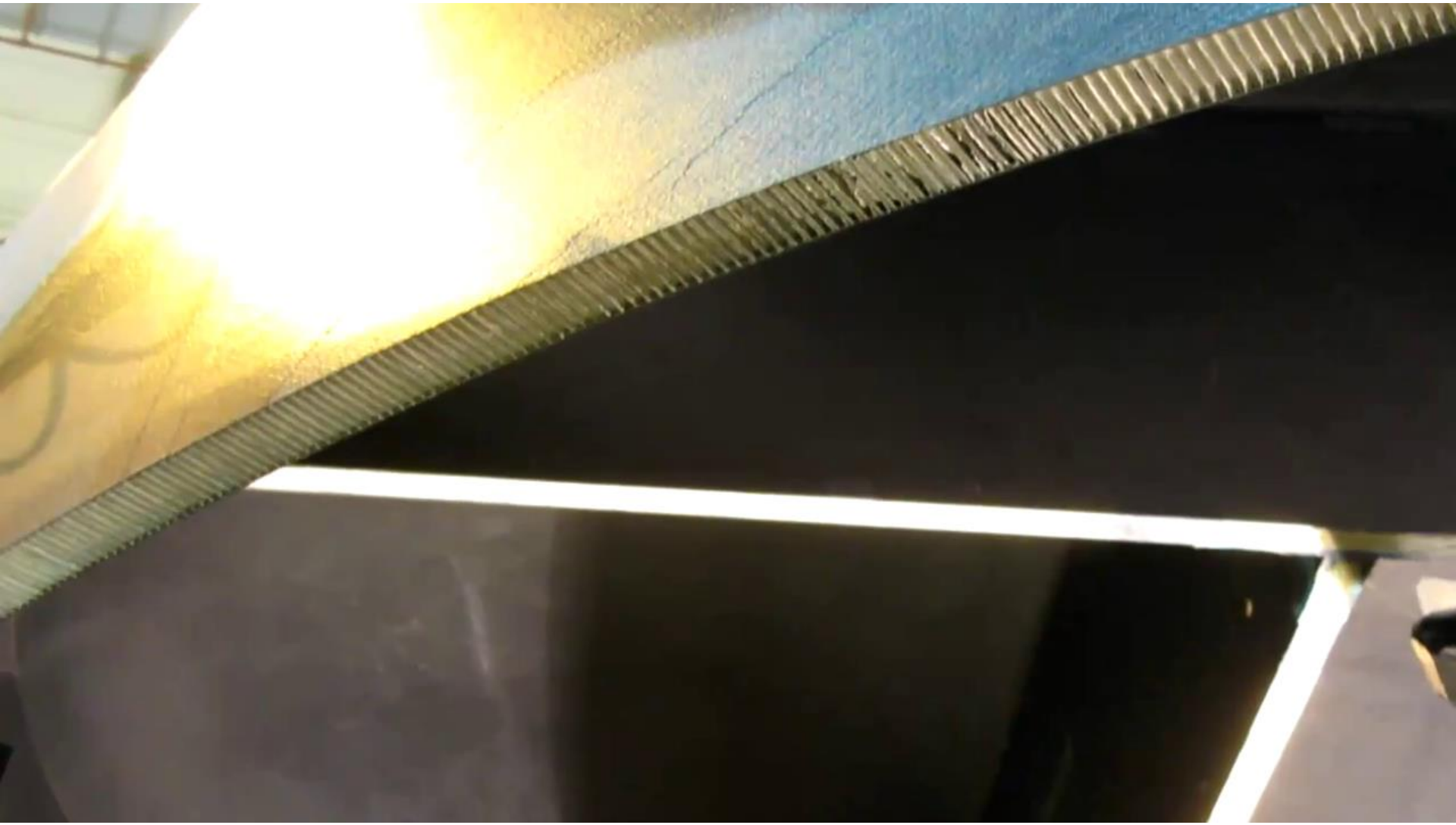

Composite sandwich structure: Aluminium honeycomb, composite facesheet

Hand Lay-up Application

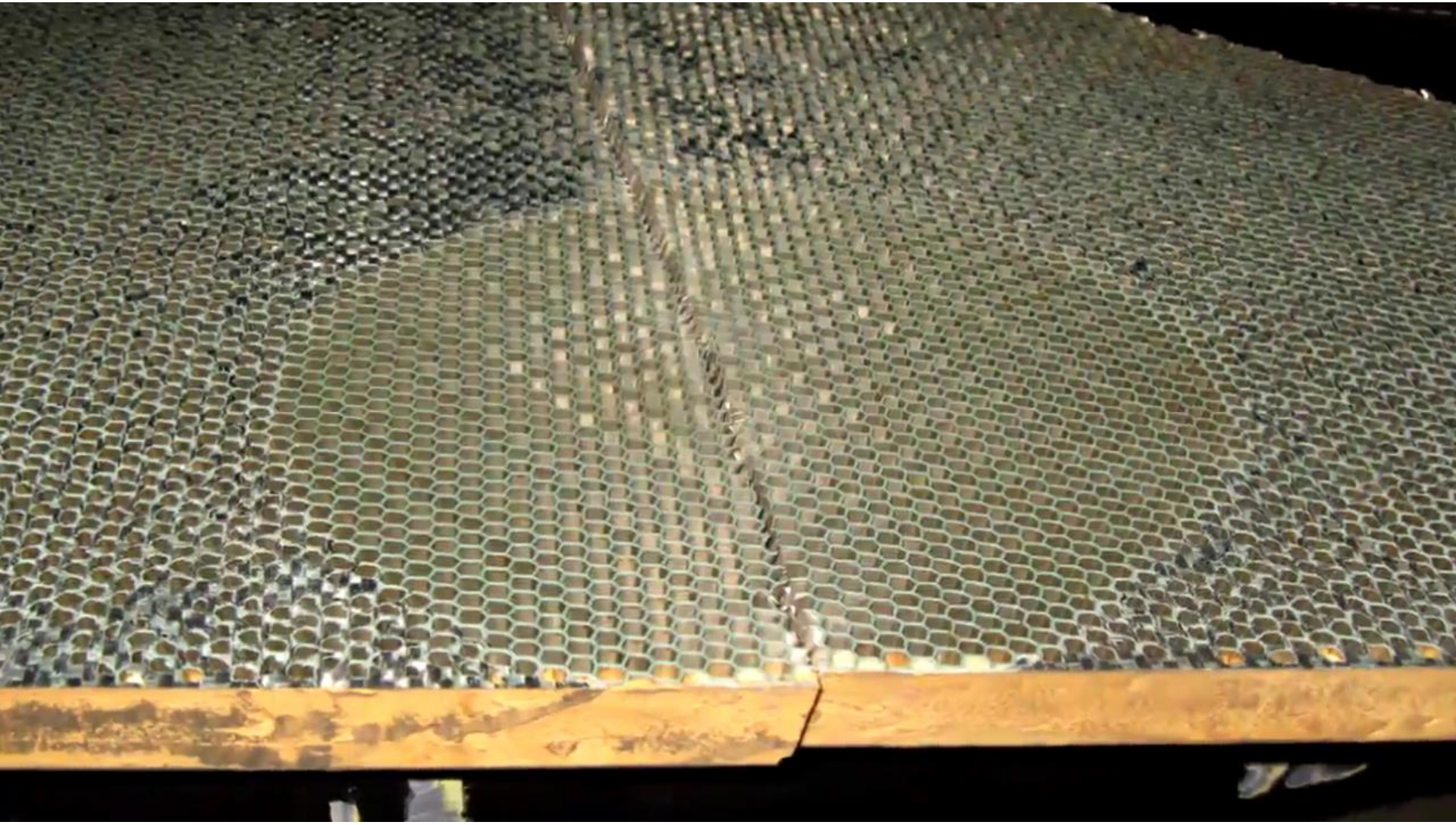

Aluminium honeycomb

Hand Lay-up Application

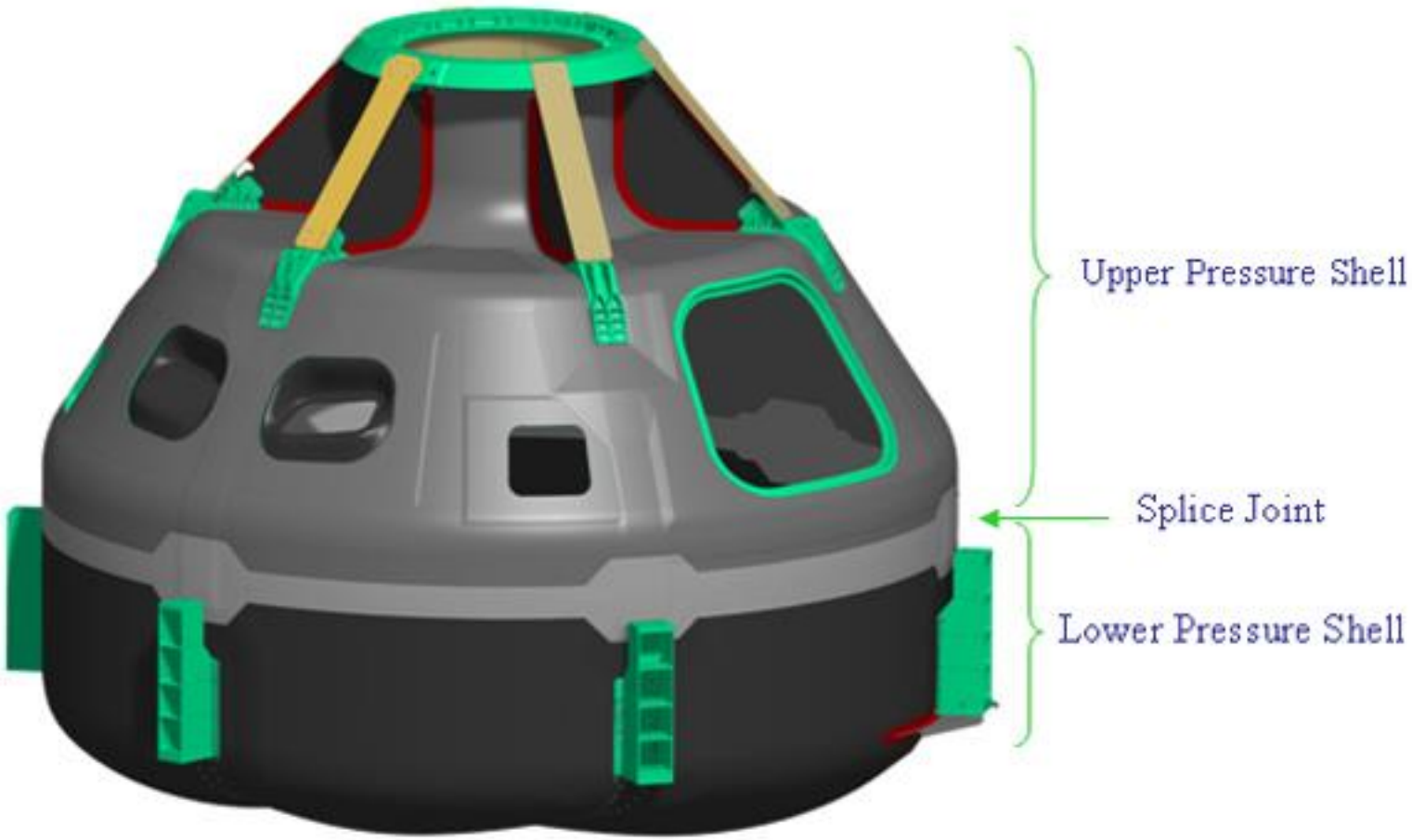

Pressure Module = Upper Pressure Shell + Splice Joint + Lower Pressure Shell

Hand Lay-up Application

Upper Pressure Shell cure tool

Hand Lay-up Application

Hand Lay-up Application

Hand Lay-up Application

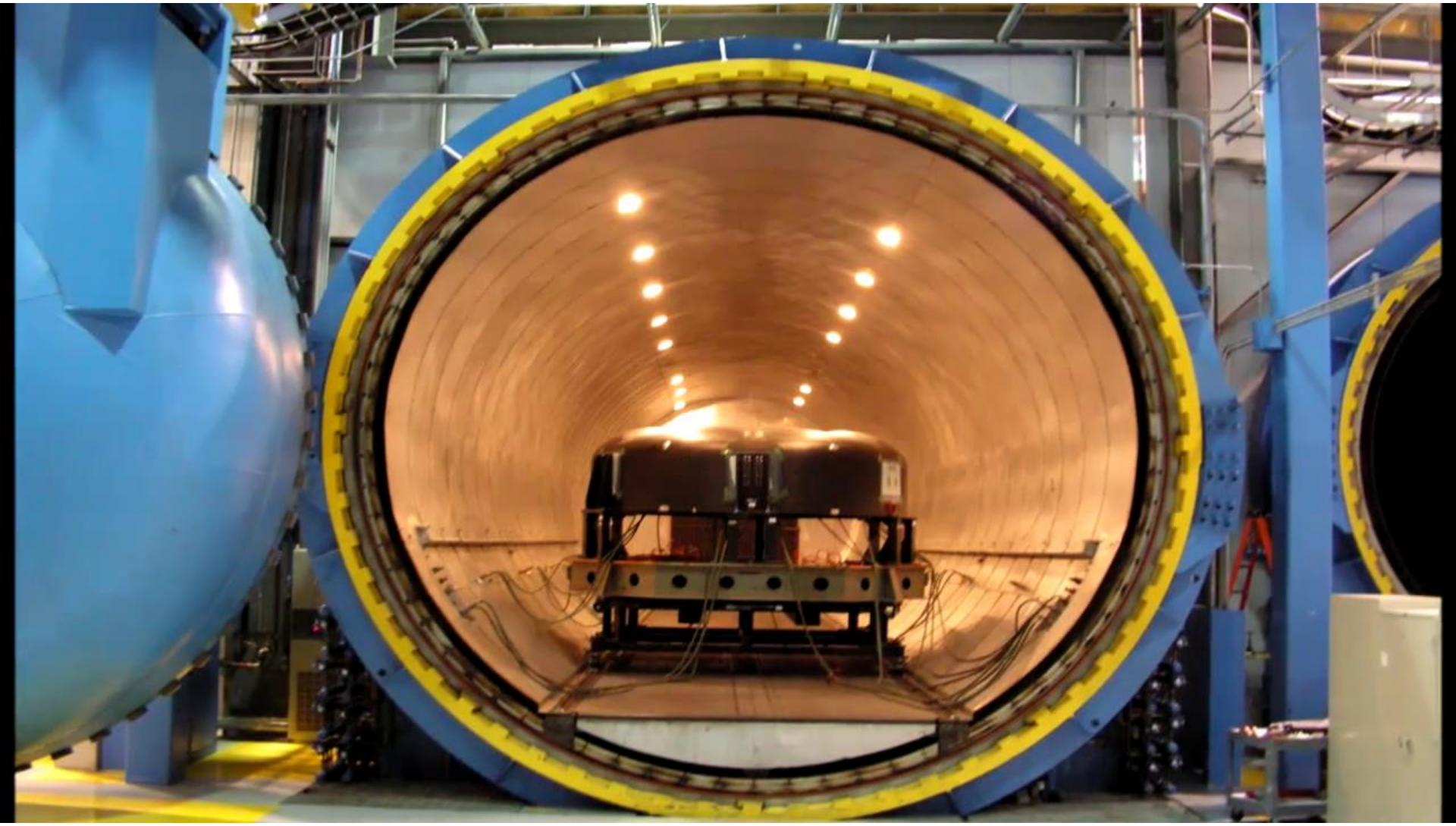

Hand Lay-up Application

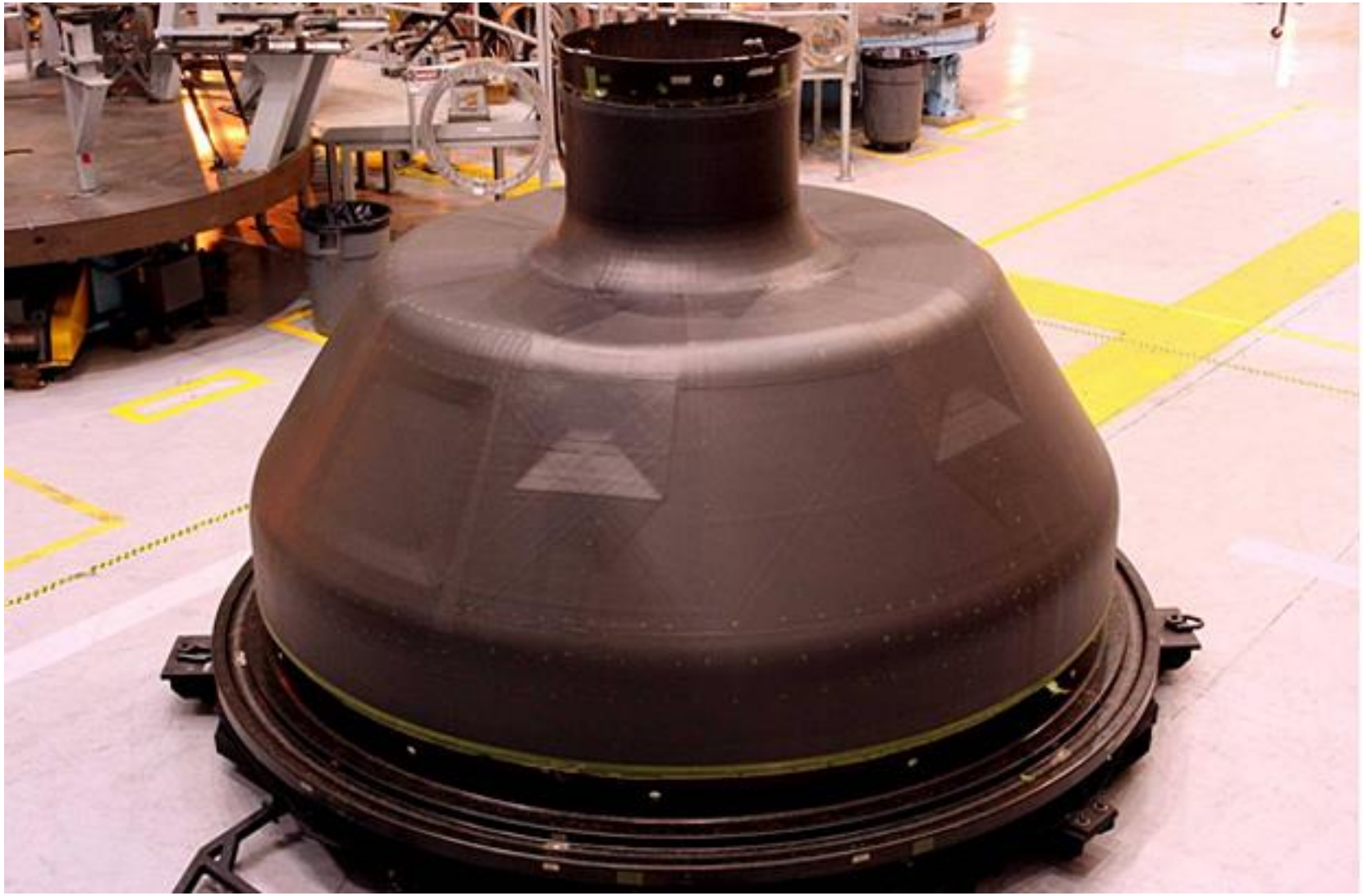

Cured Upper Pressure Shell Sandwich

Hand Lay-up Application

Hand Lay-up Application

Cured inner sandwich skin of Lower Pressure Shell

Hand Lay-up Application

Upside Down Configuration within the Self Reacting Load Frame

Success Stories: Composite Blades

GE Composite Blades

The Museum of Modern
Art of New York

[Hand lay-up example video]

Liquid Composite Moulding

- **Resin Transfer Moulding** (RTM): Mould is loaded with reinforcement and closed, resin is injected into mould and then cured. Mould is often put under vacuum, VARTM (vacuum assisted resin transfer moulding).
- **Compression moulding**: A dry mat of reinforcing material is preformed and placed into an open mould, Resin is added, and the mould halves are pressed together and heated.
- **Infusion:** An open mould process that uses vacuum pressure to drive resin into the composite laminate.

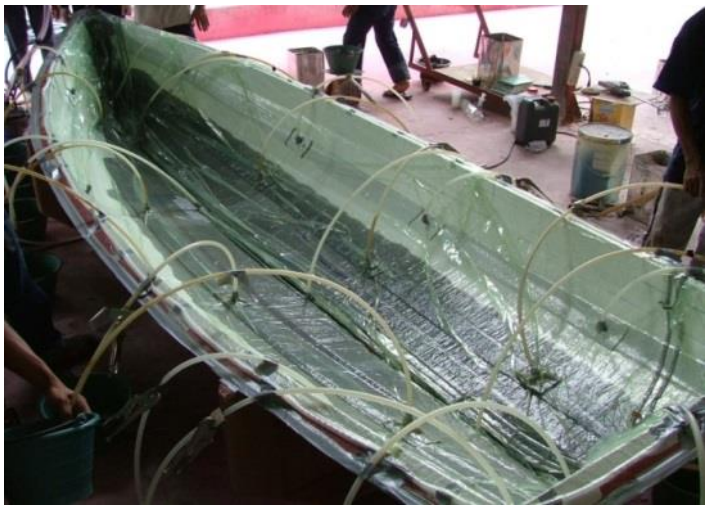

RTM Application

- The Lamborghini Aventador LP700-4 is a two-door, two-seater sports car.
- The carbon fiber composite monocoque is manufactured using an RTM process.

RTM process

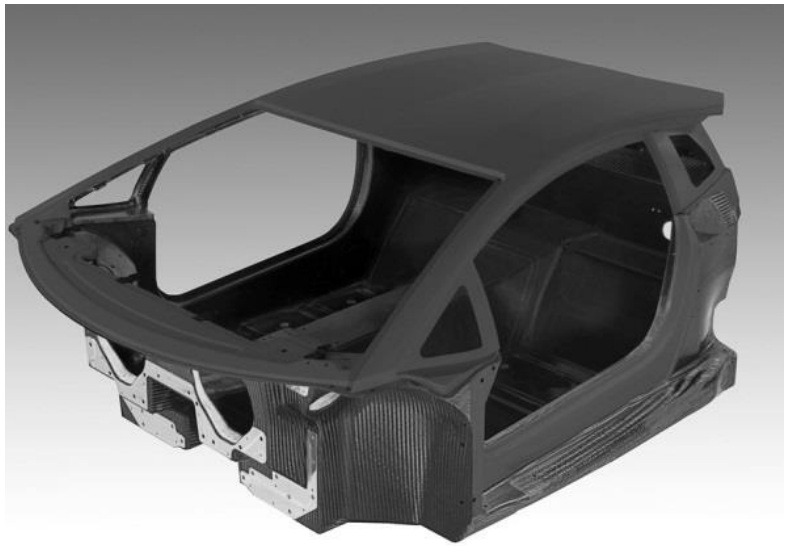

carbon fibre composite monocoque

Compression Moulding Application

- BMW i3, is an urban electric car under by BMW
- The i3 is the first mass production car to have most of its internal structure and body being made of carbon-fiber reinforced plastic (CFRP)

Compression Moulding Application

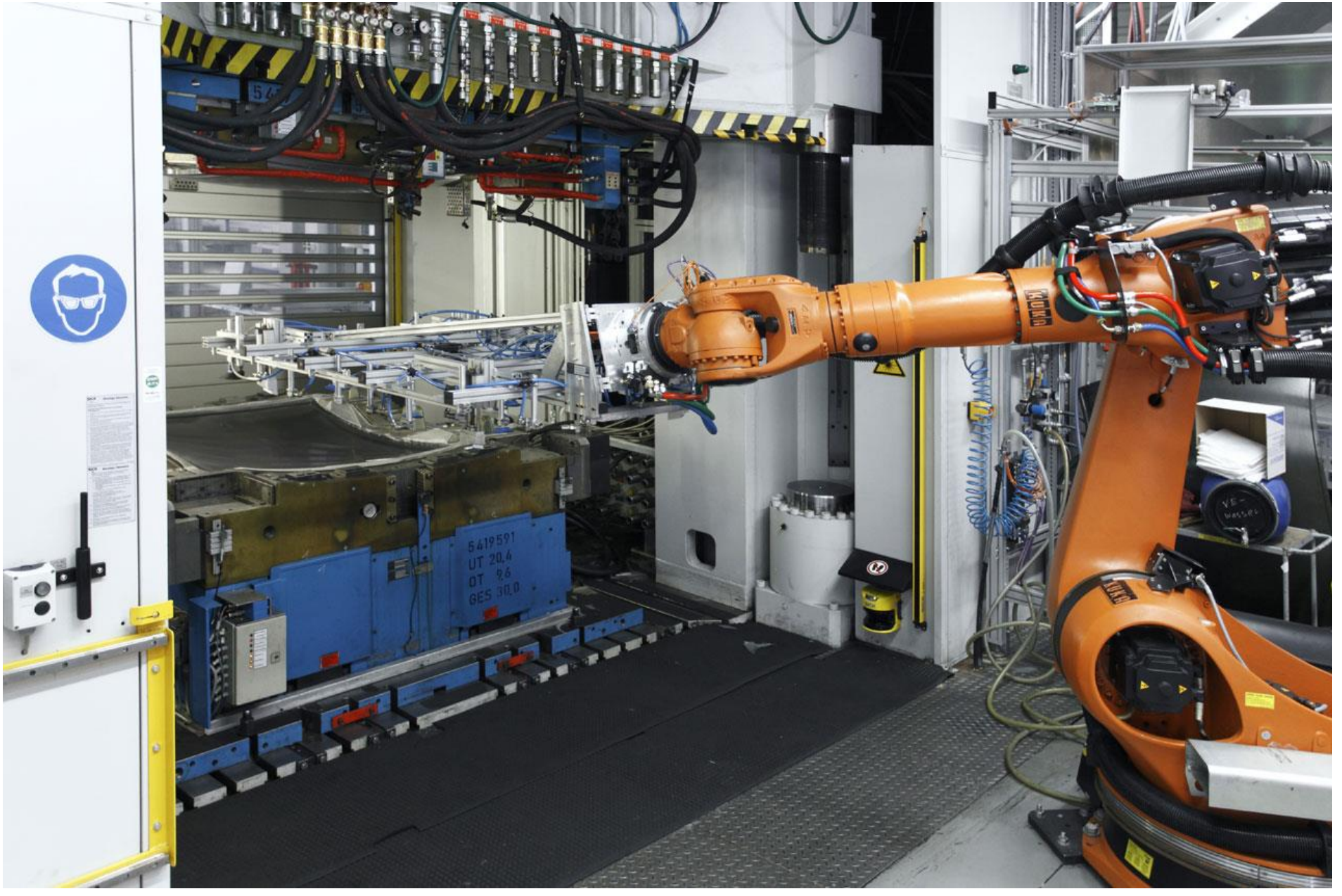

Compression Moulding Application

Processes: Wet Compression Molding: BMW 7 Series

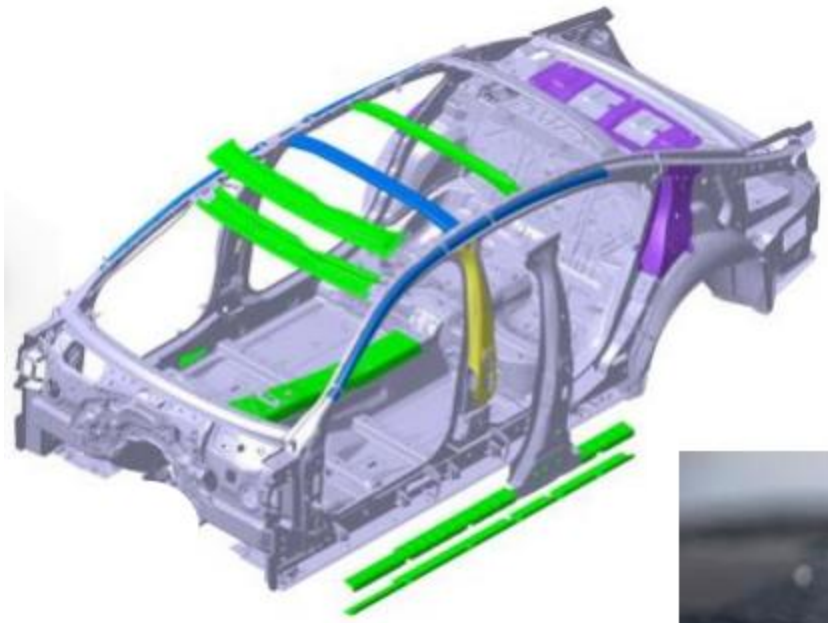

CFRP Wet Compression Molding

CFRP-Steel Hybrid

CFRP Resin Transfer Molding

CFRP Sheet Molding Compound

[example video]

CFRP Wet Compression Molding

CFRP Resin Transfer Molding

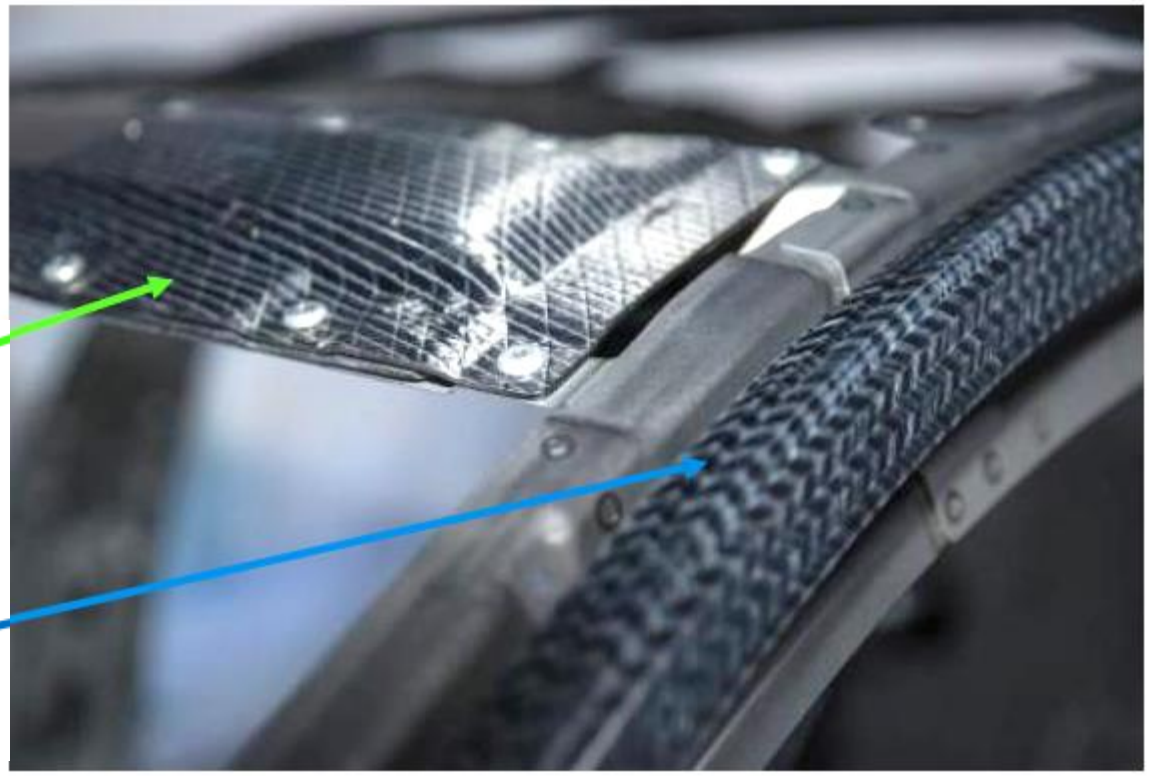

Infusion Process

25 Challenger- Maritime (9 m), Manufacturing Process

Infusion Process

Inspection and maintenance of the mold

Infusion Process

Applying gel coat for color and protection

Infusion Process

Placing glass fabric in the mould

Infusion Process

A nylon bag is placed over the entire hull mould and sealed around it

Infusion Process

Resin is drawn into the mould by using vacuum lines

Infusion Process

Infusion Process

Resin is then cured

Infusion Applications

- Horizon PC58 manufactured by the Horizon Company as a new model of luxury power catamaran (18 m)
- Fiber glass epoxy and Divinycell foam for the sandwich layers

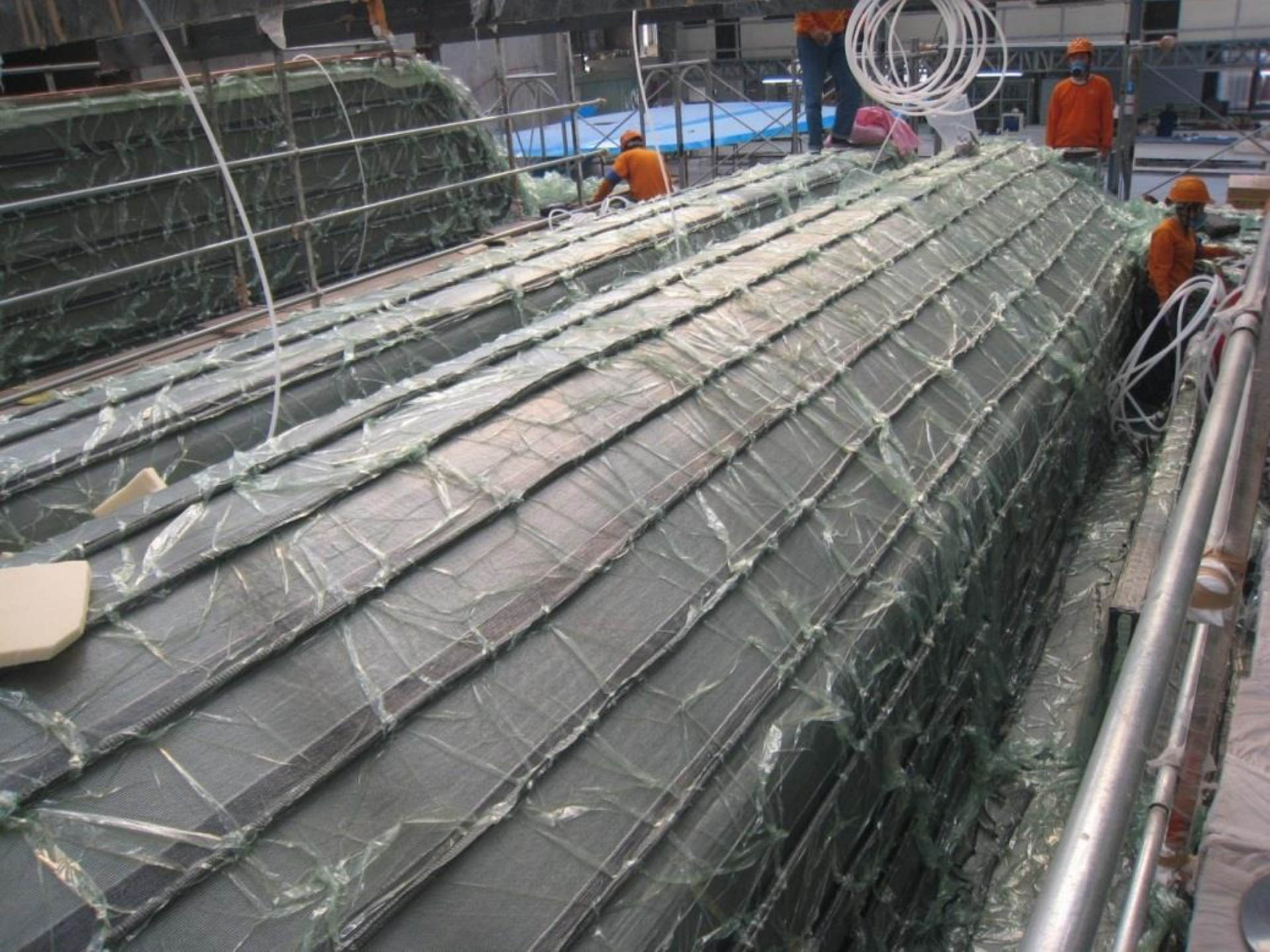

Braiding

Braiding

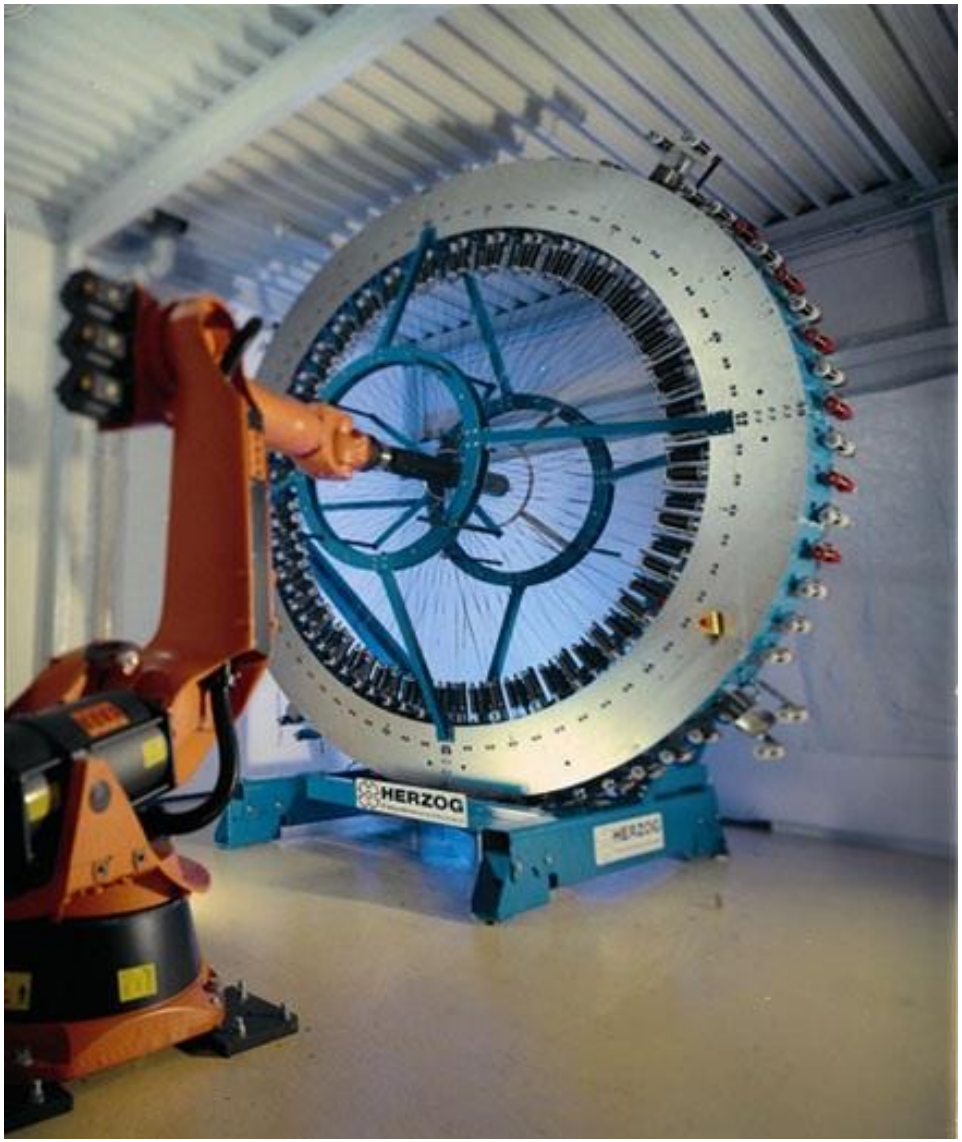

- Radial braider with 144 carriers with a robotic arm
- The speed of the machine can go up to 200 r.p.m.

Braiding Applications

Braiding is used to produce CFRP parts for Lexus LFA using a special 3D carbon-braiding machine .

Braiding Applications

Automated Fiber Placement (AFP)

- AFP uses an automated machine to place fiber onto a tool
- Two main styles:
  - Head mounted on a robotic arm
  - Head mounted on gantry system

Boeing 777x Wing

Boeing 787 Fuselage

AFP example video

Process Simulation

- For proper control of temperature and pressure history during processing, we can take advantage of process simulation.
- Currently, one of the main trends in process simulation is to break down the complexity of the system into several simpler sub-models:
  - Thermo-chemical analysis
  - Resin flow and compaction analysis
  - Stress and deformation analysis

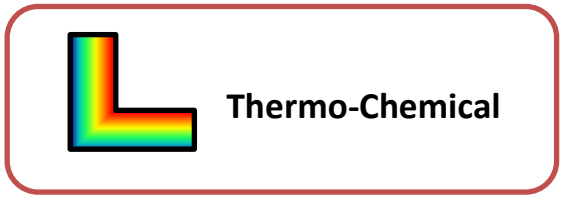

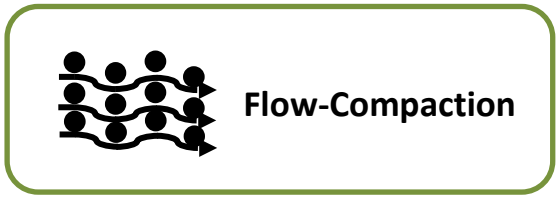

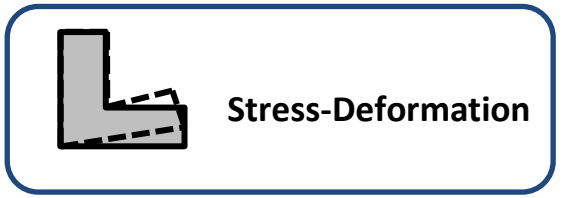

Introduction: Thermo-chemical reaction

- *Thermo-chemical reaction of the resin:*
  - Polymerization of thermoset resins is an exothermic reaction and heat is generated during the curing process. Usually, the heat of reaction is not enough to fully cure the resin and external heat is needed to advance the curing of resin. By providing enough external heat during the fabrication process, a desirable degree of cure (DOC) throughout the part is achieved. However, too much heat (sum of external and internal heats) damages the resin by burning it.

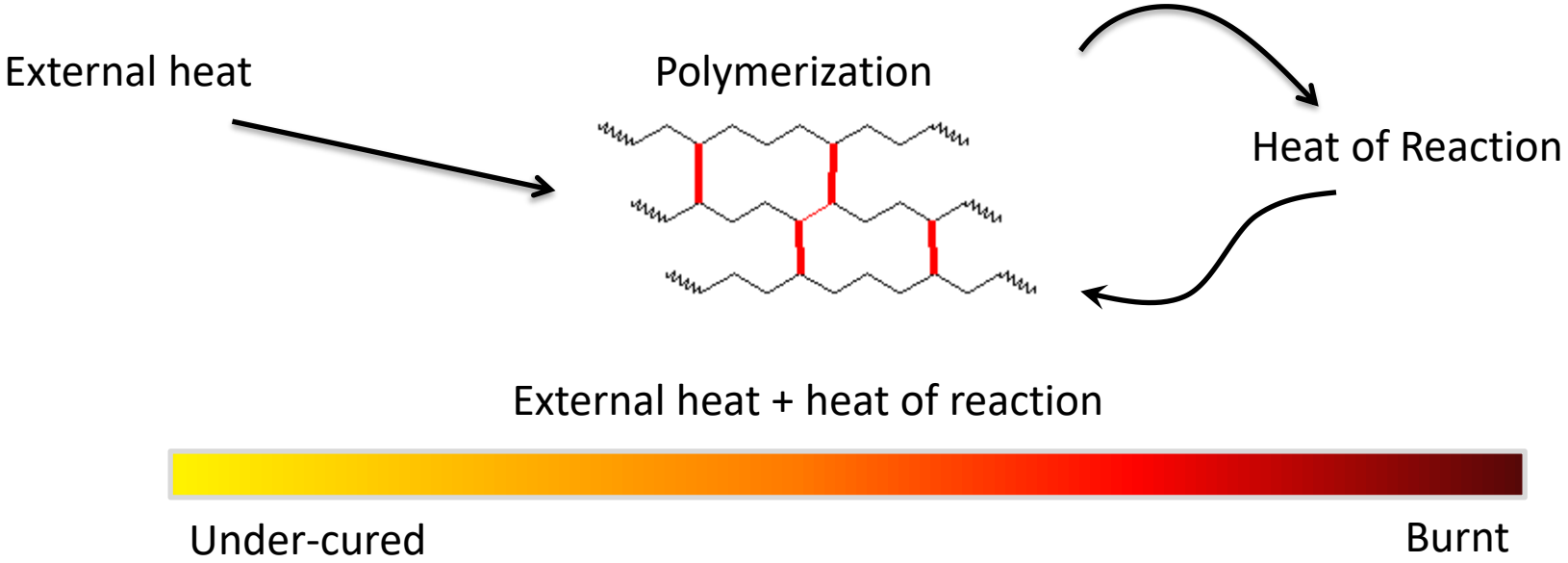

Introduction: Flow and Compaction

- *Resin flow and fiber compaction:*
  - At the beginning of the fabrication process and while the resin is still in its liquid form (before gelation), by increasing the temperature, resin viscosity drops significantly. This drop in viscosity combined with the applied pressure on the part, helps to remove trapped air bubbles in the resin through bubble migration or bubble collapse. Although heat is needed to reduce the viscosity of resin, too much heat might result in early gelation of the part before bubbles get a chance to migrate or collapse.

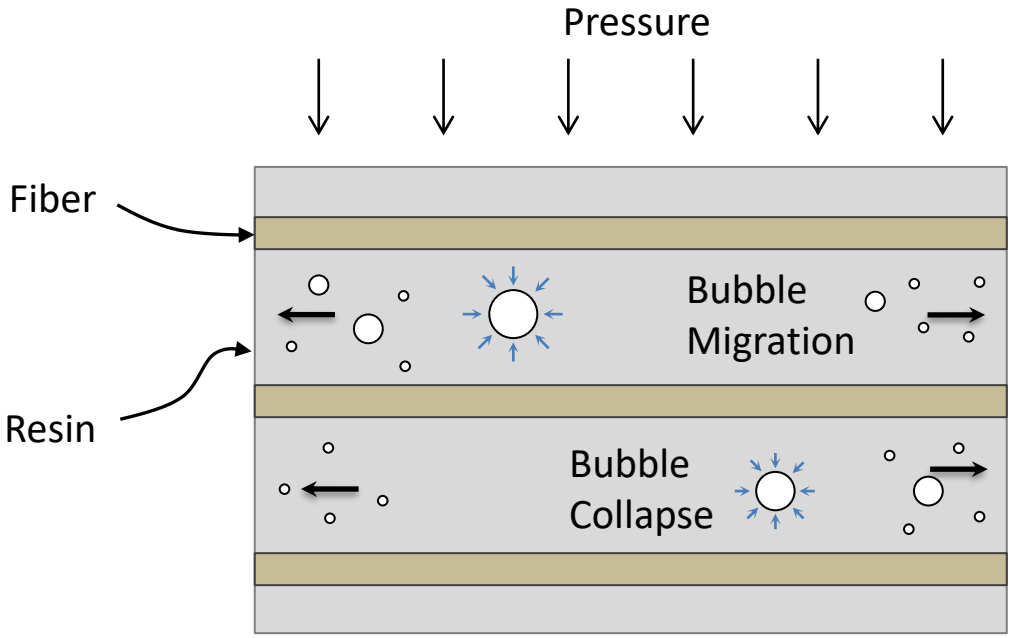

Introduction: Residual Stress and Dimensional Changes

- *Residual stress formation and dimensional changes:*
  - Composite materials have high through-thickness CTE (Coefficient of Thermal Expansion) and low in-plane CTE along the fiber direction. Tool CTE is usually different than the part CTE as well. Aside from mismatch of CTEs, during the polymerisation process, resin shrinks while fibers do not shrink. These mismatch of free strains (sum of thermal strains and resin shrinkage) between fibers, resin and tool, results in the formation of residual stresses during the fabrication process. This leads to dimensional changes in the composite part including warpage of flat parts and spring-in of curved parts.

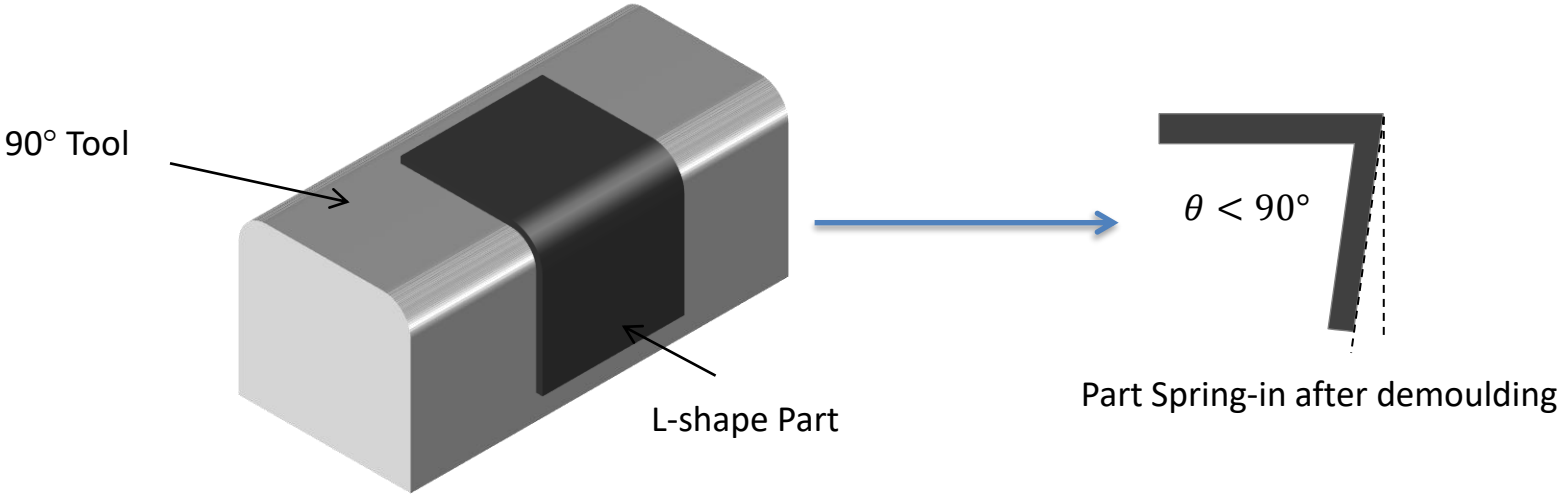

Introduction: Residual Stress and Dimensional Changes

– For example, warpage formation in flat composite parts is explained here. At the beginning of the fabrication process, as the part and tool are heated together, tool expands while the part doesn't expand as much as the tool due to the low CTE of the fibers (a). This creates a through-thickness residual stress distribution in the part due to ply slippage while the resin is still soft (b). After demoulding, this residual stress creates warpage in the part (c).

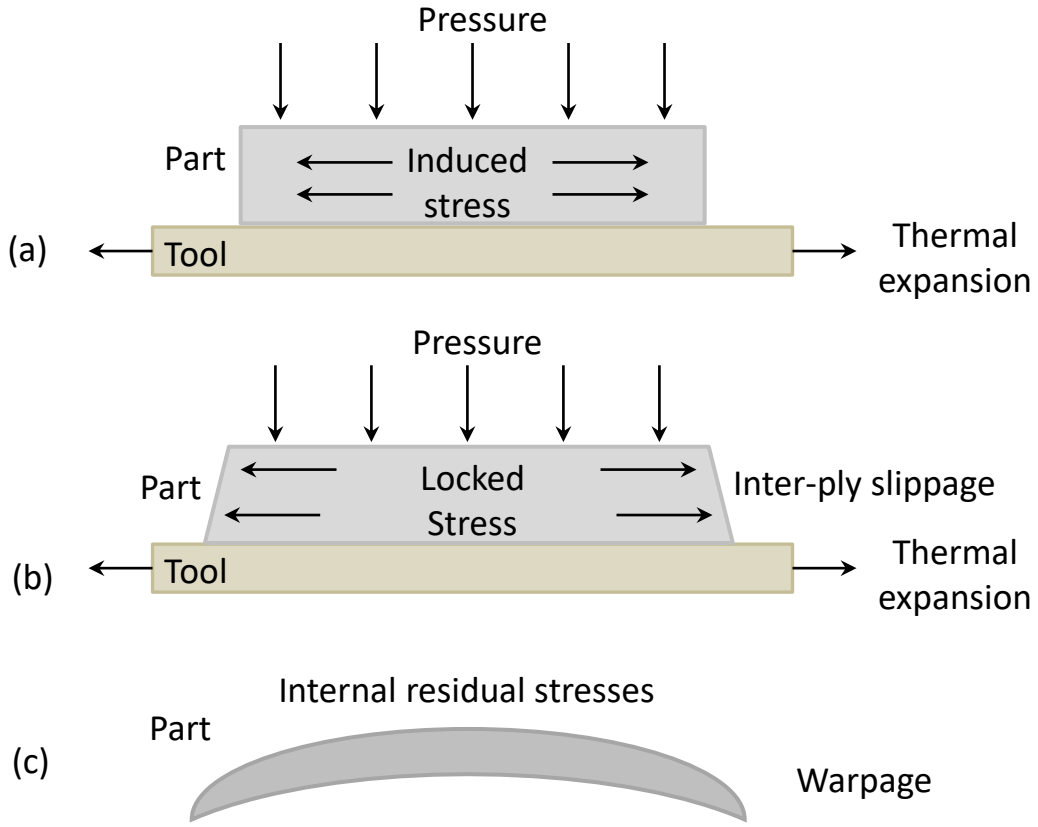

	Process Simulation			Experiment
Thermo-Chemical Analysis	1D 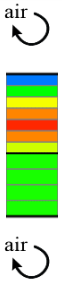	2D 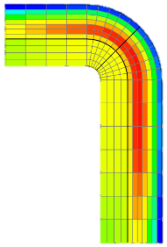	3D 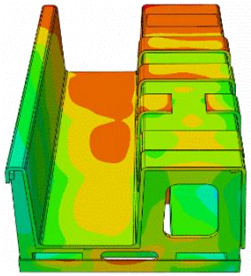	
Stress-deformation Analysis	2D (PVE) 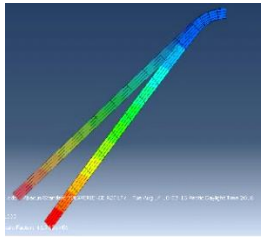	2D (VE) 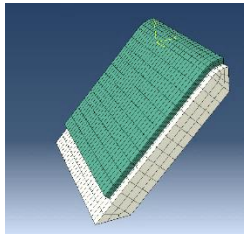	3D (TVE) 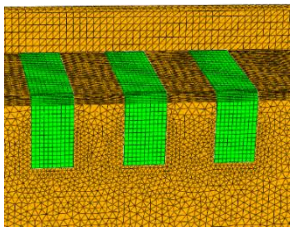	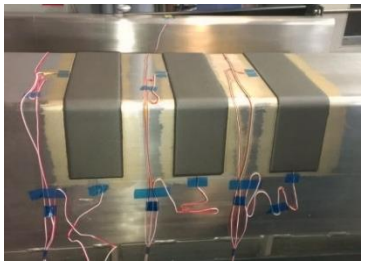
Flow and Compaction Analysis	Fast SPH 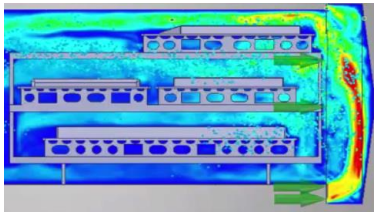	RANS-based 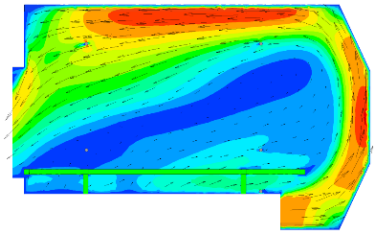		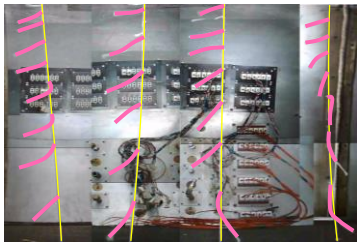
	Resin/Gas coupled flow 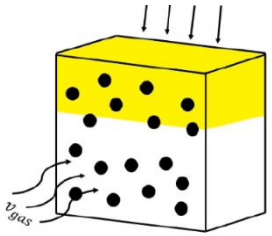	3D infusion 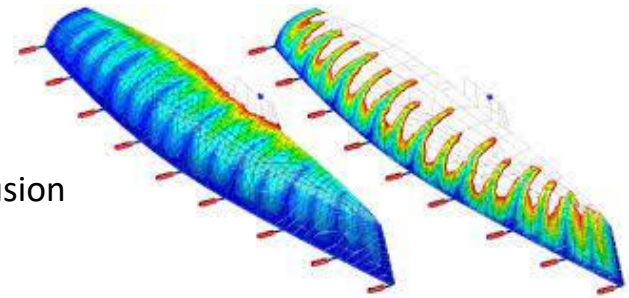		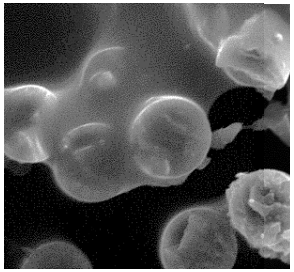

Thermo-chemical Analysis: A Cooking Analogy

- While cooking chicken, uneven thicknesses create problems.
- Thin sections are cooked first and become dry while thick sections may be partially cooked by the end
- We try to cook the chicken to an even temperature of 165 °F

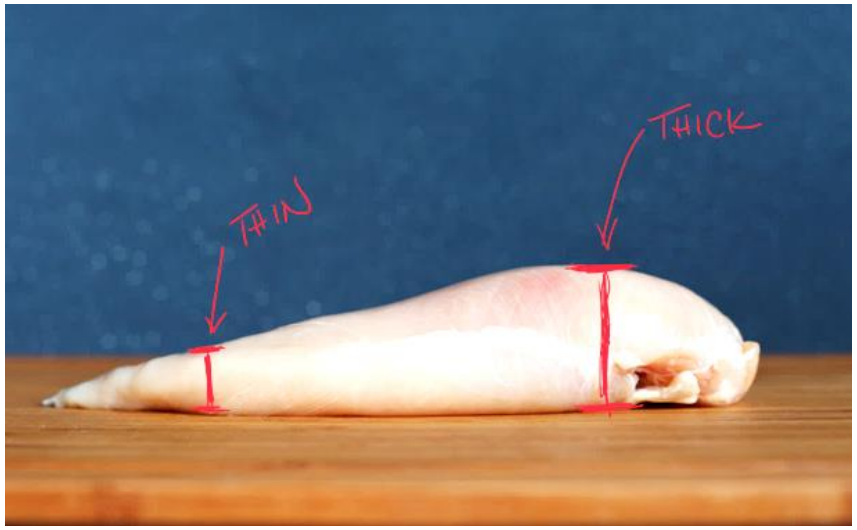

< 160 °F	165 ± 5 °F	> 170 °F
Uncooked	Cooked	Dry/Burnt

This is similar to the specifications in composites manufacturing

Thermo-chemical Analysis: A Cooking Analogy

- For a more accurate temperature control, it is better to slowly cook the chicken in a convection oven:
  - Airflow increases the rate of heat transfer and creates a uniform temperature distribution
  - Slow heating rates and long cooking times ensure uniform cooking

- This is similar to thermal management in composites manufacturing
- The main difference is the heat generation in the composite part due to the exothermic reaction
- Unlike cooking, due to cost consideration, engineers try to avoid slow heating rates and long cooking times

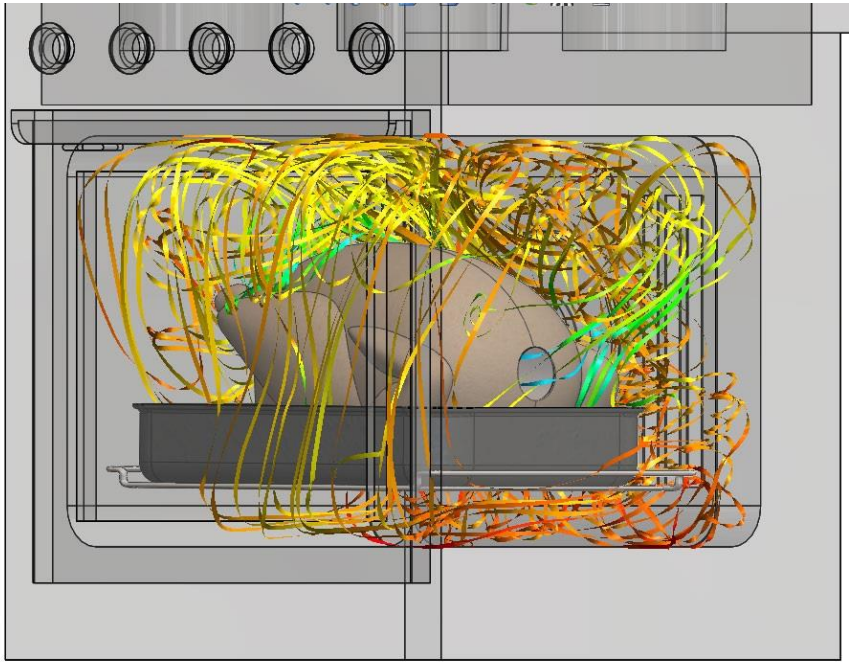

Equipment: Autoclave - Airflow

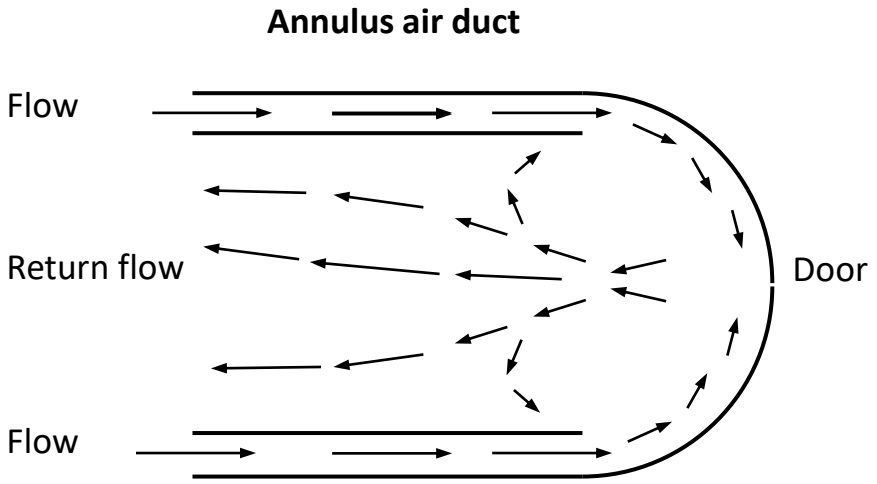

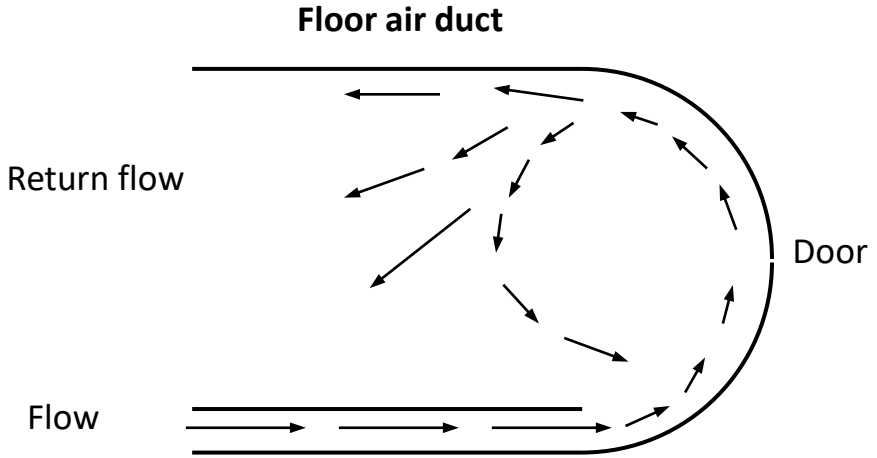

Equipment: Autoclave - Airflow

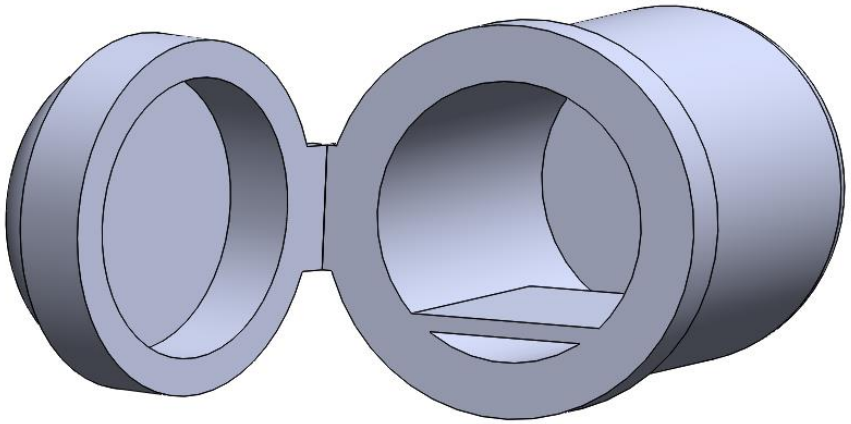

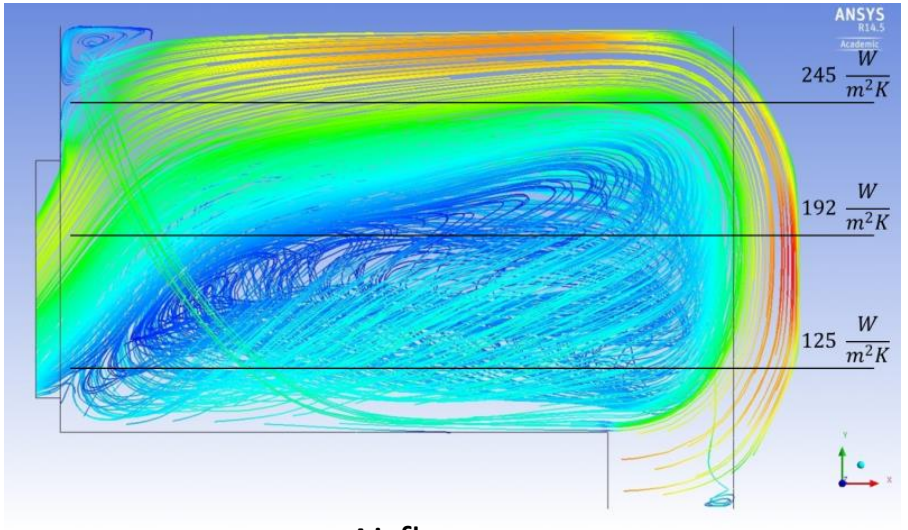

Airflow

Convective Curing of Thermoset Composites

- In convective curing (e.g. autoclave or oven curing) part and tool are heated together using convection to cure the composite part.
- Following figure, for example, schematically shows the cross-sectional view of a typical production autoclave which is loaded with three tools and parts.

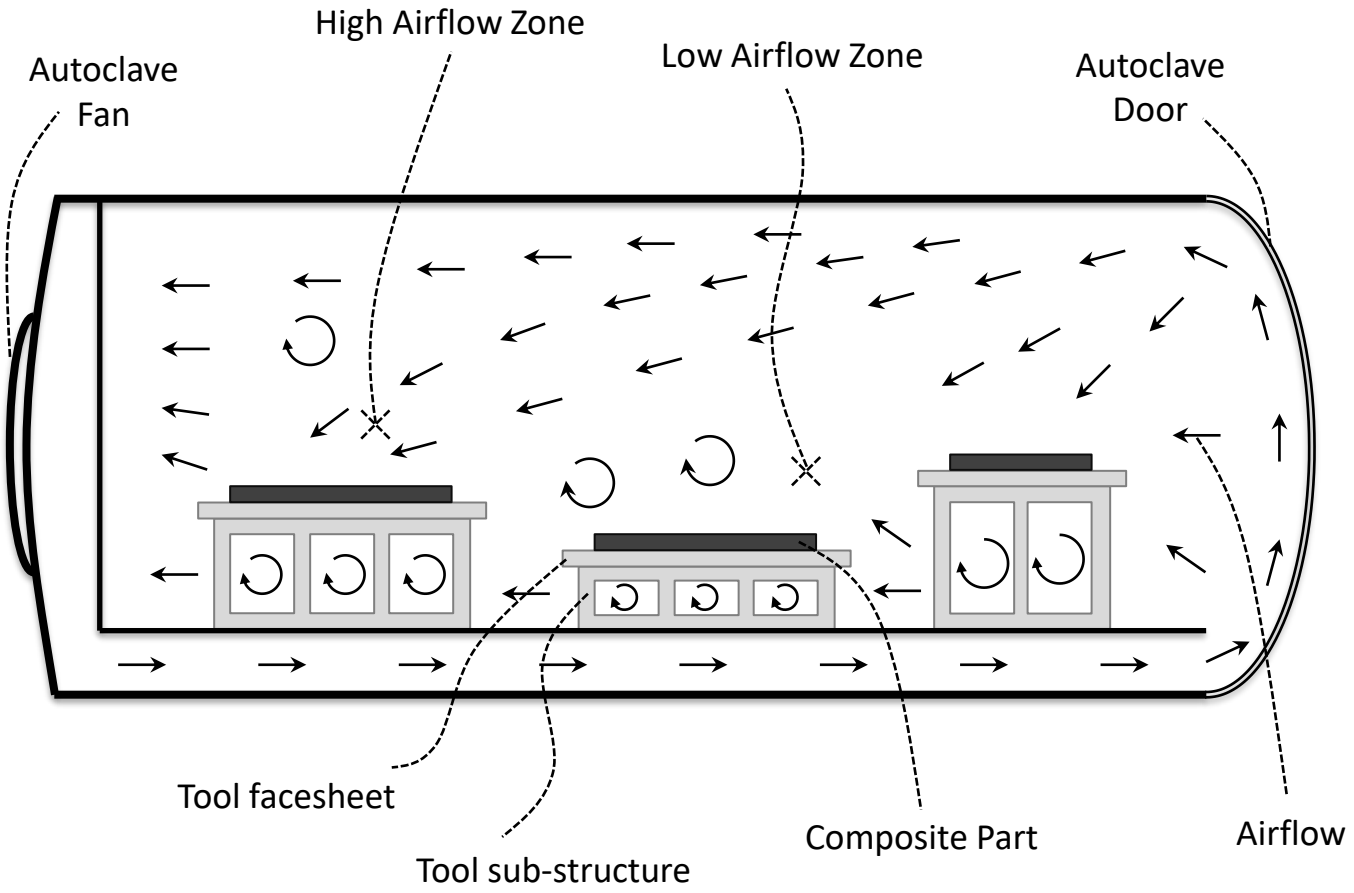

Tool - Thermal Management: Effects of Sub-structure

Good airflow: High HTC

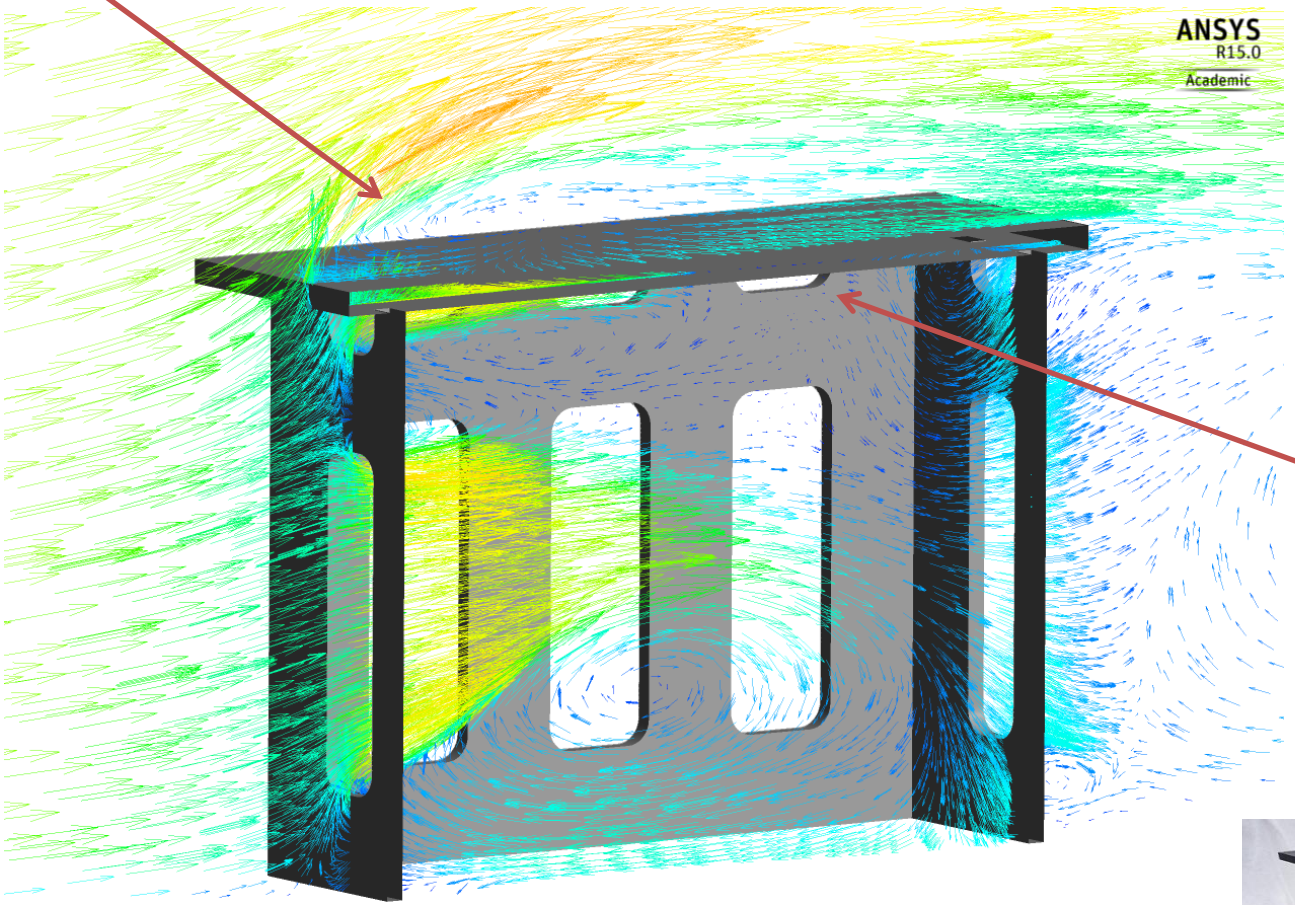

Bad airflow:
Low HTC

CFD analysis on half of a steel tool

IR Thermography To Evaluate BCs

- Tools were vacuumed bagged and then spray painted with a matte paint.
- They were heated in an autoclave before the door was opened quickly and an IR image was taken. Using temperature distribution and FE, heat transfer coefficients were back calculated:

Tool Covered with Painted Vacuum Bag

Distribution of Heat Transfer Coefficients

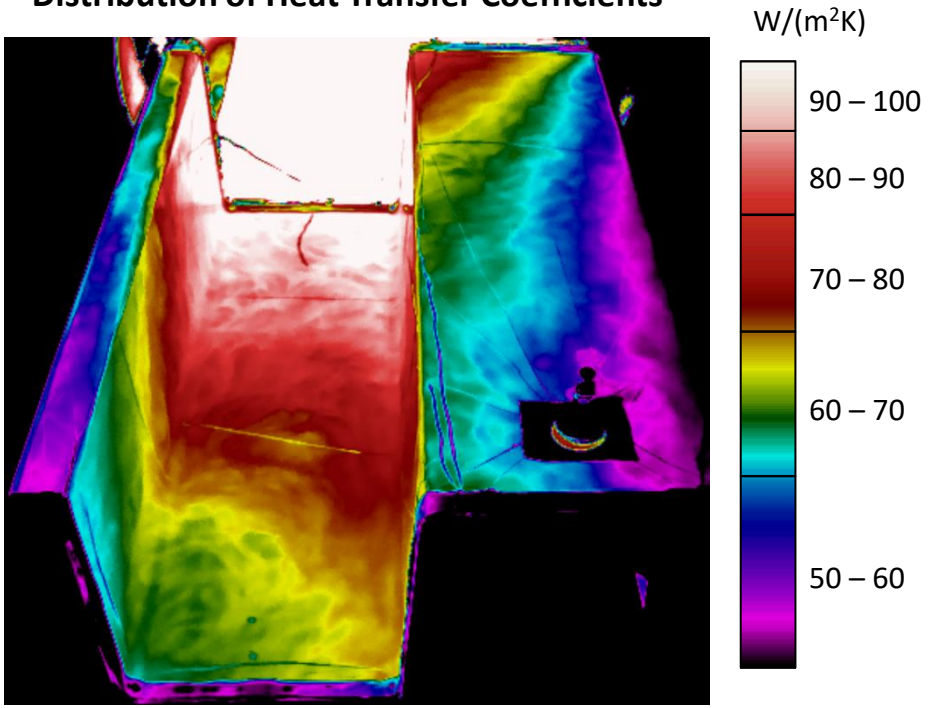

Thermo-Chemical Analysis of Composites

- Approximately, we can simplify the complex 3D thermo-chemical problem into a 1D problem.
- This is because through-thickness heat transfer is the dominant mechanism away from the edges and sub-structures.

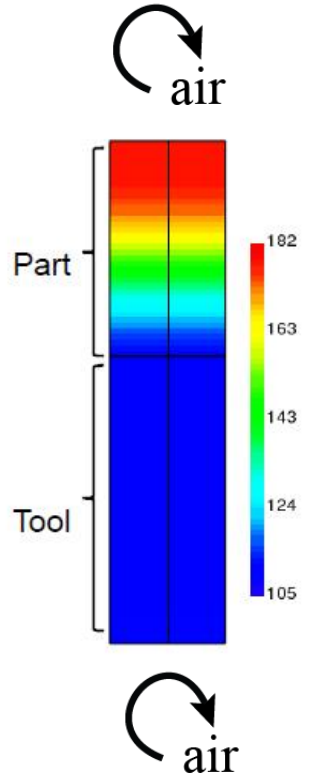

1D approximation

$$\frac{\partial}{\partial t}(\rho C_P T) = \frac{\partial}{\partial x}\left(k_{xx}\frac{\partial T}{\partial x}\right) + \frac{\partial}{\partial y}\left(k_{yy}\frac{\partial T}{\partial y}\right) + \frac{\partial}{\partial z}\left(k_{zz}\frac{\partial T}{\partial z}\right) + \dot{q}$$

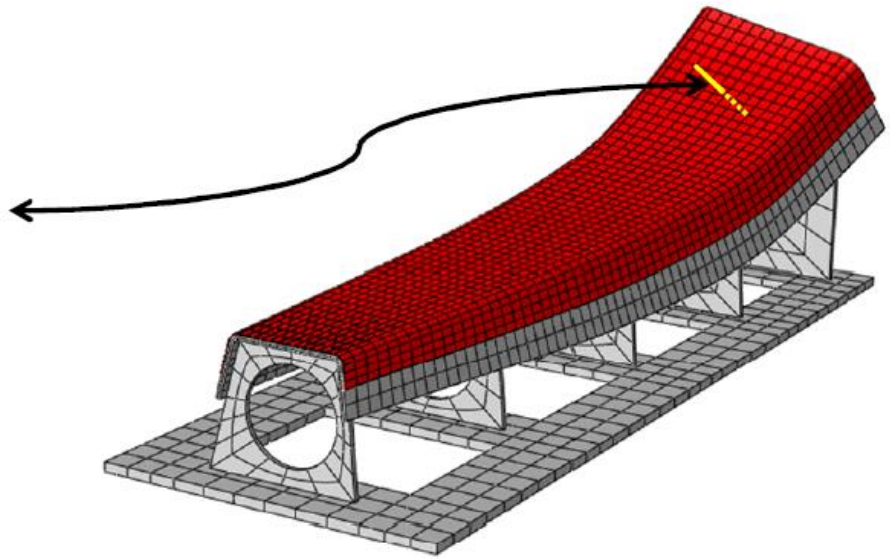

3D thermo-chemical problem

Commercial Simulation Tools

- Simulation tools are available for thermal management in composites manufacturing.

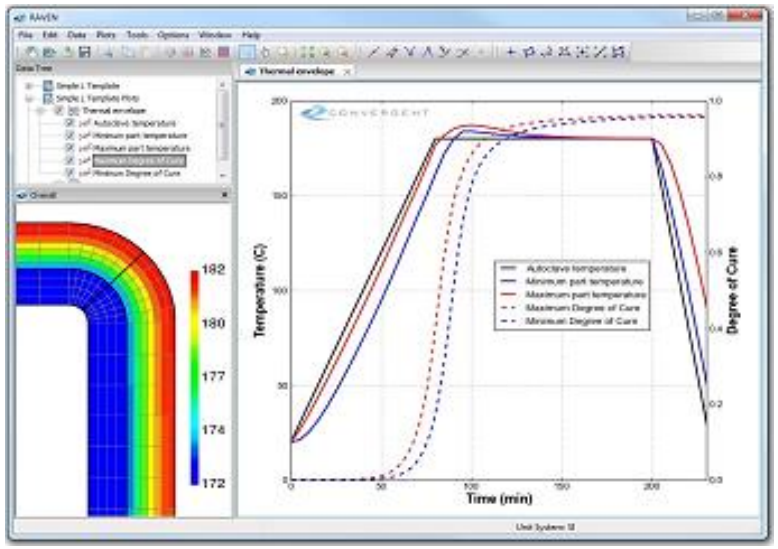

RAVEN

0D, 1D, Limited 2D

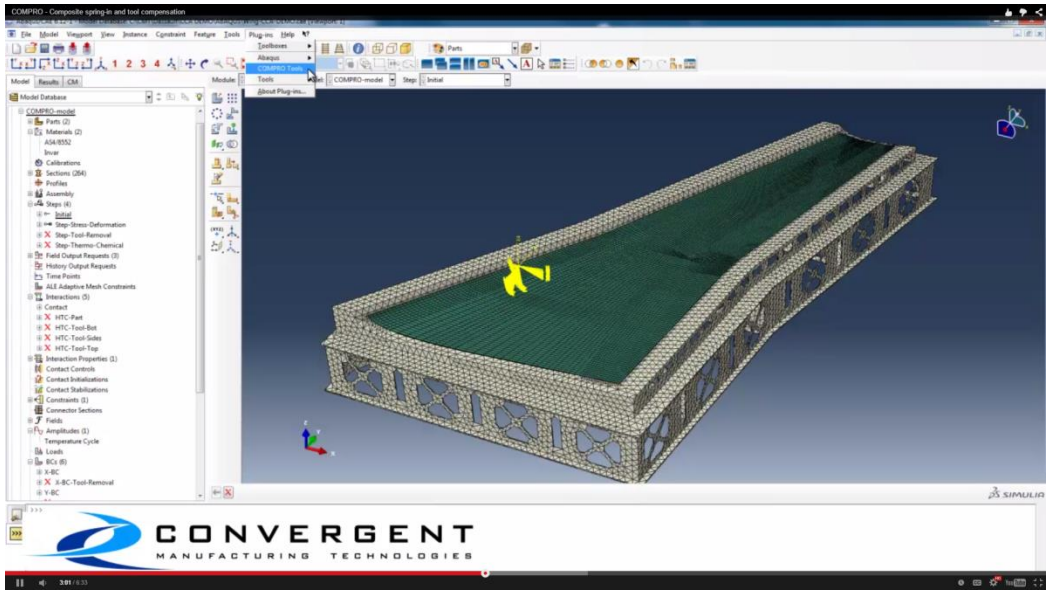

COMPRO 3D

1D System Definition: Autoclave/Oven Curing

- Heat transfer to the composite part:
  - Convective heat transfer from top of the part and bottom of the tool
  - Conductive heat transfer through the tool
- During the heat-up step, the tool transfers the heat to the composite part. During curing, tool acts as a heat sink for the exotherm energy.

System definition

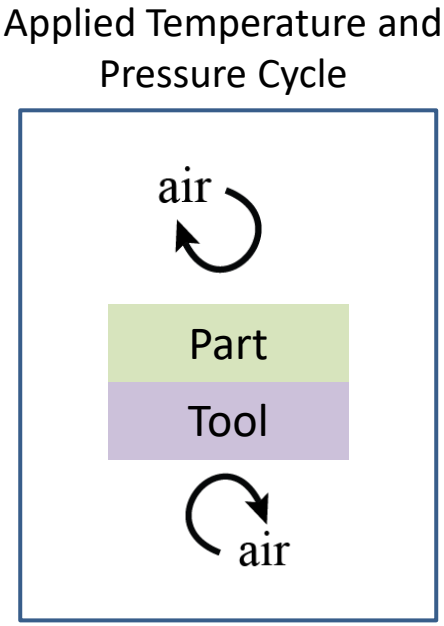

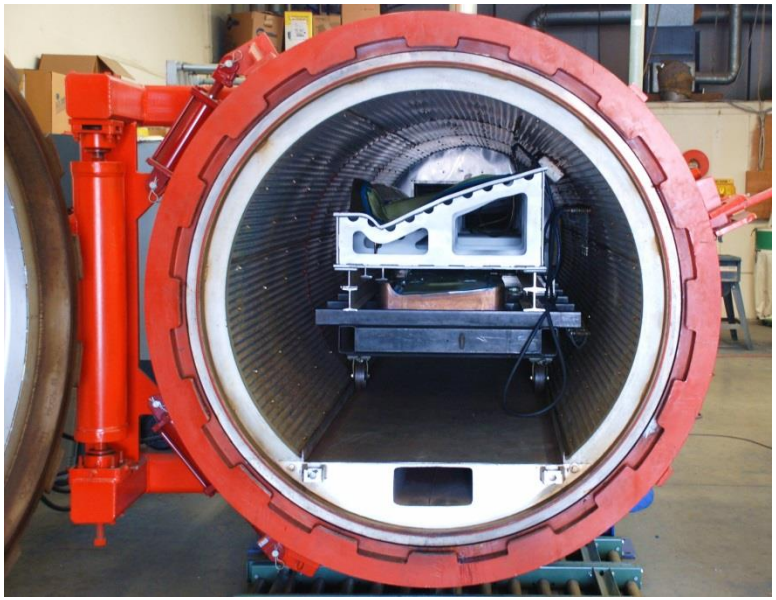

Heated mould: Closed-mould Process

- Heat transfer to the composite part:
  - Conductive heat transfer through the tool
- Manufacturing processes such as Compression Moulding or RTM use this curing process.

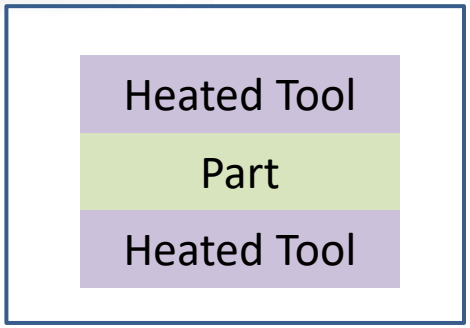

System definition

Heated Mould: 1-Sided mould

- Heat transfer to the composite part:
  - Mainly conductive heat transfer through the tool side
- Manufacturing processes such as infusion use this curing process.

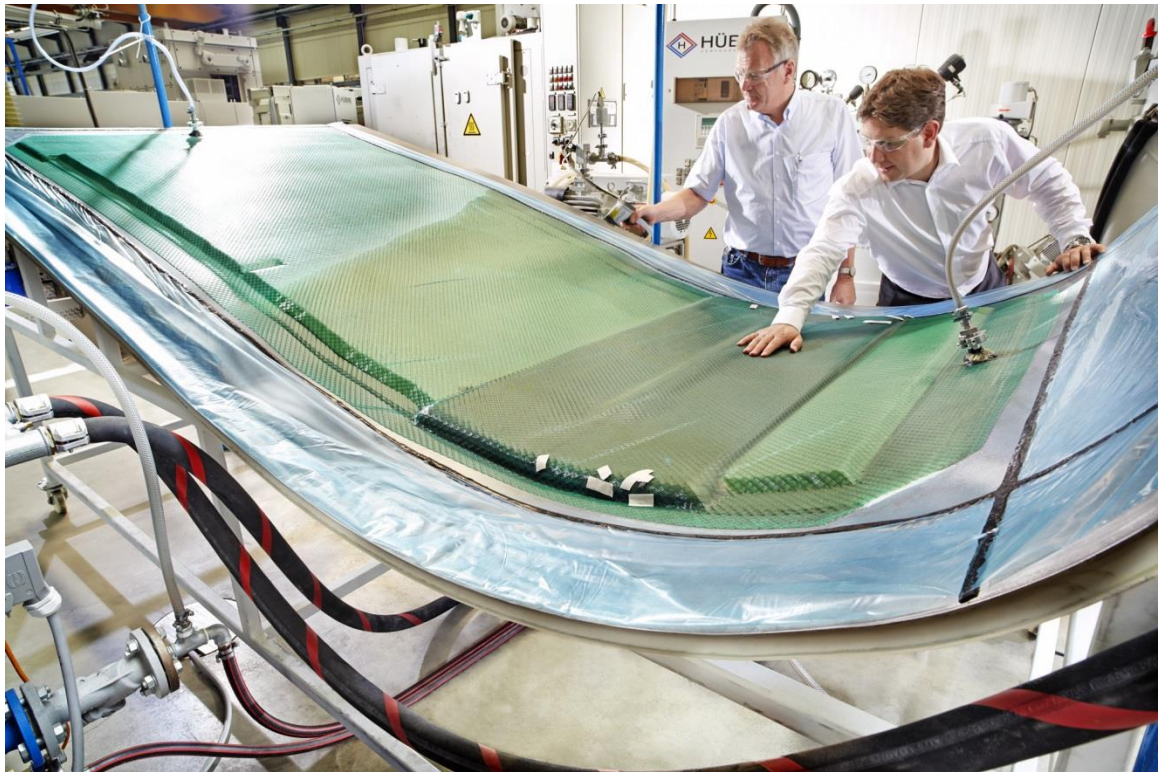

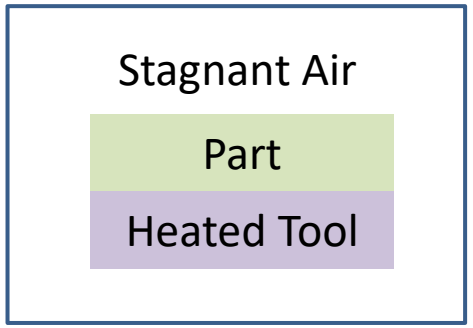

System definition

Room Temperature Curing

- Room temperature curing has very low heat transfer through the boundary (stagnant air). Consequently, there is low control over the curing process with wide distribution of temperature.

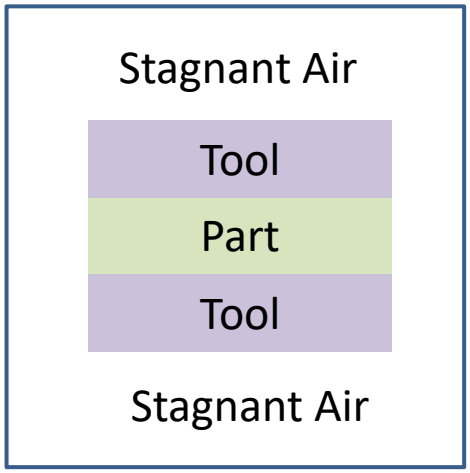

System definition

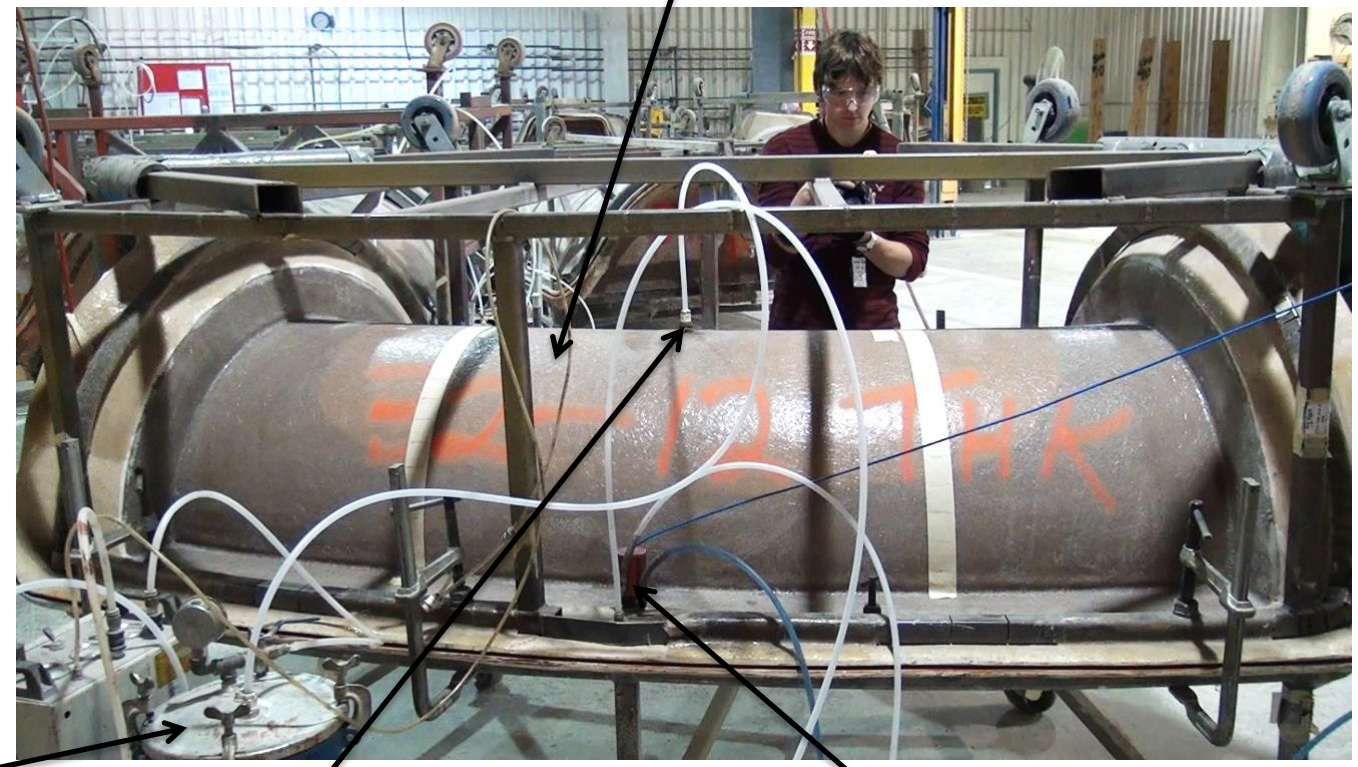

Room Temperature Curing

Wide PROCESSING TEMPERATURE DISTRIBUTION

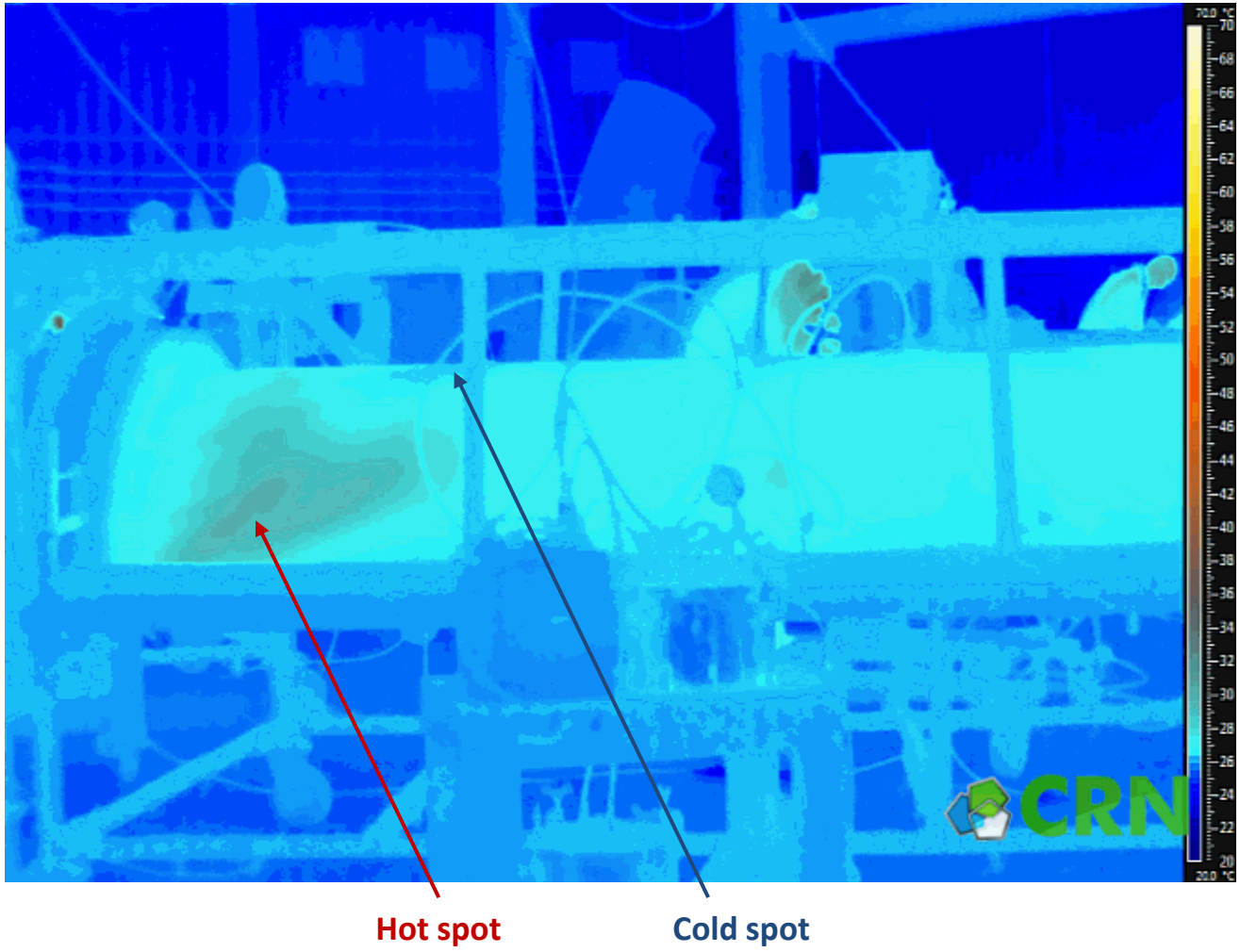

Summary: Different Curing Processes

Autoclave/Oven

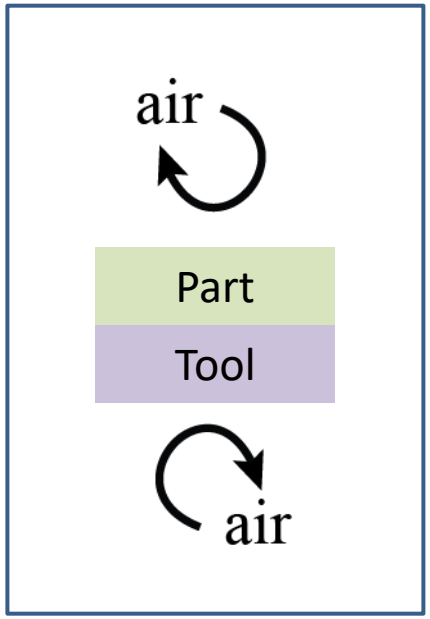

Applied Temperature and Pressure Cycle

- Aerospace
- Space
- Defense
- High-end Automotive
- Sport

Hot Press/ Heated Mould

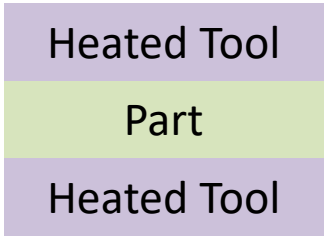

- Automotive
- Aerospace
- Sport

1-Side Heated Mould

Stagnant Air

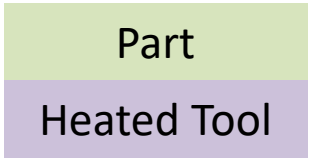

- Wind Energy

Room Temperature Cure

Stagnant Air

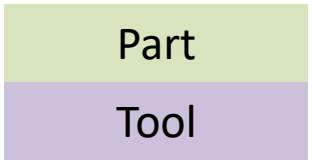

Stagnant Air

- Marine
- Sport
- Construction
- Industrial

1D Thermo-Chemical Analysis: Heat-up Step

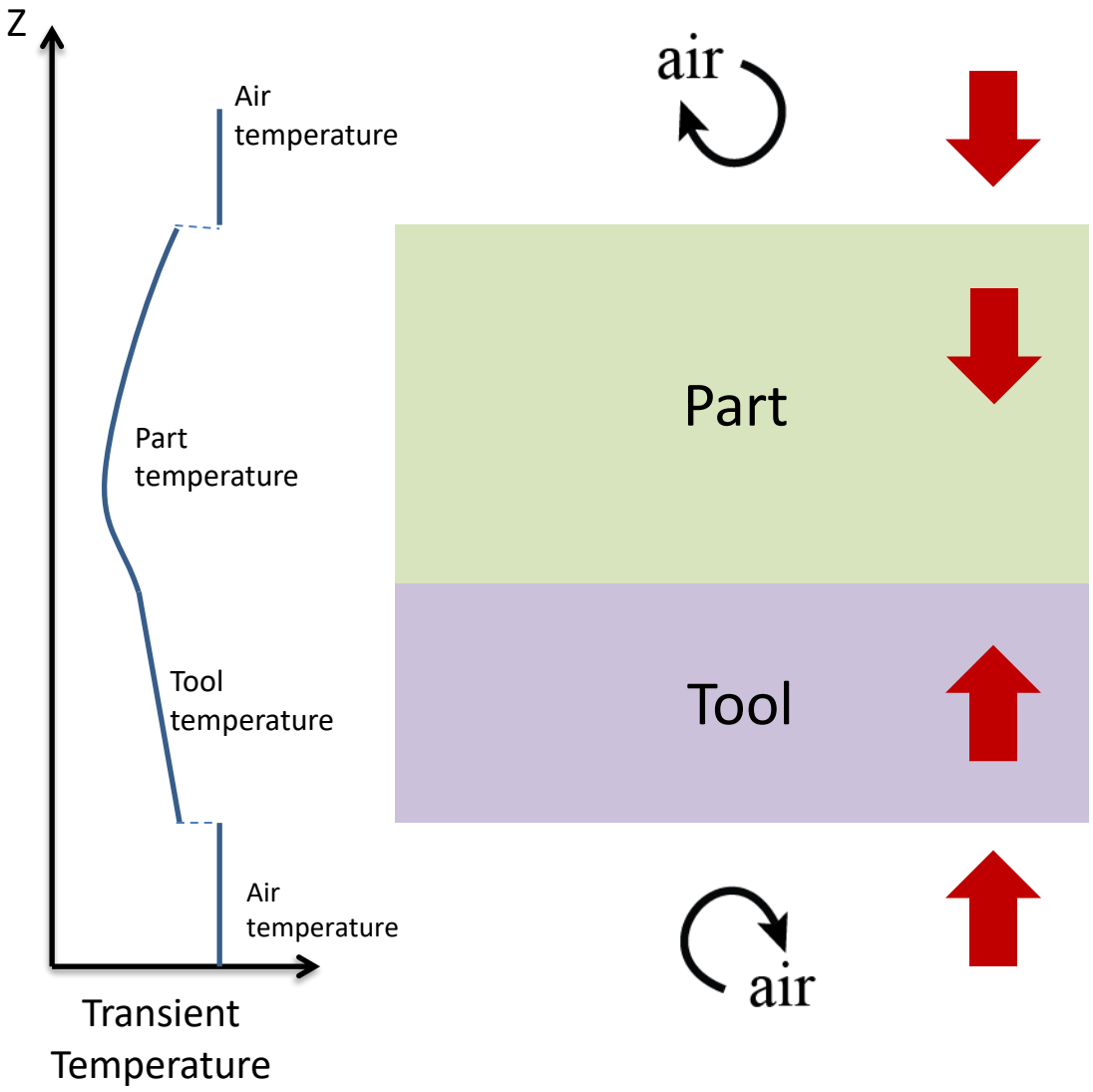

Rate of heat transfer by convection

$$\dot{Q} = HTC \times A \times \Delta T$$

Energy balance:

$$\frac{\partial}{\partial t}\left(\rho C_p T\right) = \frac{\partial}{\partial z}\left(k\frac{\partial T}{\partial z}\right)$$

rate of heat increase = rate of heat addition by conduction

Rate of heat transfer by convection

$$\dot{Q} = HTC \times A \times \Delta T$$

1D Thermo-Chemical Analysis: Polymerization Step

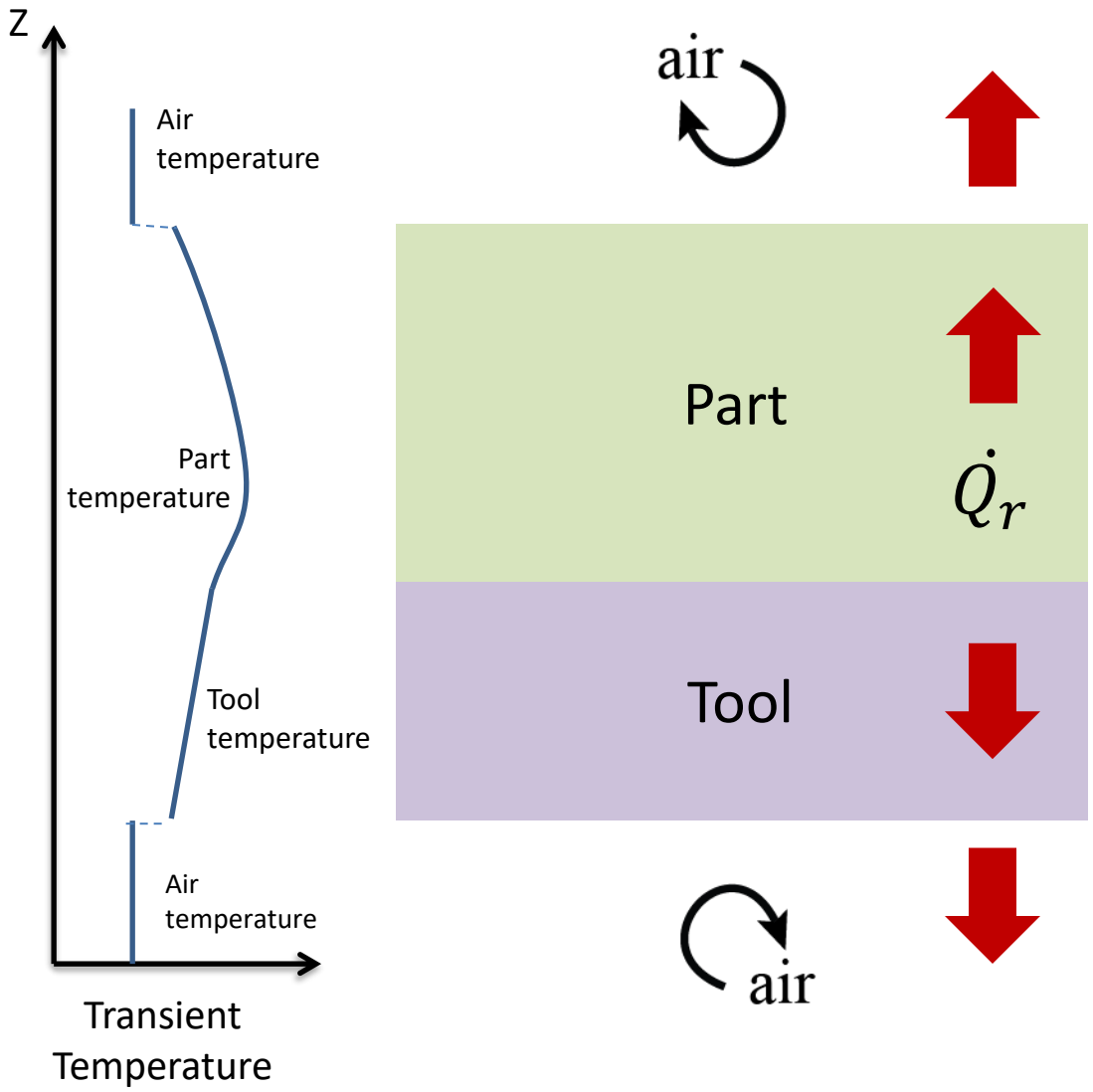

Rate of heat transfer by convection

$$\dot{Q} = HTC \times A \times \Delta T$$

Energy balance:

$$\frac{\partial}{\partial t}(\rho C_p T) = \frac{\partial}{\partial z}\left(k\frac{\partial T}{\partial z}\right) + \dot{Q}_r$$

rate of heat increase = rate of heat addition by conduction + rate of resin heat generation

Rate of heat transfer by convection

$$\dot{Q} = HTC \times A \times \Delta T$$

Cure Cycles

- Resin manufacturers usually recommend cure cycles (i.e. recipes).
- Here is a Manufacturer's recommended temperature cure cycle (MRCC) for the 8552 Epoxy resin:

Manufacturer: Hexcel

Resin: 8552 Epoxy

Usual Application: Aerospace

Autoclave Manufacturing

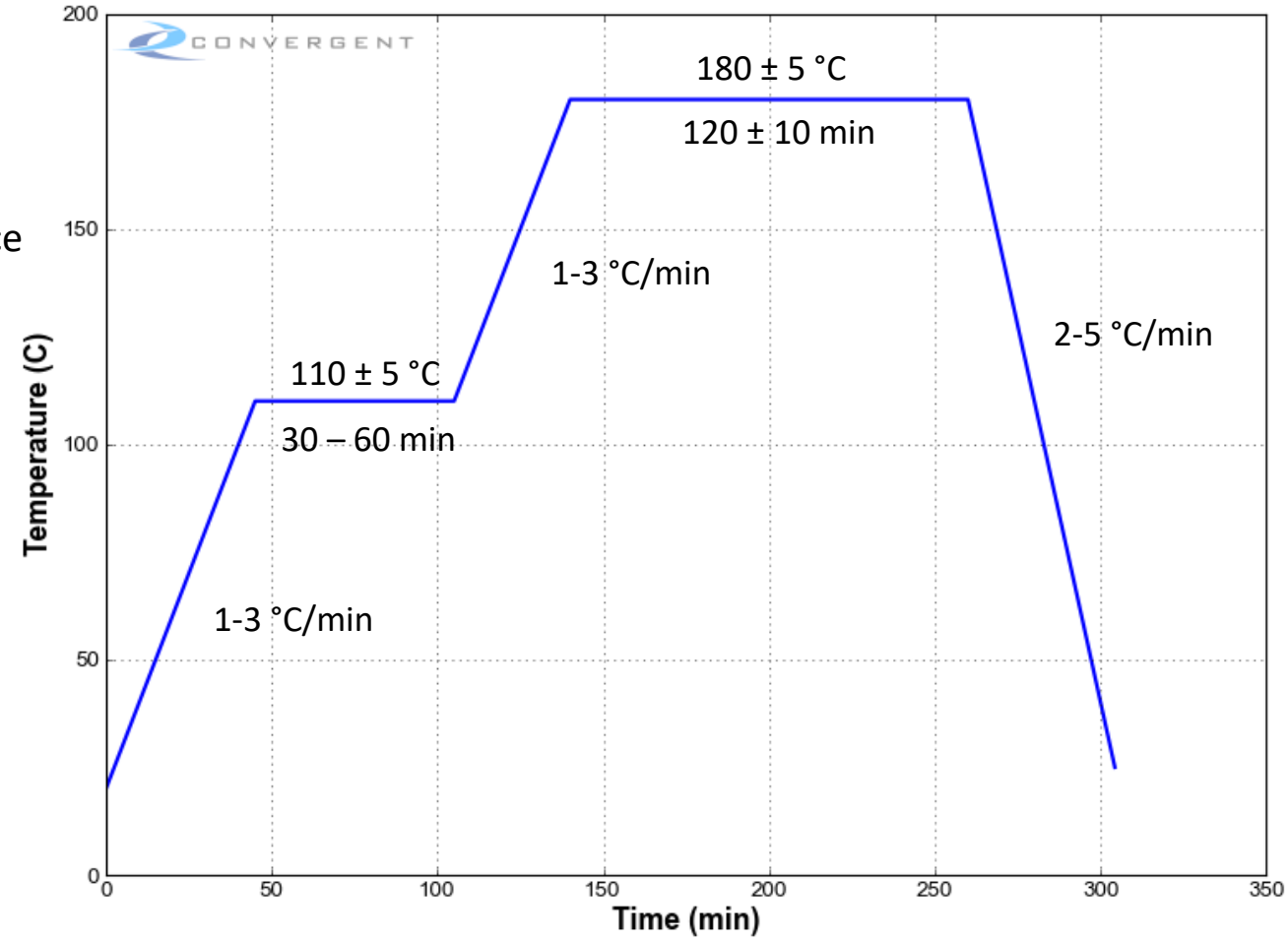

Cure Cycles vs. Specs

- Temperature limits for the part are defined by specs (industry dependent). For a part to be approved, during the manufacturing process, temperature of every point in the part should be within the defined bound.

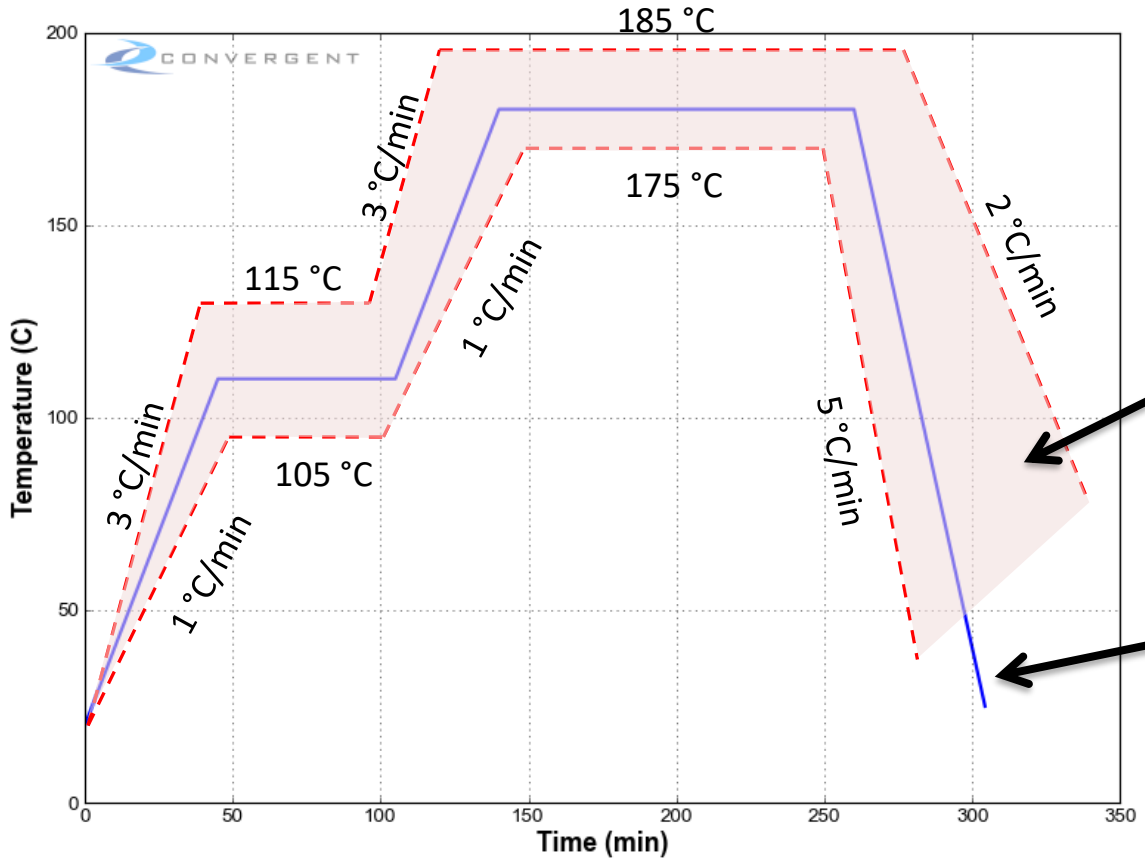

Specs: Temperature limits for the part (depends on the industry)

MRCC: Suggested cure cycle by the resin supplier

Example: Acceptable Cure Cycle

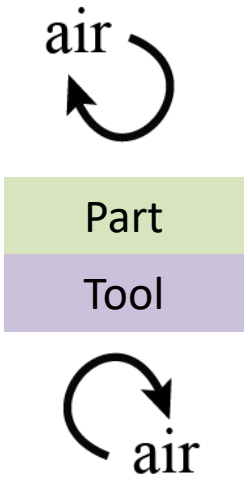

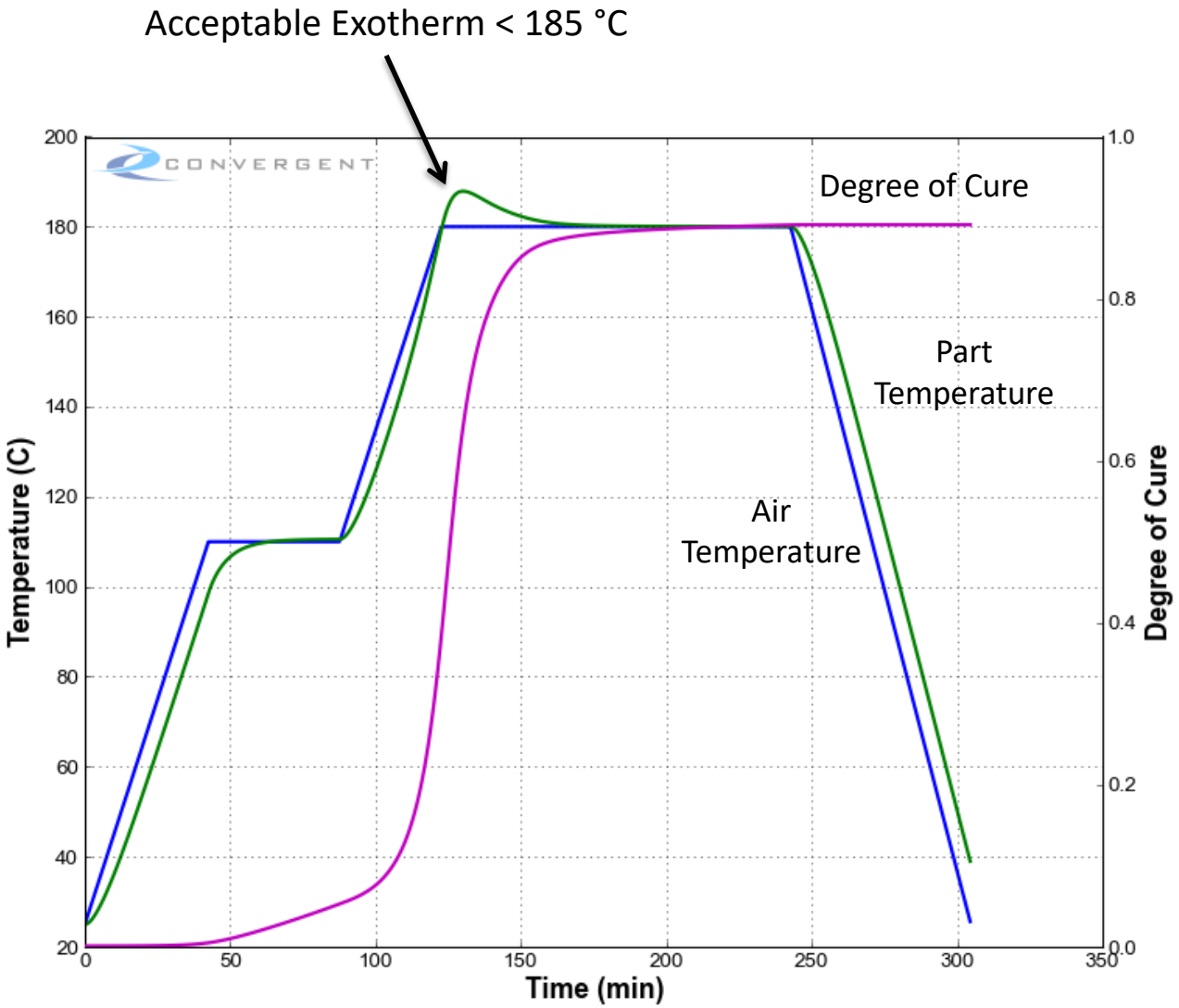

Example Problem: Tooling Material Selection

- Investigate the effect of the tooling material used to process a composite part made of Toray 2510 P707AG-15
- Select the tooling material that minimizes the exotherm and the thermal lag of the part

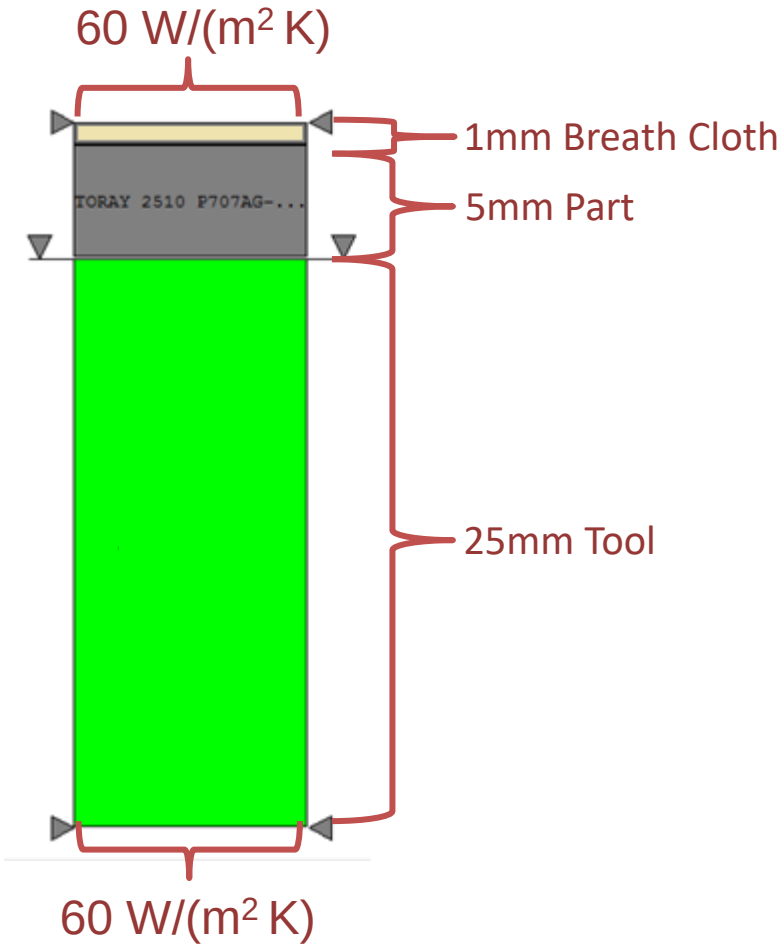

Example Problem: Tooling Material Selection

Part temperature (Top) summary:

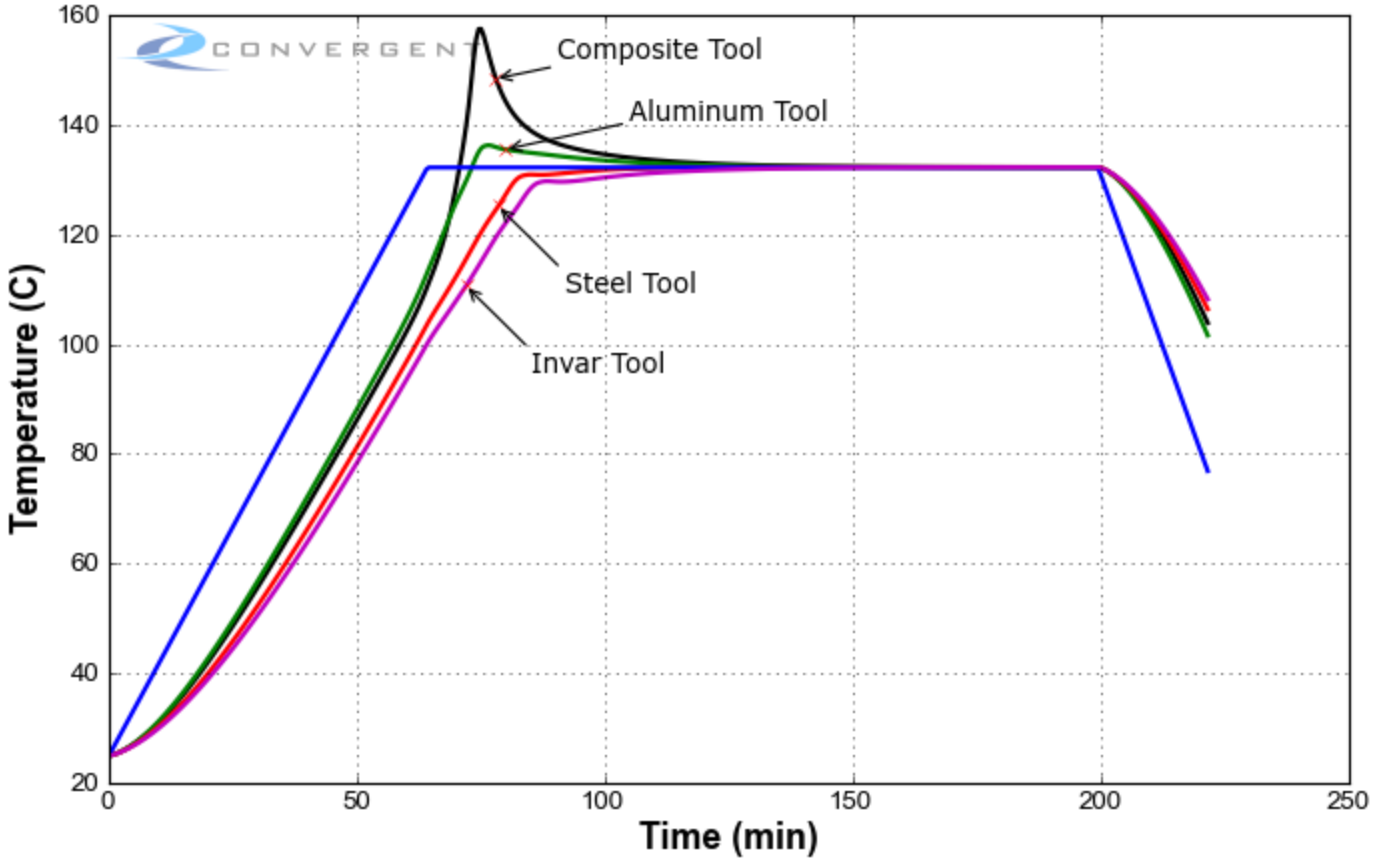

Case Study: Fabricating C-Shape Parts in an Autoclave

- Thermocouple data provided by The Canadian Composite Manufacturing R&D Inc.
- C-shaped laminates @ 16, 32, and 64 ply thickness
- T800H/3900-2 and IM7/5320-1 plain weave CFRP prepreg
- Single hold cycle: 1.7°C/min to 2-hour hold (180 or 120°C)

Rear of Vessel

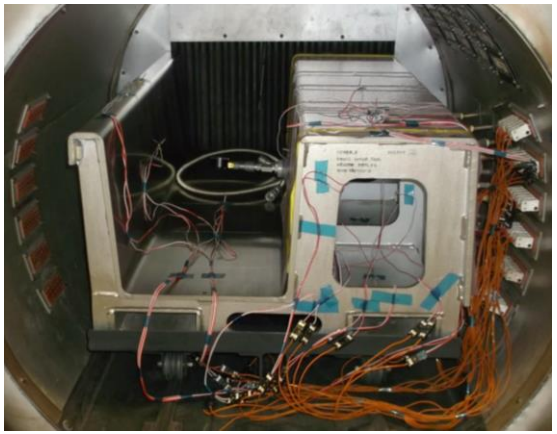

Front (Door facing)

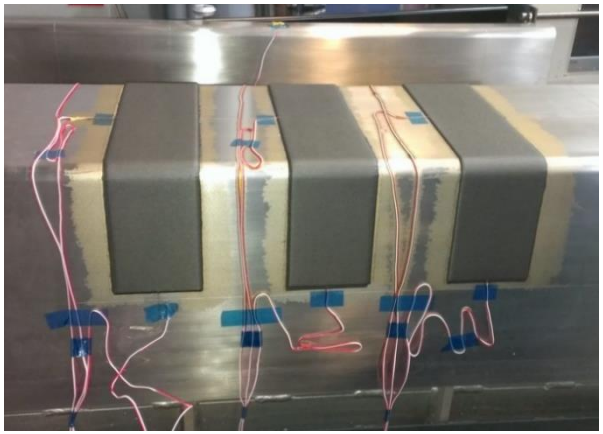

As Cured

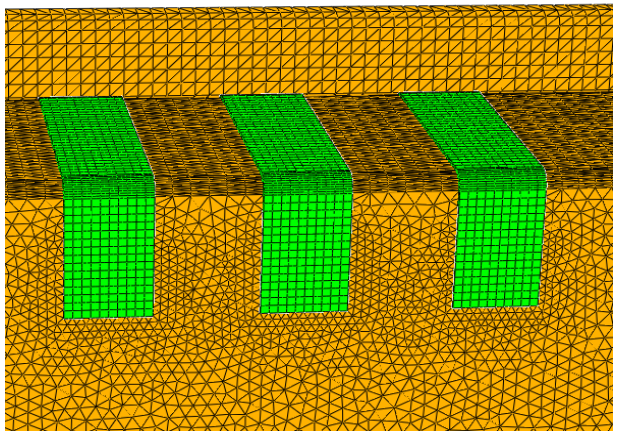

Digital Representation

Simulation Approach

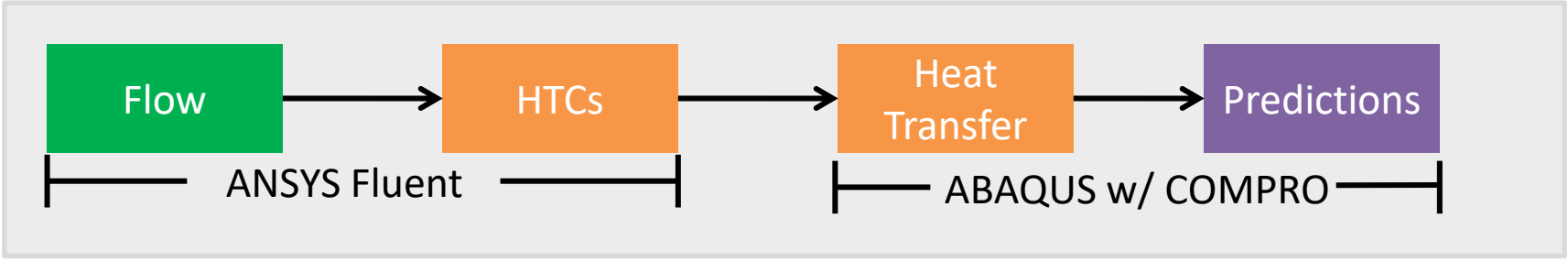

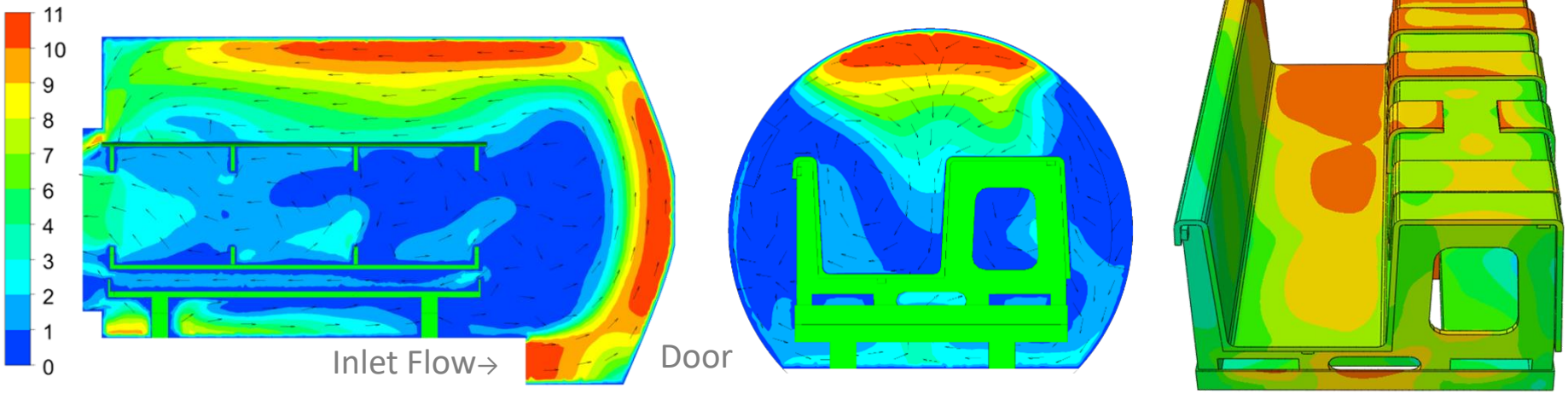

Flow Simulation and Characterization

Empty Autoclave
6.5 ft. (L) x 5 ft. (D)

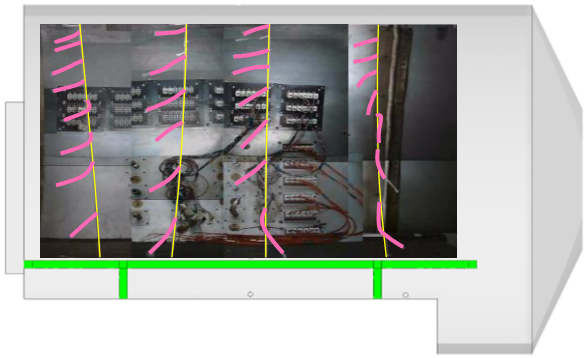

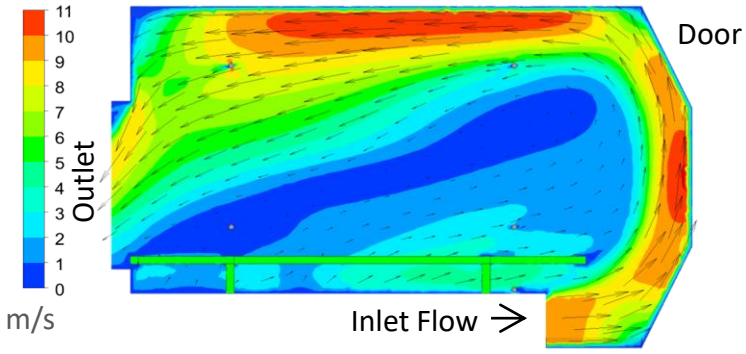

Small Tool
1 ft. (L)

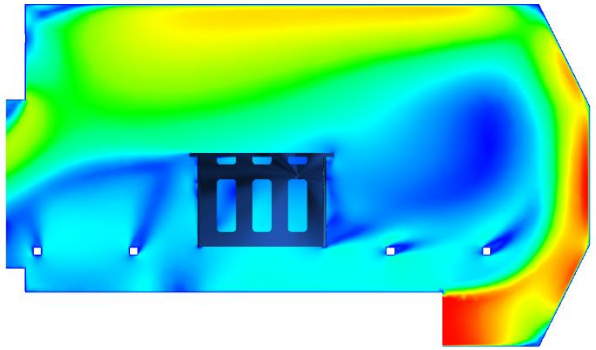

Relatively uniform HTC around tool

Large Tool
4 ft. (L) x 2.3 ft. (W) x 1.6 ft. (H)

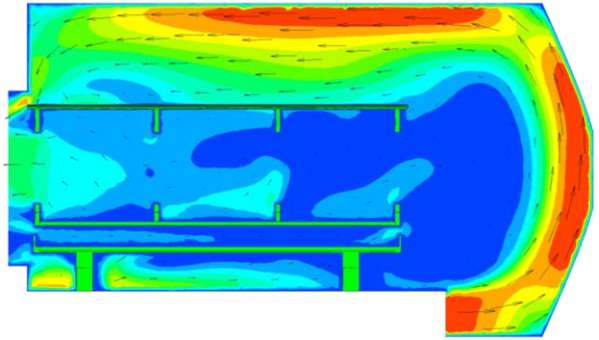

Non-uniform HTC around tool

CFD, RANS-based K-epsilon turbulence modelling, ANSYS Fluent

Tool Response: IR Thermography vs. FE Simulation

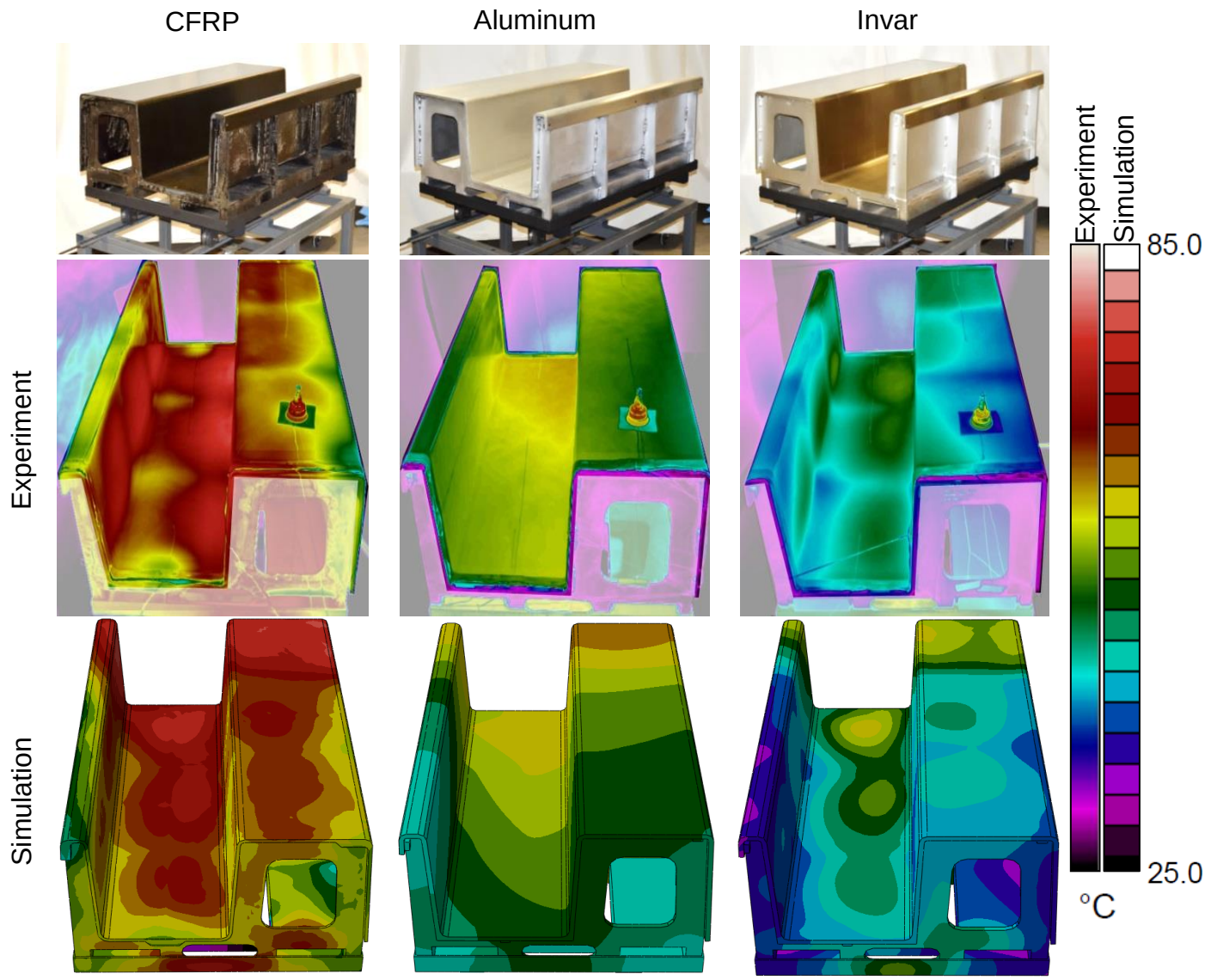

5 ℃/min to 100℃, Vacuum pressure only

Predicting Part Temperature History

- Thermocouple data by The Canadian Composite Manufacturing R&D Inc.
- Invar Tool
- C-shaped laminates @ 16, 32, and 64 ply T800H/3900-2 plain weave CFRP prepreg
- ABAQUS and COMPRO (material model)
- 1.7°C/min to 2 hour hold at 180 °C
- TC5 located at Tool – part interface

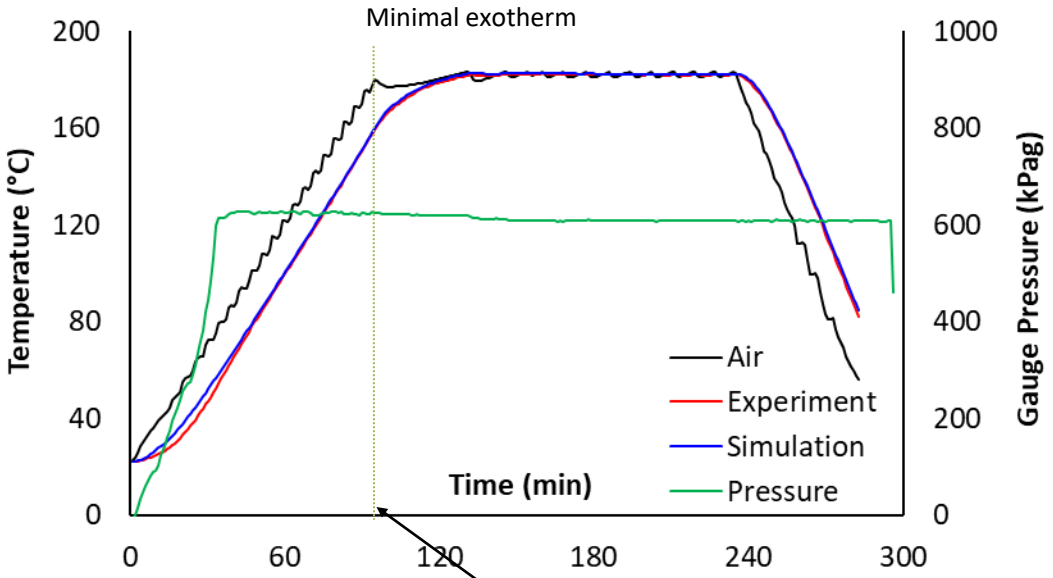

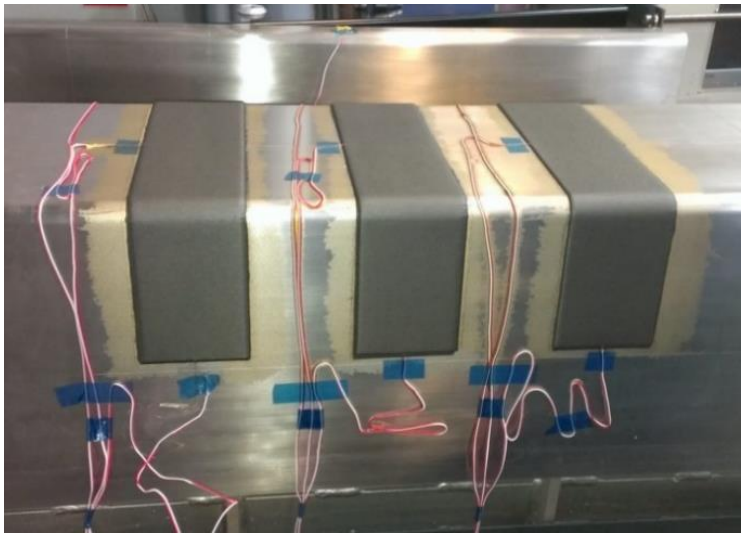

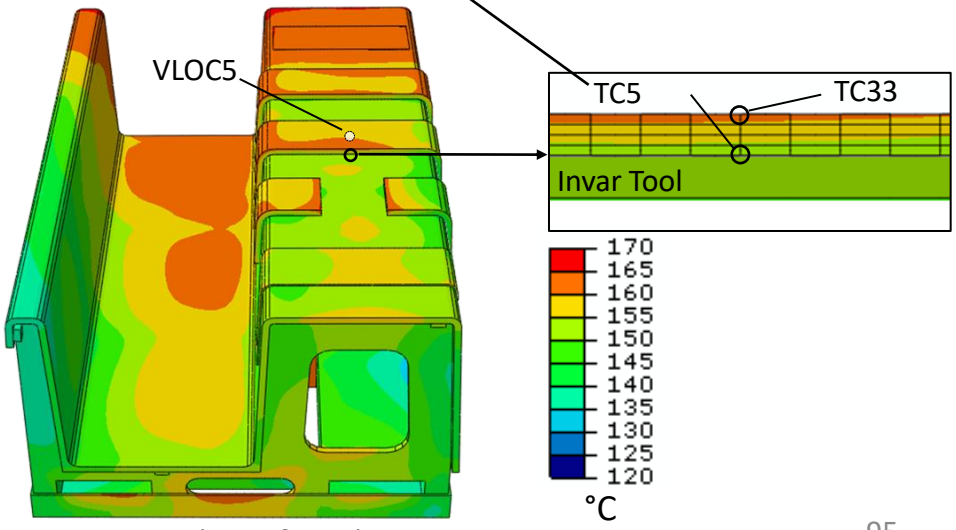

Front (Door facing)

Stress and Deformation in Composites

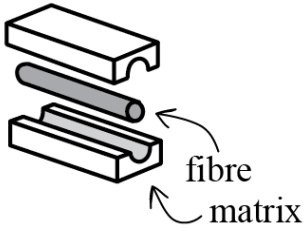

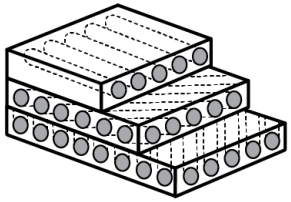

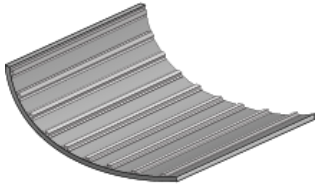

Micro-level

Laminate-level

Component- level

Residual Stress

Dimensional Changes

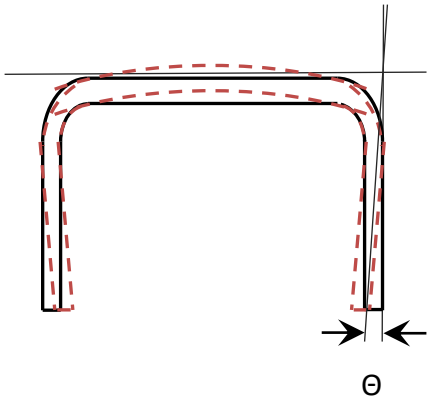

Mechanical Performance

Free strains

$$\boldsymbol{\varepsilon}_{free} = \boldsymbol{\varepsilon}_{thermal} + \boldsymbol{\varepsilon}_{phase-change} + \boldsymbol{\varepsilon}_{moisture}$$

Constitutive Models

Higher Fidelity

Thermo-Elastic (TE)

$$\sigma = E(T) \times \left(\varepsilon - \varepsilon_{free}\right)$$

Pseudo-Viscoelastic (PVE)
Cure Hardening Instantaneous Linear Elastic (CHILE)

$$\sigma(t) = \int_0^t E'(T,\alpha)\frac{d\varepsilon(\tau) - d\varepsilon_{free}(\tau)}{d\tau}d\tau$$

Linear Viscoelastic (VE)
Linear viscoelastic, thermo-rheologically simple

$$\sigma(t) = \int_0^t E(E,\alpha,t-\tau)\frac{d\varepsilon(\tau) - d\varepsilon_{free}(\tau)}{d\tau}d\tau$$

Thermo-Viscoelastic (TVE)
Linear viscoelastic, thermo-rheologically complex

$$\sigma_x = E_e\epsilon_x + a_F\int_0^\xi \Delta E(\xi-\xi')\frac{d\epsilon_x}{d\xi'}d\xi' - \beta_e\Delta T - a_F\int_0^\xi \Delta\beta(\xi-\xi')\frac{d\left(\frac{\Delta T}{a_F}\right)}{d\xi'}d\xi'$$

Nonlinear Viscoelastic (NVE)
Nonlinear viscoelastic, thermo-rheologically complex

Lower Computational Cost

Lower Characterization Cost

Constitutive Models

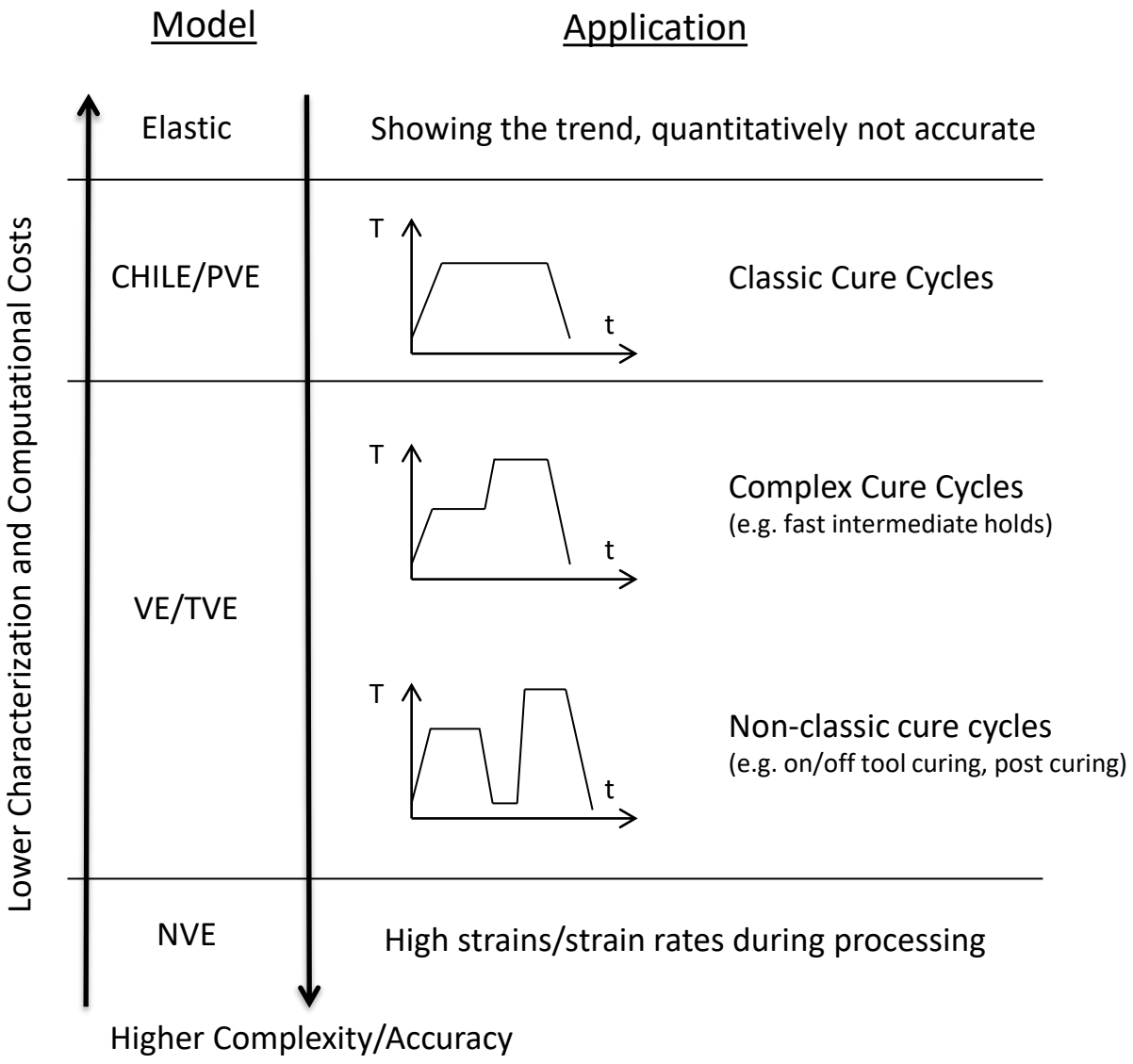

Effect of Cure Cycle: AS4/8552

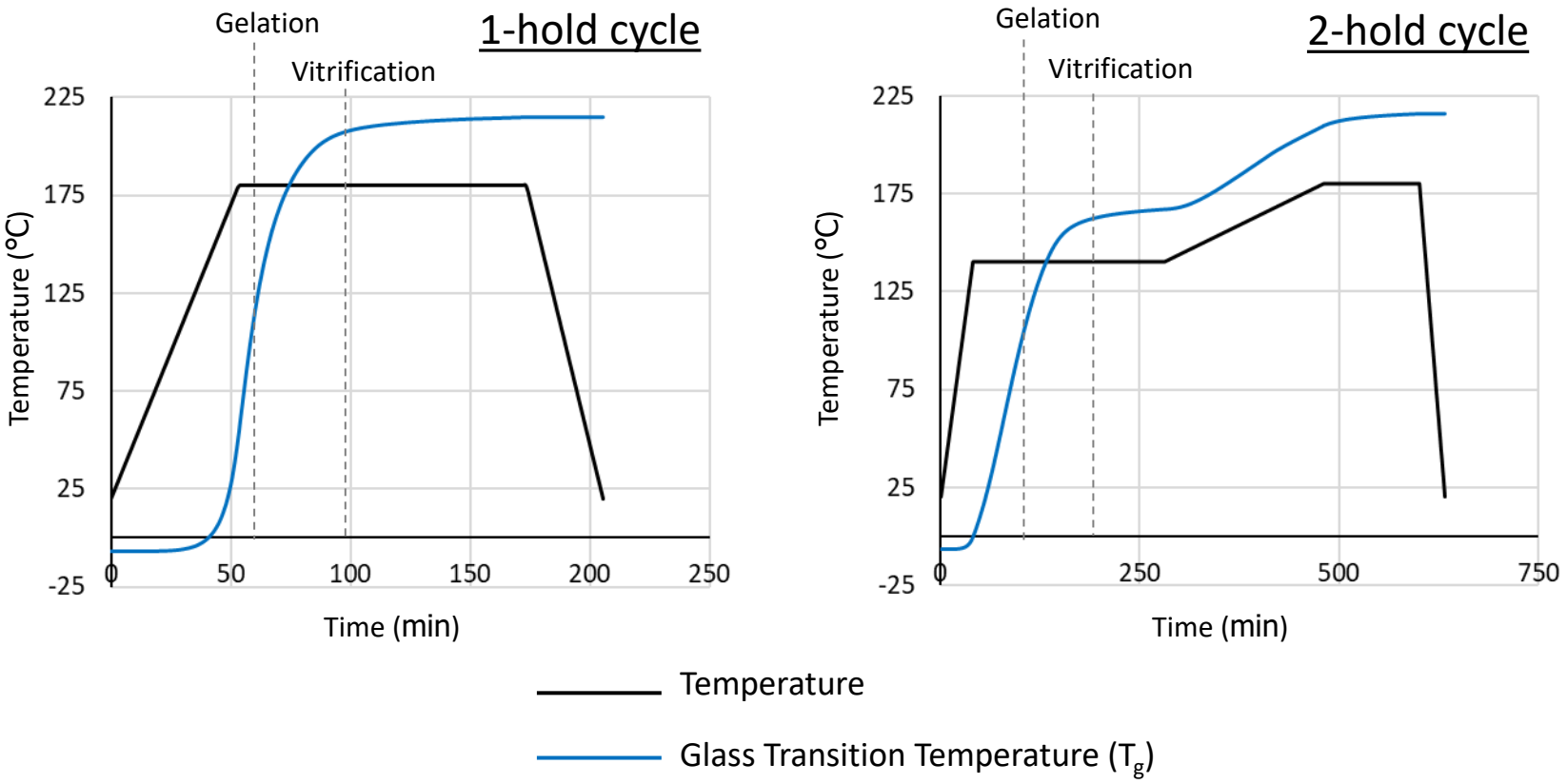

Cycle	heat-up	dwell	heat -up	dwell	cool-down
1	3 °C/min			2 hrs. @ 180 °C	5 °C/min
2	3 °C/min	4 hrs. @ 140 °C	0.2 °C/min	2 hrs. @ 180 °C	5 °C/min

Residual Stress in Cross-Ply Laminates

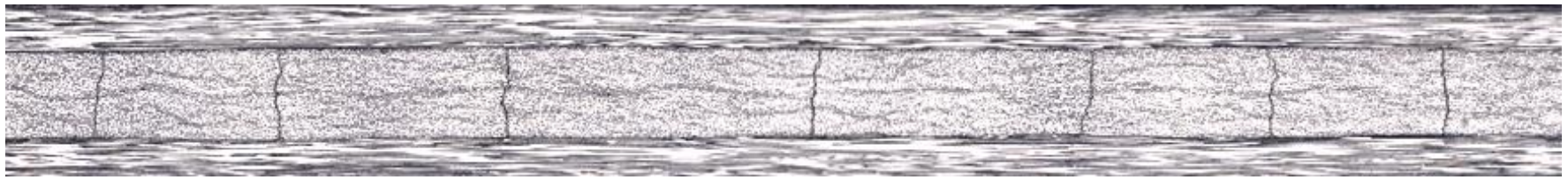

Predictions of Residual Stresses in $[0/90]_s$ Laminates

$$\sigma_{residual} = \frac{-E_0 t_0}{\sum E_i' t_i} \int E_{90}' d\varepsilon_{free}$$

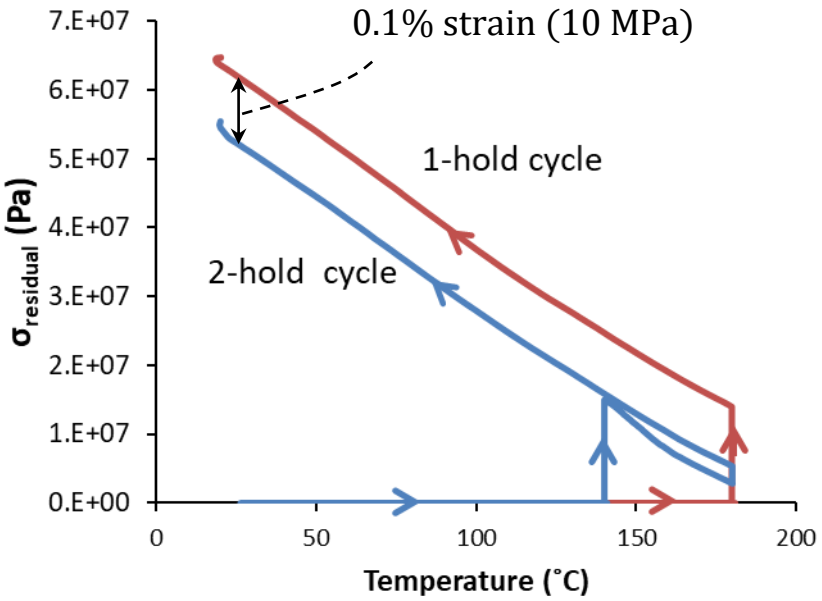

Matrix Cracking Tests on $[0/90]_s$ Laminates

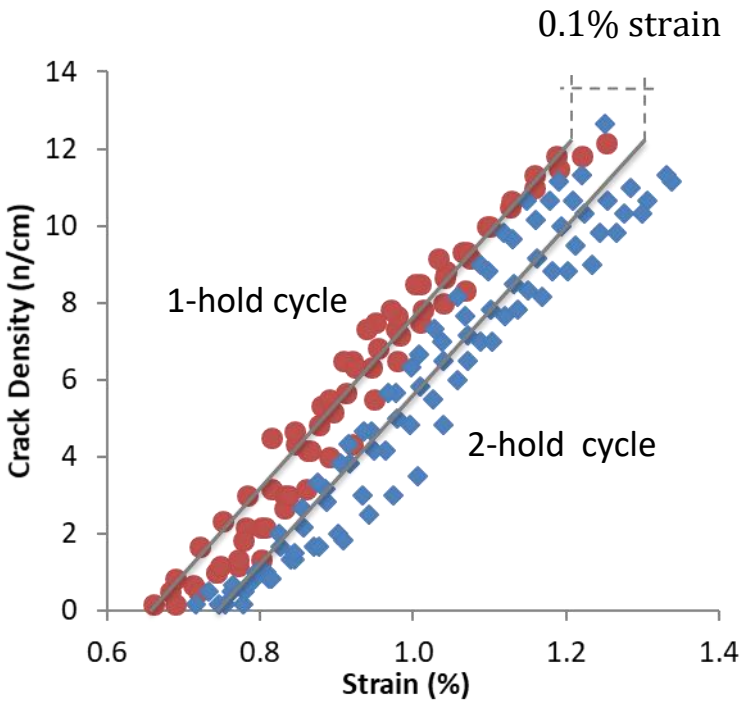

Zobeiry N., Forghani A., Li C., Thorpe R., Gordnian K., Vaziri R., Fernlund G., Poursartip A. (2016). Multi-scale characterization and representation of composite materials during processing, *Philosophical Transactions of the Royal Society of London A: Mathematical, Physical and Engineering Sciences*, DOI: 10.1098/rsta.2015.0278, 374:20150278

Part Deformation Simulation

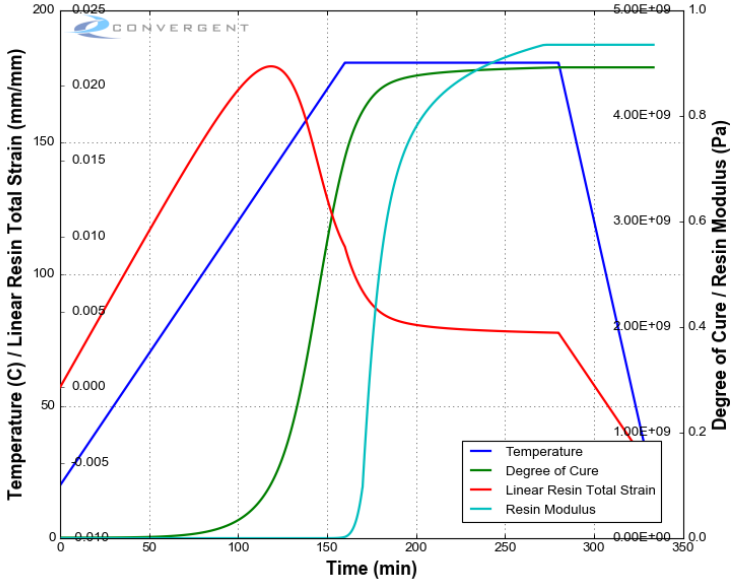

ABAQUS and COMPRO

NCAMP material model

Element type C3D20

frictionless tool-part

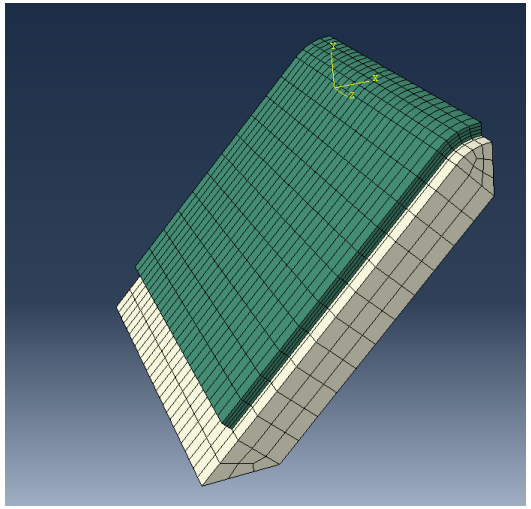

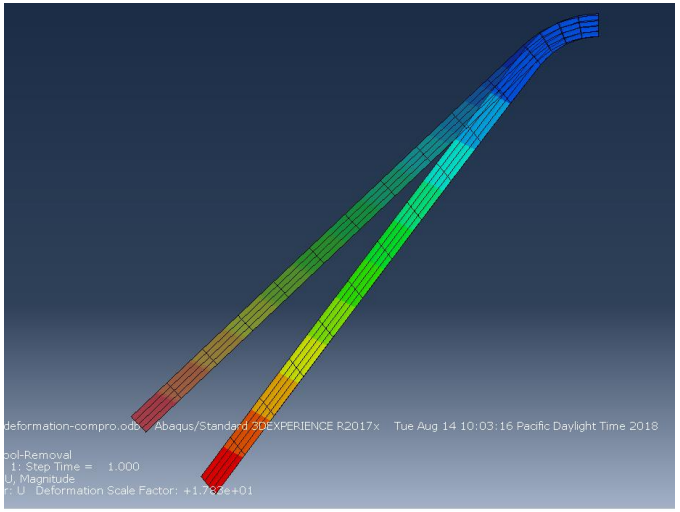

Process-Induced Deformation by COMPRO

– Tool geometry compensation in CATIA

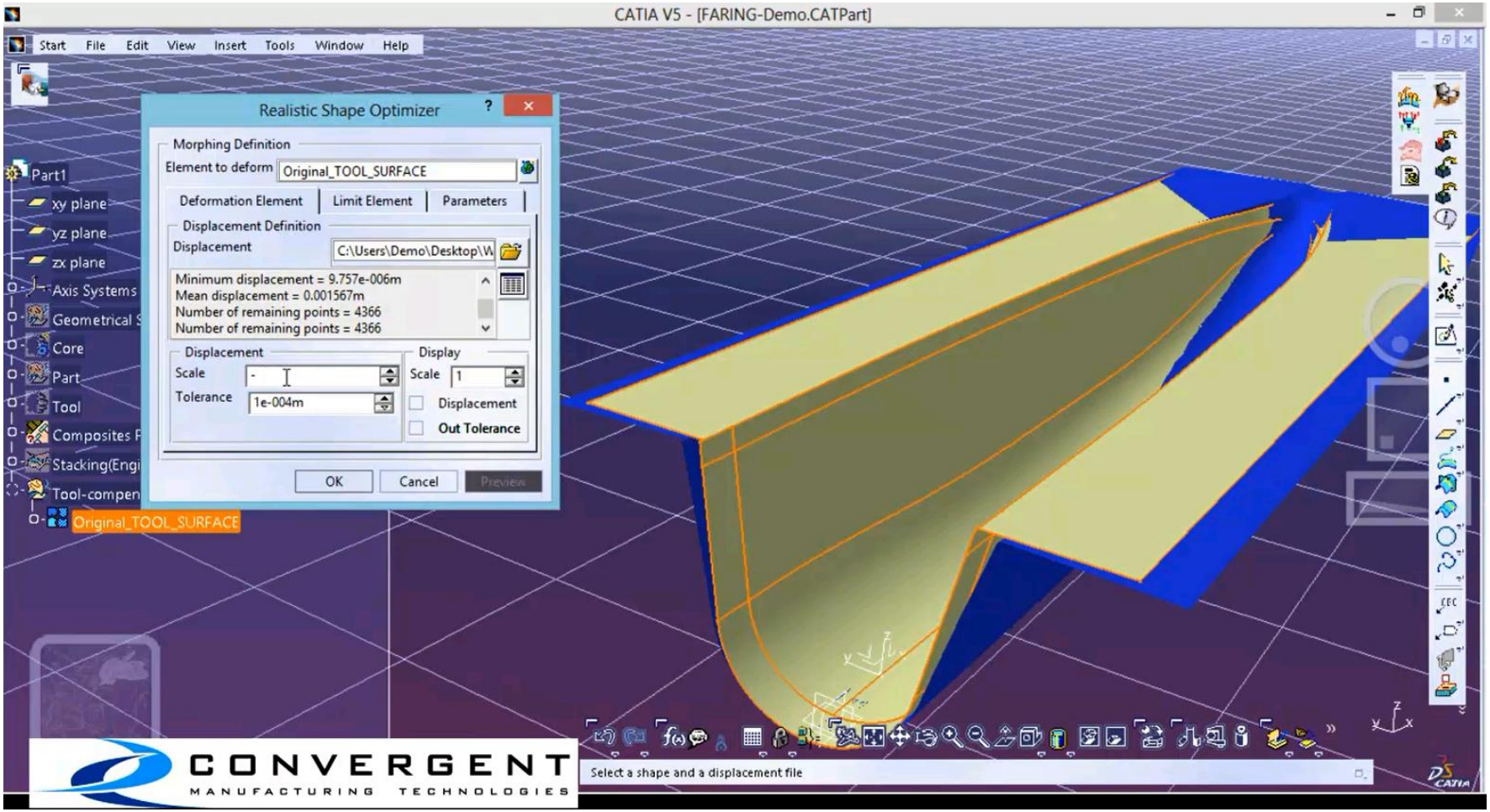

Process-Induced Deformation by COMPRO

– Current tool geometry compensation workflow

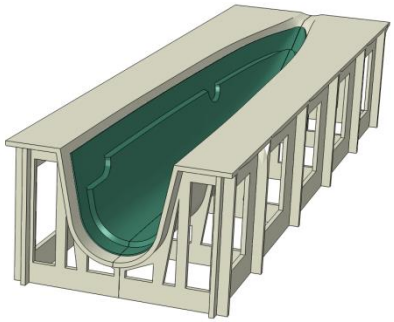

+

Material Characterization

CATIA

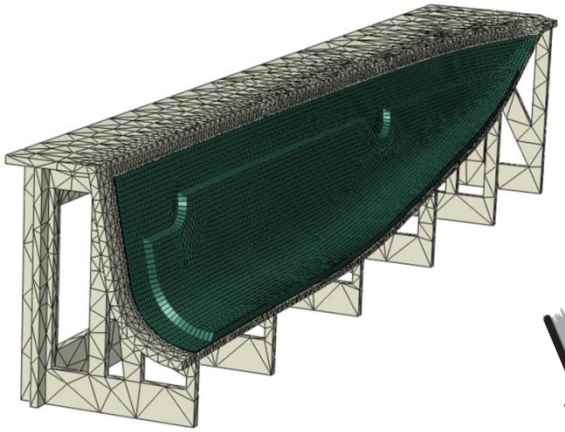

ABAQUS
COMPRO

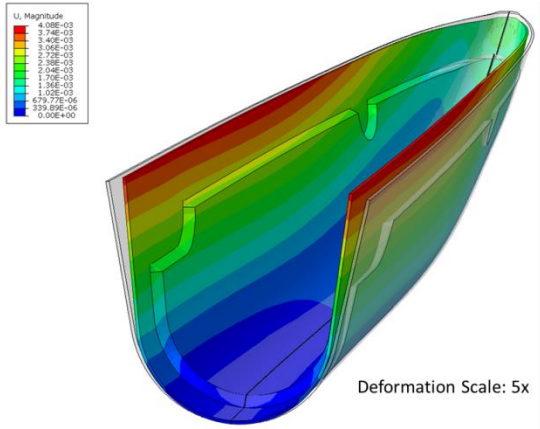

CATIA

Tool Geometry
Compensation

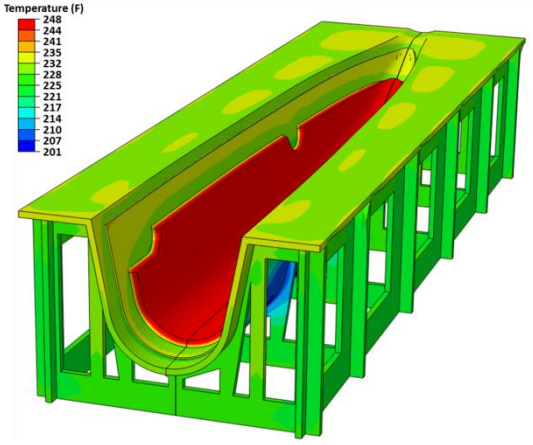

Thermo-chemical analysis
Flow-compaction analysis
Stress-deformation Analysis

Initial Prepreg Condition

- HEXCEL AS4/8552 carbon-epoxy UD prepreg
- Made using the hot melt process

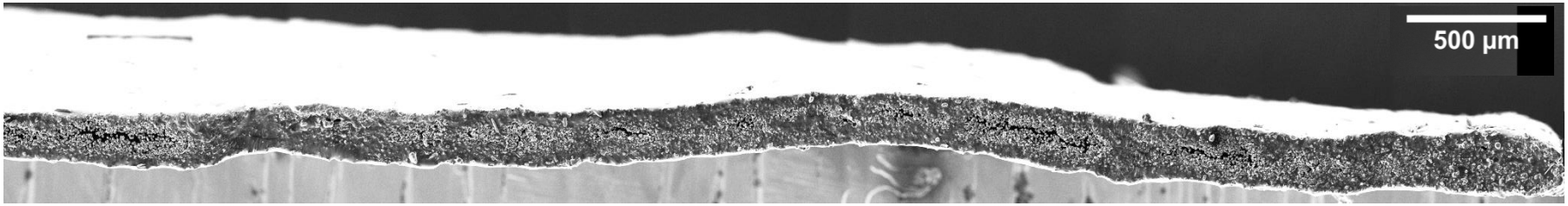

AS4/8552 cut at room temperature
SEM Image (X200 Magnification)

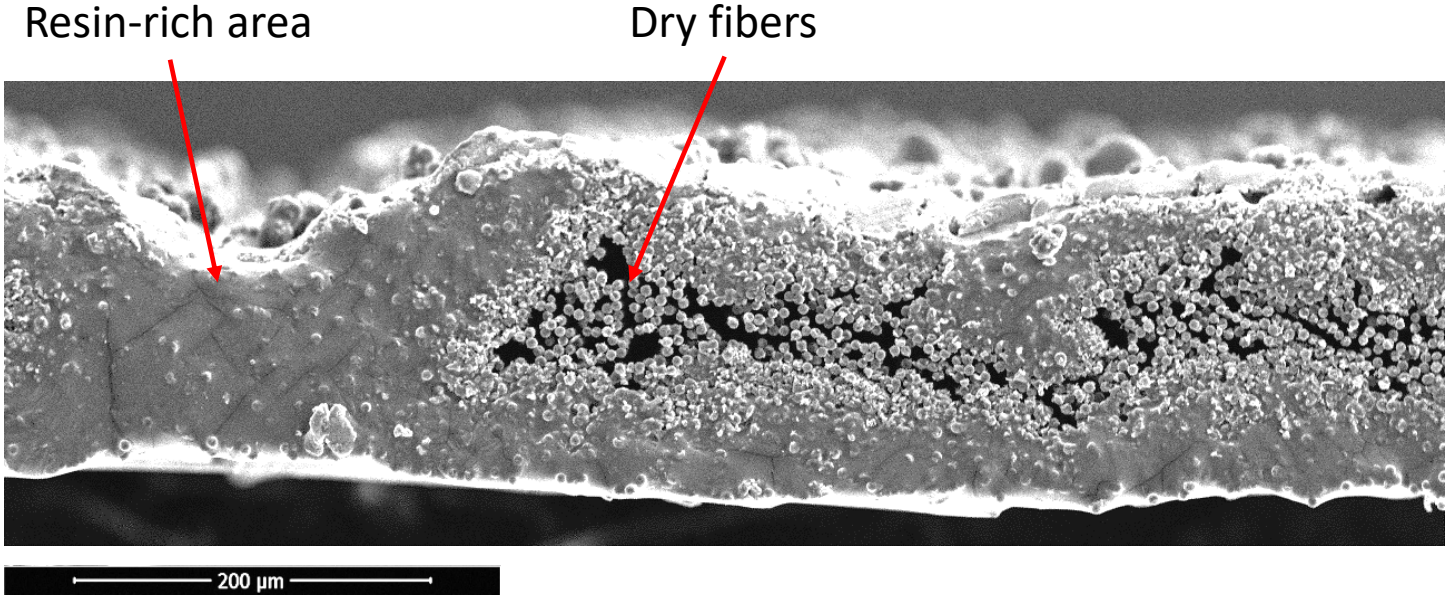

Effect of Pressure

Uncured Prepreg (Room Conditions)	15 min @ 40 °C (104 °F) (Under vacuum)	15 min @ 60 °C (140 °F) (Under vacuum)	15 min at 80 °C (176 °F) (Under vacuum)
Thickness = 200 – 220 µm			Thickness = 165 – 185 µm

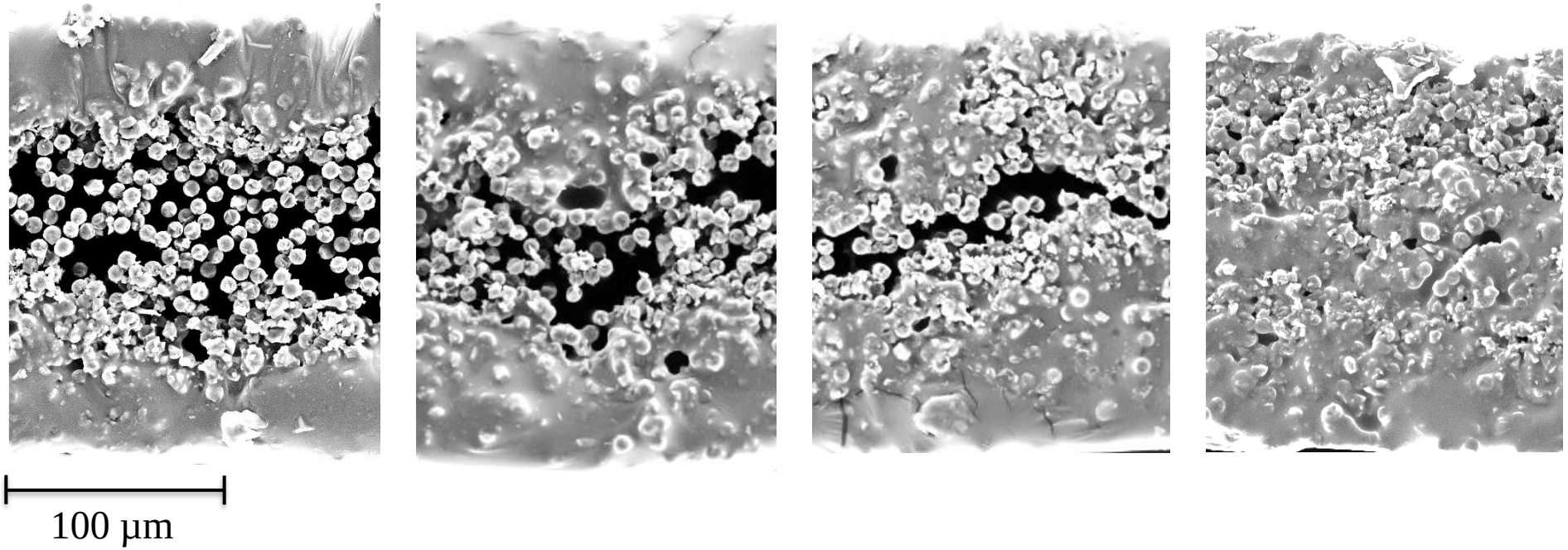

Consolidation Under Vacuum Pressure

- Effect of Cure Cycle on Porosity:

Ply thickness = 0.196 mm
(≈ 7% porosity)

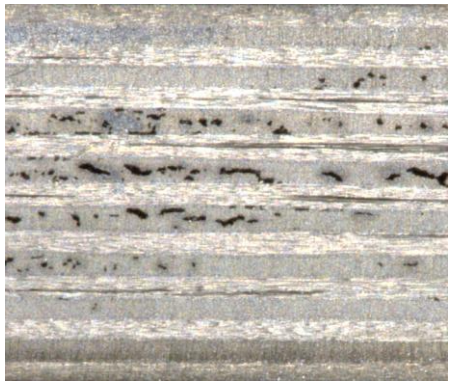

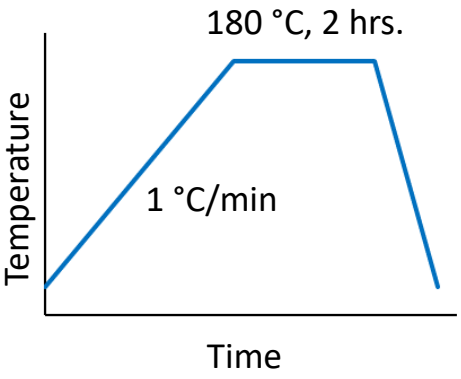

Ply thickness = 0.189 mm
(≈ 3.5% porosity)

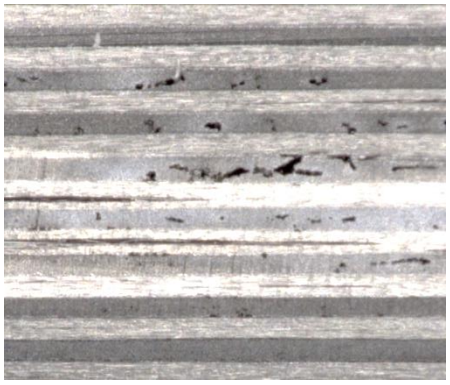

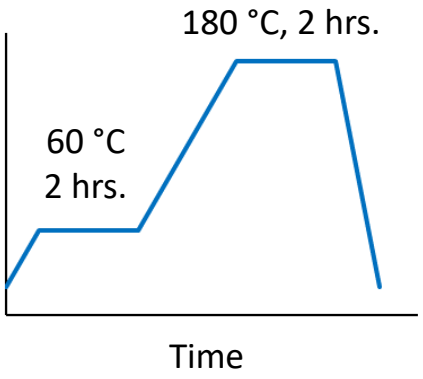

Ply thickness = 0.182 mm
(< 0.5% porosity)

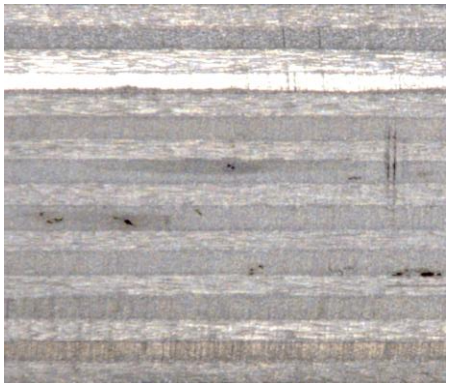

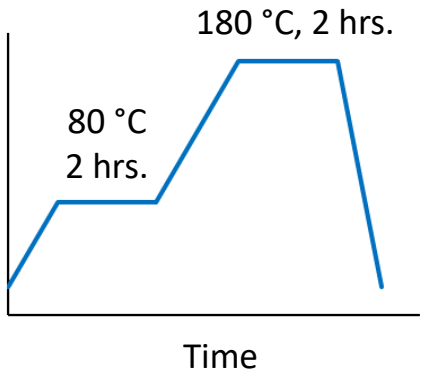

Ply thickness = 0.192 mm
(≈ 5% porosity)

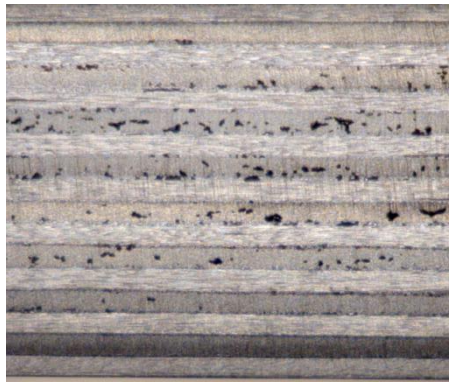

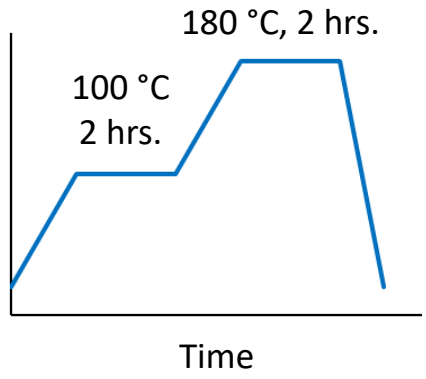

Coupled Gas/Resin Transport Model

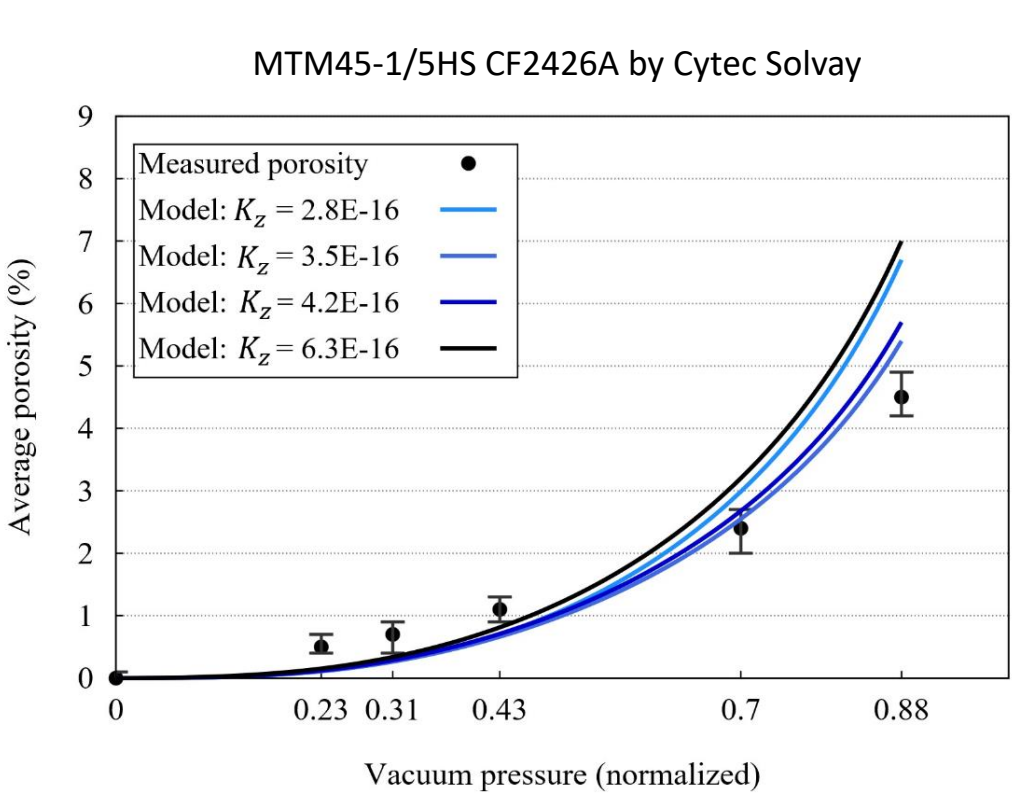

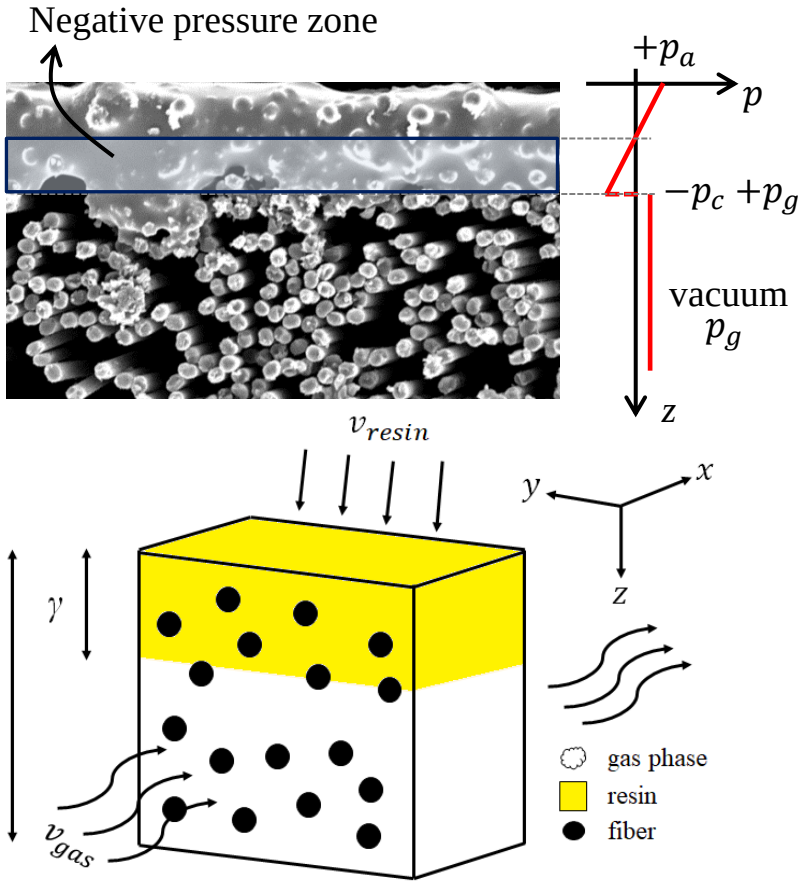

$$\begin{cases} \varphi \dfrac{\partial P_g}{\partial t} = \dfrac{K_{x0}}{\mu_g} \dfrac{\partial}{\partial x}\left(\left(1+\dfrac{b}{P_g}\right) P_g \dfrac{\partial P_g}{\partial x}\right) + \dfrac{K_z}{h^2 \mu_r (1-V_f)} \dfrac{P_g (P_a - P_g + P_c)}{(1-\varphi)} \\ \dfrac{d\varphi}{dt} = -\dfrac{K_z}{h^2 \mu_r (1-V_f)} \dfrac{P_a - P_g + P_c}{(1-\varphi)} \end{cases}$$

Gas flow in x direction

Resin flow in z direction

Evolution of properties during processing and characterization methods

2021-06-09

Navid Zobeiry, PhD (navidz@uw.edu)
Assistant Professor
Materials Science & Engineering
University of Washington

BE BOUNDLESS

Aerospace Composite Materials

Typical toughened thermoset composites

Laminate

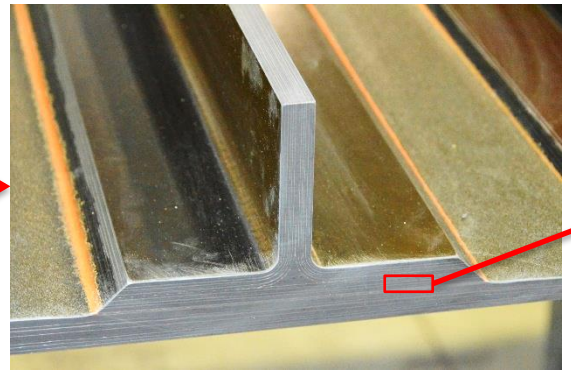

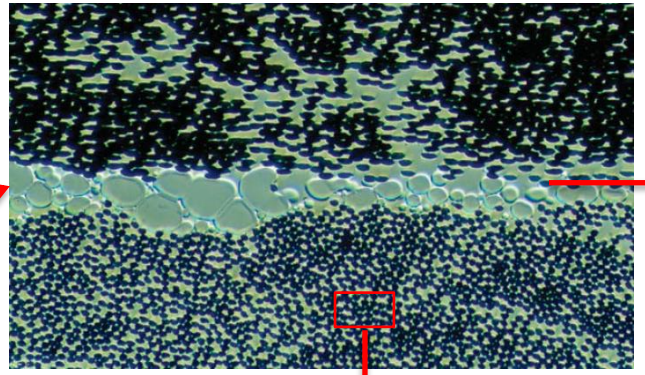

Layer 1

Interply Thermoplastic Particles

Layer 2

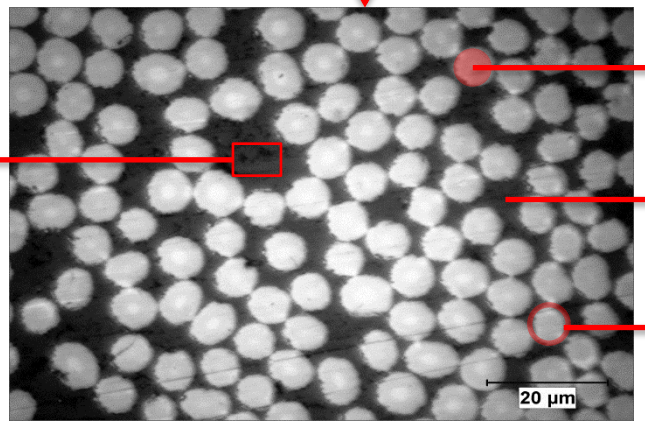

Carbon fiber

Toughened thermoset resin

Sizing

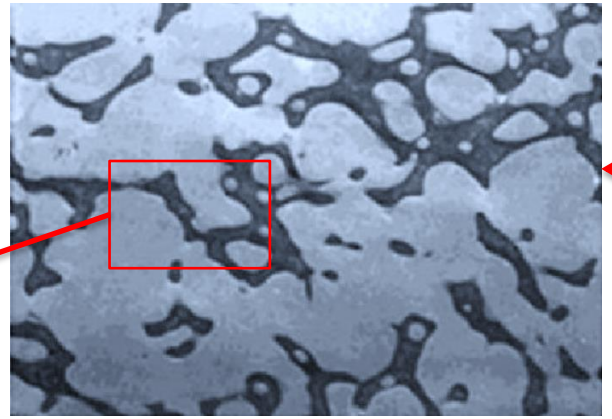

Matrix ≈
80% Thermoset resin +
20% Thermoplastic resin

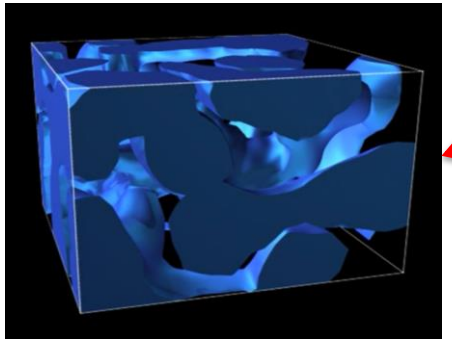

Aerospace Composite Materials

Typical semi-crystalline thermoplastic composites

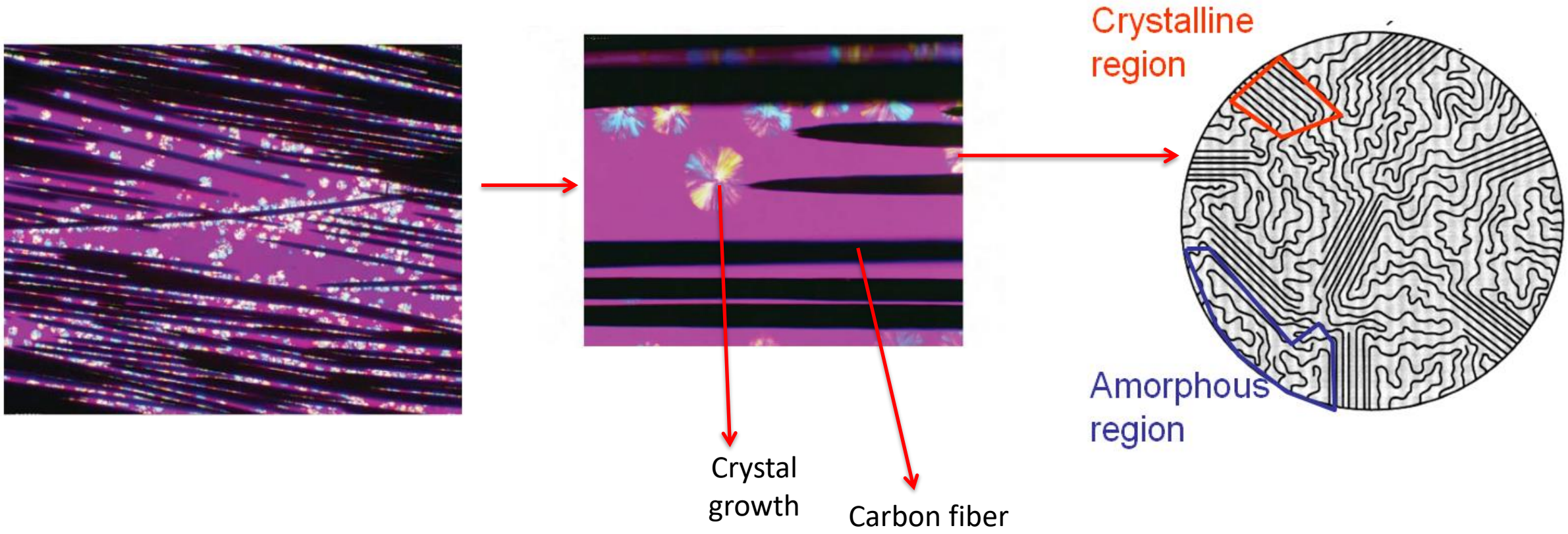

Curing Process in Thermosets

- During polymerization, material goes through different phases.
- At gelation, it changes form a viscous liquid to a rubbery gel
- As the curing advances, the rubbery gel transforms into glassy solid at vitrification

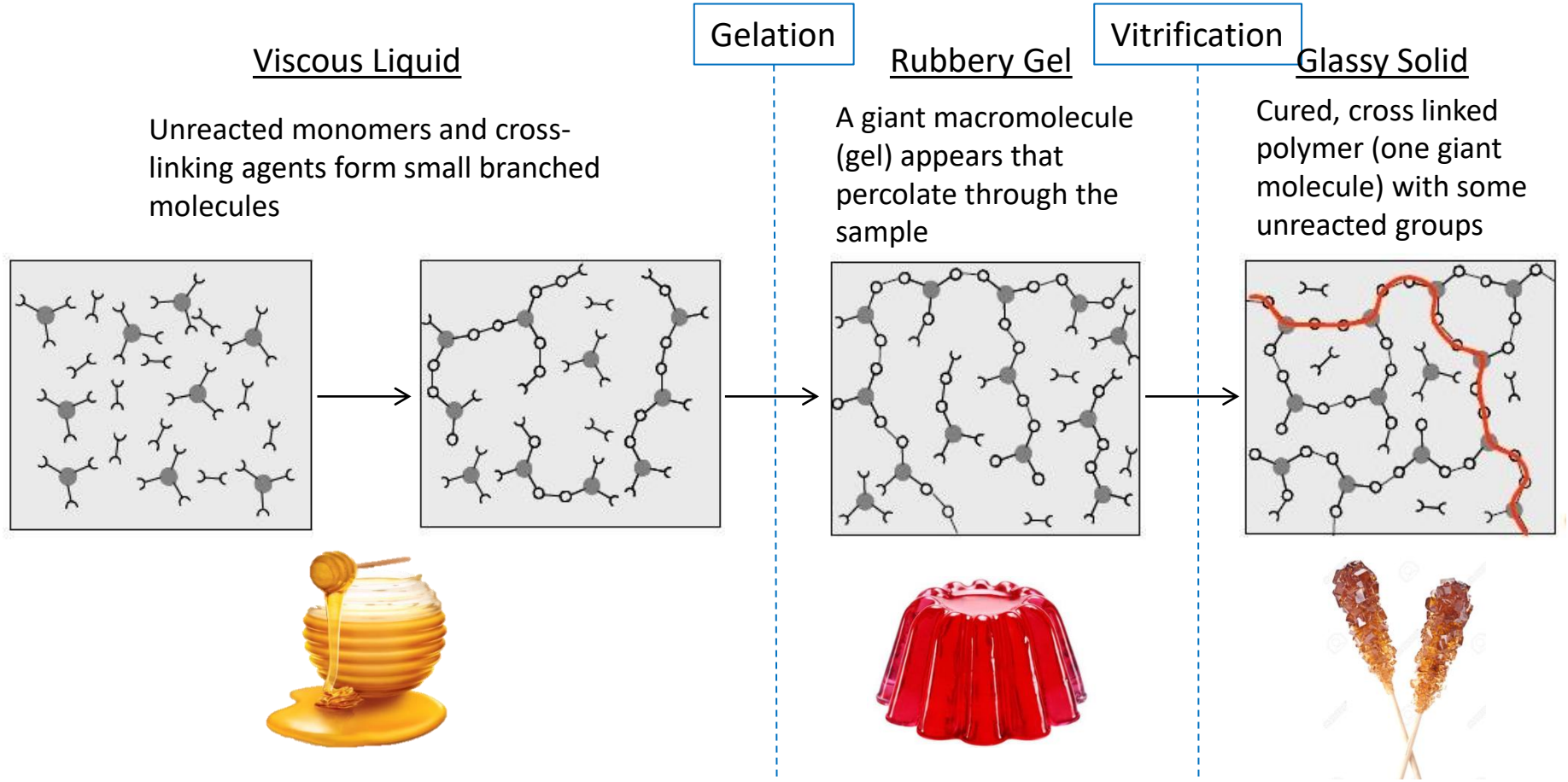

Curing Process in Thermosets

- Example: HEXCEL AS4/8552 (aerospace grade toughened epoxy prepreg)
  - 65% by weight AS4 carbon fiber, 35% by weight 8552 resin
  - 8552 resin: ≈ 75% epoxy + 25% PES

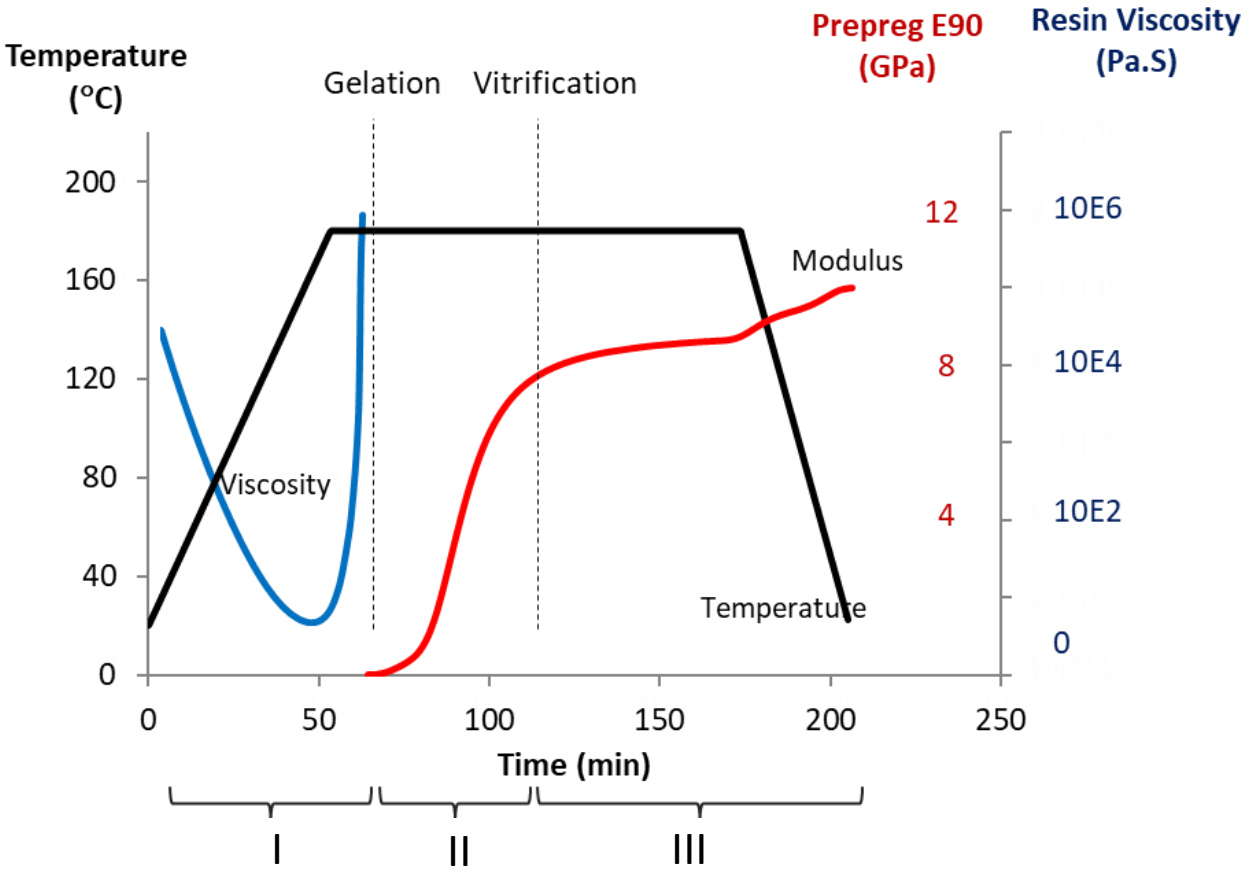

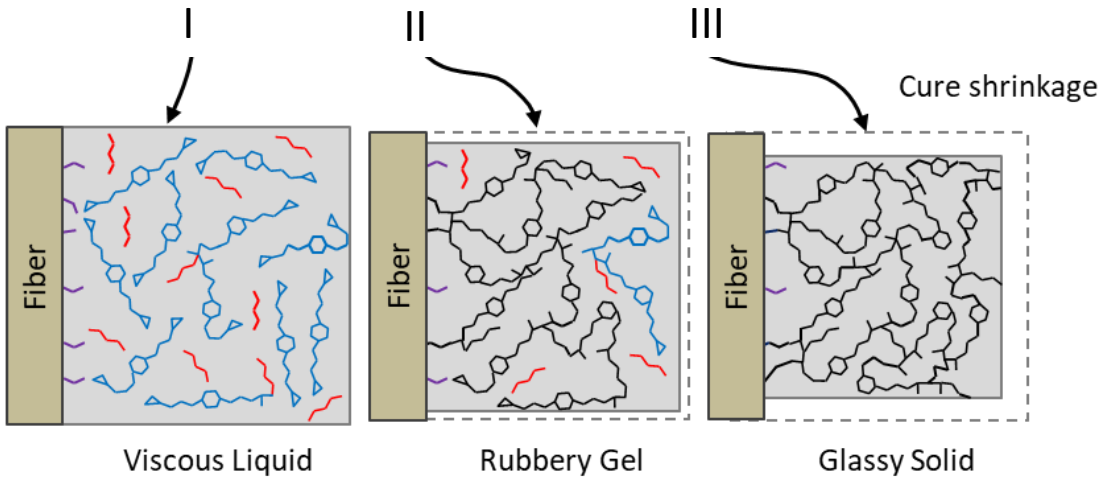

Thermosets and Heat

- If heated after cured, thermosets soften initially and then transform into char at very high temperatures.

Heat →

Glassy Solid	Rubbery Gel	Burnt
Cured, cross linked polymers	Increase of chain mobility when temperature goes above T_g	Oxidation and breaking of covalent bonds

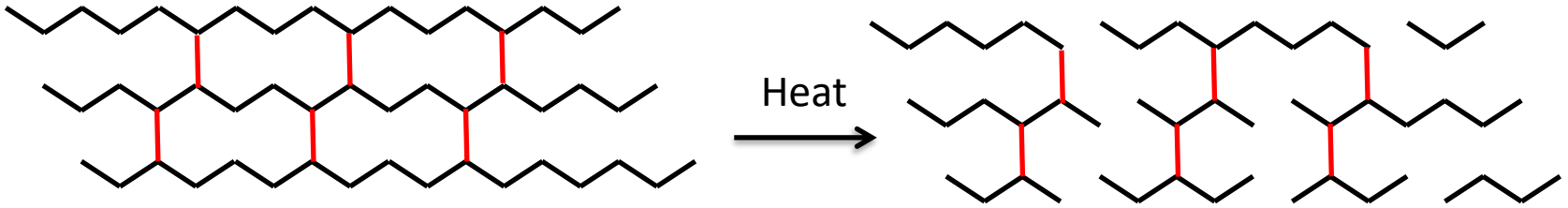

Degradation

Glassy (thermoelastic)

Rubbery (viscoelastic)

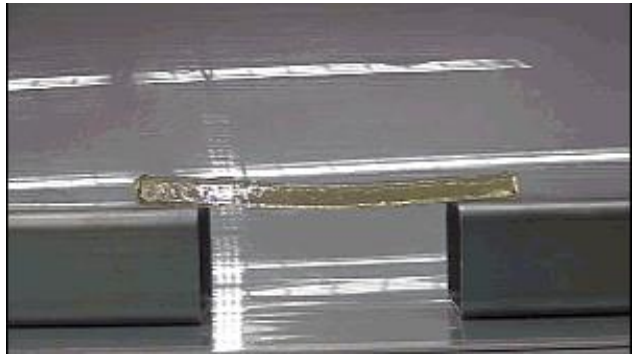

Heat of Reaction

- Curing of thermoset resins is an exothermic and heat is generated. The heat of reaction during polymerization is measured using a Differential Scanning Calorimeter (DSC) equipment.
- DSC measures how much energy/heat comes out of the reaction for a small resin sample

Loading a composite sample

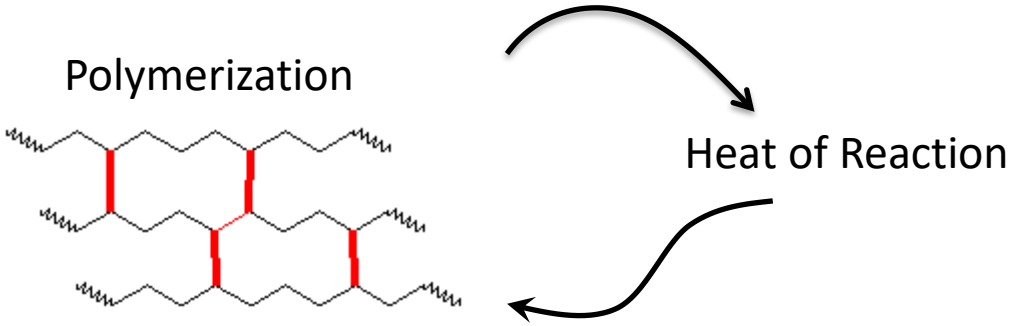

Degree of Cure

- Using heat of reaction, Degree of cure (DOC) is calculated.
- DOC is defined between 0 and 1 and is an indication of how far the crosslinking is advanced in a thermoset resin.

Low Degree of Cure
Low mechanical properties

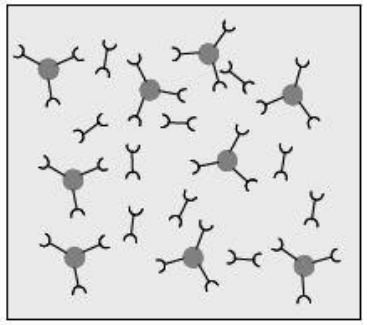

High Degree of Cure
High mechanical properties

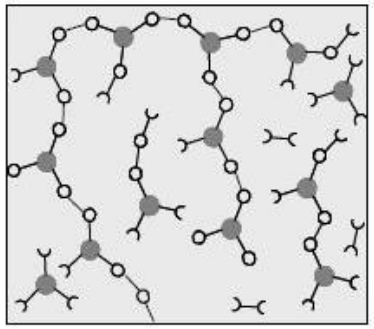

Effect of curing temperature on degree of cure

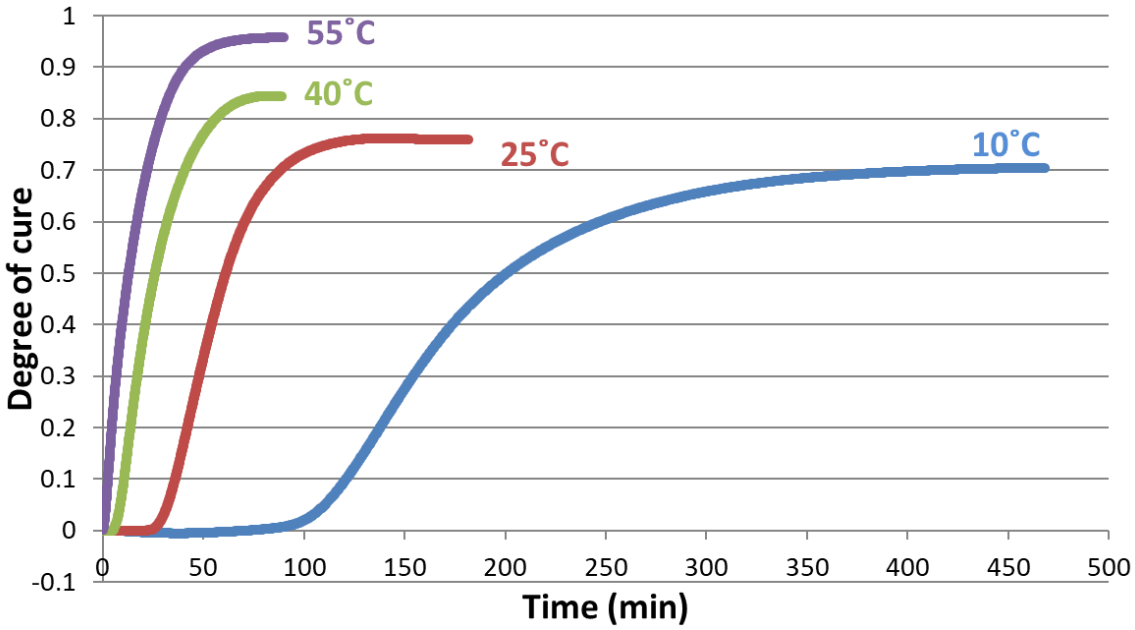

Volume: Thermosets vs Thermoplastics

- Here, the effect of temperature on volume of thermosets and thermoplastics are compared:

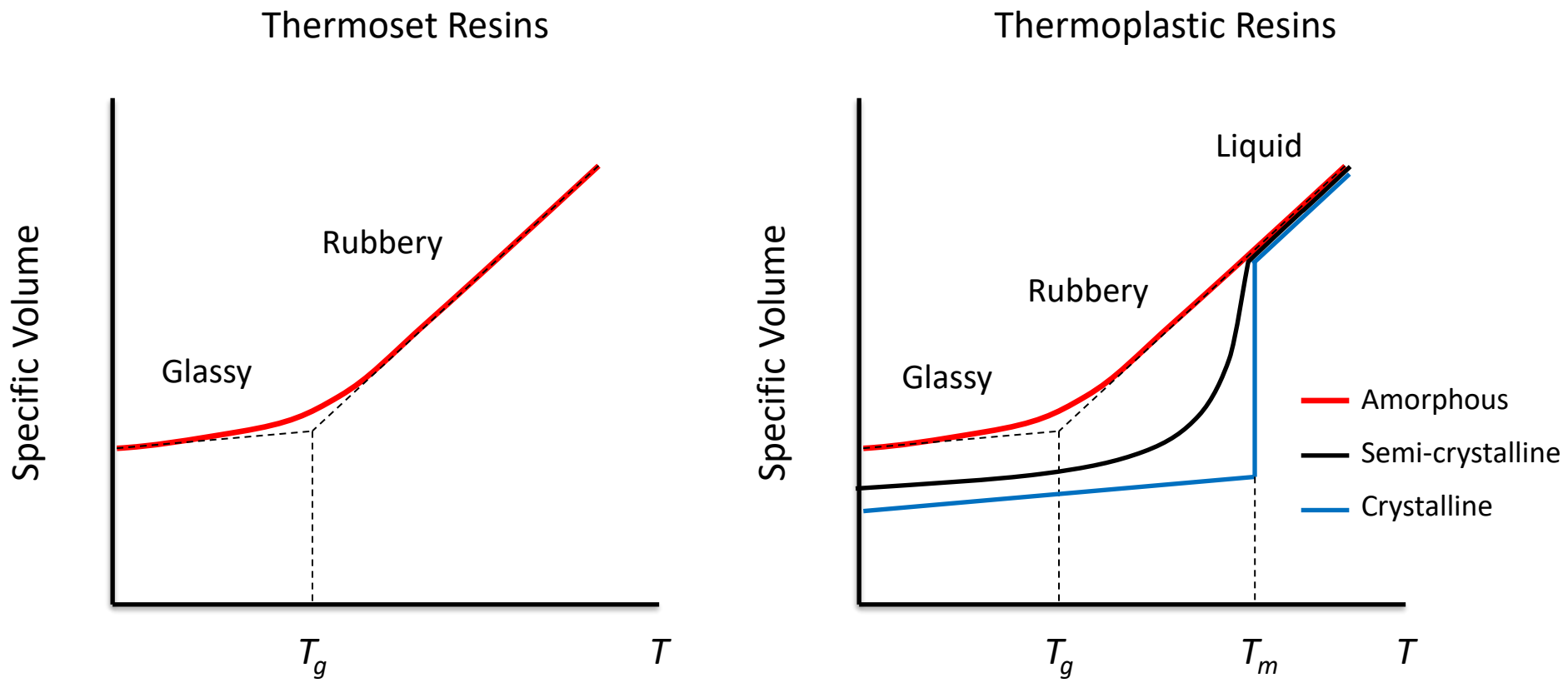

Free Strains in Composites

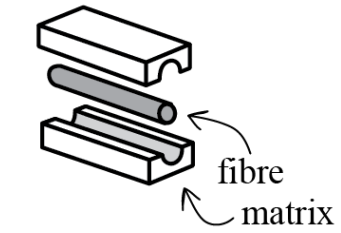

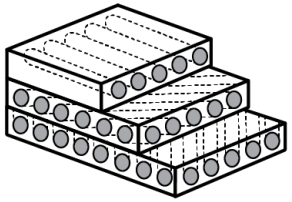

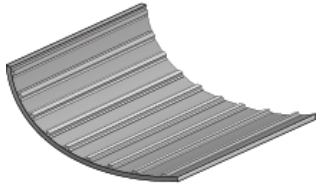

Micro-level

Laminate-level

Component- level

Residual Stress

Dimensional Changes

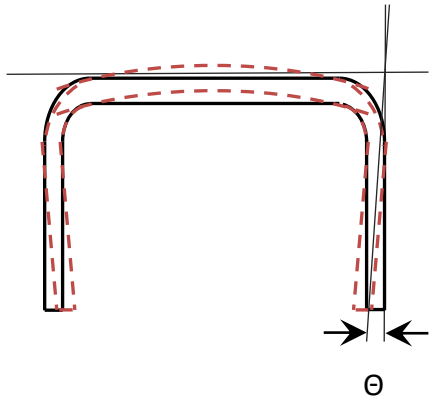

Mechanical Performance

Free strains

$$\boldsymbol{\varepsilon}_{free} = \boldsymbol{\varepsilon}_{thermal} + \boldsymbol{\varepsilon}_{phase-change} + \boldsymbol{\varepsilon}_{moisture}$$

Characterizing Volume Change During Processing

Thermomechanical Analyzer (TMA)

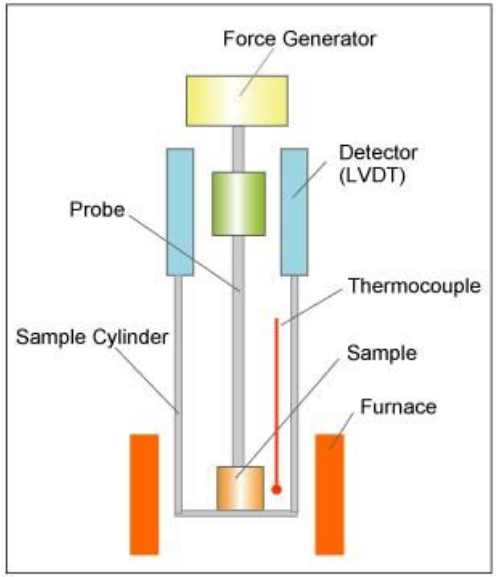

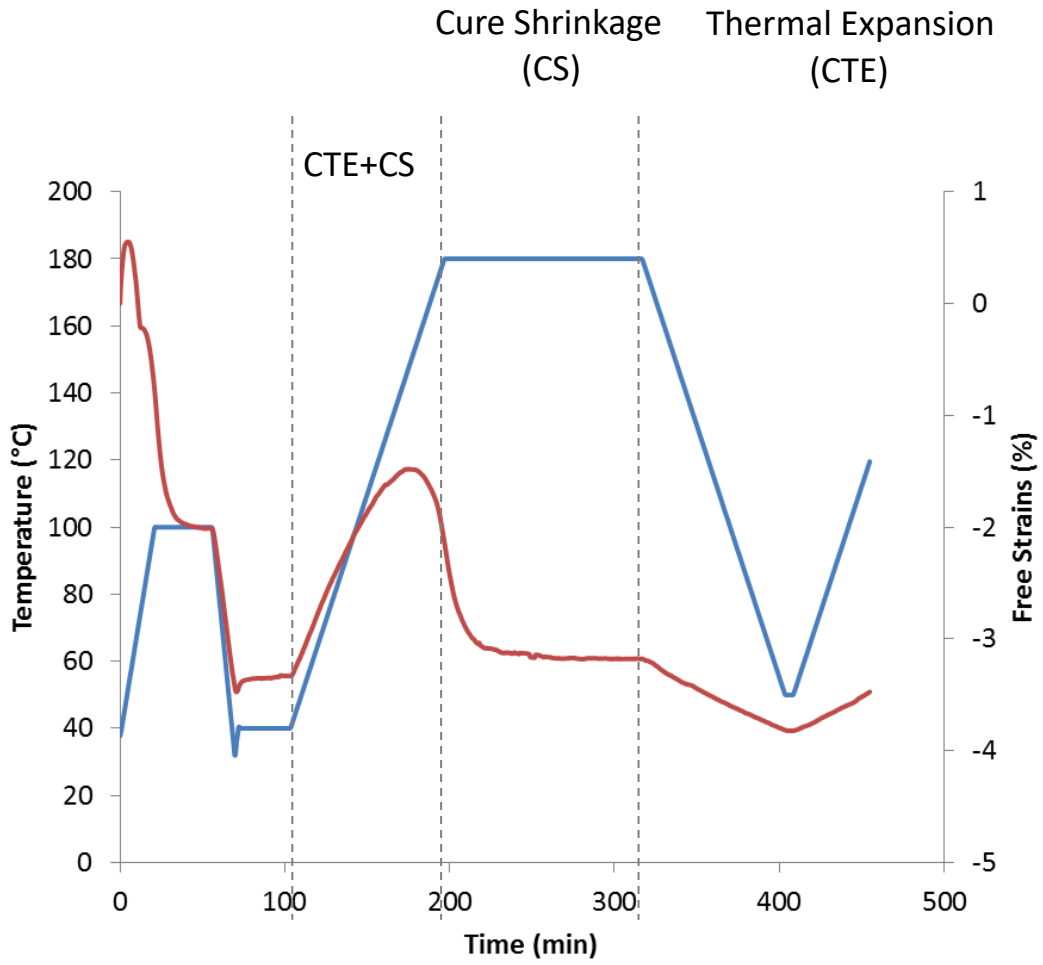

Characterizing Evolution of Viscoelastic Properties

Dynamic Mechanical Analyzer (DMA)

Dynamic Test

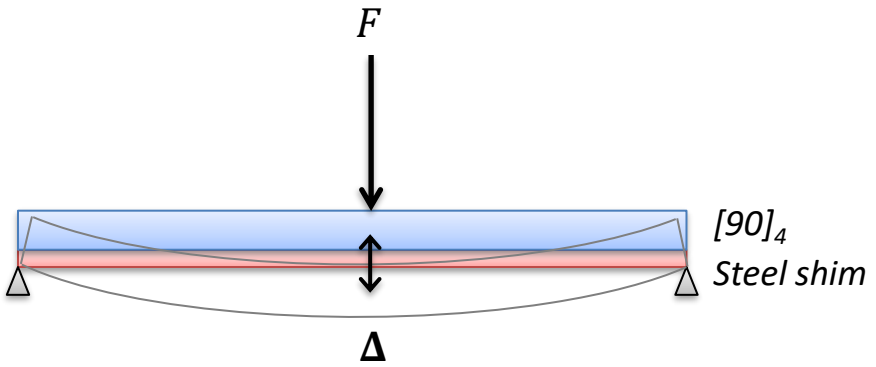

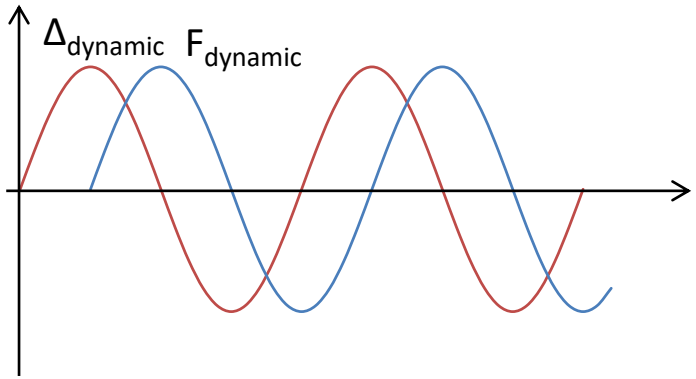

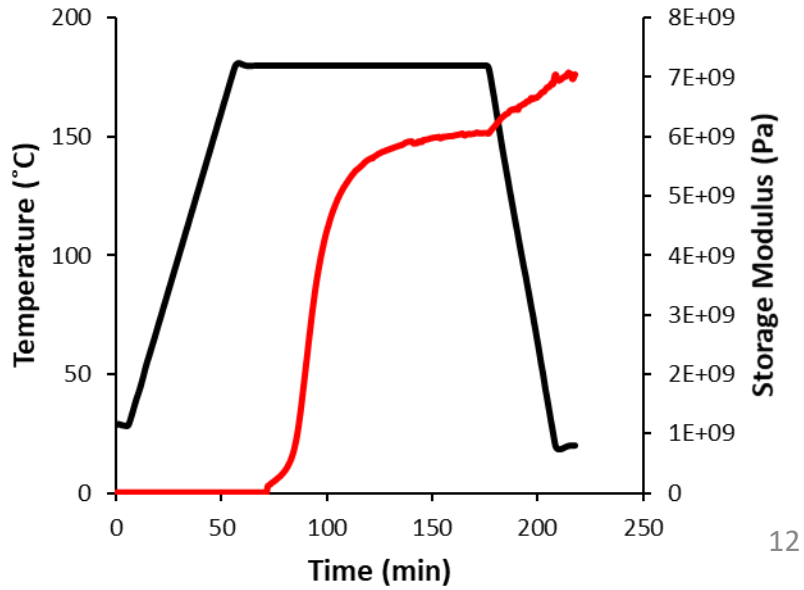

Characterizing Evolution of Viscoelastic Properties

Dynamic Mechanical Analyzer (DMA)

Relaxation Tests (prepreg beam, AS4/8552)

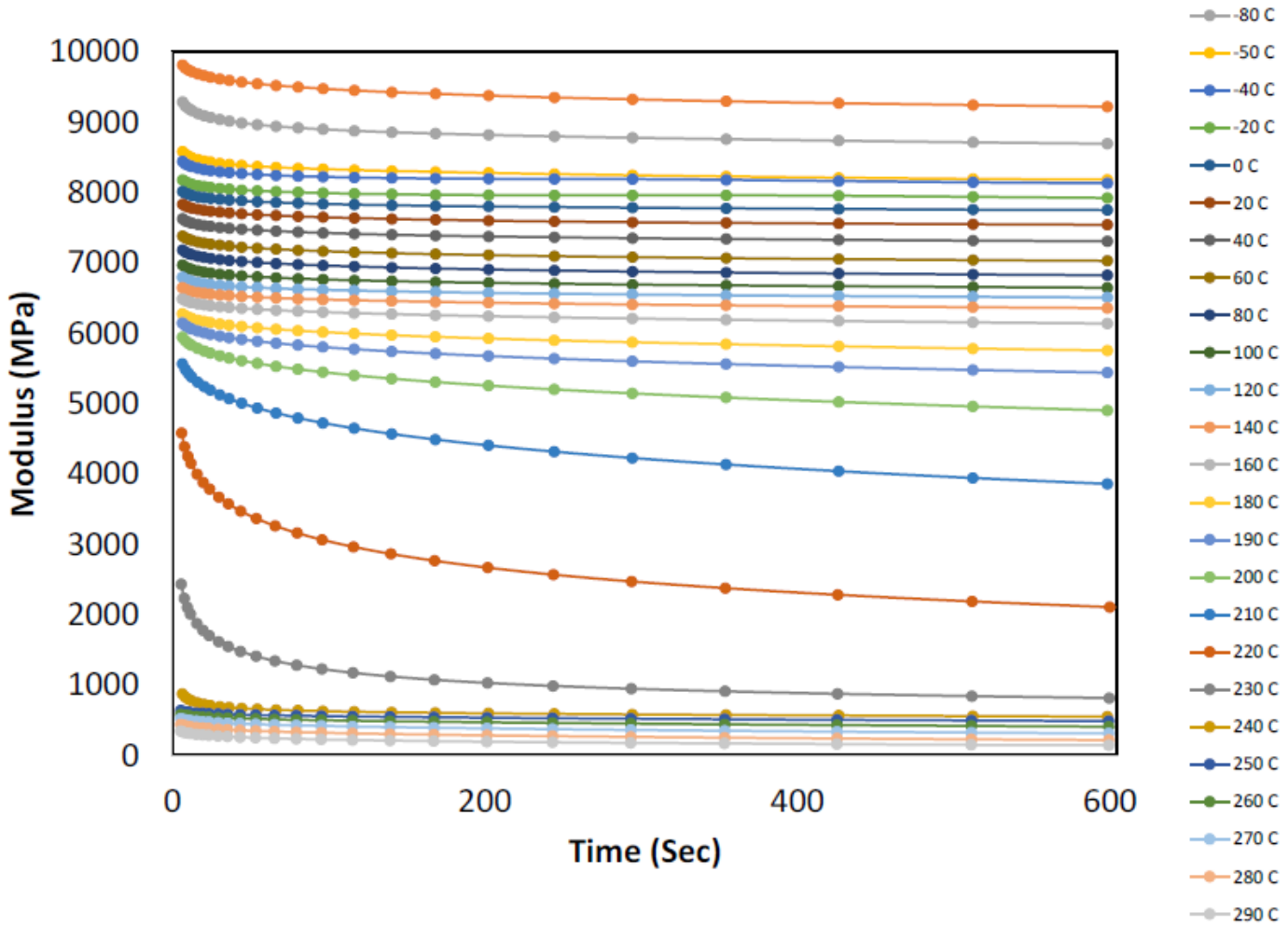

Constitutive Models

Higher Fidelity

Thermo-Elastic (TE)

$$\sigma = E(T) \times \left(\varepsilon - \varepsilon_{free}\right)$$

Pseudo-Viscoelastic (PVE)
Cure Hardening Instantaneous Linear Elastic (CHILE)

$$\sigma(t) = \int_0^t E'(T,\alpha)\frac{d\varepsilon(\tau) - d\varepsilon_{free}(\tau)}{d\tau}d\tau$$

Linear Viscoelastic (VE)
Linear viscoelastic, thermo-rheologically simple

$$\sigma(t) = \int_0^t E(E,\alpha,t-\tau)\frac{d\varepsilon(\tau) - d\varepsilon_{free}(\tau)}{d\tau}d\tau$$

Thermo-Viscoelastic (TVE)
Linear viscoelastic, thermo-rheologically complex

$$\sigma_x = E_e\epsilon_x + a_F\int_0^\xi \Delta E(\xi-\xi')\frac{d\epsilon_x}{d\xi'}d\xi' - \beta_e\Delta T - a_F\int_0^\xi \Delta\beta(\xi-\xi')\frac{d\left(\frac{\Delta T}{a_F}\right)}{d\xi'}d\xi'$$

Nonlinear Viscoelastic (NVE)
Nonlinear viscoelastic, thermo-rheologically complex

Lower Computational Cost

Lower Characterization Cost

Initial Prepreg Condition

- HEXCEL AS4/8552 carbon-epoxy UD prepreg
- Made using the hot melt process

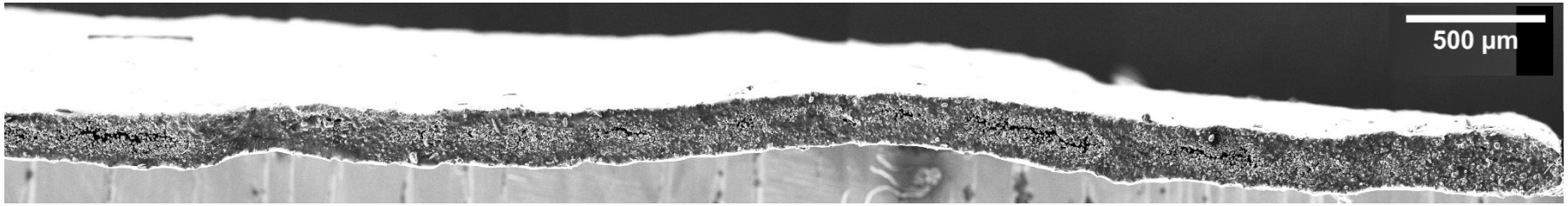

AS4/8552 cut at room temperature
SEM Image (X200 Magnification)

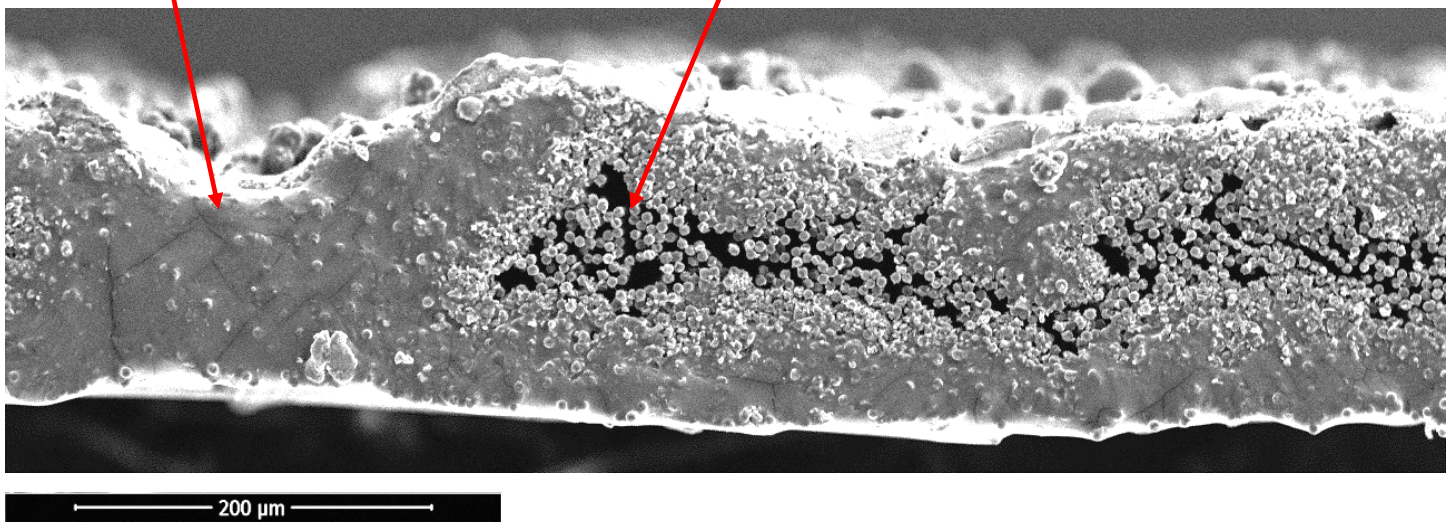

Effect of Pressure

Uncured Prepreg (Room Conditions)	15 min @ 40 °C (104 °F) (Under vacuum)	15 min @ 60 °C (140 °F) (Under vacuum)	15 min at 80 °C (176 °F) (Under vacuum)
Thickness = 200 – 220 µm			Thickness = 165 – 185 µm

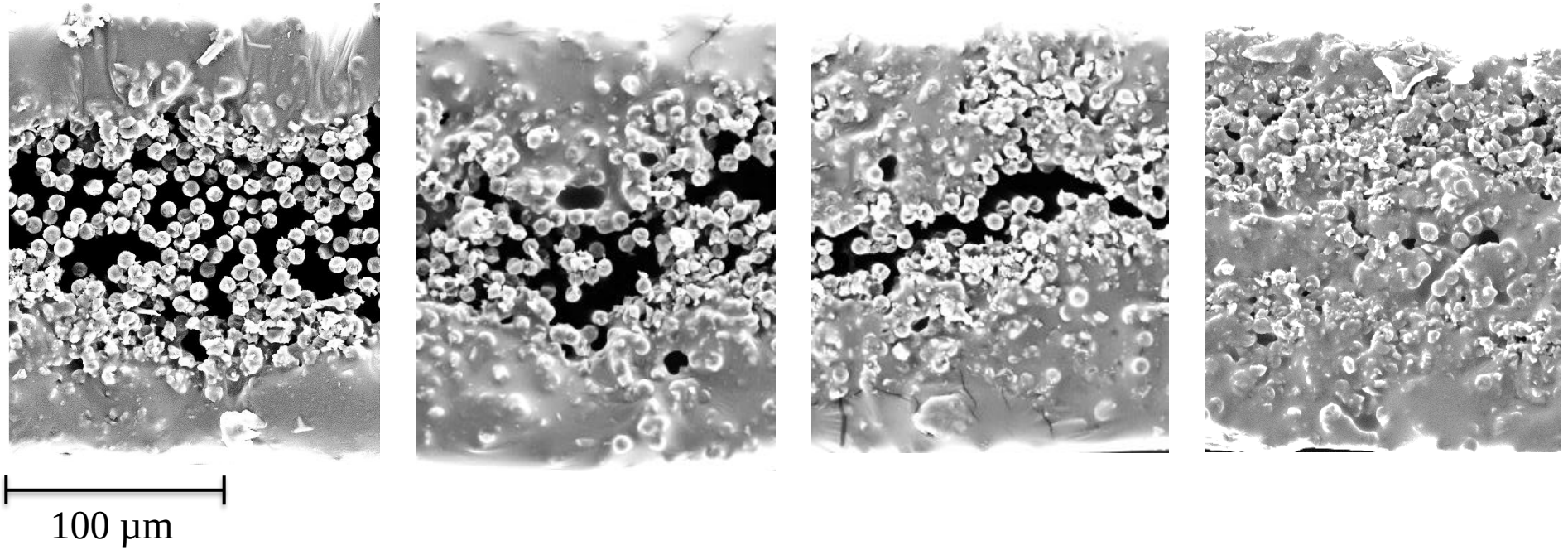

Characterizing Viscosity

Rheometer

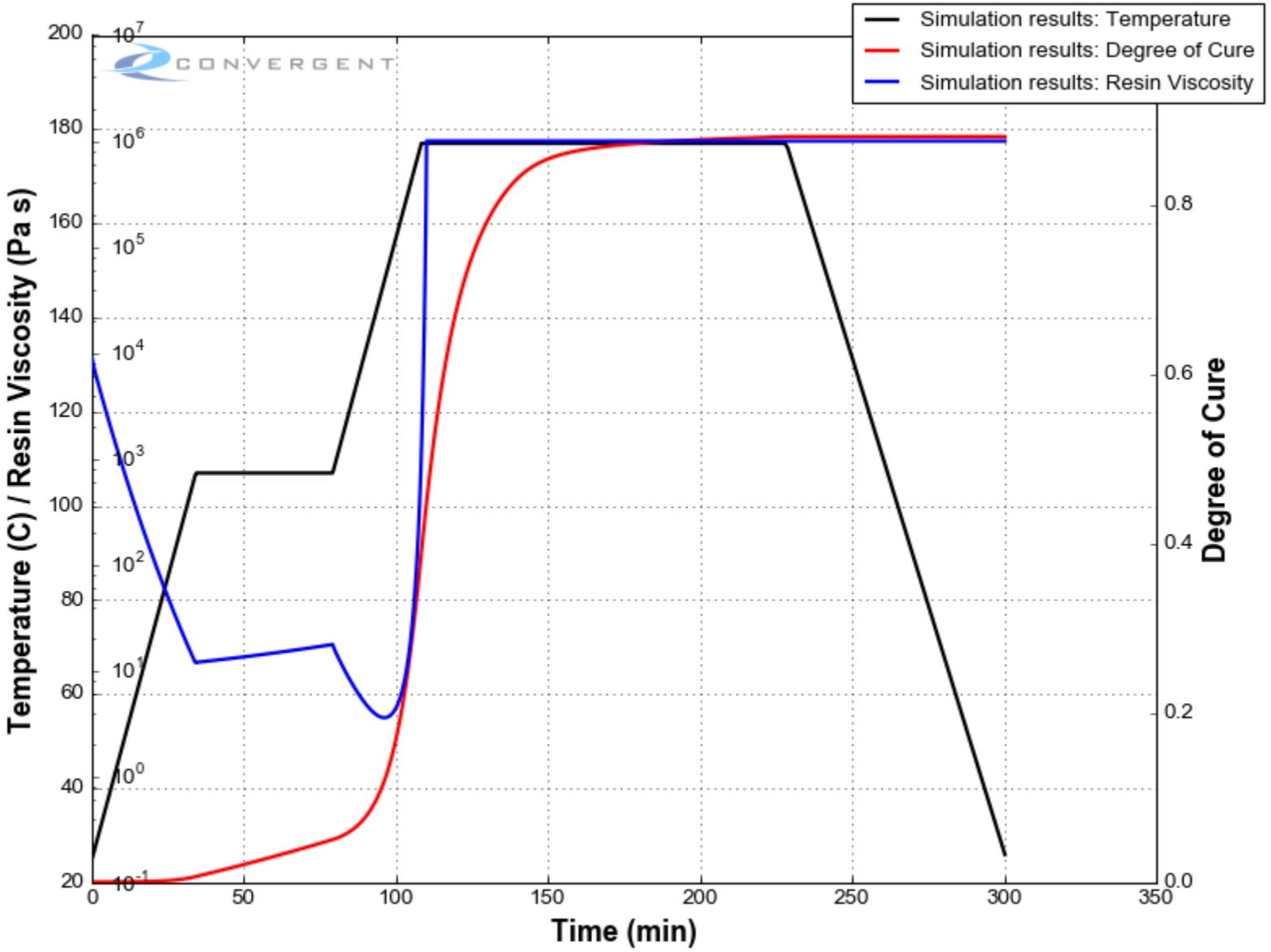

Case Study 1: Fabricating C-Shape Parts in an Autoclave

- We want to conduct the thermo-chemical analysis for fabricating C-Shape composites parts using an autoclave:
  - C-shaped laminates @ 16, 32, and 64 ply thickness
  - Material T800H/3900-2 CFRP prepreg
  - Single hold cycle: 1.7°C/min to 2-hour hold (180 °C)

Autoclave

Rear of Vessel

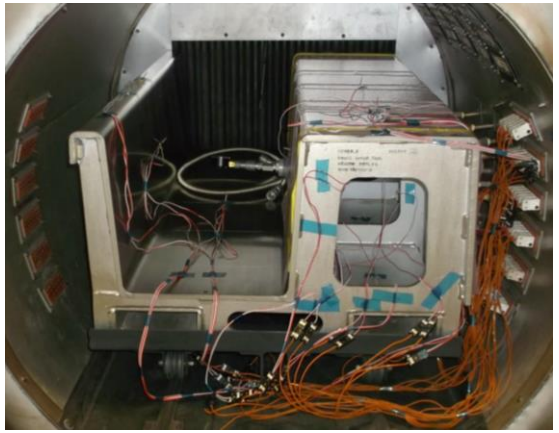
Front (Door facing)

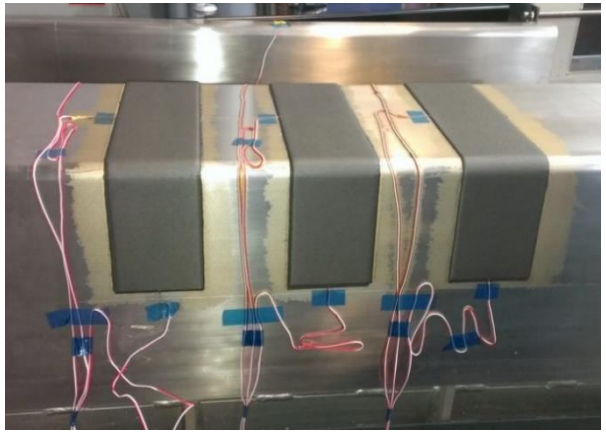
Parts on Tool

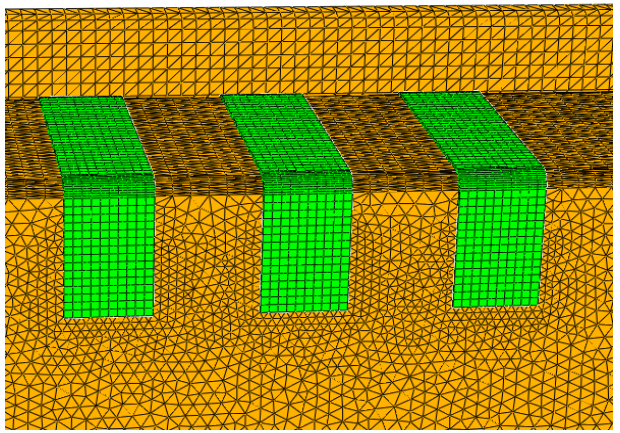
Digital Representation

Step I: Material Characterization

- To conduct thermochemical analysis, first we need to characterize the following material properties:
  - Part cure kinetics (heat of reaction and evolution of cure)
  - Part thermal properties (thermal conductivity, specific heat capacity, density)
  - Tool thermal properties (thermal conductivity, specific heat capacity, density)

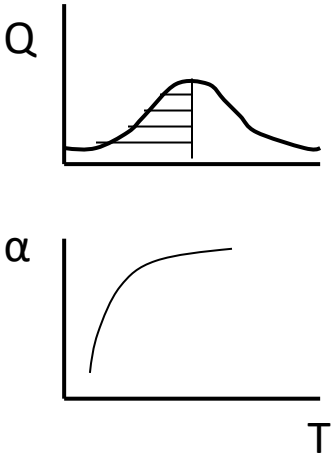

cure kinetics model

$$K = A\exp^{-E/RT}$$

$$\frac{d\alpha}{dt} = \frac{K\alpha^m(1-\alpha)^n}{1+e^{C[\alpha-(\alpha_{C0}+\alpha_{CT}T)]}}$$

Step II: Equipment Characterization

- We need to characterize the airflow and heat transfer coefficient in the autoclave:

Empty Autoclave
6.5 ft. (L) x 5 ft. (D)

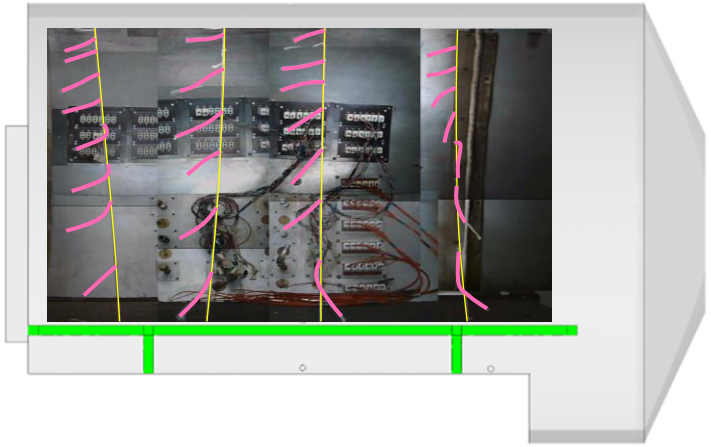

CFD, RANS-based K-epsilon turbulence modelling, ANSYS Fluent

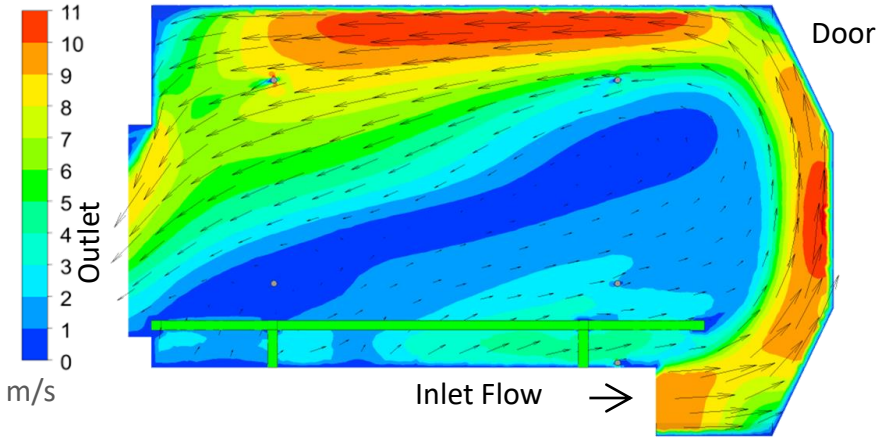

With a Large Tool
4 ft. (L) x 2.3 ft. (W) x
1.6 ft. (H)

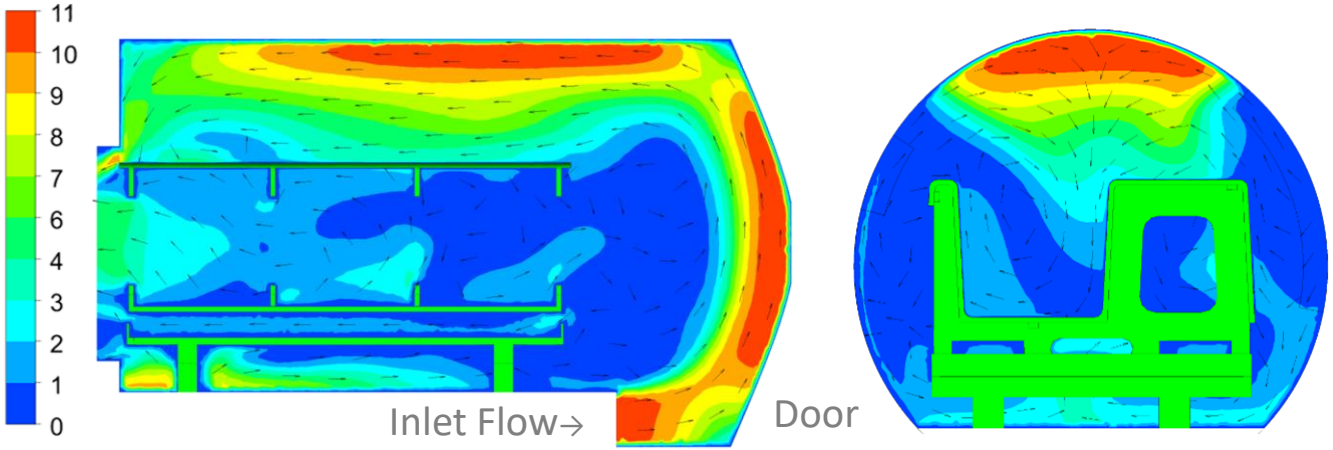

Validation of Boundary Conditions

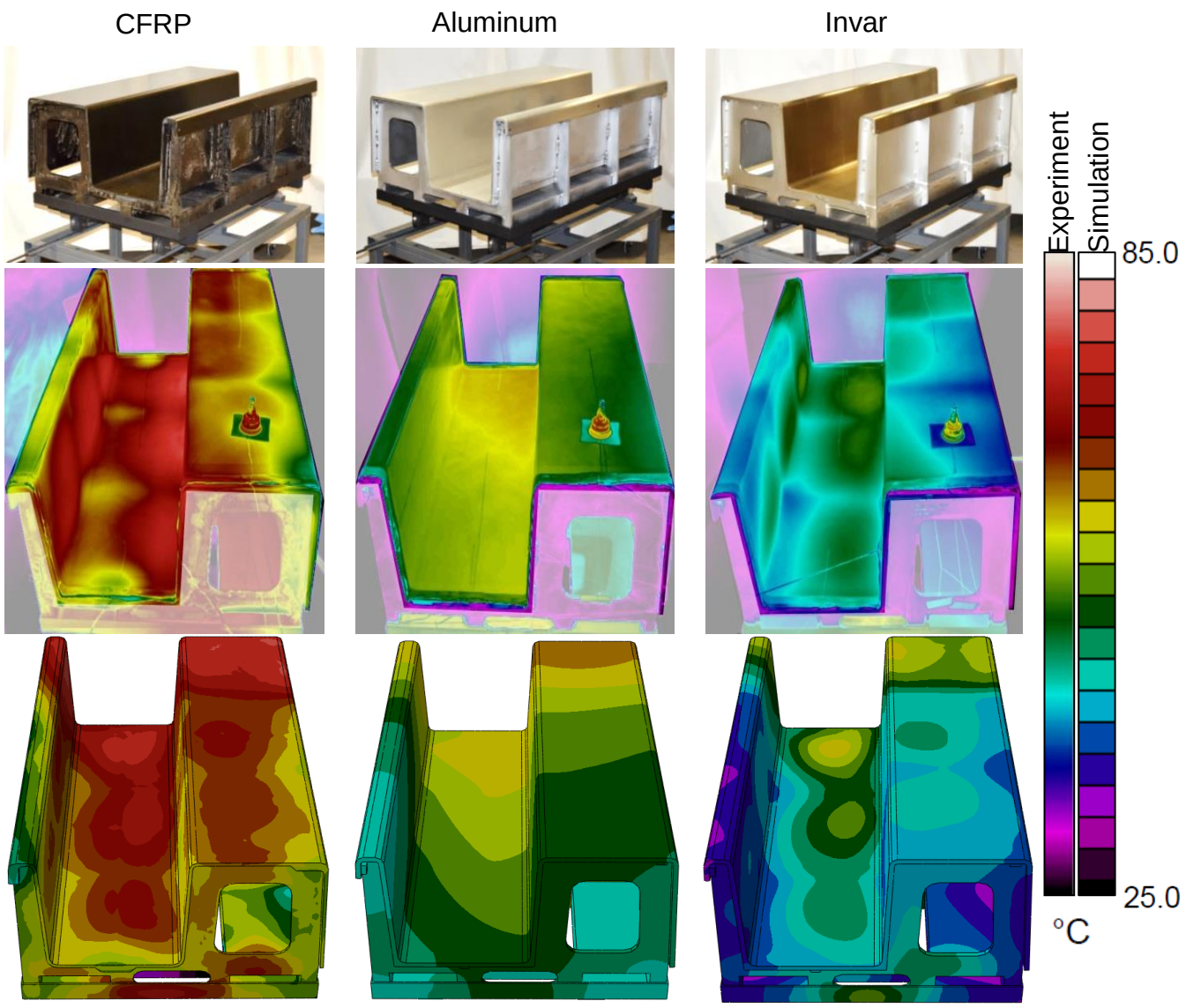

IR Thermography
Experiment

Heat Transfer Simulation
Abaqus

Predicting Part Temperature History

- FE Simulation was conducted using ABAQUS and implementing cure kinetics model in COMPRO
- TC data was succefuly compared with FE predictions

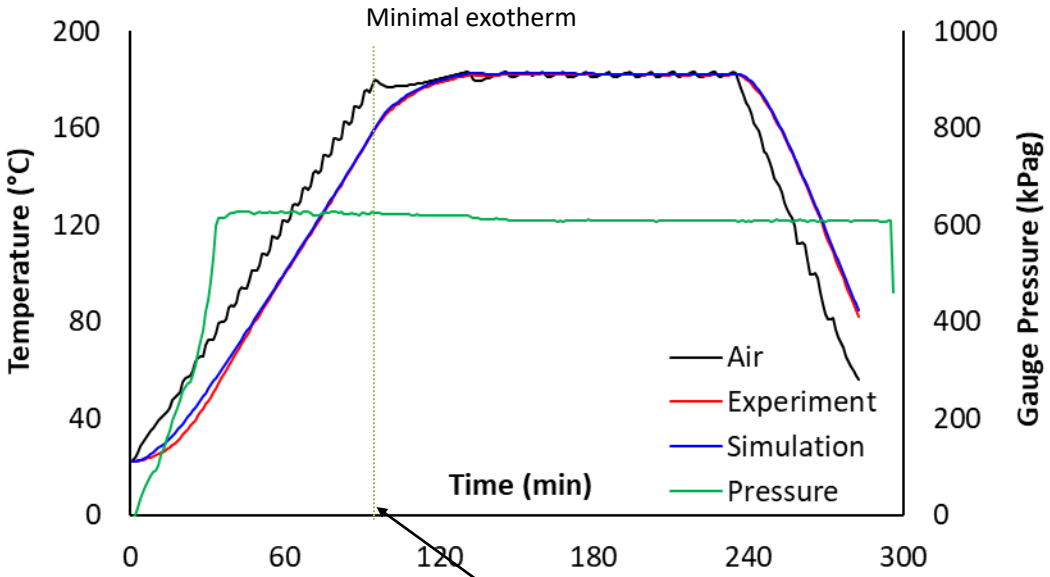

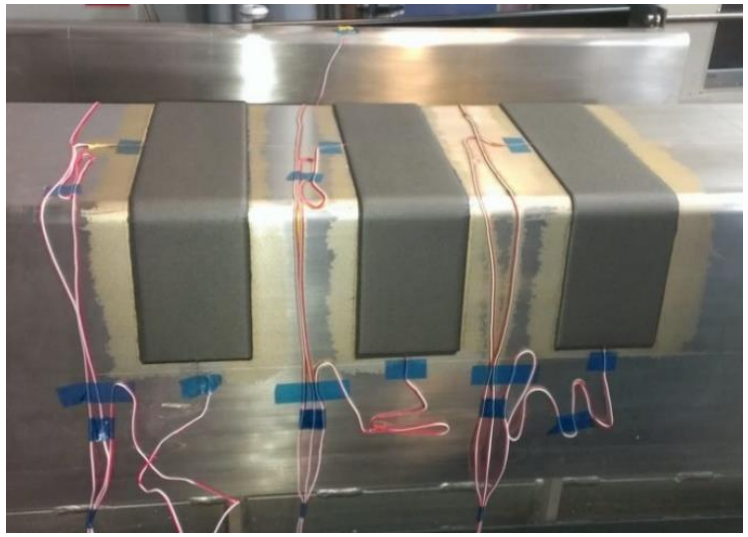

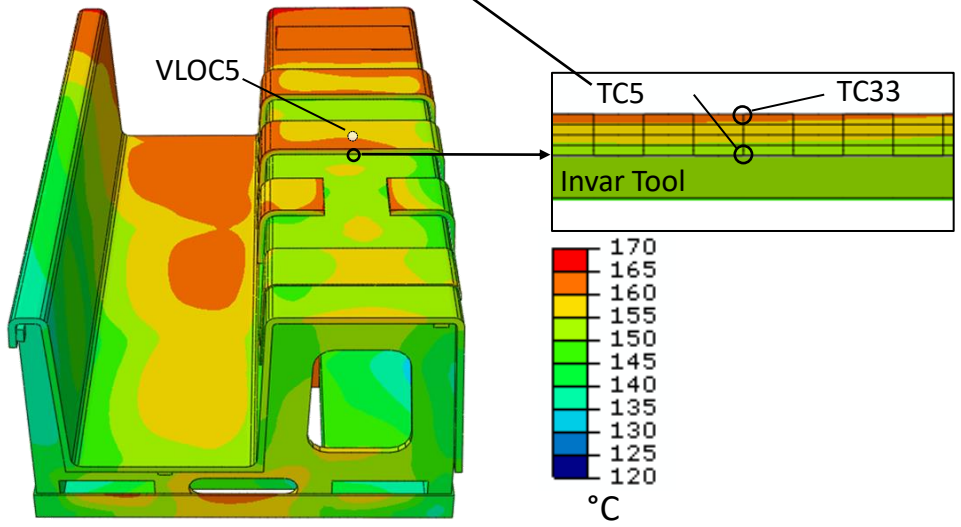

Front (Door facing)

Case Study 2: Effect of Process Parameters on Residual Stresses

- In this study, we will investigate effect of cure cycle on residual stress and micro-crack evolution in composites:
  - Material: HEXCEL AS4/8552
  - Two cure cycles

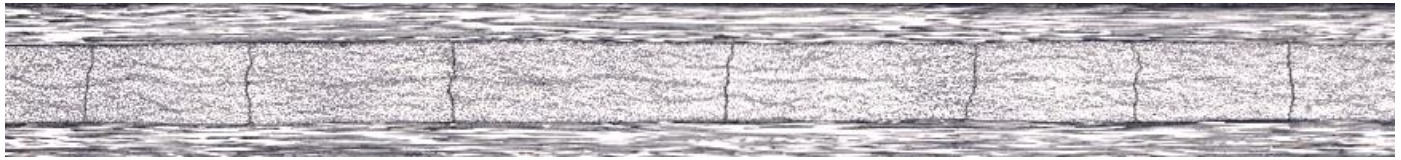

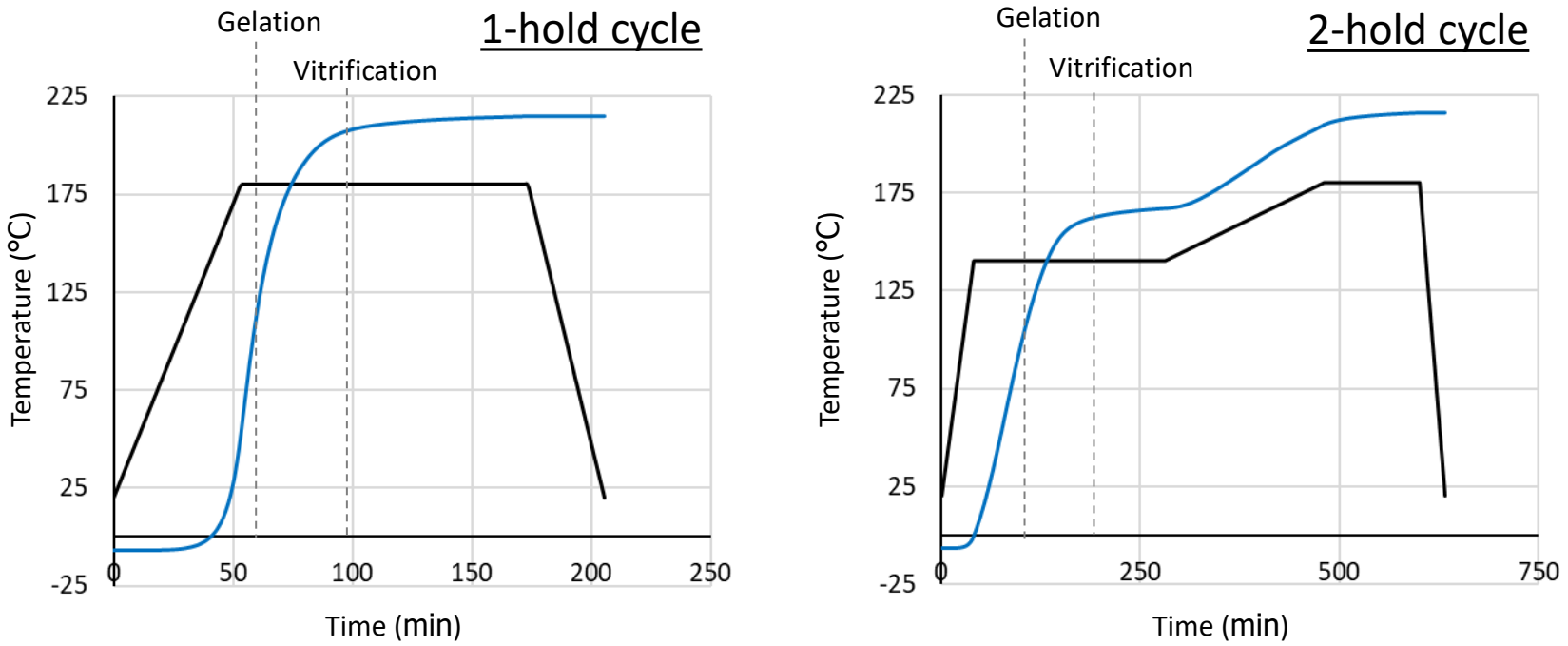

Material Characterization

- We need to characterize the following material properties:
  - Cure kinetics
  - Free strains: Cure shrinkage and CTE
  - Viscoelastic modulus evolution

DSC

DMA

TMA

Characterization of Viscoelastic Properties

Fully Cured 8552 resin and AS4/8552 prepreg beams

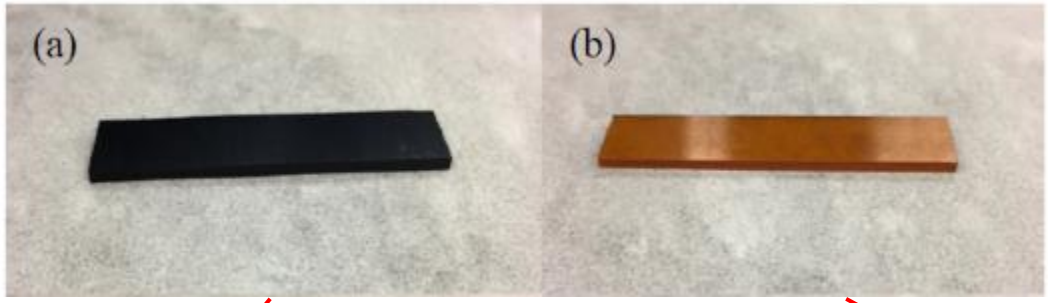

3-point bend clamp for relaxation test

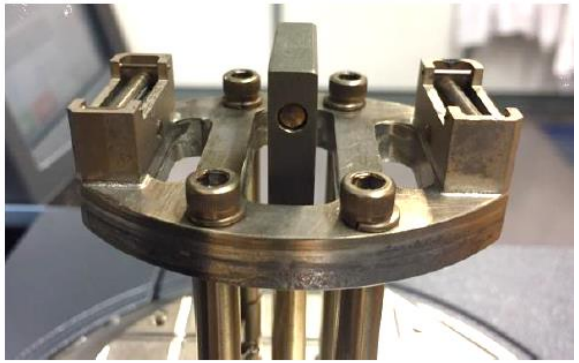

Prepreg

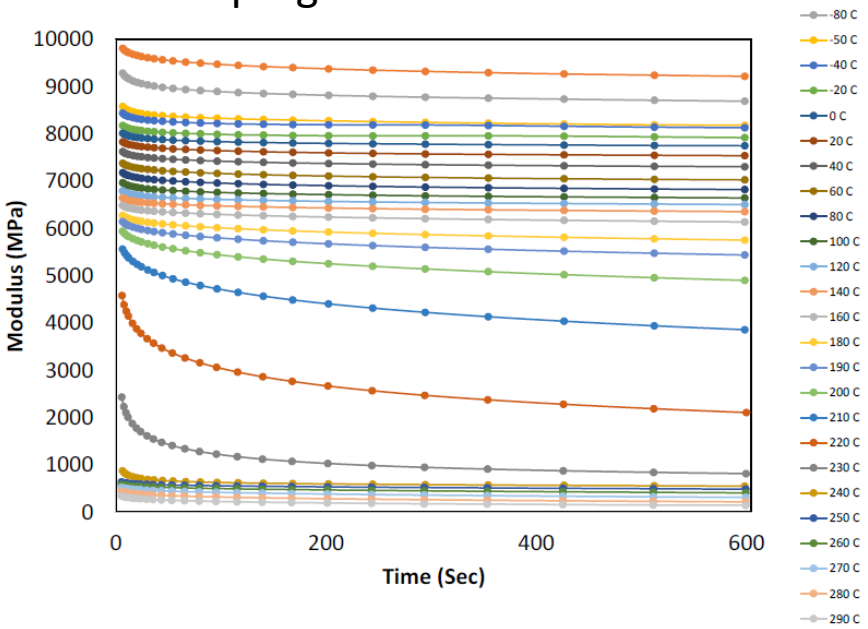

Resin

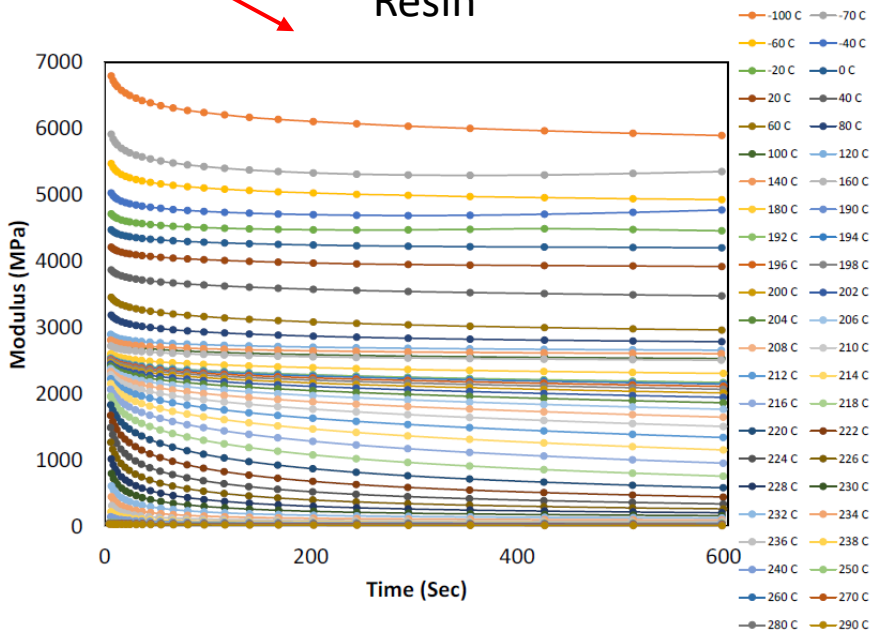

Characterization of Viscoelastic Properties

- Generalized Maxwell Model can be characterized to describe G' (Storage Modulus), G" (Loss Modulus) and G (Relaxation Modulus)

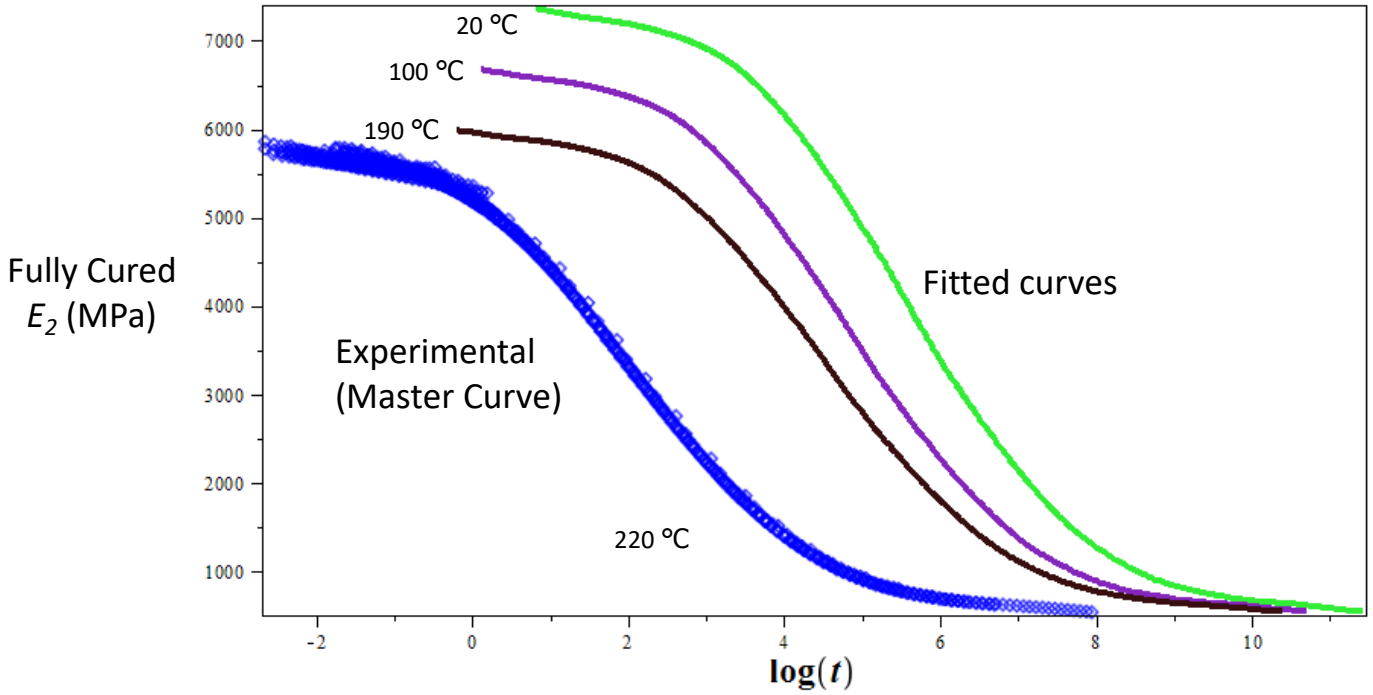

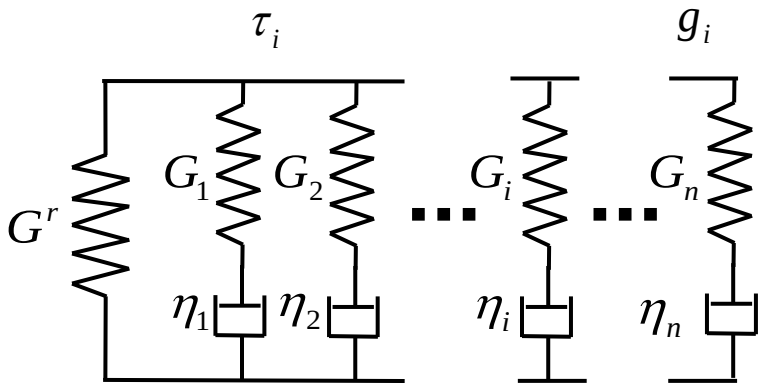

$$\tau_i = \frac{G_i}{\eta_i}$$

$$G'(\omega,T,X) = G^r(X,T) + [G^u(T) - G^r(X,T)]\sum g_i \frac{\omega^2 a_{T,X}^2 \tau_i^2}{1+\omega^2 a_{T,X}^2 \tau_i^2}$$

$$G''(\omega,T,X) = [G^u(T) - G^r(X,T)]\sum g_i \frac{\omega a_{T,X} \tau_i}{1+\omega^2 a_{T,X}^2 \tau_i^2}$$

$$G(t,T,X) = G^r(X,T) + [G^u(T) - G^r(X,T)]\sum g_i e^{-(t/a_{T,X}\tau_i)}$$

Storage Modulus and Free Strain Characterization Results

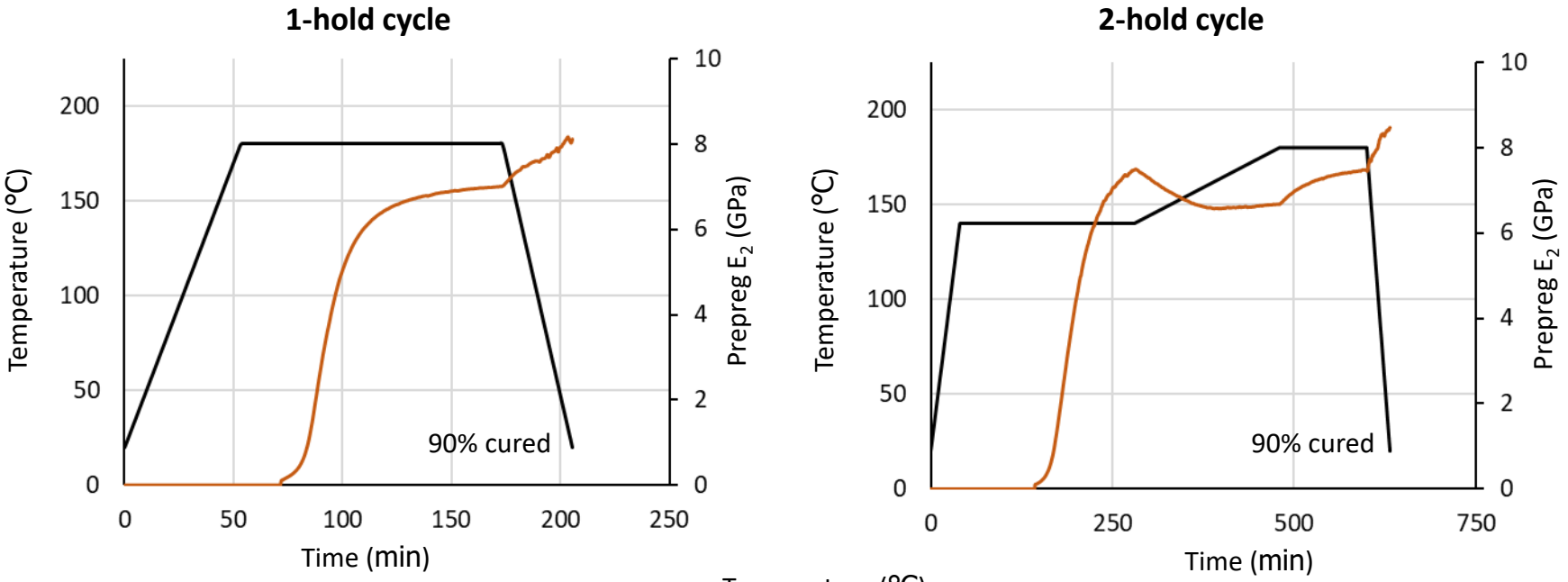

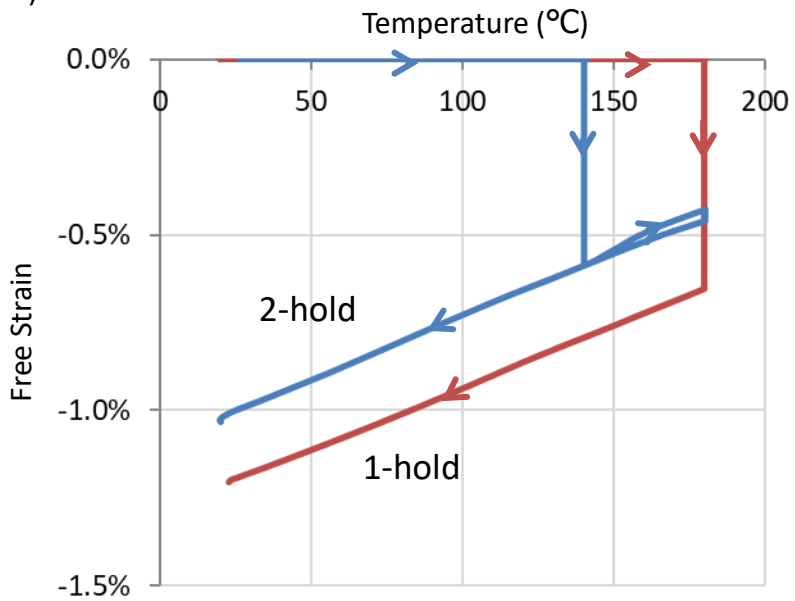

Predicting Residual Stress in $[0/90]_s$ Laminates using Characterized Properties

$$\begin{Bmatrix} dN \\ dM \end{Bmatrix} = \begin{bmatrix} A' & B' \\ B' & D' \end{bmatrix} \begin{Bmatrix} d\varepsilon_0 \\ d\kappa \end{Bmatrix} - \begin{Bmatrix} dN_{free} \\ dM_{free} \end{Bmatrix} \rightarrow$$

$$\begin{Bmatrix} 0 \\ 0 \end{Bmatrix} = \begin{bmatrix} A' & 0 \\ 0 & D' \end{bmatrix} \begin{Bmatrix} d\varepsilon_0 \\ 0 \end{Bmatrix} - \begin{Bmatrix} E'_{90} t_{90} d\varepsilon_{free} \\ 0 \end{Bmatrix} \rightarrow$$

$$d\varepsilon_0 = \frac{E'_{90} t_{90}}{A'} d\varepsilon_{free} \rightarrow$$

$$\sigma_{residual} = \int d\sigma_{residual} = \frac{-E_0 t_0}{\sum E'_i t_i} \int E'_{90} d\varepsilon_{free}$$

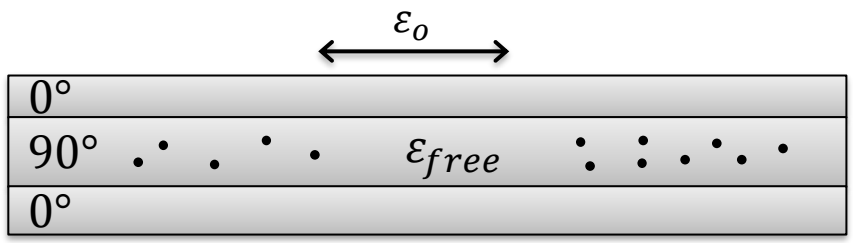

Cure Cycle	Total Strain ε_o (%)	Residual Stress $\sigma_{residual}$ (MPa)
1-hold	0.648	64.8
2-hold	0.554	55.4
Δ	0.09	9.4

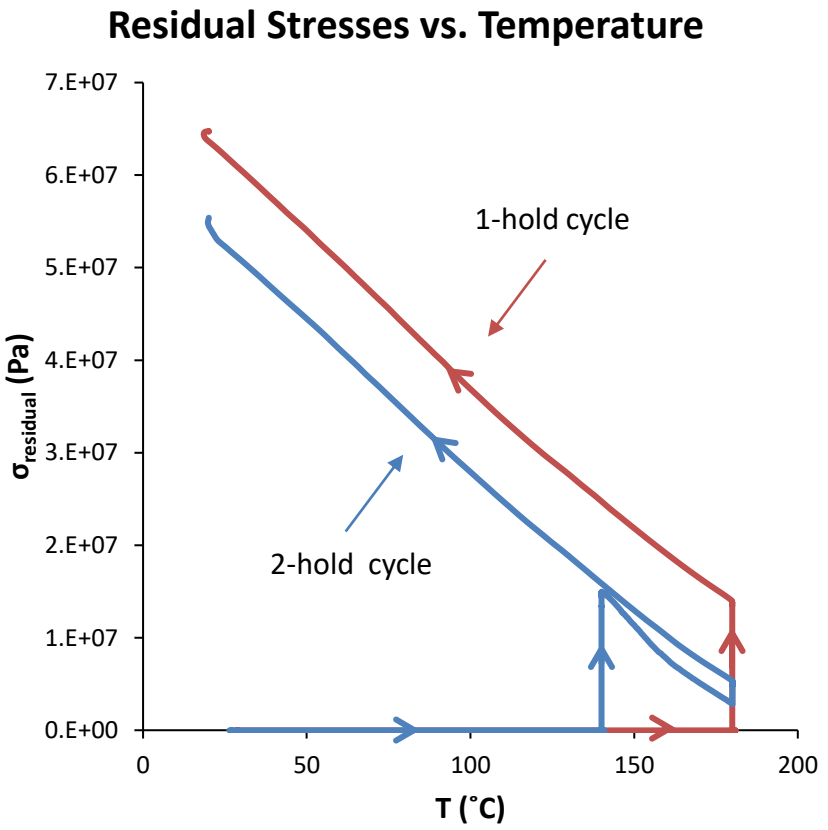

Validation of Results

- Laminates were manufactured using the two cure cycles.
- Tensile coupons were prepared and tested while one polished edge of the coupon was monitored using a microscope.

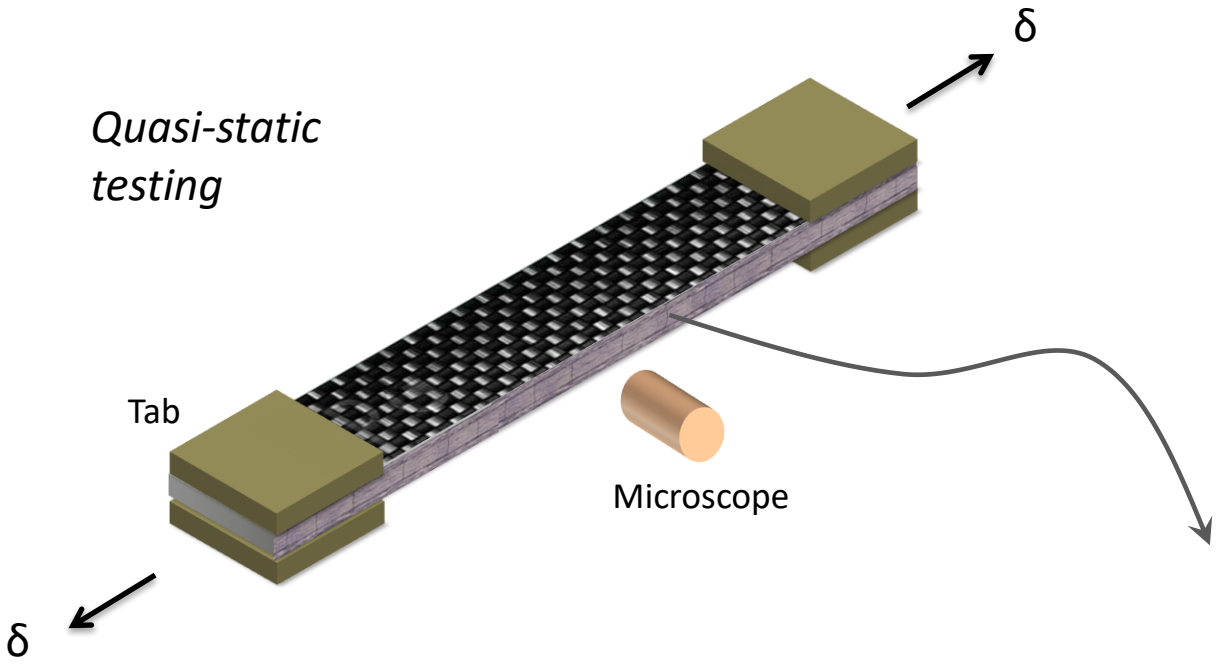

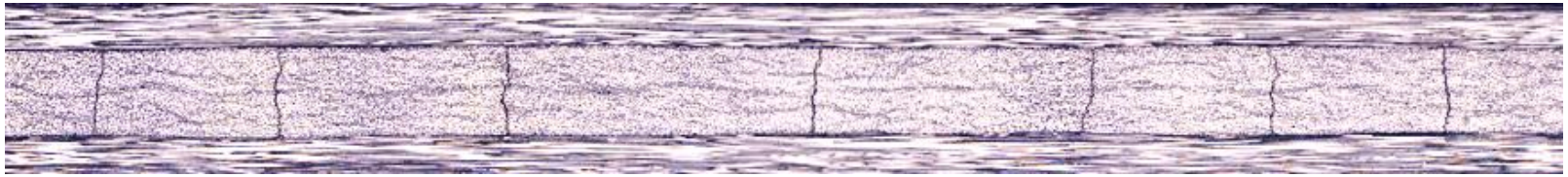

Residual Stress in Cross-Ply Laminates

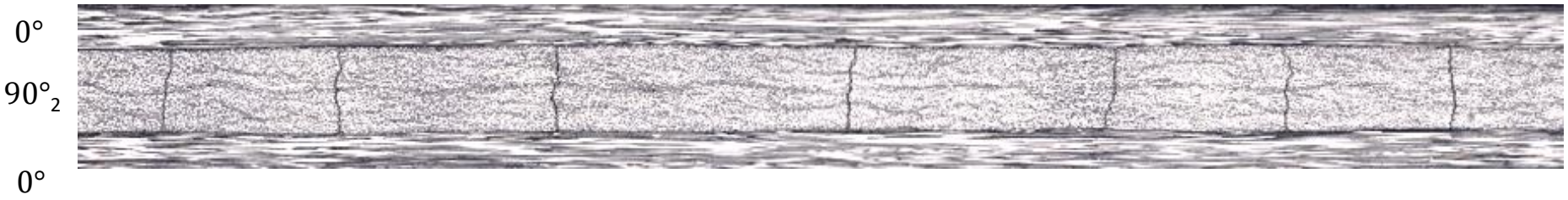

Predictions of Residual Stresses in $[0/90]_S$ Laminates

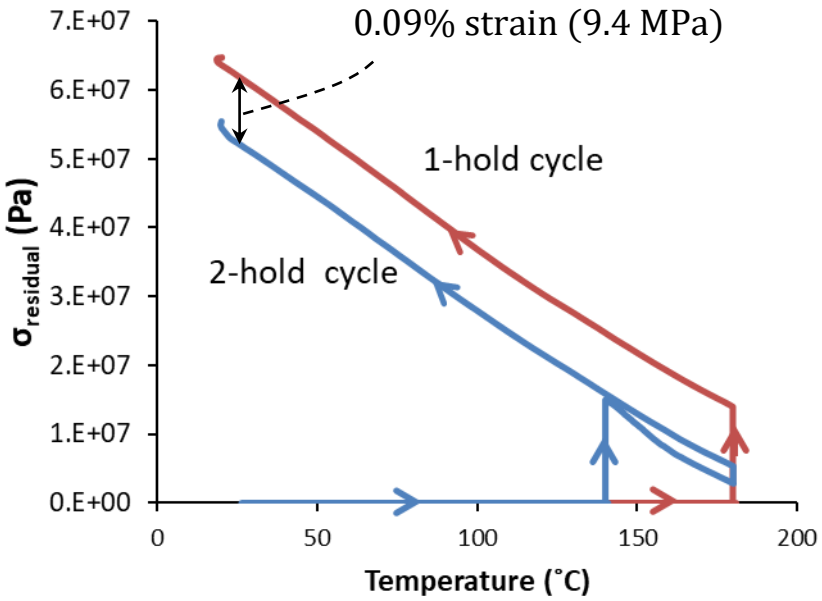

Matrix Cracking Tests on $[0/90]_S$ Laminates

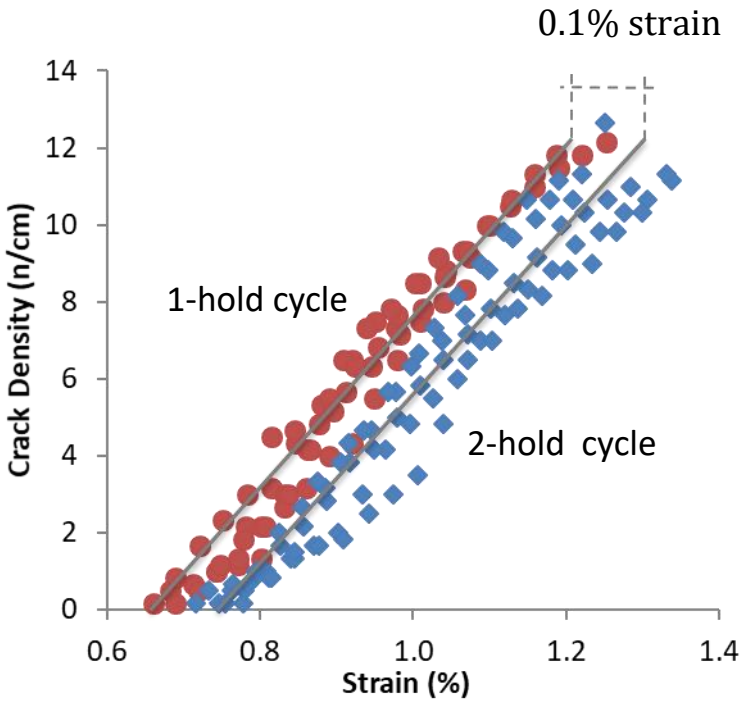

Zobeiry N., Forghani A., Li C., Thorpe R., Gordnian K., Vaziri R., Fernlund G., Poursartip A. (2016). Multi-scale characterization and representation of composite materials during processing, *Philosophical Transactions of the Royal Society of London A: Mathematical, Physical and Engineering Sciences*, DOI: 10.1098/rsta.2015.0278, 374:20150278

Effect of Process Parameters on Porosity

- Effect of Cure Cycle on Porosity (Toray T800/3900-2):

Ply thickness = 0.196 mm
(≈ 7% porosity)

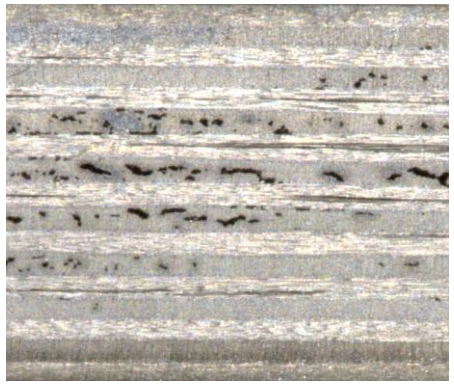

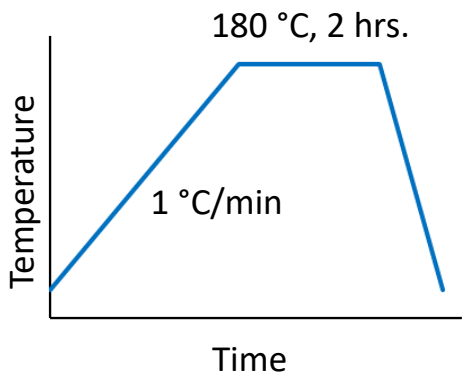

Ply thickness = 0.189 mm
(≈ 3.5% porosity)

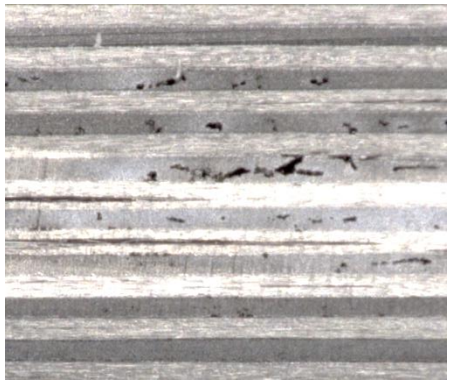

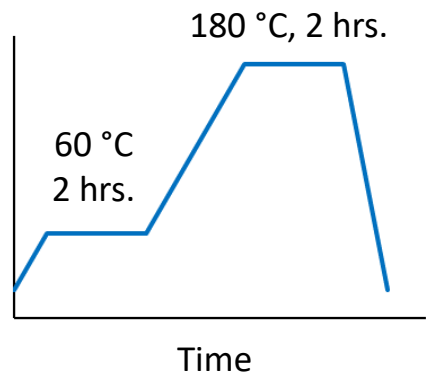

Ply thickness = 0.182 mm
(< 0.5% porosity)

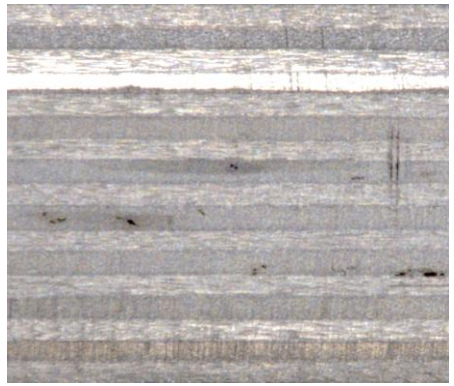

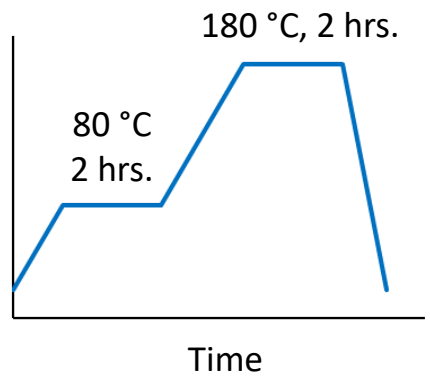

Ply thickness = 0.192 mm
(≈ 5% porosity)

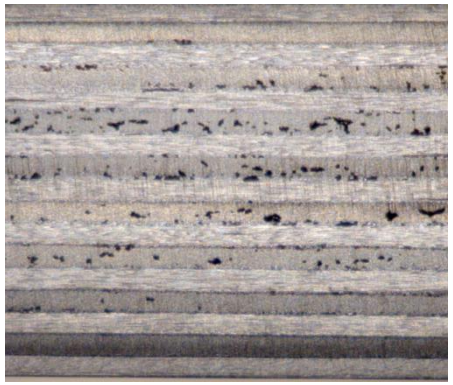

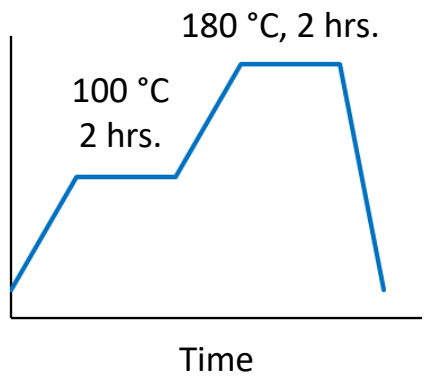

Material Characterization

- We need to characterize the following material properties:
  - Cure kinetics
  - Resin viscosity
  - Prepreg permeability

In-plane (resin infusion)

Through-thickness (prepreg)

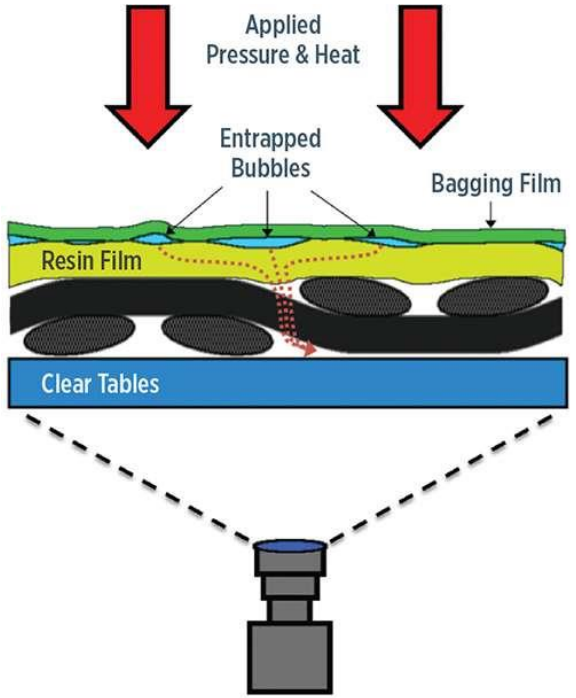

Coupled Gas/Resin Transport Model

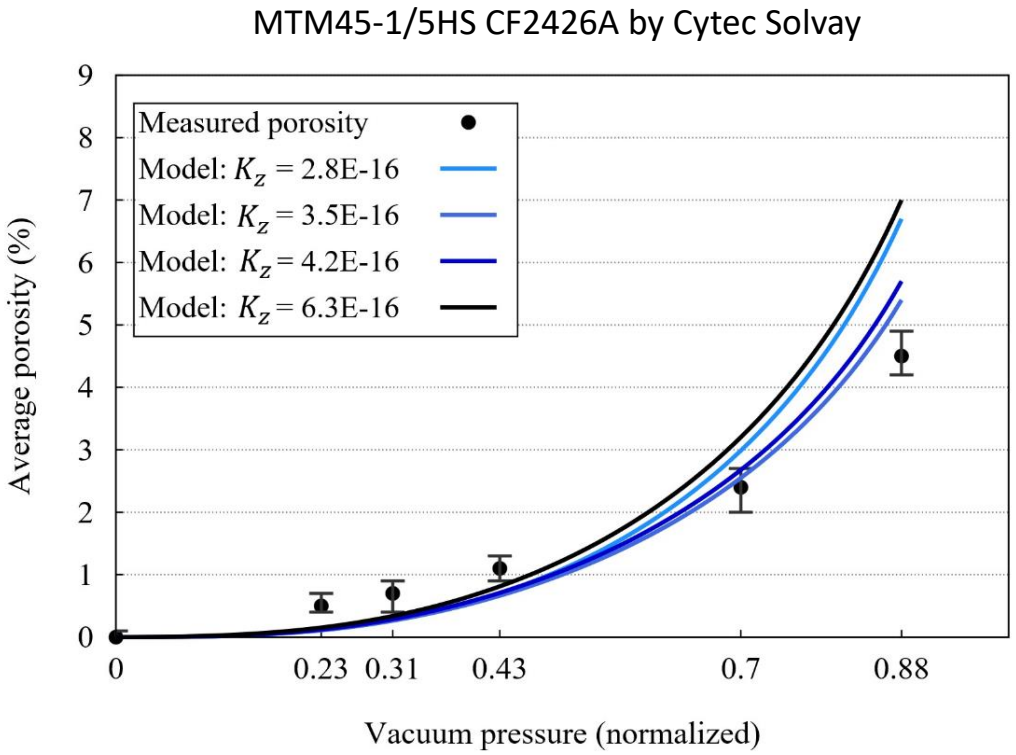

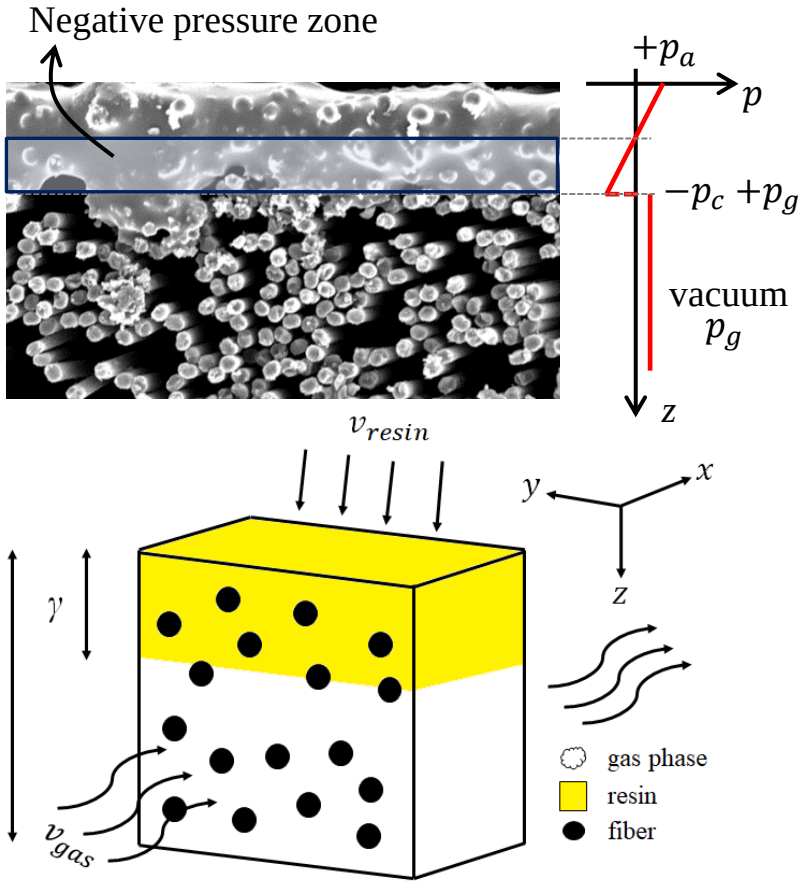

$$\begin{cases} \varphi \dfrac{\partial P_g}{\partial t} = \dfrac{K_{x0}}{\mu_g} \dfrac{\partial}{\partial x}\left(\left(1+\dfrac{b}{P_g}\right) P_g \dfrac{\partial P_g}{\partial x}\right) + \dfrac{K_z}{h^2 \mu_r (1-V_f)} \dfrac{P_g (P_a - P_g + P_c)}{(1-\varphi)} \\ \dfrac{d\varphi}{dt} = -\dfrac{K_z}{h^2 \mu_r (1-V_f)} \dfrac{P_a - P_g + P_c}{(1-\varphi)} \end{cases}$$

Gas flow in x direction

Resin flow in z direction

Example: Commercial Tools for Dimensional Changes

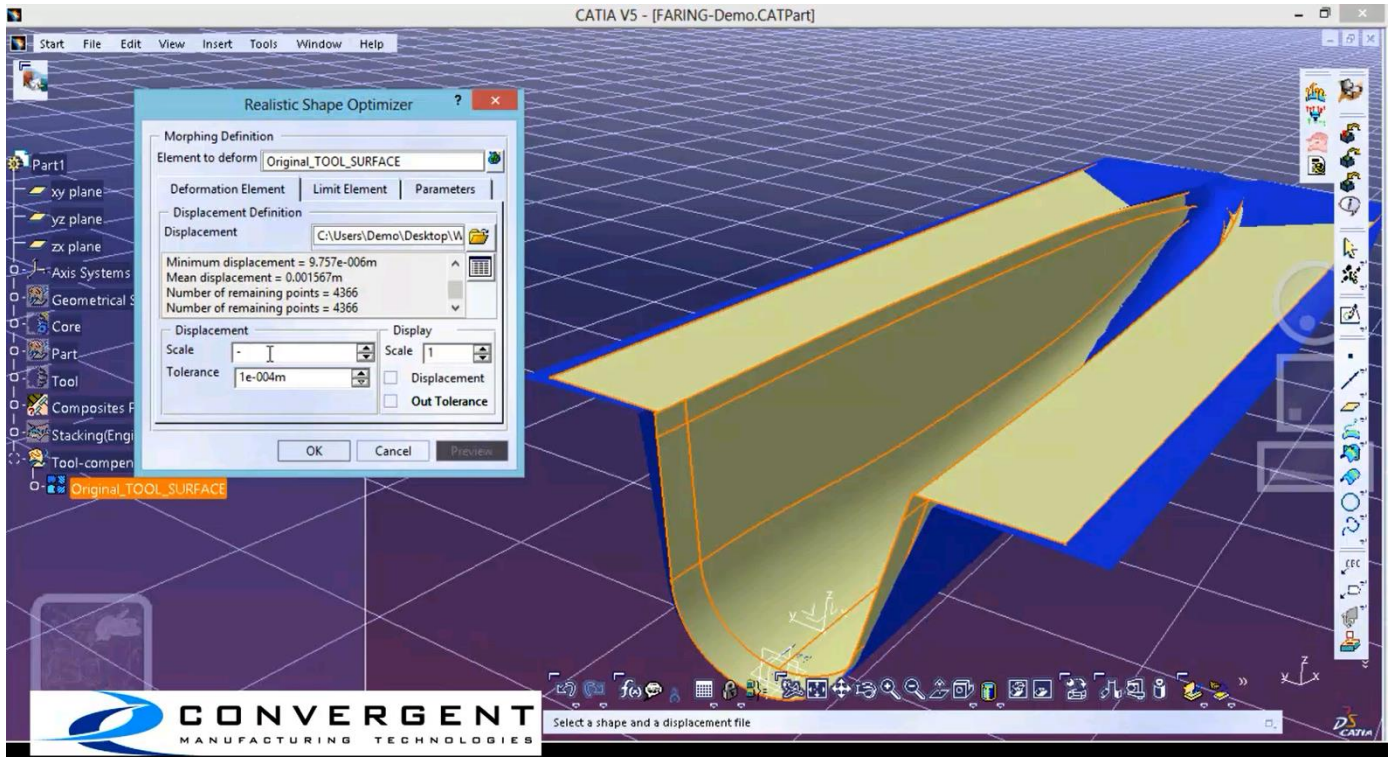

Process-Induced Deformations by COMPRO

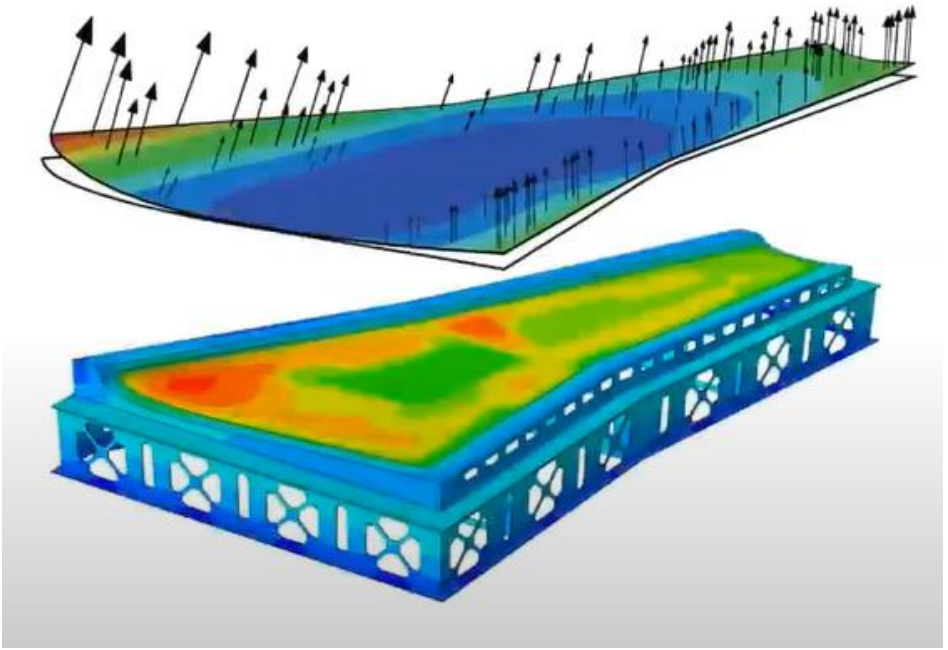

Industry Approach

Material Characterization

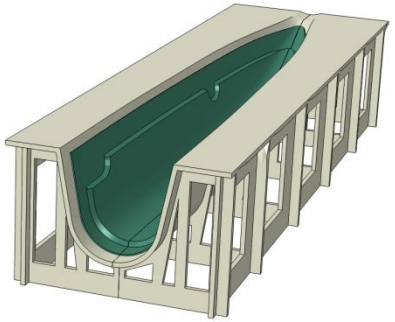

CATIA

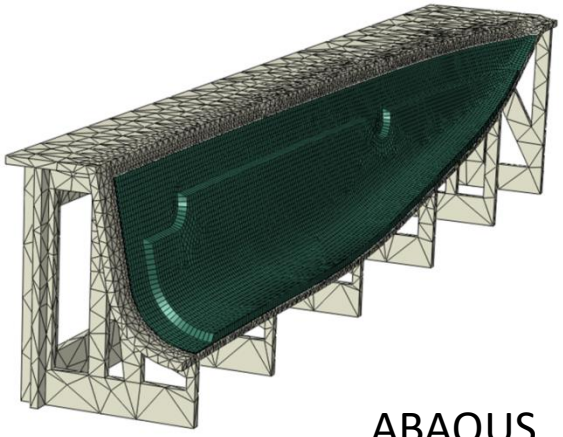

ABAQUS COMPRO

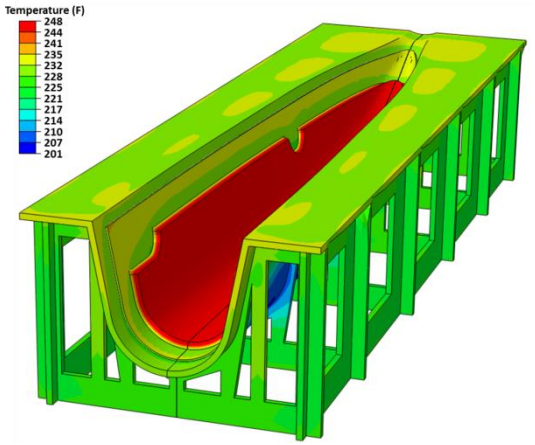

Thermo-chemical analysis

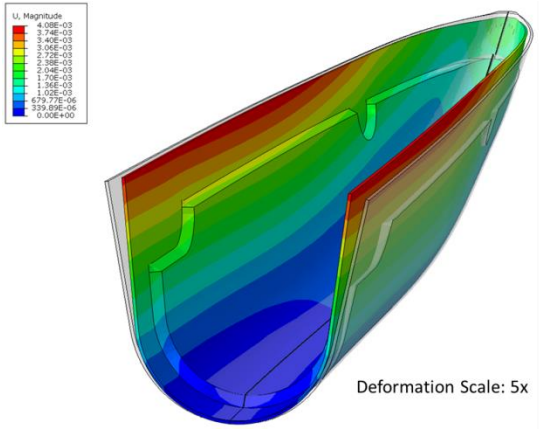

Stress-deformation analysis

Tool Geometry Compensation